

**Synthesis of Cardiotonic Steroids Oleandrigenin and Rhodexin B and Studies Toward the  
Synthesis of Bufalin**

by

Zachary A. Fejedelem

A dissertation submitted in partial fulfillment  
of the requirements for the degree of  
Doctor of Philosophy  
(Chemistry)  
in the University of Michigan  
2021

Doctoral Committee:

Associate Professor, Pavel Nagorny, Chair  
Professor John Montgomery  
Professor Nouri Neamati  
Associate Professor Paul Zimmerman

Zachary A. Fejedelem

[zfejedel@umich.edu](mailto:zfejedel@umich.edu)

ORCID iD: [0000-0003-1415-3019](https://orcid.org/0000-0003-1415-3019)

© Zachary Alan Fejedelem 2021

## **Dedication**

I dedicate this thesis to my friends and family. Without their support, nothing would be possible. Especially to my mother, Mary, I love you very much.

## **Acknowledgements**

I would like to express special appreciation to my advisor, Pavel Nagorny, for his constant support and guidance. Dr. Nagorny has been a true mentor to me, and I am honored to have been part of his group at the University of Michigan. His wealth of chemical knowledge is boundless.

I would also like to acknowledge and thank my dissertation committee members, Dr. John Montgomery, Dr. Paul Zimmerman, and Dr. Nouri Neamati for their support throughout my graduate studies. I want to acknowledge my current and former lab mates Dr. Hem Khatri, Dr. Tay Rosenthal, Dr. Bijay Bhattarai, Dr. Jeonghyo Lee, Nicolas Diaz, Rami Hourani, Siyuan Sun, Sibin Wang, Nolan Carney, Ryan Rutkoski, and Sungjin Kim for their friendship and scientific advice. I will forever cherish the memories.

I have been truly blessed to have forged strong and invaluable friendship with Wesley Pein, if I did not befriend you in Michigan, I would probably become a recluse. Thank you for your never-ending support and encouragement helped me stay motivated and sane throughout graduate school.

## Table of Contents

Dedication.....	ii
Acknowledgements.....	iii
List of Tables .....	vii
List of Figures.....	viii
List of Schemes.....	xiii
List of Abbreviations .....	xv
Abstract.....	xix
Chapter 1 Introduction .....	1
1.1 Introduction to relevance of bufadienolides.....	1
1.2 Selected examples of plant sources of bufadienolides .....	5
1.3 Select examples of animal sources of bufadienolides.....	7
1.4 Selected examples of the <i>de novo</i> synthesis of bufadienolides.....	9
1.5 Proposed biosynthesis pathway.....	18
1.6 Summary .....	19
1.7 References .....	22
Chapter 2 Studies Towards the Total Synthesis of Cardiotonic Steroid Family: Bufadienolides	24
2.1 Introduction.....	24

2.2 Regioselective hydrogenation of 2-pyrone-coupled bufadienolides .....	26
2.3 Developments of regioselective hydrogenation of Stille-coupled bufalin-like steroids .....	26
2.3.1 Preliminary data with model substrates.....	26
2.3.2 Preliminary data of full reduction of pyrone model substrates .....	32
2.4 Oxidation of cyclic lactones to pyrones .....	35
2.5 Attempts of pyrone olefin masking for selective hydrogenation studies .....	41
2.6 Modifications for furan-amide <sup>1</sup> O <sub>2</sub> cycloaddition.....	45
2.6.1 Initial optimization of endoperoxide rearrangement .....	49
2.6.2 Furan-endoperoxide rearrangement toward forming alpha-pyrones: Generation 2 .....	60
2.7 Conclusions .....	68
2.8 Experimental information .....	71
2.9 References .....	101
Chapter 3 Total Synthesis of Cardiotonic Steroid Family: Synthesis of Cardiotonic Steroids Oleandrigenin and Rhodexin B.....	103
3.1 Introduction .....	103
3.2 Direct installation of βC-16 oxygenation.....	121
3.2.1 Direct C-16 oxidation of butanolide containing steroid .....	121
3.3 Directed C16 oxidation of furan-containing steroid .....	126
3.4 Conclusions .....	142
3.5 Future Directions.....	143

3.6 Experimental .....	143
3.7 References .....	184
Chapter 4 Site-Selective Glycoside Cleavage.....	186
4.1 Introduction .....	186
4.2 Research Aim: Site-selective deglycosylation .....	188
4.3 Superacid reactions in literature .....	190
4.4 Initial studies with pseudo-disaccharides .....	192
4.5 Conclusions .....	198
4.6 Experimental information .....	200
4.7 References .....	212
Chapter 5 Closing Remarks .....	214

## List of Tables

Table 2.1. Optimization of Rh/Al <sub>2</sub> O <sub>3</sub> hydrogenation screening. ....	33
Table 2.2. Oxidation conditions screening of 2-23.....	37
Table 2.3. Attempts of cyclizing furan amide 2-88 to pyrone.....	66
Table 3.1. Select examples from Wicha's cytotoxic (IC <sub>50</sub> ; μM; 72 h) assay study against cancer cell lines. <sup>13</sup> .....	111
Table 3.2. Initial optimization of epoxide ring opening. ....	129
Table 3.3 <sup>1</sup> H NMR (CDCl <sub>3</sub> ) comparison of reported synthetic (left) vs. synthetic (right) oleandrigenin with reported data from the literature. ....	168
Table 3.4 <sup>13</sup> C NMR (CDCl <sub>3</sub> ) comparison of reported synthetic (left) vs. synthetic (right) oleandrigenin with reported data from the literature. ....	169
Table 3.5. <sup>1</sup> H NMR (CD <sub>3</sub> OD) comparison of isolated (left) vs. synthetic (right) rhodexin B (i.e. tupichinolide) with reported data from the literature.....	182
Table 3.6. <sup>13</sup> C NMR (CD <sub>3</sub> OD) comparison of isolated (left) vs. synthetic (right) rhodexin B (i.e. tupichinolide) with reported data from the literature.....	183
Table 4.1. Comparison study of various acids for the deglycosylation of 4-24. ....	196
Table 4.2. Comparison study of various acids for the deglycosylation of 4-29. ....	197
Table 4.3. Comparison study of various acids for the deglycosylation of 4-19. ....	198



## List of Figures

Figure 1.1. Steroid core ‘U’-shaped fused ring system. ....	2
Figure 1.2. Most used cardio inotropes in the United States, digitoxin 1-4 and digoxin 1-5. ....	3
Figure 1.3. Representative examples of bufadienolide and cardienolide, respectively. ....	3
Figure 1.4. Representative examples of endogenously present bufadienolides in human tissues. .	4
Figure 1.5. Daigremontianin 1-8, bersaldegennin 1,3,5- orthoacetate 1-9. ....	6
Figure 1.6. Hellebrigenin 1-10, lanceotoxin A, 1-11 and lanceotoxin B, 1-12. ....	6
Figure 1.7. Representative structure of bufotoxin. ....	7
Figure 1.8. Epoxybufadienolides extracted from Chan’ Su toad venom. ....	8
Figure 1.9. Representative example from snake venom in the nuchal glands of <i>Rhabdophis tigrinus</i> . ....	9
Figure 1.10. Proposed biogenesis of bufadienolides. ....	19
Figure 1.11. Illustration of steroid targets with complex D-ring functionalizations ....	20
Figure 2.1. Effects of structural modifications on bufadienolides. ....	25
Figure 2.2. Hilton’s regioselective hydrogenation of a pyrone-steroid. ....	26
Figure 2.3. Discovery of competitive double bond reactivity in pyrone ring of bufadienolides ..	31
Figure 2.4. Transformation of $\delta$ -valerolactone to silyl enol ether lactol. ....	36
Figure 2.5. Dong's Cu(I) oxidation of lactone. ....	39
Figure 2.6. Baran's electrochemically driven desaturation method. ....	39
Figure 2.7. Replicative experiments of Dong's Cu(I) oxidation of lactone 2-24. ....	40
Figure 2.8. Replicative experiments of Dong's Cu(I) oxidation of lactone 2-20A. ....	40

Figure 2.9. Attempted Cu(I) oxidation of 5 $\alpha$ -bufadienolide model 2-21. ....	41
Figure 2.10. Prior art towards iron-masking of pyrones. ....	42
Figure 2.11. Complexation of various bromo-substituted 2-pyrones with Fe <sub>2</sub> (CO) <sub>9</sub> via Fairlamb's method. ....	43
Figure 2.12. Hydrogenation of iron-carbonyl masked pyrone. ....	44
Figure 2.13. Iron-carbonyl masking on 5 $\alpha$ -bufadienolide. ....	44
Figure 2.14. Hydrogenation of iron-masked 5 $\alpha$ -bufadienolide and proposed iron(0) complexes. ....	45
Figure 2.15. Wiesner's route for making intermediate 2-49. ....	47
Figure 2.16. Wiesner's complete synthesis of bufalin from intermediate 2-49. ....	48
Figure 2.17. Proposed route of furan to pyrone with the pre-installed C-14 $\beta$ -OH. ....	50
Figure 2.18. Model studies with C5' ester containing furan (by Dr. Khatri). ....	52
Figure 2.19. Model studies with C5' ortho-ester containing furan (by Dr. Khatri). ....	53
Figure 2.20. Model studies with C5'-OTIPS furan ester. ....	55
Figure 2.21. Initial diisopropyl furan amide test reactions (by Dr. Khatri). ....	56
Figure 2.22. Diisopropylfuran amide on model steroid (with Dr. Khatri). ....	58
Figure 2.23. Proposed side product formation mechanism (by Dr. Khatri). ....	59
Figure 2.24. Proposed mechanism for N,O- acyl rearrangement. ....	61
Figure 2.25. Synthesis of 2-81. ....	62
Figure 2.26. Further optimization of furan amide cyclization. ....	63
Figure 2.27. Synthesis of 2-85 and 2-17 for model steroid studies. ....	64
Figure 2.28. Synthetic route for building intermediate 2-88. ....	65
Figure 2.29. Proposed observed side products from crude HRMS analysis of experiments in Table 2-3. ....	67

Figure 3.1. Structural representation of oleandrin, oleandrigenin. ....	104
Figure 3.2. Structural representation of rhodexin B (tupichinolide).....	104
Figure 3.3. Wicha's synthesis ketone 3-13 from 3-4.....	106
Figure 3.4. Wicha's synthesis 3-19 from 3-13 .....	108
Figure 3.5. Wicha's completed synthesis of oleandrigenin (3-2).....	109
Figure 3.6. Wicha's mechanistic proposal for photooxidation endo-peroxide rearrangement for transformation of 3-20 to 3-21.....	110
Figure 3.7. Fernandez-Mateos selected example of stereospecific epoxide ring opening with Lewis acid.....	112
Figure 3.8. Retrosynthetic proposal for C-16 oxidation and mechanistic proposal for C-16 oxidation via House-Meinwald rearrangement.....	113
Figure 3.9. Inoue's synthesis of bufadienolide precursor 3-34. ....	115
Figure 3.10. Inoue's synthesis of 3-37. ....	116
Figure 3.11. Mechanistic proposal by Inoue for the observed transformations with 3-35 and TMSOTf (path A), and InCl <sub>3</sub> (path B).....	117
Figure 3.12. Inoue's synthesis of bufotalin and scheme leading to bufalin.....	119
Figure 3.13. Inoue's completed synthesis of bufalin. ....	120
Figure 3.14. Stille cross-coupling for making model butenolide 3-43. ....	121
Figure 3.15. Hydroboration oxidation on model butanolide 3-43. ....	122
Figure 3.16. Attempted Lewis acid epoxide ring opening on model butanolide 3-43.....	123
Figure 3.17. Asakawa's BF <sub>3</sub> •OEt <sub>2</sub> , Lewis acid ring opening with pre-installed C16-ketone. <sup>17</sup>	124
Figure 3.18. Mechanistic proposal for transformation of epoxide 3-47 to spirocyclic intermediate 3-48. ....	125

Figure 3.19. Asakawa's proposed decomposition pathways with 3-47.....	126
Figure 3.20. Suzuki coupling to make model substrate 3-54.....	127
Figure 3.21. Synthetic route for building steroid core of oleandrigenin.....	131
Figure 3.22. Synthetic route for completion of the synthesis of oleandrigenin.....	133
Figure 3.23. First attempt of glycosylation towards rhodexin B. (donor 3-59 was graciously donated by Ryan Rutkoski).....	135
Figure 3.24. Second attempt of glycosylation towards rhodexin B. (Donor 3-65 was graciously donated by Nolan Carney) .....	137
Figure 3.25. Yb(OTf) <sub>3</sub> mediated deprotection attempt on 3-66 and proposed products based on crude <sup>1</sup> H NMR and HRMS analysis. ....	138
Figure 3.26. Synthesis of rhamnoside donor 3-73 from Nguyen <sup>21</sup> (synthesized by Nolan Carney). .....	139
Figure 3.27. Optimization of Nguyen's glycosylation method with digitoxigenin. ....	140
Figure 3.28. Nguyen's proposed mechanism for cationic Pd(II)-catalyzed stereoselective formation of α-glycosides <sup>21</sup> .....	141
Figure 3.29. Successful glycosylation and deprotection towards rhodexin B. ....	142
Figure 3.30. <sup>1</sup> H NMR spectrum corresponding to oleandrigenin (3-2). ....	166
Figure 3.31. <sup>13</sup> C NMR spectrum corresponding to oleandrigenin (3-2). ....	167
Figure 3.32. <sup>1</sup> H NMR spectrum corresponding to rhodexin B (3-3). ....	179
Figure 3.33. <sup>13</sup> C NMR spectrum corresponding to rhodexin B (3-3). ....	180
Figure 4.1. Classic mechanism for glycoside hydrolysis.....	186
Figure 4.2. Bols <sup>8</sup> findings for understanding substituent effects for glycoside hydrolysis reactivity. .....	187

Figure 4.3. Previous preliminary results for mimicking glycosylases. (by Jeongyho Lee and Jeremy O'Brien). .....	189
Figure 4.4. Proposal for potential anomeric enrichment of glycosides in organic solvents .....	190
Figure 4.5. Observed NMR intermediates for glycosyl donors in superacid medium. ....	191
Figure 4.6. Synthesis of glucose pseudo-disaccharide model 4-19. ....	193
Figure 4.7. Synthesis of mannose pseudo-disaccharide model.....	193
Figure 4.8. Synthesis of galactose pseudo-disaccharide model.....	194
Figure 4.9. Proposal for poly-saccharide site recognition with chiral Bronsted acid catalysts. .	199

## List of Schemes

Scheme 1.1. Representative examples of butenolide installation. (A. Inoue <sup>22</sup> , B. Baran <sup>23</sup> , C. Nagorny <sup>24</sup> ).....	10
Scheme 1.2. Sondheimer's construction of the $\alpha$ -pyrone ring involving the Vilsmeier–Haack reaction.....	12
Scheme 1.3. Yoshii et. al. procedure for making 3 $\beta$ -OAc-resibufagenin. <sup>26</sup> .....	13
Scheme 1.4. Welzel et. al. procedure for making 3 $\beta$ -OAc-bufalin. <sup>27</sup> .....	15
Scheme 1.5. Bauer's procedure for making 3 $\beta$ -hydroxy-5 $\beta$ ,14 $\alpha$ -bufa-20,22-dienolide from deoxycorticosterone. ....	16
Scheme 1.6. Kabat's procedure for making 14-deoxybufadienolide derivatives. ....	17
Scheme 1.7. Meinwald's procedure for direct 2-pyrone installation.....	18
Scheme 2.1. Synthetic route for developing model steroid core .....	27
Scheme 2.2. Synthesis of pyrone cross-coupling partner. ....	28
Scheme 2.3. Synthesis of 5 $\alpha$ -bufadienolide.....	28
Scheme 2.4. Installation of C14 $\beta$ -alcohol TMS protecting group.....	29
Scheme 2.5. Results of Wilkinson's catalyst with model bufadienolide .....	29
Scheme 2.6. Synthesis of protected bufalin .....	30
Scheme 2.7. Stille coupling of 2-pyrone containing model substrates. ....	32
Scheme 2.8. Optimized hydrogenation procedure on model substrate 2-20, and proposed side products.....	34

Scheme 2.9. Optimized hydrogenation conditions with <i>trans</i> -androsterone model and proposed side products. ....	35
Scheme 2.10. Attempted formation of silyl enol ether on model substrates 2-20A and 2-21.....	38
Scheme 2-11 Synthesis of 2-76 (by Dr. Khatri). ....	57

## List of Abbreviations

$\alpha$ : alpha

Acac: acetylacetone

Ar: aryl

$\beta$ : beta

Bu: butyl

Bz: benzoyl

c: cyclo

C: Celsius

cat: catalyst

Cp: cyclopentadienyl

CPME: *cyclo*-pentyl methyl ether

Cu: copper

DCM: dichloromethane

DDQ: 2,3-dichloro-5,6-dicyano-1,4-benzoquinone

DG: directing group

DME: dimethoxyethane



DMF: dimethylformamide

DMSO: dimethyl sulfoxide

dr: diastereomeric ratio

er: enantiomeric ratio

Et: ethyl

EtOAc: ethyl acetate

Equiv.: equivalent

GC-FID: gas chromatography-flame ionization detector

GCMS: gas chromatography-mass spectrometry

Fe: iron

h: hour

HRMS: high resolution mass spectroscopy

*hν*: ultraviolet light

i: iso

i-Bu: isobutyl

i-Pr: isopropyl

L: ligand

LG: leaving group

$\mu$ : micro

MBG: marinobufagenin

M: molarity, transition metal

Me: methyl

mg: milligram

n-Bu: butyl

n-Hex: hexyl

n-Pent: pentyl

n-Pr: propyl

NMR: nuclear magnetic resonance

Pd: palladium

*p*-TsOH: *para*-toluene sulfonic acid

PG: protecting group

Ph: phenyl

Piv: pivalate

Pr: propyl

R: generic group

r.t.: room temperature

SAR: structure activity relationship

t: tertiary

t-Bu: *tert*-butyl

TBS: *tert*-butyldimethyl silyl

TBDPS: *tert*-butyldiphenylsilyl

TES: triethylsilyl

Tf: triflate

THF: tetrahydrofuran

TIPS: triisopropylsilyl

TMS: trimethylsilyl

X: halogen, leaving group, generic group

## Abstract

Organic chemistry is an ever-evolving field, which produces constant development of new synthetic methods featuring novel technologies. This is critical in driving innovation, especially in total synthesis. Total synthesis is an ever-present topic, with nature still providing new discoveries of natural compounds that can unlock newly discovered therapeutic understandings. However, the natural world can often provide only limited quantities of materials for biological explorations. With most isolation techniques requiring extraction of once living material, natural sources are finite. Total synthesis methods allow scientists the opportunity to preserve natural life by producing natural products with commercially abundant materials. Total synthesis also takes inspiration from the literature to modify and improve upon existing methods for making targets more efficiently. Nature makes specific products for a variety of reasons that are necessary for survival, while boasting the means to achieve regio- and stereoselectively. Described herein is the development of novel strategies for building late-stage, poly-functionalized steroid cores, containing sensitive substituents, including bufadienolide core-scaffolds, thereby allowing the development of more efficient methods to synthesize steroids in general. The first chapter will focus on introducing the relevance of bufadienolides by discussing their unique structural motif and describing their endogenous production in human tissues and the regulatory processes they engage in. This will continue to overview sources of bufadienolides found in nature and provide a brief summary of the progression of synthetic routes that were developed leading to the present-day literature. From there, chapter 2 will describe methods regarding our investigations into developing a strategy for synthesizing bufadienolides via selective hydrogenation. This will

advance toward a brief discussion of subsequent oxidation studies of the resulting reduced lactone through applying recently discovered literature methods and Saegusa and Wacker-type oxidations developed in our research group. Chapter 2 will also discuss an investigation on improving known methods of synthesizing pyrone moieties via a photooxidation of carbonyl furans, toward a more stream-lined method from the reported literature. This chapter will also offer some additional strategies and future directions for optimization studies. Chapter 3 will discuss the synthesis and novel methods utilized to generate the second, and most efficient synthesis to date, of oleandrigenin through a House-Meinwald rearrangement strategy. To complete the synthesis of oleandrigenin, a similar photooxidation procedure is used to transform a furan into a butenolide moiety from optimizations based on literature precedent. The synthesis of oleandrigenin provides the foundation for developing a novel glycosylation protocol towards the first synthetic route of rhodexin B (*vida infra*). The glycosylation method described herein is the first reported strategy of glycosylating in the presence of sensitive C-16 oxidized and protected functionalities, followed by selective orthogonal deprotection. Chapter 4 will describe current strategies and methods for developing site-selective glycoside cleavage under mild reaction conditions. The preliminary studies and optimizations describe how using catalytic amounts of superacid reagents can be used in anhydrous organic solvent, can induce selective anomeric cleavage of a mixture of pseudo-disaccharides. This chapter concludes by discussing future directions of using chiral Bronsted super acidic catalysts to induce selective glycoside cleavage via inherent site recognition of glycoside linkages. Finally, chapter 5 will provide a brief overview of the present gaps in the field of the synthesis of bufadienolides and how this dissertation describes efforts to close these gaps. This concluding chapter will also provide future objectives that are currently being investigated.

## Chapter 1

### Introduction

#### 1.1 Introduction to relevance of bufadienolides

Cardiac glycosides, and their steroidal aglycones are responsible for increasing the contractile force of the heart by inhibiting the enzyme  $\text{Na}^+$ ,  $\text{K}^+$ -ATPase.<sup>1</sup> This enzyme is the main receptor for these cardiotoxic steroids, and its function is the transfer of intercellular  $\text{Na}^+$  in exchange for extracellular  $\text{K}^+$ . This in turn induces a positive inotropic effect and is a treatment for congestive heart failure, cancer, and Alzheimer's disease.<sup>1</sup> The principle molecular mechanism of pharmacological action of cardiotoxic steroids and their derivatives involves the induction of a local increase of  $\text{Na}^+$  concentration due to the inhibition of a carrier enzyme:  $\text{Na}^+/\text{K}^+$ -ATPase (EC 3.6.1.37; the sodium pump), commonly described as a "digitalis-like" effect.<sup>4,5</sup>  $\text{Na}^+/\text{K}^+$ -ATPase is responsible for maintaining of electrochemical gradient of  $\text{Na}^+$  and  $\text{K}^+$  through the cell membrane.<sup>2</sup> Keeping a low  $\text{Na}^+$  and a high  $\text{K}^+$  intracellular concentration, can cause a change in membrane potential, and this is crucial for activation of nerves and muscle cells (including cardiomyocytes), as well as, for the secondary active transport.<sup>2</sup> Bufadienolides also can alter myocardial ion balance resulting in an increase of intracellular  $\text{Ca}^{2+}$  concentration via a backward running of the  $\text{Na}^+/\text{Ca}^{2+}$  exchanger, and consequently, leading to stronger contractions of cardiac and arterial myocytes. The cardiotoxic steroids can affect membrane tissues via  $\alpha$ -isoforms.<sup>3</sup> The  $\alpha_1$ -isoform is predominant in the kidneys and liver and is often upregulated in cancerous cells. The  $\alpha_2$ -isoform is present mostly in the brain, heart muscle, and skeletal muscle. The  $\alpha_3$ -isoform is

present in the central nervous system, cardiac muscle, skeletal muscle, and placental tissue. Finally, the  $\alpha_4$ -isoform is found primarily active in spermatozoa cells<sup>3</sup> It has been discovered that suppression of  $\alpha_4$  activity reduces sperm motility, depolarizes the membrane potential, and increases intracellular sodium<sup>3</sup>, whereas overexpression of  $\alpha_4$  increases motility<sup>3</sup> These various  $\alpha$ -subunit isoforms are expressed differently in different tissues<sup>2</sup> and cardiotonic steroids can access them due to their unique physical properties. The cardiotonic steroids possess a ‘U’-shaped, four fused-ring system that is oriented in an A/B-cis, B/C-trans, C/D-cis fashion to build the steroid core (Figure 1.1). The top of the steroid core is commonly referred to as the ‘ $\beta$ -face’ (beta-face) and the bottom side of the steroid is commonly referred to as the ‘ $\alpha$ -face’ (alpha-face). The steroid core can contain various functionalities throughout the 6,6,6,5-tetracyclic core.

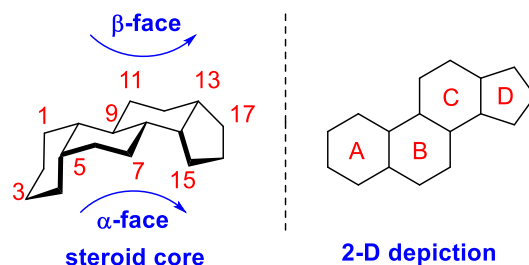


**Figure 1.1.** Steroid core ‘U’-shaped fused ring system.

Most clinical attention is directed to the cardiotonic glycosides owing to their availability and well-studied therapeutic use. For example, digitoxin **1-4** and digoxin **1-5** are the two most widely used digitalis inotropes that patients are receiving in the United States for congestive heart failure (Figure 1.2).<sup>4</sup>

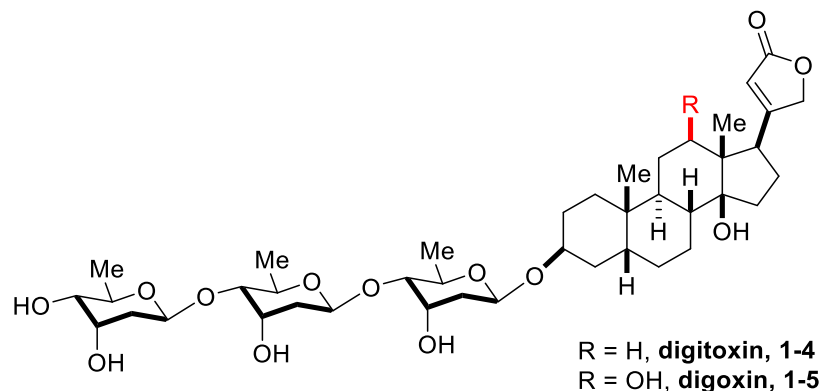


**Figure 1.2.** Most used cardio inotropes in the United States, digitoxin **1-4** and digoxin **1-5**.

Bufadienolides and cardenolides are both classified as cardiotoxic steroids. The main difference between the two classes of cardiotoxic steroids is the unsaturated heterocyclic lactone substituent at C-17 (Figure 1.3). Bufadienolide (**1-6**) possesses a pentadienolide (i.e. alpha pyrone, Figure 1.3) while a butenolide for the cardenolides (i.e. ouabagenin **1-7**, Figure 1.3), respectively.

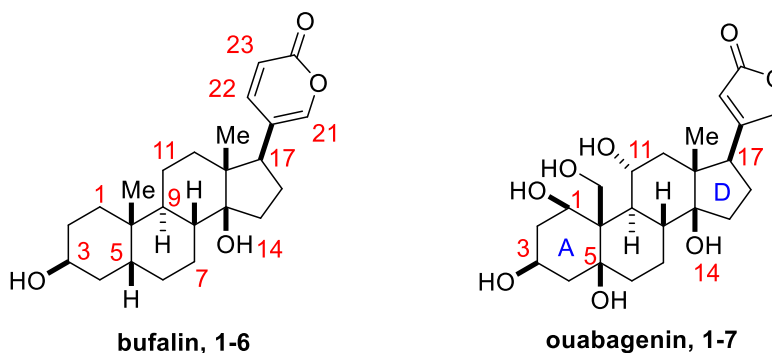


**Figure 1.3.** Representative examples of bufadienolide and cardenolide, respectively.

The bufadienolides are an important group of steroids containing the 2-pyrone functionality connected at the C-17 position of the steroid framework. Bufalin **1-6** is a very potent  $\text{Na}^+/\text{K}^+$ -ATPase inhibitor.<sup>4</sup> Some of the first bufadienolide derivatives were discovered endogenously in mammals, including human brain tissue.<sup>4</sup>

Bufadienolides were first detected in human bile and plasma, with marinobufagenin (MBG) (*cf.* Figure 1.4) being as a primary compound. MBG was first discovered from venom extracted



from certain Asiatic toads species, and is a main component in the traditional Chan'Su treatment.<sup>5</sup> It was discovered that enhanced production of MBG had been demonstrated in humans with volume expansion<sup>5</sup> and in patients with preeclampsia<sup>4</sup>, hypertension, primary aldosteronism<sup>5</sup>, and end-stage renal disease,<sup>5</sup> and at concentrations comparable with in vivo plasma levels of this hormone, MBG produces vasoconstriction in isolated human pulmonary and mesenteric arteries<sup>5</sup>

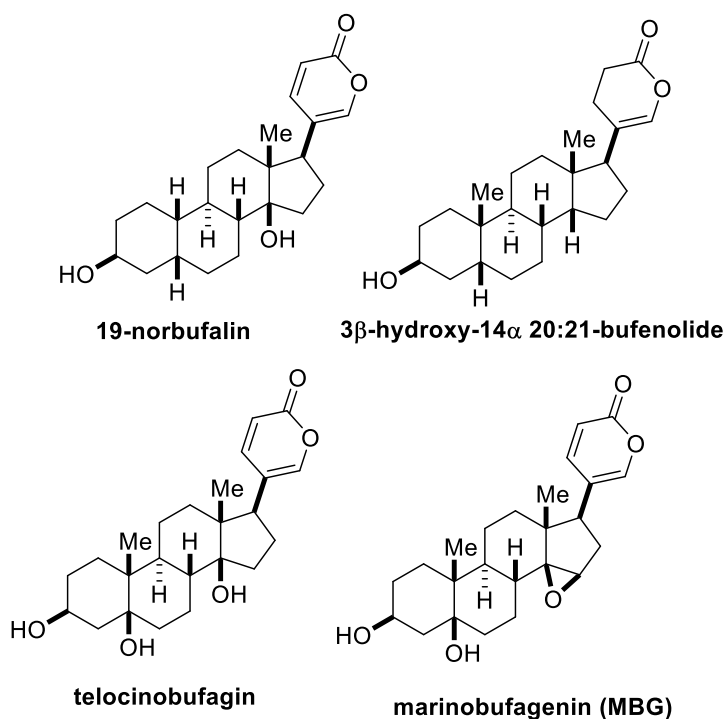


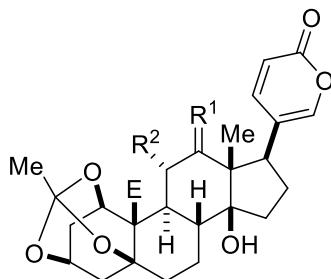
**Figure 1.4.** Representative examples of endogenously present bufadienolides in human tissues.

Bufadienolides can also be found in several families of plants and animals with diverse biological activity. Floral sources include the families *Crassulaceae*, *Hyacinthaceae*, *Iridaceae*, *Melanthaceae*, *Ranunculaceae* and *Santalaceae*. The species *Cotyledon* and *Tylecodon* from the family *Crassulaceae* can cause the symptoms of cardiac poisoning in animals particularly to livestock, where alternative forage is scarce, with the main active ingredient being bufadienolides<sup>6</sup>. Bufadienolide producing plants can also create problems in agriculture<sup>7</sup> due to their toxicity to livestock who consume them. Kellerman and co-workers<sup>8</sup> reported that bufadienolides, and their

corresponding glycosides, represent the most common cause of mortality, due to plant poisoning among cattle in South Africa. These naturally occurring cardiotonic steroids were studied and were found to possess antineoplastic and cell growth inhibitory properties<sup>9</sup> as well as, effects on the central nervous system<sup>10</sup>, which is of great pharmacological importance.<sup>2</sup> The animal sources of bufadienolides include the *Photinus* (fireflies), *Rhabdophis* (snake) and *Bufoidea* or toad. Over eighty bufadienolides have been isolated from the toad sources. The Asiatic toad skin extract Ch'an Su, was found to significantly inhibit P-388 lymphocytic leukemia.<sup>11</sup> Ch'an su is traditionally ingested orally or applied topically to reduce swelling, and alleviate pain. It is said to "expel summer heat and dampness, open the orifices, and awaken the spirit". Chan su dosage in pills and powders is usually between 10-30 mg<sup>12</sup> These dosages are not regulated, and the strength can range to being almost a placebo effect, and other times can be a lethal dosage level. Even with these risk factors involved, there is still widespread use of these herbal medicines.<sup>12</sup>

## **1.2 Selected examples of plant sources of bufadienolides**

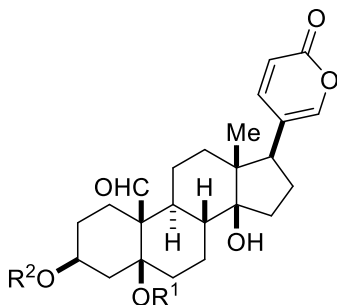
Certain species of the *Cotyledon*, *Tylecodon* and *Kalanchoe*<sup>2</sup> can cause acute and subacute intoxication in sheep and cattle, which are a significant economic resource in South Africa and Australia. *Kalanchoe* species are used in traditional medicine for the treatment of several ailments, such as various infections and inflammation, and extracts of *Kalanchoe* plants have shown to possess immunosuppressive effects.<sup>13</sup> Along with inducing the typical symptoms of cardiac poisoning, small, repeated doses of the bufadienolide extracts also cause cotyledonosis,<sup>9</sup> an intoxicating affect towards the nervous and muscular systems of animals.<sup>14</sup> Daigremontianin **1-8**, bersaldegenin 1,3,5-orthoacetate **1-9** (Figure 1.5), are examples of isolated bufadienolides that not only exhibited the expected strong positive inotropic effect, but also performed a sedative effect with small doses, with larger doses having more harmful effects, like paralysis.



**1-8**  $R^1 = O$ ;  $R^2 = OH$ ,  $E = CHO$   
**1-9**  $R^1 = H$ ,  $R^2 = H$ ,  $E = CHO$

**Figure 1.5.** Daigremontianin **1-8**, bersaldegennin 1,3,5- orthoacetate **1-9**.

The bufadienolides that induce toxic effects from *Kalanchoe lanceolata*, have been attributed to derivatives of hellebrigenin **1-10** (Figure 1.6) as well as similar structural isoforms assigned as 3-*O*-acetyl-hellebrigenin, the rhamnoic acid ester of 5-*O*-acetylhellebrigenin (lanceotoxin A, **1-11**) and 5-*O*-acetyl-3-*O*- $\alpha$ -L-rhamnosylhellebrigenin (lanceotoxin B, **1-12**).<sup>15</sup>



**1-10**  $R^1 = R^2 = H$   
**1-11**  $R^1 = Ac$ ,  $R^2 =$

**1-12**  $R^1 = Ac$ ,  $R^2 =$

**Figure 1.6.** Hellebrigenin **1-10**, lanceotoxin A, **1-11** and lanceotoxin B, **1-12**.

### 1.3 Select examples of animal sources of bufadienolides

Bufadienolides are also prevalent in animal sources and are typically stored in specialized glands or organs that are isolated from the rest of the somatic cells of the organism. Bufadienolides and the more polar conjugates, the bufotoxins, are present in the bodies of toads, specifically the skin, of the genus *Bufo*. The toad bufadienolides occur not only in the unconjugated form, but several C-3 conjugates are also known sulfates, dicarboxylic esters and amino acid - dicarboxylic acid esters. The arginine– suberoyl ester, bufotoxin **1-13** (Figure 1.7), is one such example.<sup>1</sup>

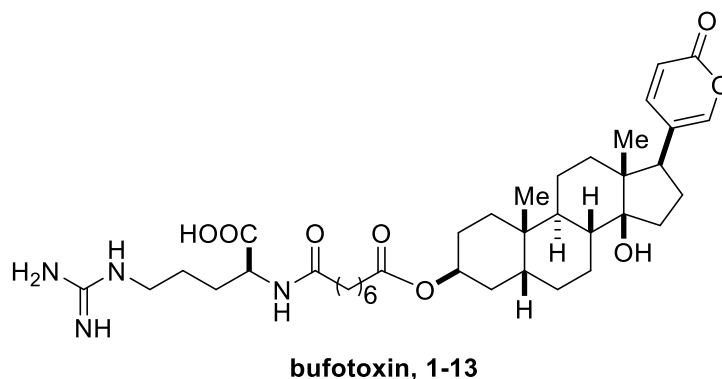


**Figure 1.7.** Representative structure of bufotoxin.

There are several variations of these compounds where the suberoyl ester can be substituted by succinyl, glutaryl, adipyl, pimelyl residues, or amino acids. Preliminary evidence suggests that by virtue of their potency as inhibitors of Na<sup>+</sup>,K<sup>+</sup>-ATPase, bufadienolides and their derivatives may be important in sodium homeostasis in toads that migrate between fresh and salt water environments.<sup>16</sup>

One of the most studied extracts that contain a concoction of bufadienolides is the Chinese traditional drug, Ch'an Su which is prepared from skin secretions of *Bufo gargarizans*, or *Bufo melano* toads.<sup>17</sup> The most notable functionality of this extract is that the pyrone moiety contains an epoxy group on the C4/C5 of the 2-pyrone system, or the C-14/15 position on the steroid core

is epoxidized (Figure 1.8, labelled with red text, i.e. **1-14**). Resibufogenin **1-14** is also reported to have antiproliferative effects against cancer cells, inducing cell cycle arrest by suppressing the expression of cyclin D1, which is an important regulator of cell cycle progression and can function as a transcription co-regulator. Overexpression of cyclin D1 has been linked to the development of cancer.<sup>18</sup>

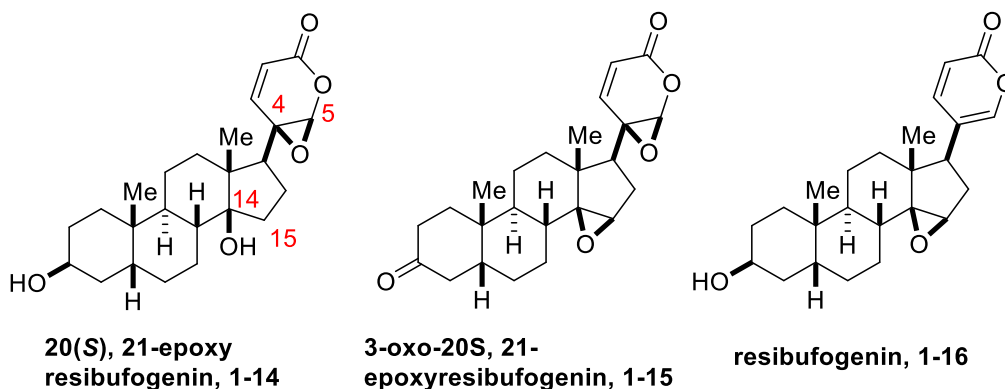
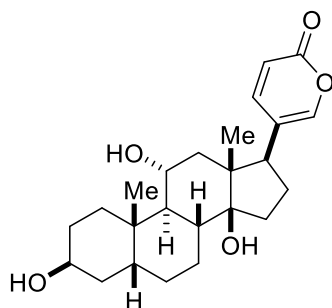


**Figure 1.8.** Epoxybufadienolides extracted from Chan' Su toad venom.

The Asian snake *Rhabdophis tigrinus* has specialized defensive glands located on its neck, which contain steroidal toxins of the bufadienolide class.<sup>19</sup> A recent investigation reported the presence of seventeen bufadienolides in the nuchal gland fluid of *R. tigrinus*. Further observations have confirmed that the defensive steroids are not synthesized by *R. tigrinus* itself. Instead, the snake is dependent on a diet of toads from which it can sequester these compounds.<sup>20</sup>



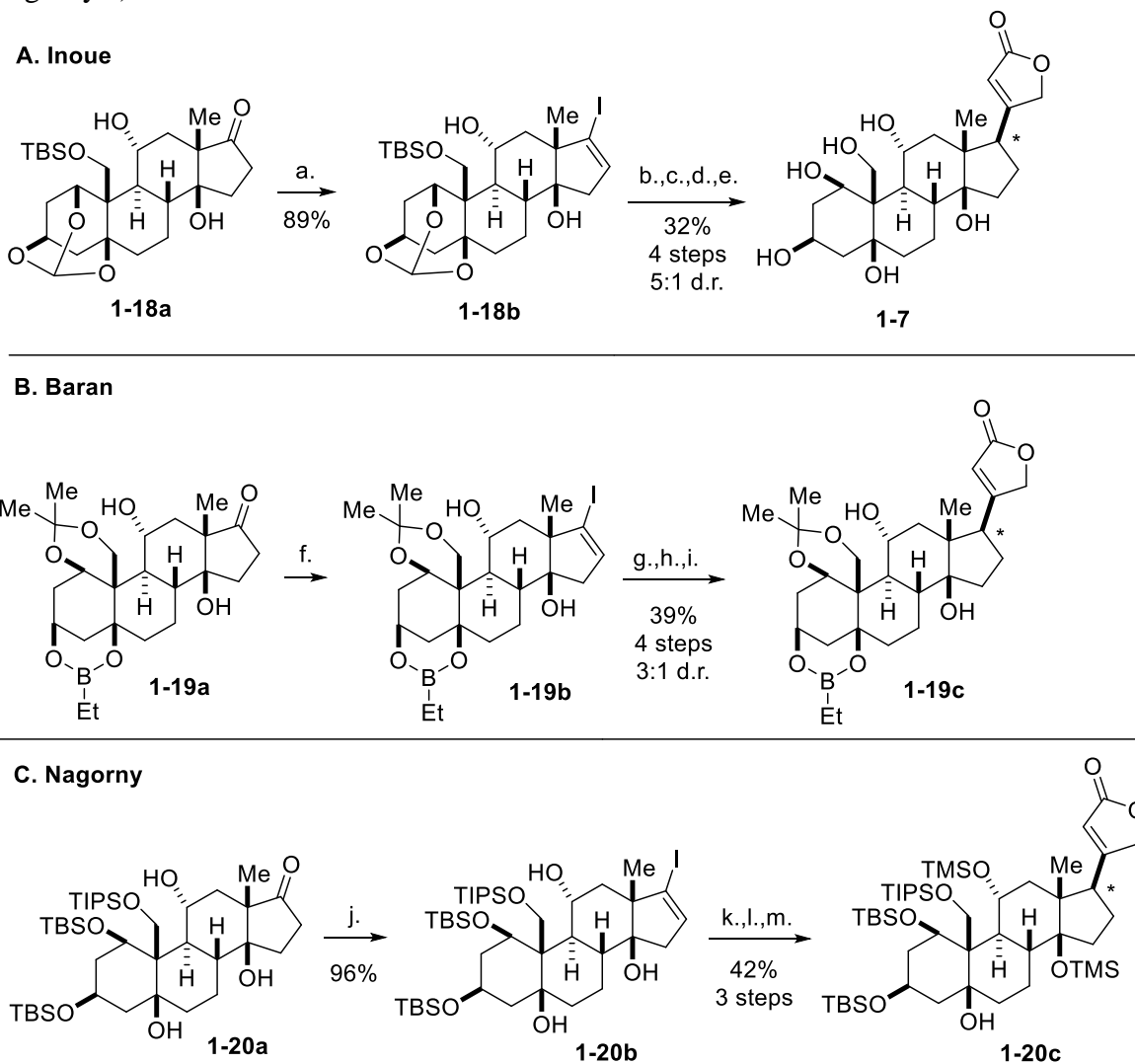
**gamabufotalin, 1-17**

**Figure 1.9.** Representative example from snake venom in the nuchal glands of *Rhabdophis tigrinus*.

#### 1.4 Selected examples of the *de novo* synthesis of bufadienolides

The chief challenge encountered in the synthesis of bufadienolides, as discussed by Sondheimer<sup>21</sup> in 1965, was installing both an  $\alpha$ -pyrone ring and a labile 14-hydroxyl moiety (or epoxide) on the D-ring, while keeping the thermodynamically stable configuration of the *cis*-C/D ring junction (Figure 1.1). In contrast to the cardenolides, which have a multitude of established preparations and can be prepared efficiently (Scheme 1.1).

**Scheme 1.1.** Representative examples of butenolide installation. (A. Inoue<sup>22</sup>, B. Baran<sup>23</sup>, C. Nagorny<sup>24</sup>).



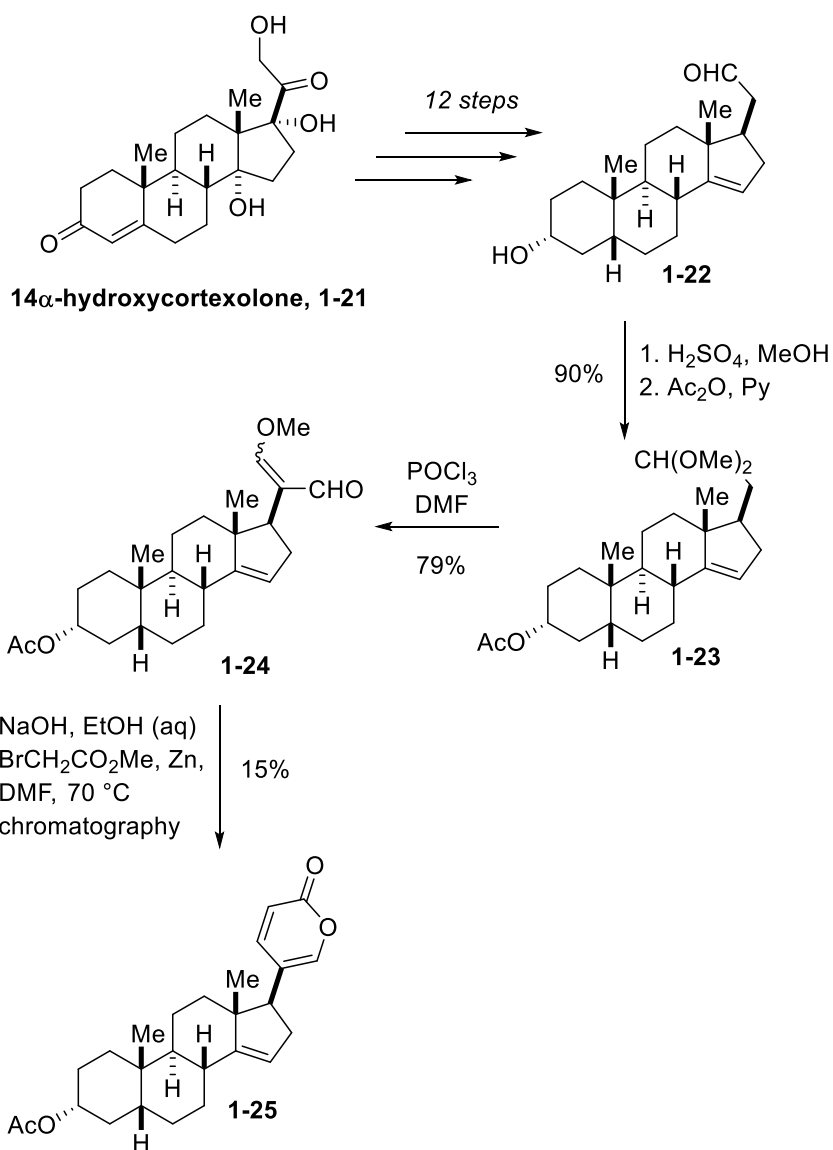
**A.** a.)  $(\text{H}_2\text{N})_2 \cdot \text{H}_2\text{O}$ ,  $\text{Et}_3\text{N}$ ,  $\text{EtOH}$ ,  $50\text{ }^\circ\text{C}$ , then,  $\text{I}_2$ ,  $\text{Et}_3\text{N}$ ,  $\text{THF}$ ,  $\text{rt}$ ; b.) 4-(tributylstannyl)-2,5-dihydrofuran-2-one,  $\text{Pd}(\text{PPh}_3)_4$ ,  $\text{LiCl}$ ,  $\text{CuCl}$ ,  $\text{DMSO}$ ,  $60\text{ }^\circ\text{C}$ .; c.)  $\text{TMSOTf}$ , 2,6-lutidine,  $\text{CH}_2\text{Cl}_2$ ,  $\text{SiO}_2$ .; d.)  $\text{H}_2$ ,  $\text{Pd/C}$ ,  $\text{EtOAc}$ ; e.) 3M aqueous  $\text{HCl}$ ,  $\text{MeOH}$ .; **B.** f.)  $\text{N}_2\text{H}_4$ ,  $\text{Et}_3\text{N}$ , 4:1  $\text{DCM}:\text{EtOH}$ ,  $50\text{ }^\circ\text{C}$ ., then,  $\text{I}_2$ ,  $\text{Et}_3\text{N}$ ,  $\text{THF}$ ,  $\text{rt}$ ; g.) 4-(tributylstannyl)-2,5-dihydrofuran-2-one,  $[\text{Ph}_2\text{PO}_2][\text{NBu}_4]$ ,  $\text{Pd}(\text{PPh}_3)_4$ ,  $\text{CuTC}$ ,  $\text{DMF}$ ,  $23\text{ }^\circ\text{C}$ ; h.)  $\text{CoCl}_2 \cdot 6\text{H}_2\text{O}$ ,  $\text{NaBH}_4$ ,  $\text{EtOH}$ , 0 to  $23\text{ }^\circ\text{C}$ ; i.) 2-*t*-butyl-1,1,3,3-tetramethylguanidine (BTMG),  $\text{C}_6\text{H}_6$ ,  $100\text{ }^\circ\text{C}$ .; **C.** j.)  $\text{N}_2\text{H}_4$ ,  $\text{Et}_3\text{N}$ ,  $\text{EtOH}$ ,  $50\text{ }^\circ\text{C}$ , then,  $\text{I}_2$ ,  $\text{Et}_3\text{N}$ ,  $\text{THF}$ ,  $\text{rt}$ ; k.) 4-(tributylstannyl)-2,5-dihydrofuran-2-one,  $\text{Pd}(\text{PPh}_3)_4$ ,  $\text{LiCl}$ ,  $\text{CuCl}$ ,  $\text{DMSO}$ ,  $50\text{ }^\circ\text{C}$ .; l.)  $\text{TMSCl}$ , imidazole,  $\text{DMF}$ ,  $\text{r.t.}$ ; m.)  $\text{H}_2$ ,  $\text{Pd/C}$ ,  $\text{EtOAc}$ ,  $\text{r.t.}$

The installation of an  $\alpha$ -pyrone moiety throughout previous literature examples occurred before introduction of  $\beta\text{C}-14$  oxidation. This is due to the harsh conditions typically required to promote the pyrone cyclization to occur, which typically requires strong acid with high

temperatures.<sup>1</sup> This subsection aims to highlight a few selected methods of advancement from the literature.

In 1969, Sondheimer<sup>21,25</sup> laid the foundational investigations to make synthetic samples of bufalin and resibufogenin targeting the  $\alpha$ -pyrone formation before C-14 hydroxyl installation. 14 $\alpha$ -Hydroxycortexolone **1-21** (Scheme 1.2), was transformed into 14-ene-aldehyde **1-22** which was then converted to an acetal **1-23**. Acetal **1-23** was subjected to the Vilsmeier–Haack reaction to provide compound **1-24**. Chromatography yielded the *Z* isomer of product **1-24** was obtained in 60% yield (*E*-isomer in 19% yield). Hydrolysis of the *Z*-isomer, **1-24**, led to a mixture of enolized dialdehydes which was subjected to the Reformatsky reaction by heating with methyl bromoacetate and zinc in DMF at 70 °C. The required 2-pyrone derivative **1-25** was isolated in a 15% yield.

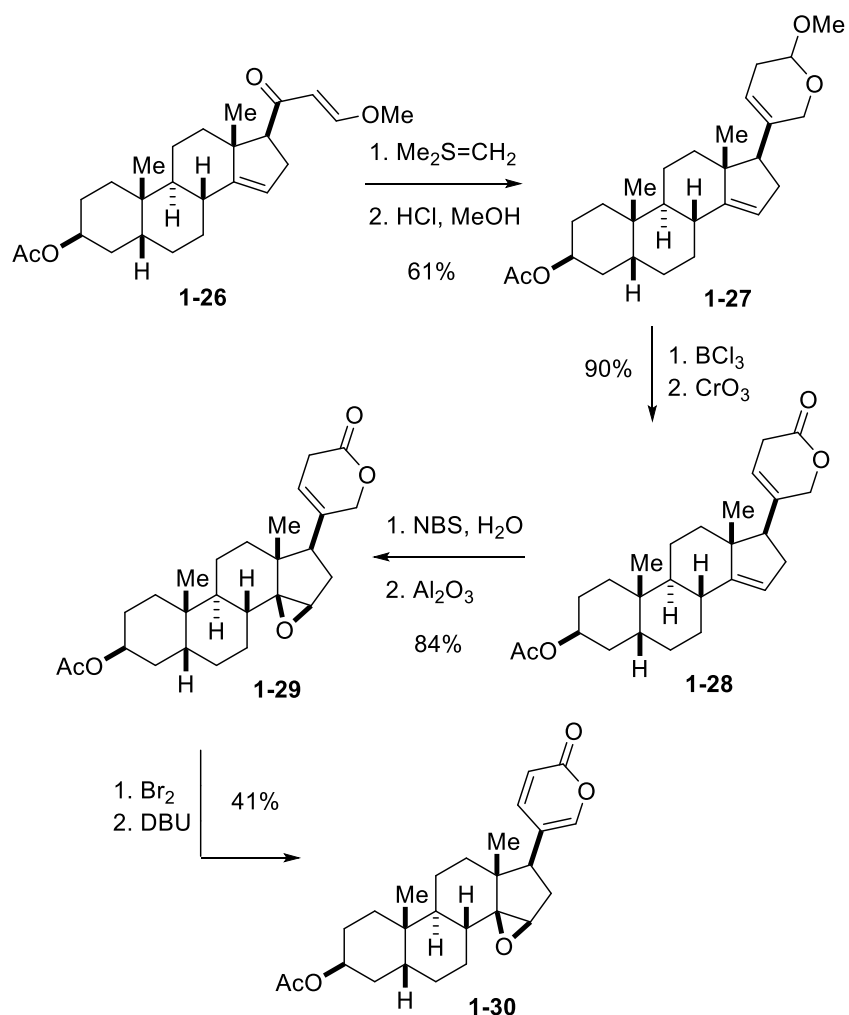




**Scheme 1.2.** Sondheimer's construction of the  $\alpha$ -pyrone ring involving the Vilsmeier–Haack reaction.

Yoshii *et al.*<sup>26</sup> used 5 $\beta$ -pregn-14-en-3 $\beta$ -ol-20-one acetate as the starting material for their attempted synthesis of resibufagin (Scheme 1.3). Acid-catalyzed condensation of the starting material with trimethyl orthoformate, and subsequent treatment of the product with acidic methanol, yielded the  $\beta$ -methoxyvinyl ketone **1-26**. The product was then reacted with dimethylsulfonium methylide, followed by hydrolysis and oxidation of **1-27** yielded the dehydrolactone **1-28**. The more reactive C14,15-double bond was transformed into the epoxide

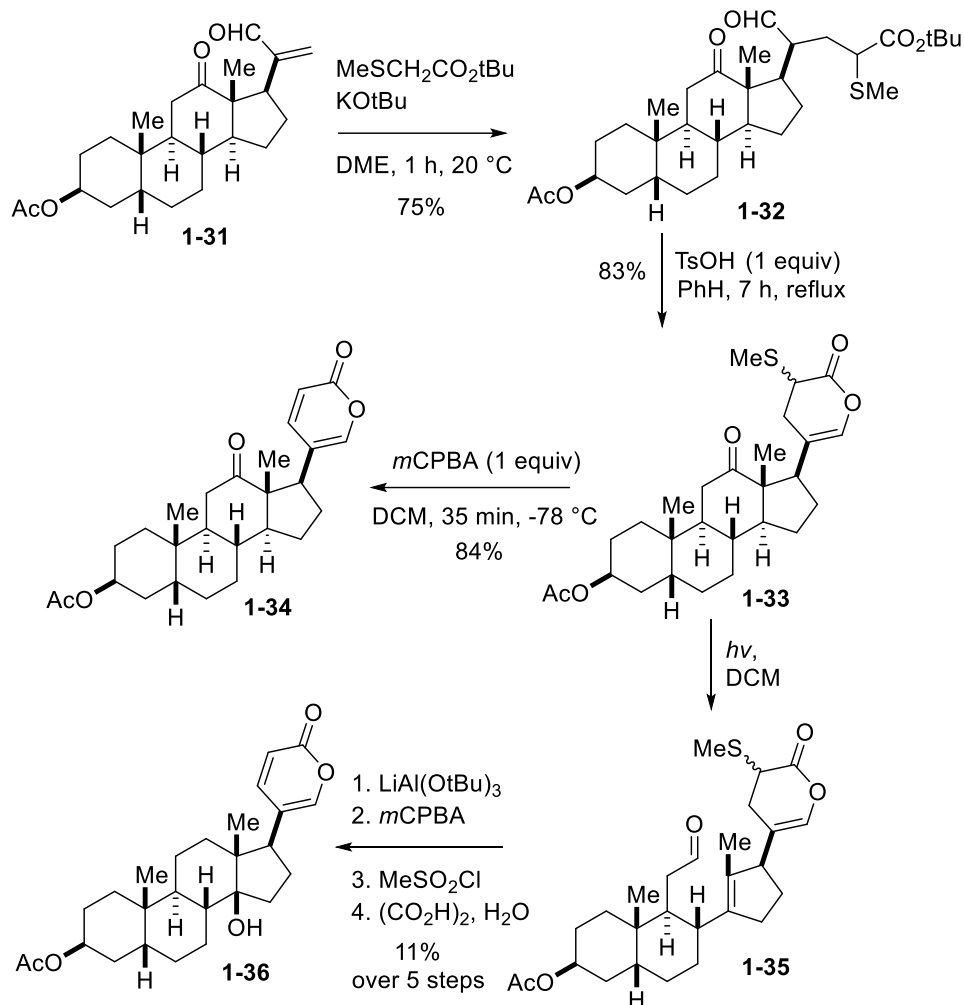
via a bromohydrin intermediate to form **1-29**. Reaction of the C20,22-enolide with bromine followed by treatment with DBU, yielded 3-*O*-acetylresibufagin **1-30**. The synthesis was stopped at this point since the other reactions of reductive cleavage of the epoxide ring were established previously to forward synthesis.<sup>26</sup>



**Scheme 1.3.** Yoshii et. al. procedure for making 3 $\beta$ -OAc-resibufagenin.<sup>26</sup>

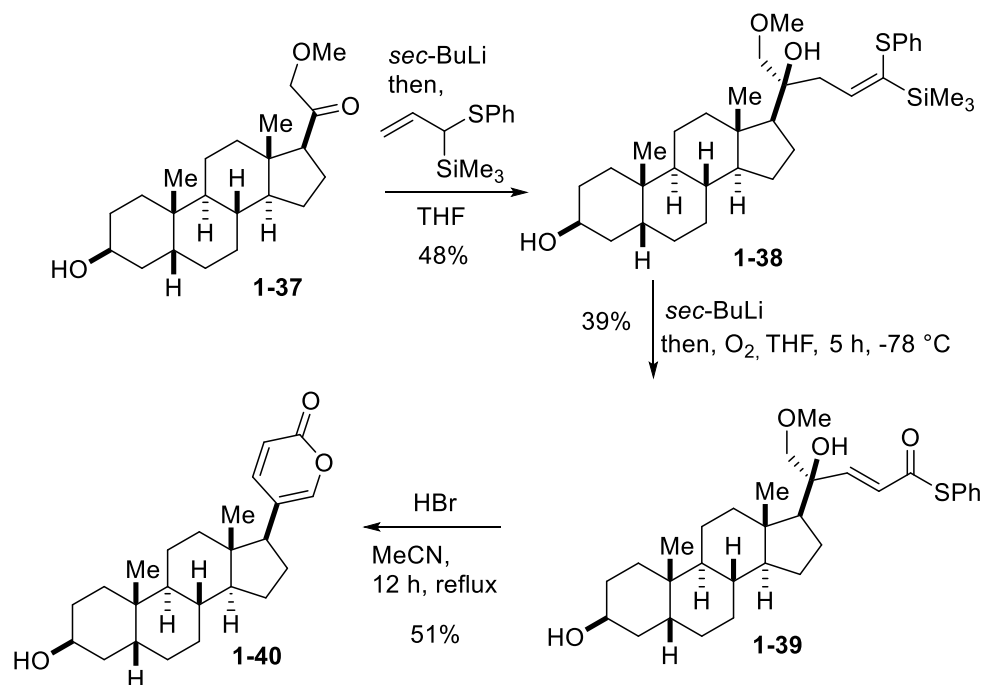
Welzel and co-workers<sup>27</sup> used deoxycholic acid as starting material for their strategy for the syntheses of bufadienolides and cardenolides. In their manuscript, they reported synthetic steps starting from **1-31**, which was produced from deoxycholic acid in 4 steps.<sup>27</sup> **1-31** was then reacted with a stabilized anion prepared from tert-butyl phenylsulfanylacetate to give **1-32** as a mixture of

four stereoisomers, in 75% yield. **1-32** was then refluxed in a benzene solution of **5b** (mixture of stereoisomers) in the presence of *p*-toluenesulfonic acid (1 equiv.) to give **1-33** as a 1:1 mixture of isomers in 83% yield. The isomeric mixture of **1-33** were oxidized with *m*-chloroperbenzoic acid then worked up in a CH<sub>2</sub>Cl<sub>2</sub> solution and allowed to stand at room temperature for 36 h to provide **1-34** in 84% yield. Their photorearrangement process of **1-33** gave them some trouble but, they were able to apply their best procedure through irradiation until about 50% of **1-33** was consumed, followed by immediate reduction with LiAlH(O*t*Bu)<sub>3</sub>, which they also found does not react with **1-33** under the experimental conditions. Reduction of the aldehyde **1-35**, followed by, oxidation, mesylation, and then solvolytic ring closure yielded the 14β-hydroxy steroid **1-36** in 11% yield over 5 steps (Scheme 1.4).



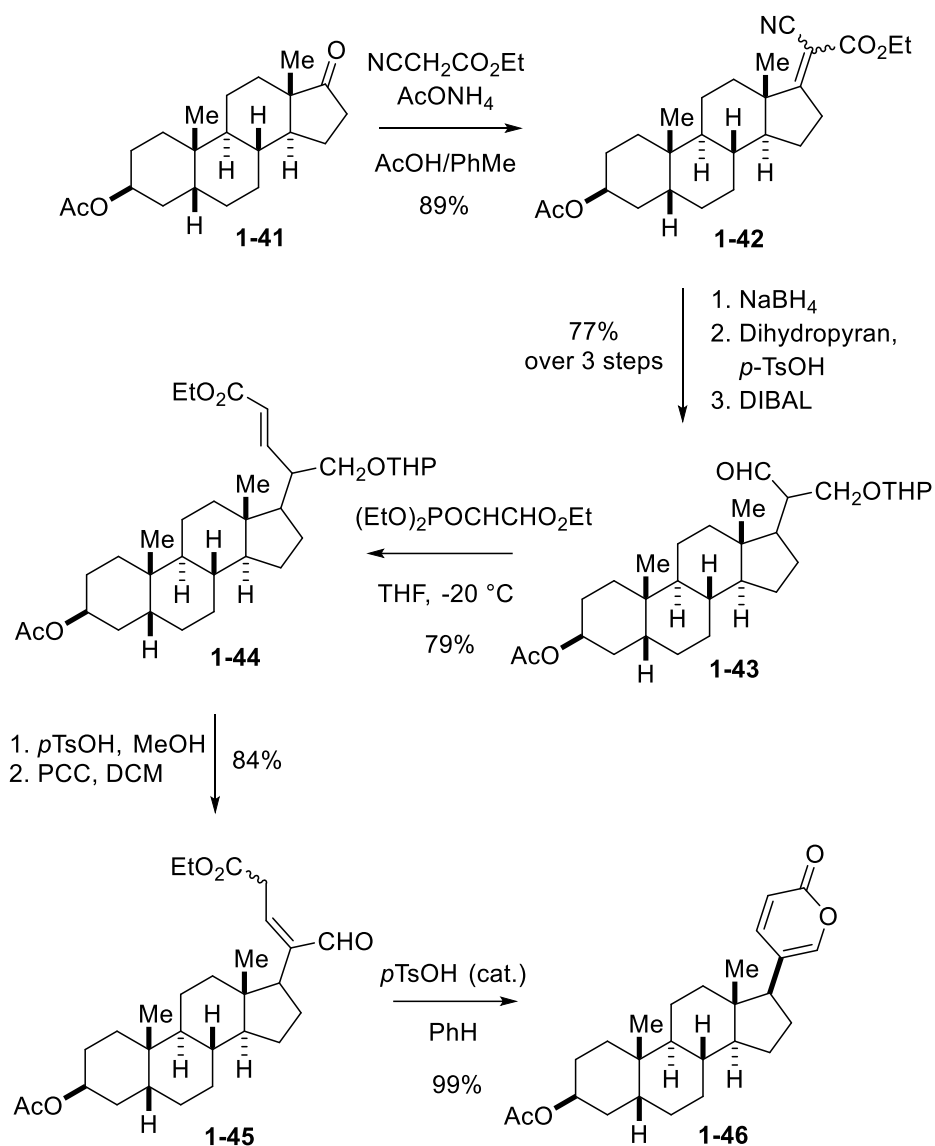
**Scheme 1.4.** Welzel et. al. procedure for making 3 $\beta$ -OAc-bufalin.<sup>27</sup>

Other preparations for 14-deoxybufadienolides have also been published to generate pyrone moieties without concern of the  $\beta$ 14-hydroxyl being eliminated or installed as a late-stage transformation. Bauer et al.<sup>28</sup>, employed 11-deoxycorticosterone as their starting material, and in 3 steps, were able to obtain intermediate **1-37** (cf. Scheme 1.5) in 73% overall yield. The next step was the synthesis of a  $\gamma$ -hydroxy- $\alpha,\beta$ -unsaturated thiol ester **1-39** by reaction of the 1-phenylthio-1-trimethylsilylprop-2-enyl anion with compound **1-37**, followed by oxidation of intermediate **1-38** to make **1-39**. The product was then dissolved in acetonitrile and refluxed in the presence of HBr to complete the cyclization affording **1-40** (Scheme 1.5).



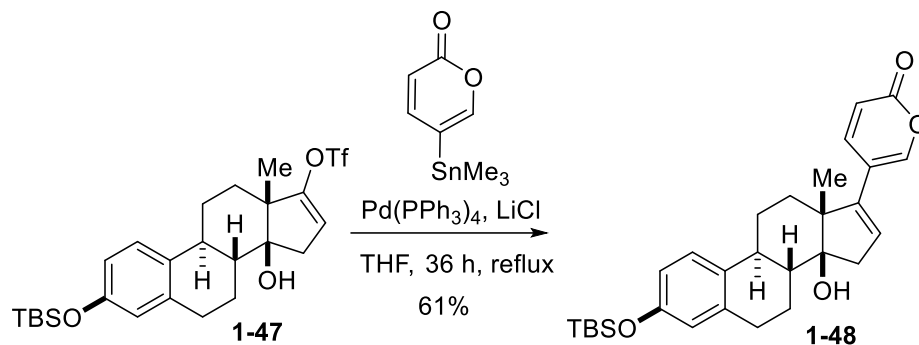
**Scheme 1.5.** Bauer's procedure for making 3 $\beta$ -hydroxy-5 $\beta$ ,14 $\alpha$ -bufa-20,22-dienolide from deoxycorticosterone.

Kabat et al.<sup>29</sup> produced their 14-deoxybufadienolide **1-46** via the key intermediate **1-42** by condensation of ethyl cyanoacetate with a 17-oxoandrostane **1-41** (Scheme 1.6). Compound **1-42** was transformed into **1-43** via functional group interconversion of the ketone into the cyano-containing compound **1-42**, followed by two reductive steps. Then, **1-44** was made via a Horner-Wadsworth-Emmons reaction, followed by deprotection of tetrahydropyran with acid, and subsequent oxidation to produce **1-45**. Acid-mediated cyclization then completed the synthesis of 14 $\alpha$ -bufadienolide. **1-46**.



**Scheme 1.6.** Kabat's procedure for making 14-deoxybufadienolide derivatives.

A more direct approach to installing the  $\alpha$ -pyrone moiety towards the synthesis of bufadienolides was published by Liu and Meinwald.<sup>30</sup> It involved a Stille coupling of 5-trimethylstannyl-2H-pyran-2-one (prepared from 5-bromo-2H-pyran-2-one)<sup>30</sup> with a 14 $\beta$ -hydroxy-16-ene-17-ol triflate steroid derivative **1-47** to obtain the bufadienolide analogue **1-48** in 61% yield (Scheme 1.7). Although only an estrone derived bufadienolide **1-48** was prepared, this method presents an efficient and elegant approach to bufadienolides.



**Scheme 1.7.** Meinwald's procedure for direct 2-pyrone installation.

### 1.5 Proposed biosynthesis pathway

The biosynthetic pathway of acetic acid  $\rightarrow$  mevalonic acid  $\rightarrow$  isopentenyl pyrophosphate  $\rightarrow$  squalene  $\rightarrow$  squalene 2,3-oxide  $\rightarrow$  lanosterol  $\rightarrow$  cholesterol is well established.<sup>31</sup> Pregnenolone is synthesized from cholesterol.<sup>32</sup> This conversion involves hydroxylation of the side chain at the C-20 and C-22 positions, with cleavage of the side chain.<sup>32</sup> The enzyme performing this task is cytochrome P450<sub>sc</sub>, (or CYP11A1), located in the mitochondria inner membrane. Pregnenolone is not itself a hormone but is the immediate precursor for the biosynthesis of steroidal hormones,<sup>33</sup> and the plant-derived bufadienolides (Figure 1.10). The conversion of pregnenolone into digitoxigenin requires the inclusion of an acetate group.<sup>32</sup> Whereas in the biogenesis of the  $\alpha$ -pyrone is formed by the condensation of a pregnane derivative with one molecule of oxaloacetic acid.<sup>1</sup> It is important to highlight that, all the toad (*Bufo*) steroids have the  $5\beta$  stereochemistry, the plant cardiotonic steroids can be divided into three major groups: the 4,5-dehydro derivatives, the  $5\beta$ -hydroxy derivatives and the  $5\alpha$ -bufadienolides. The change in configuration at C-5 in the plant-derived bufadienolides indicates a divergent biosynthesis. For cardenolide biosynthesis, Stuhlemmer and Kreis<sup>33</sup> reported that progesterone  $5\beta$ -reductase and progesterone  $5\alpha$ -reductase may compete for the same substrate in *Digitalis lanata*. This finding could be crucial to

understanding the formations *cis* and *trans* A/B ring junctions observed in certain cardiac glycosides.

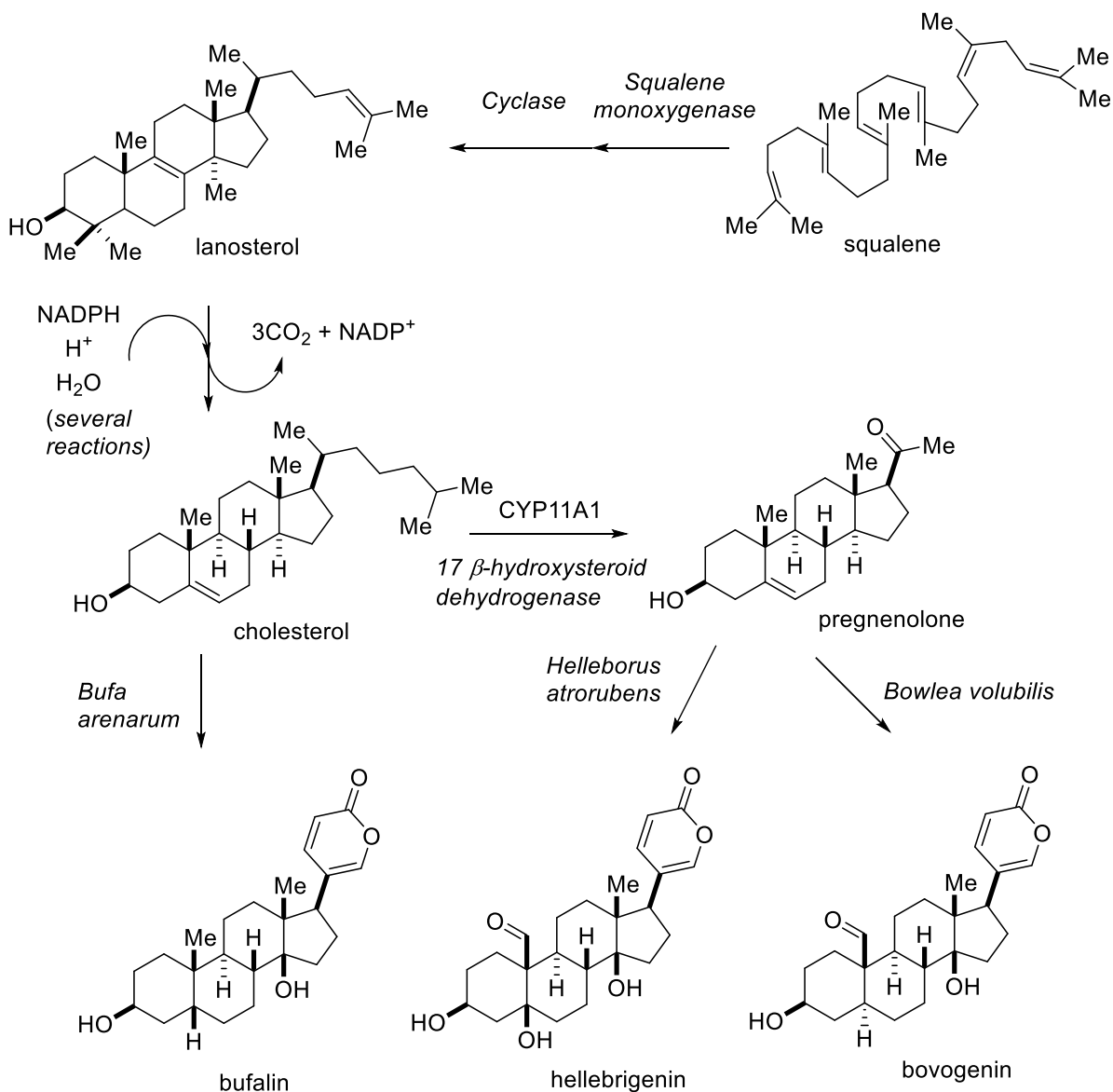


**Figure 1.10.** Proposed biogenesis of bufadienolides.

## 1.6 Summary

As more natural products are discovered and elucidated, a story is pieced together regarding how life defends itself from predators, and/or the environment via chemical means. Consequently, the lifeforms containing these small molecules have been used throughout the historical literature



as traditional medicines that claim to cure common ailments. In the time since, chemists have uncovered the compounds that illicit the therapeutic, toxic, and dangerous effects and repurposed them to treat and cure various diseases. While these compounds are interesting and have growing demands, the supply of these products is small and requires the sacrifice of many lifeforms. Through total synthesis, the supply of potentially therapeutic natural products can be dramatically increased by developing synthetic methods that allow for cheap, readily available chemical feedstocks to be combined, utilized, and transformed into the target structures. The following chapters of this dissertation aim to discuss novel strategies and approaches to build new pathways towards strategies of D-ring steroid modifications, specifically towards the C-14 and C-16 position of the D-ring, along with investigating methods for making late-stage modifications in the presence of sensitive C-17 heterocycles, like  $\alpha$ -pyrones, which are a critical component for making bufadienolides. The scientific motivation for these investigations is to add to the scientific literature since there is a current lack of methods for installing late-stage D-ring modifications in the presence of an  $\alpha$ -pyrone, due to its inherent sensitivity and reactivity. Along with the current methods established in the literature require harsh conditions that would be non-compatible with a C-14 hydroxyl group, which are vital for making natural steroid cores.

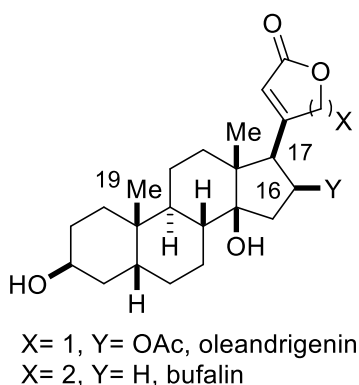


**Figure 1.11.** Illustration of steroid targets with complex D-ring functionalizations

The lack of a C-19-OH group limits the use of previously established Nagorny group chemistry<sup>24</sup> for building complex and polyfunctionalized steroid cores. While it is useful for installing the C-14-OH functionality, removal of the subsequent C-19-OH is non-trivial. Therefore, other steroid core derivatives, lacking the C-19 oxidation are utilized as the starting materials, and the subsequent chapters in this thesis aim to describe the new methods generated toward making D-ring modifications and address current issues involved in making sensitive  $\alpha$ -pyrones in the presence of late-stage C-14 and C-16-OH functionalizations, as well as, describing efforts towards improving the general overall synthesis of steroids.

## 1.7 References

- (1) Steyn, P.; Heerden, F., *Nat. Prod. Rep.*, **1998**, *15*, 397-413
- (2) Kolodziejczyk-Czepas, J.; Stochmal, A.; *Phytochem Rev* **2017**, *16* (6), 1155–1171..
- (3) Felipe Gonçalves-de-Albuquerque, C.; Ribeiro Silva, A.; Ignácio da Silva, C.; Caire Castro-Faria-Neto, H.; Burth, P.; *Molecules* **2017**, *22* (4), 578. Clausen, M. V.; Hilbers, F.; Pulsen, H. *Front Physiol.* **2017**; *8*: 371.
- (4) Repke, K.; Megges, R. S.; *Expert Opinion on Therapeutic Patents* **1997**, *7* (11), 1297–1306.
- (5) Bagrov, A. Y.; Shpairo, J. I.; Fedorova, O. V., *Pharmacol Rev.* **2009**, *61*, 9–38
- (6) S. Steyn, P.; R. van Heerden, F.; *J. Chem. Soc. Perkin Trans.* **1984**, 965.
- (7) McKenzie, R. A.; Franke, F. P.; Dunster, P. J.; *Australian Veterinary Journal* **1987**, *64* (10), 298–301.
- (8) Kellerman, T. S.; Naudé, T. W.; Fourie, N.; *Onderstepoort J Vet Res* **1996**, *63* (2), 65–90.
- (9) Kupchan, S. M.; Ognyanov, I.; Moniot, J. L., *Bioorg. Chem.*, **1971**, *1*, 13.
- (10) Naudé, T. W.; Schultz, R. A.; *Onderstepoort J Vet Res* **1982**, *49* (4), 247–254.
- (11) Nogawa, T.; Kamano, Y.; Yamashita, A.; Pettit, G. R.; *J. Nat. Prod.* **2001**, *64* (9), 1148
- (12) Shaw, D.; *Planta Med* **2010**, *76* (17), 2012–2018.
- (13) Rossi-Bergmann, B.; Costa, S. S.; Borges, M. B. S.; Silva, S. A. da; Noleto, G. R.; Souza, M. L. M.; Moraes, V. L. G.; *Phytotherapy Research* **1994**, *8* (7), 399–402.
- (14) Wagner, H.; Lotter, H.; Fischer, M.; *Helvetica Chimica Acta* **1986**, *69* (2), 359–367.
- (15) Anderson, L. A. P.; Steyn, P. S.; van Heerden, F. R.; *J. Chem. Soc., Perkin Trans.*, **1984**, *1*, 1573
- (16) Flier, J.; Edwards, M. W.; Daly, J. W.; Myers, C. W.; *Science* **1980**, *208* (4443), 503–505.
- (17) Nogawa, T.; Kamano, Y.; Yamashita, A.; Pettit, G. *J. Nat. Prod.* **2001**, *64*, 1148-1152
- (18) Ichikawa, M.; Sowa, Y.; Iizumi, Y.; Aono, Y.; Sakai, T.; *PLoS One*, **2015**, *10* (6).
- (19) Krenn, L.; Kopp, B. *Phytochemistry*, **1998**, *48*, 1.
- (20) Hutchinson, D.; Mori, A.; Savitzky, A.; Burghardt, G.; Wu, X.; Meinwald, J.; Schroeder,

- F.; *Proc. Natl. Acad. Sci.*, **2007**, *104*, 2265.
- (21) S Sondheimer, F.; McCrae, W.; Salmond, W. G., *J. Am. Chem. Soc.*, **1969**, *91*, 1228–1230.
- (22) Mukai, K.; Urabe, D.; Kasuya, S.; Aoki, N.; Inoue, M.; *Chem. Sci.*, **2015**, *6*, 3383.
- (23) Renata, H.; Zhou, Q.; Dünstl, G.; Felding, J.; Merchant, R.; Yeh, C.; Baran, P.  
*Journal of the American Chemical Society*, **2015**, *137* (3), 1330-1340.
- (24) Khatri, H.; Bhattarai, B.; Kaplan, W.; Li, Z.; John, M.; Long, C.; Aye, Y. Nagorny, P.,  
*Journal of the American Chemical Society*, **2019**, *141* (12), 4849-4860.
- (25) Michalak, M.; Michalak, K.; Wicha, J., *Nat. Prod. Rep.*, **2017**, *34*, 361–410.
- (26) Yoshi, E.; Oribe, T.; Koizumi, T.; Hayashi, I.; Tumura, K., *Chem. Pharm. Bull.* **1977**, *25*  
(9), 2249-2256. (28)
- (27) Hoppe, H.; Welzel, P., *Tetrahedron Letters*, **1986**, *27*, (22), 2459-2462.
- (28) Bauer, P.; Kyler, K.; Watt, D., *J. Org. Chem.* **1983**, *48*, 34-39.
- (29) Kabat, M.; Kurek, A.; Wicha, J., *J. Org. Chem.* **1983**, *48*, 4248-4251.
- (30) Liu, Z.; Meinwald, J., *J. Org. Chem.* **1996**, *61*, 6693-6699
- (31) Little, H. N.; Bloch, K., *Journal of Biological Chemistry*, **1950**, *183* (1), 33-46.; Berg, J.M.;  
Tymoczko, J.L.; Stryer, L. *Biochemistry*. 5th edition. New York: W H Freeman; 2002.  
Section 26.2,
- (32) Foye, W. O.; Roche, V. F.; Zito, S. W.; Williams, D. A., *Foye's Principles of Medicinal  
Chemistry*, 6<sup>th</sup> edition; Lippincott Williams & Wilkins, **2007**.
- (33) Tschesche, R.; Lilienweiss, G., *Z. Naturforsch., Teil B*, **1964**, *19*, 265.

## Chapter 2

### Studies Towards the Total Synthesis of Cardiotonic Steroid Family: Bufadienolides

#### 2.1 Introduction

Bufadienolides are an important class of cardiotonic steroids that are structurally like cardenolides but differ by their respective C-17 heterocyclic substituent. The base of their chemical structure is a steroidal aglycone.<sup>1</sup> Plant and animal extracts containing cardenolides and bufadienolides were widely used in Chinese and Japanese culture as traditional medicines.<sup>1</sup>

Structure activity relationship studies on known isolated cardiotonic steroids show variation in the location and quantity of hydroxyl groups has great impact on the compounds biological activity. From the literature, the most important site of the steroid core is located at the C-3 position.<sup>1</sup> Studies show the 3 $\beta$ -OH orientation is the most favorable conformer and the  $\alpha$ -isomer or ketone, yields lower reactivity.<sup>1</sup> Although, if glycosides are attached at that position instead, the reactivity dramatically increases (Figure 2.1). Across the rest of the steroid core, various oxidative modifications seem to decrease the biological activity bufadienolides. Bufalin has been detected in human plasma and has been shown to be involved in a signal cascade related to inhibition of Na<sup>+</sup>/K<sup>+</sup>-ATPase activity.<sup>2</sup> Currently, there is a commercially available assay for ouabain characterization, whereas measurements of marinobufagenin, telocinobufagin, and bufalin still require research assays.<sup>2</sup> Plasma levels of ouabain and marinobufagenin in humans are in the range of 200 to 1500 pM.

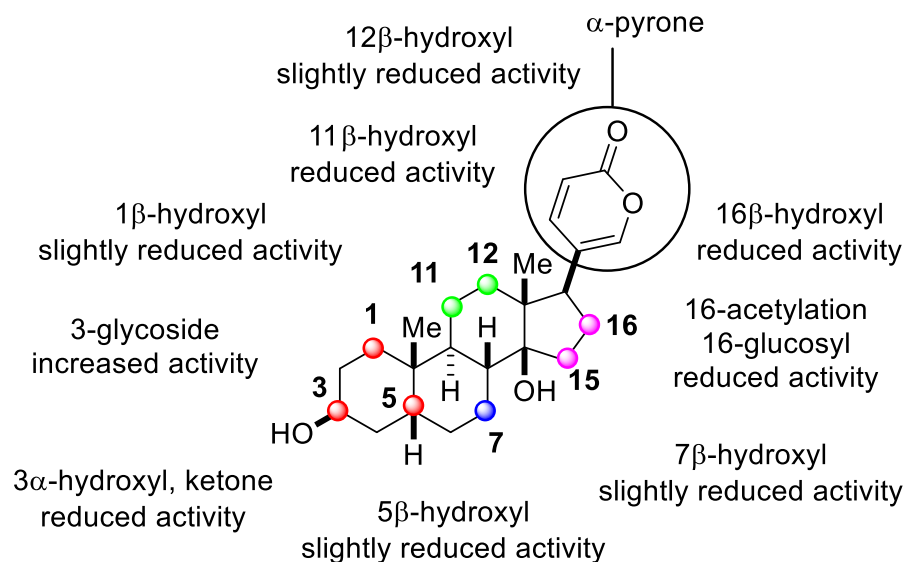


**Figure 2.1.** Effects of structural modifications on bufadienolides

The scarcity of the bufadienolide natural sources, leads to a limited quantity of isolatable compounds and thus limited knowledge of their therapeutic potential. Together with their side effects and adverse drug interactions, this class of therapeutics would require more investigations before they are included among standard medicines. To help achieve the highest standard of care, efficient syntheses of bufadienolides must be developed to help supply the demand for these compounds. Modern and efficient routes to cardenolides have been recently developed,<sup>3</sup> while many total syntheses of bufadienolides were reported only in the 1970s and 1980s.<sup>4,5</sup> The 2-pyrone ring construction in these syntheses involves tedious and harsh stepwise manipulations from a linear or saturated precursor. The need for direct installation of the 2-pyrone moiety would enhance the synthesis of bufadienolides. These challenging modifications have been approached in the literature with some elegant routes to making bufadienolides with late-stage modifications in the presence of a pre-installed pyrone substituent.

## 2.2 Regioselective hydrogenation of 2-pyrone-coupled bufadienolides

Direct and selective hydrogenation is a common synthetic transformation and has been done on a wide range of compounds and butenolide-containing cardiotonic steroids (Figure 2.2).<sup>3</sup> The most direct method to date, was discovered by Hilton<sup>6</sup> where it was shown that selective hydrogenation can be done at the C-16/C-17 alkene of the *cis*-C/D ring junction of **2-1** using Wilkinson's hydrogenation catalyst with a good conversion.<sup>6</sup>

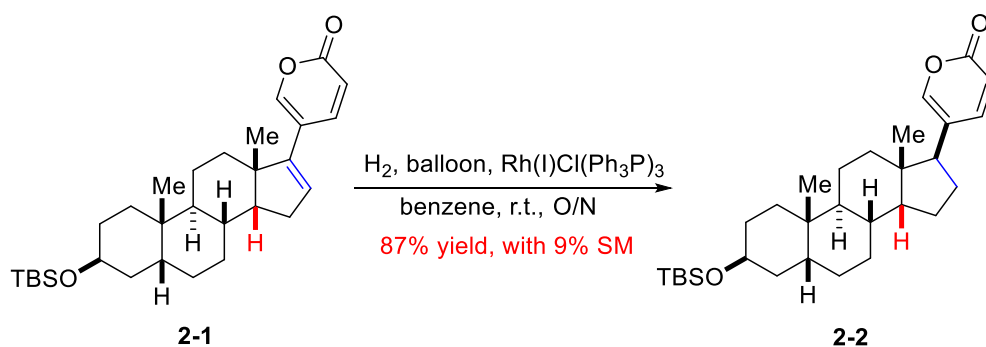


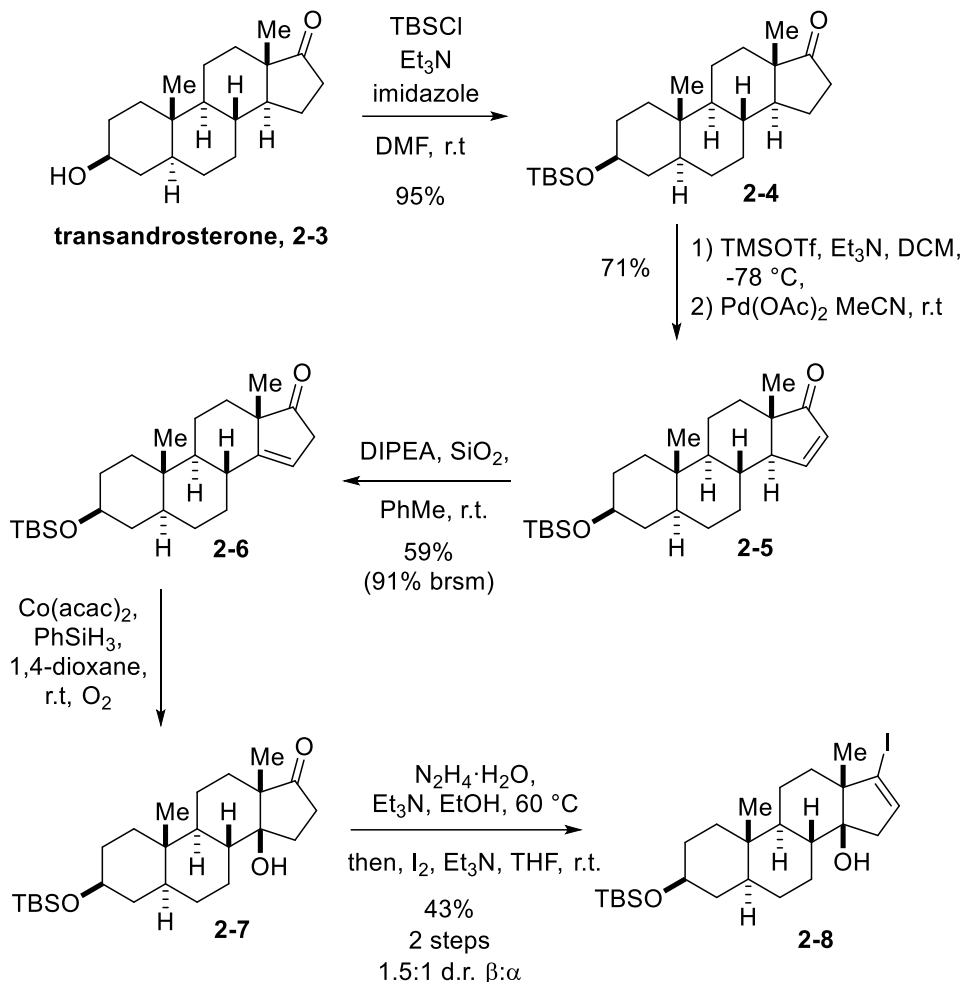
**Figure 2.2.** Hilton's regioselective hydrogenation of a pyrone-steroid.

They took the reaction one-step further to attempt selective reduction of the pyrone moiety, but this method resulted in a complex mixture of diastereomers that were not separable by traditional column chromatography. There is no evidence of performing this selective hydrogenation of C-16/C-17 alkene in the presence of a  $\beta$ -C-14 alcohol or TMS protected alcohol moiety. The development of this method motivated the experimental design herein.

## 2.3 Developments of regioselective hydrogenation of Stille-coupled bufalin-like steroids

### 2.3.1 Preliminary data with model substrates

For these studies, the model steroid substrates used came from *trans*-androsterone **2-3** which allowed for faster access to the desired C/D ring configuration necessary to simulate the chemical environment for developing important late-stage transformations.



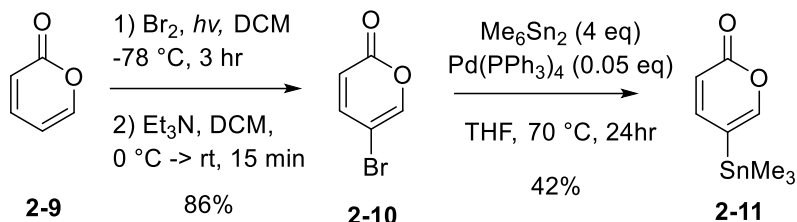
**Scheme 2.1.** Synthetic route for developing model steroid core

*Trans*-androsterone was converted to the C-3 *tert*-butyldimethylsilyl ether **2-4** in greater than 95% yield. This was followed by Saegusa-Ito oxidation to obtain intermediate **2-5** in 71% yield. Olefin rearrangement in the presence of Hünig's base and silica gel gave compound **2-6**. Next, Mukaiyama hydration was used to obtain **2-7**, which was then subjected to the following Barton iodination reaction to yield model steroid core vinyl-iodide **2-8** (Scheme 2.1) in 11% overall yield over 6 steps. The final vinyl iodide **2-8** compound was the main model used to investigate the transformations described in this chapter.

After the core of the steroid model was built, the  $\alpha$ -pyrone coupling partner was then synthesized via addition of bromine under photochemical conditions, using a floodlamp as the

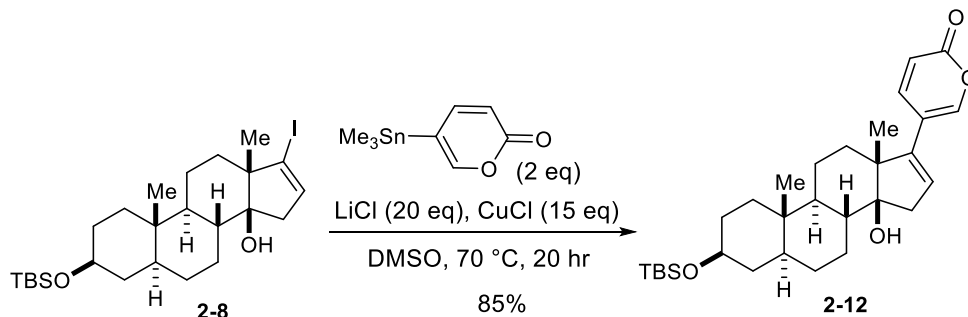


light source and subsequent solvent removal and elimination with triethylamine to produce the C3-brominate pyrone **2-10** in 86% yield (Scheme 2.2). This in turn was subjected to trans-metalation with hexamethylditin to produce the Stille coupling substrate **2-11** in 42% yield.



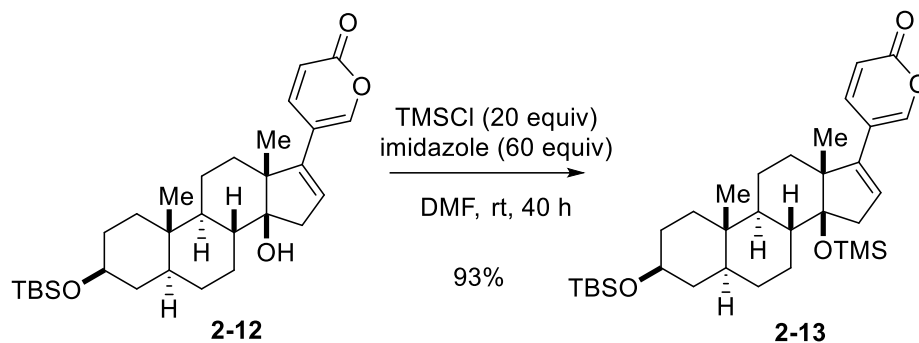
**Scheme 2.2.** Synthesis of pyrone cross-coupling partner.

Compound **2-11** was then used in a variety of ways to build the various model steroid systems used to investigate the selective hydrogenation of bufadienolides. Starting with the vinyl iodide steroid **2-8** (Scheme 2.1), the A/B trans isomer model pyrone **2-12** was synthesized in 85% yield using a classical Stille coupling reaction (Scheme 2.3).



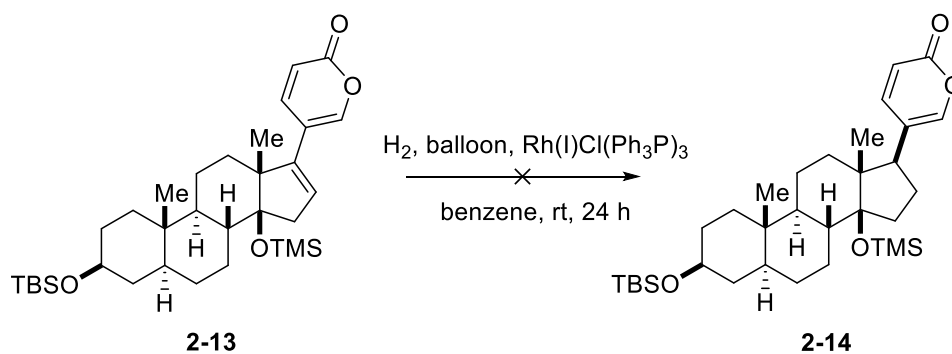
**Scheme 2.3.** Synthesis of 5 $\alpha$ -bufadienolide

The next step was to protect the C14 $\beta$ -alcohol with a TMS silyl protecting group. This helps limit complexation of the alcohol to the hydrogenation catalyst and the added steric bulk would help improve the regioselectivity of the reaction. The overall yield from the TMS protection reaction of **2-12** was carried out in 78% yield (Scheme 2.4).



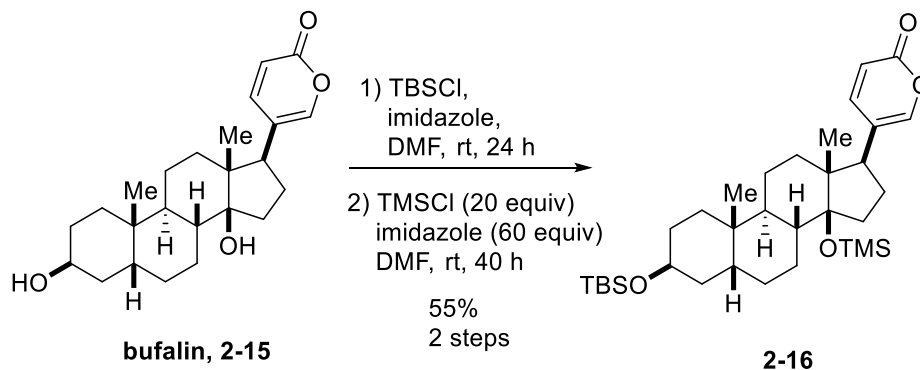
**Scheme 2.4.** Installation of C14 $\beta$ -alcohol TMS protecting group

The product **2-13** was then subjected to the hydrogenation conditions established by Hilton,<sup>6</sup> but surprisingly, no reduction product was observed from the reaction (Scheme 2.5). Even with larger loading of Wilkinson's catalyst or higher hydrogen pressure, the reaction remained unsuccessful.



**Scheme 2.5.** Results of Wilkinson's catalyst with model bufadienolide

Other conditions were explored beginning with the utilization of Rh/Al<sub>2</sub>O<sub>3</sub>, along with increase hydrogen pressure, which led to a complex mixture of hydrogenation products. To understand how the reaction was progressing, a comparison study was conducted alongside a model sample of bufalin **2-15** to monitor if at any point of the reaction any of the desired hydrogenation reaction was occurring (Scheme 2.6).



### Scheme 2.6. Synthesis of protected bufalin

It was found that the reaction was slow enough at a high hydrogen pressure (150-200 psi) to allow tracking of complex mixture of hydrogenation products that seemed to be forming from competitive reduction of the pyrone olefins and the steroidal olefin. Based on TLC, HRMS, and NMR analysis, shows the C-22/C-23 (*cf.* Figure 2.3, highlighted in blue) reacts competitively, and this observation was reinforced by subjecting a pure sample of bufalin derivative **2-16** to the reduction conditions and observing similar TLC, NMR, and HRMS profiles for the resultant product. (Figure 2.3). TLC analysis between **2-14** and **2-16** showed starting material  $R_f$  values to be 0.5 and 0.4 in 20% EtOAc/hexanes, respectively. However, both would react similarly to give a single spot at  $R_f = 0.25$  in 20% EtOAc/hexanes. This single spot was analyzed by HRMS and  $^1\text{H}$  NMR to show that there was a complex mixture of products. HRMS analysis was taken at varying time intervals to monitor the reaction, but, while starting material remained, and even mixture of reduction products and a minor amount of a rearranged tetrasubstituted olefin side product, which could only be consumed by allowing the reaction to go longer. This would unfortunately also consume all of the olefins which could not be separated by chromatography.

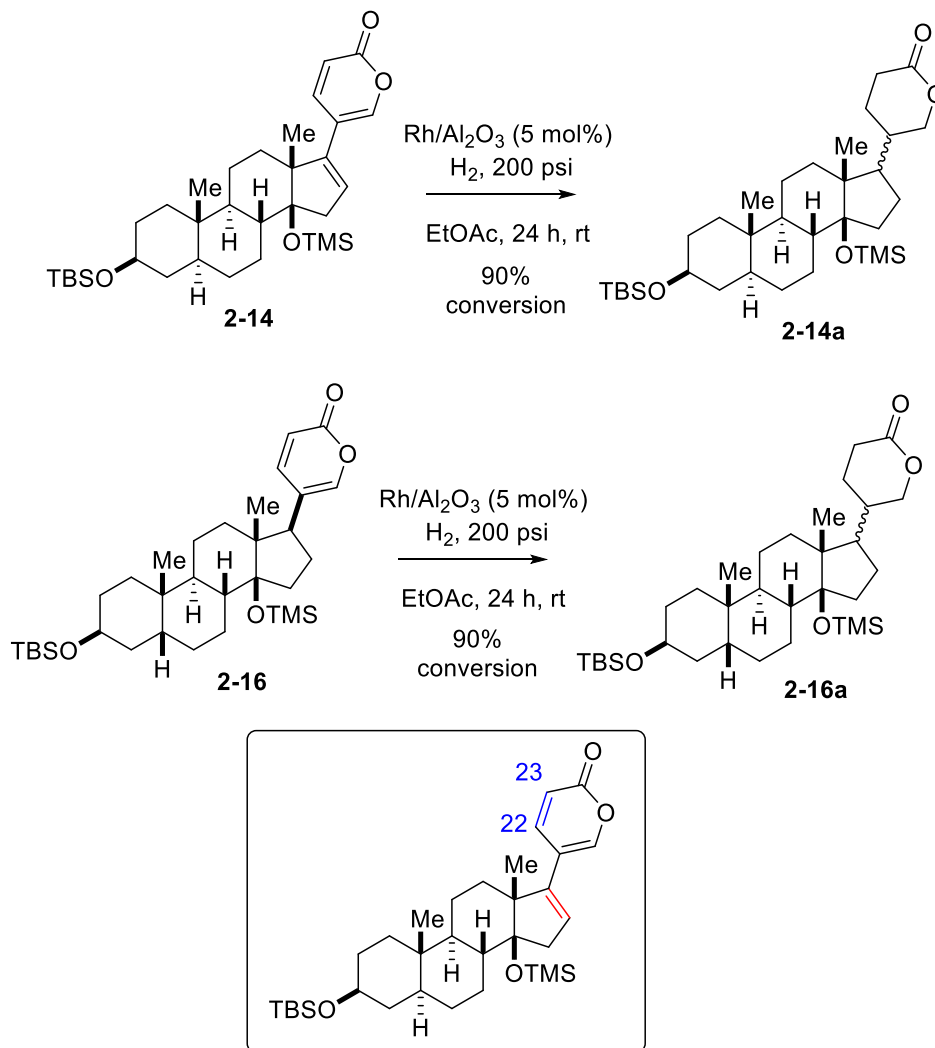


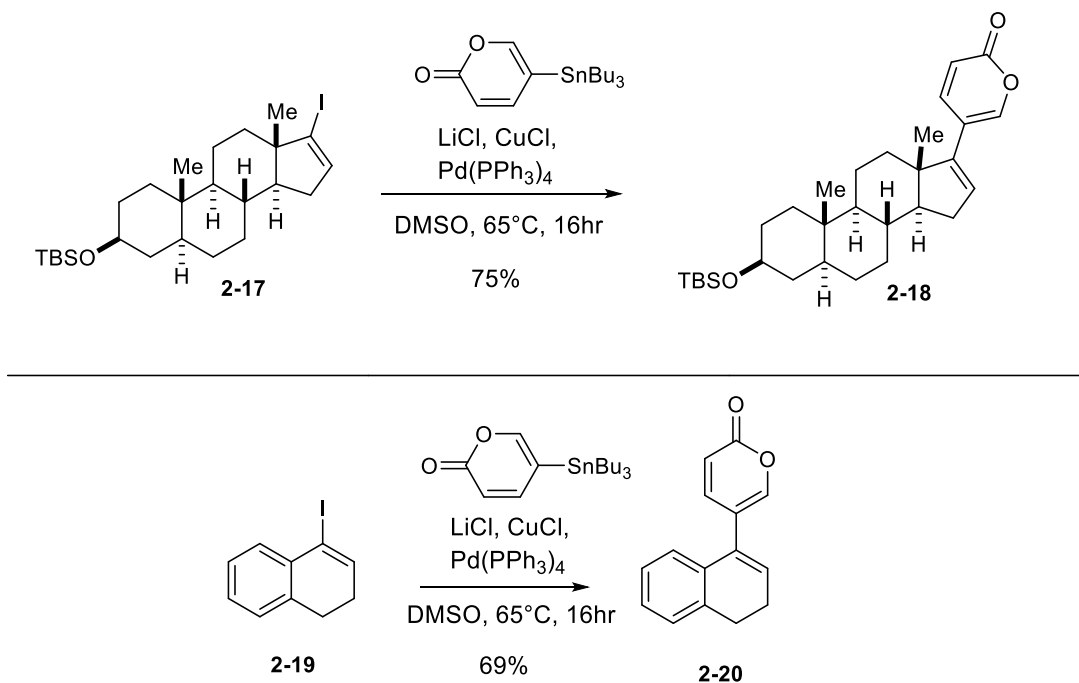
**Figure 2.3.** Discovery of competitive double bond reactivity in pyrone ring of bufadienolides

$^1\text{H}$  NMR analysis further confirmed the mixture of fully reduced products **2-14a** and **2-16a** respectively. The ratio of compounds was determined by NMR analysis on the complex mixture by looking for characteristic peaks for the corresponding compounds. The products **2-14a** and **2-16a** could be observed to be approximately a 20-25% ratio of the complex mixture of recovered mass. This unfortunate outcome led to the development of some other strategies to circumvent this hurdle. The quickest and most direct way was to approach the hydrogenation by completely reducing the entirety of the pyrone moiety along with the steroid hydrogenation. This would then

be followed by oxidation back to the desired unsaturated 2-pyrone, a transformation that has not been described in literature to date.

### 2.3.2 Preliminary data of full reduction of pyrone model substrates

To gain a better understanding of the hydrogenation reactions, we pursued the synthesis and studies of simplified models **2-18** and **2-20** (*cf.* Scheme 2.7). Stannane **2-11** was also used to make the simpler models of steroid backbone via a vinyl iodide *trans*-androsterone **2-17** in 75% yield and indene-based substrate **2-19** in 69% yield, respectively. These were used to investigate the complete hydrogenation screening.

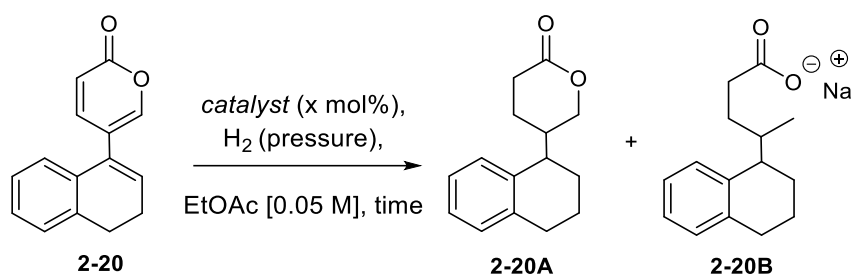


**Scheme 2.7.** Stille coupling of 2-pyrone containing model substrates.

To investigate and replicate the ability of the hydrogenation profile, substrate **2-20** was first investigated to simplify analysis while trying to understand the hydrogenation activity of the many olefins in the pyrone ring system. To begin, **2-20** was subjected to standard hydrogenation conditions with  $\text{PtO}_2$  under a hydrogen balloon atmosphere and it was found that an inconsistent hydrogenation profile was observed. Based on TLC and HRMS analysis, it could be discerned that

the desired *tris*-reduction of the pyrone was successful but, subsequent ring opening was a significant side product of the reaction. Other hydrogenation conditions with Pd/C provided no reaction with a hydrogen balloon, however conversion was observed with the employment of a high-pressure system. This came at a significant consequence of a complex mixture of side products. Finally, when Rh/Al<sub>2</sub>O<sub>3</sub> was used, the desired reduction profile was the more dominant result and minimal side product was observed with 10 mol% catalyst loading. Surprisingly, Wilkinson's catalyst (Rh(PPh<sub>3</sub>)<sub>3</sub>Cl) was not successful in forming any reaction on the model substrate.

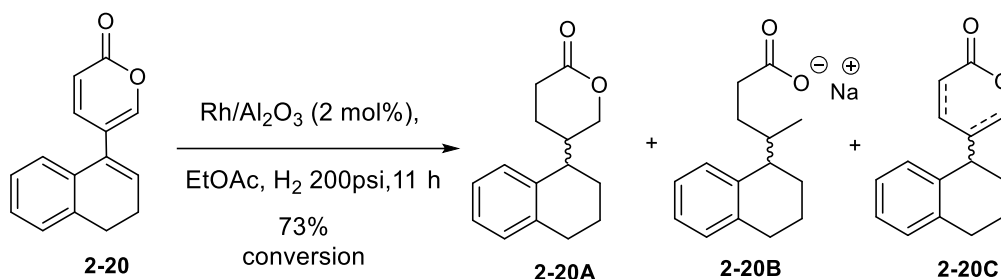
**Table 2.1.** Optimization of Rh/Al<sub>2</sub>O<sub>3</sub> hydrogenation screening.



Entry	Catalyst	Cat. Loading	H <sub>2</sub> Pressure	Time	Conversion <sup>a</sup>	Ratio (A:B) <sup>b</sup>
1	PtO <sub>2</sub>	10 mol%	balloon	1 h	Full	1:1
2	Pd/C	5 mol%	100 psi	1 h	Partial	<i>complex</i>
3	Rh/Al <sub>2</sub> O <sub>3</sub>	10 mol%	200 psi	6 h	Full	2:1
4	Rh/Al <sub>2</sub> O <sub>3</sub>	5.6 mol%	150 psi	1 h	Full	7:1
5	Rh/Al <sub>2</sub> O <sub>3</sub>	4 mol%	150 psi	1 h	Full	9.7:1
6	Rh/Al <sub>2</sub> O <sub>3</sub>	2.5 mol%	150 psi	4 h	Full	11.5:1
7	Rh/Al <sub>2</sub> O <sub>3</sub>	0.7 mol%	150 psi	3 d	Full	60:1
8	Rh/Al <sub>2</sub> O <sub>3</sub>	0.2 mol%	150 psi	6 d	Low	<i>N/A</i>
9	Rh(PPh <sub>3</sub> ) <sub>3</sub> Cl	5 mol%	balloon	4 h	None	<i>N/A</i>
10	Rh(PPh <sub>3</sub> ) <sub>3</sub> Cl	5 mol%	150 psi	4 h	None	<i>N/A</i>

<sup>a</sup> Conversion was based on TLC analysis. <sup>b</sup> Ratio was determined by using crude <sup>1</sup>H NMR and HRMS analysis. The ratio of products could not be separated by chromatography and mixtures were moved forward as complex mixtures.

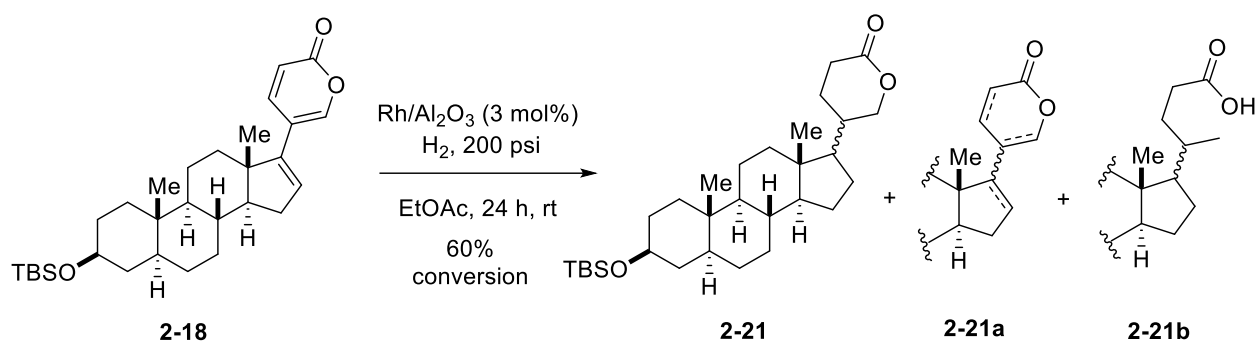
The screening process was further optimized to lower the potential Rh/Al<sub>2</sub>O<sub>3</sub> loading to be near 2 mol% while maintaining a nominal hydrogen pressure of 150-200 psi to achieve full conversion with low side product formation in 73% conversion to obtain a crude complex mass mixture (Scheme 2.8). The HRMS characterization showed that product was present by HRMS but, a complex mixture of pyrone opened side products remained. The reaction was observed to be slow enough to be monitor by TLC, however the products had similar chromatographic properties and could not be readily separated by chromatography. These side products have been proposed based on HRMS analysis and crude <sup>1</sup>H NMR analysis.



**Scheme 2.8.** Optimized hydrogenation procedure on model substrate **2-20**, and proposed side products.

Another goal of this investigation was to discover if the selective hydrogenation by Hilton, could be replicated on a C-14 OH containing bufadienolide steroid. First, the reduction was repeated on a trans-androsterone model system to test the reaction conditions and observe if full conversion could be achieved in one step, rather than with multiple iterations of the hydrogenation conditions. While trying to replicate Hilton's procedure with a H<sub>2</sub> balloon, a significant amount of starting material remained. To bypass the inconsistent conversion, a bomb reactor was used with the optimized hydrogenation pressure developed in Table 2.1 (Entry 6), to drive hydrogenation reaction to completion. The result was a complex mixture of products by <sup>1</sup>H NMR that also

contained multiple carbon peaks in the 160-175 ppm range, which can be associated with potential pyrone ring opening. The complex mixture was isolated in 60% conversion of a complex mixture of reduced compounds and pyrone ring opening side product based on data analyzed by HRMS and crude  $^1\text{H}$  NMR analysis.



**Scheme 2.9.** Optimized hydrogenation conditions with *trans*-androsterone model and proposed side products.

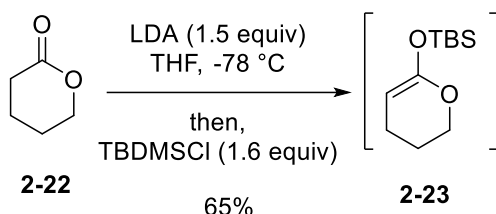
With these results for full reduction of the steroid moiety, it shows that the reduction does not lead to clean conversion into one of the products. However, to circumvent this issue, the next strategy was to investigate the re-oxidation of the lactone and see if the complex mixture could be separated after oxidation.

## 2.4 Oxidation of cyclic lactones to pyrones

Since the total hydrogenation conditions create an inseparable complex mixture, we investigated the possibility of using these products to regenerate the  $\alpha$ -pyrone moiety back under the oxidative conditions. To date, the most effective method remains from Hilton<sup>6</sup> where their completely reduced bufadienolide was then oxidized via phenylselenium chloride and subsequent oxidation with peroxide and elimination to achieve the mono-oxidized lactone. They did not go any further to perform another oxidation to obtain the necessary alpha pyrone. To this degree, an investigation was necessary to discover a more efficient process to oxidize the 6-membered saturated lactone back into a 2-pyrone substituent. The simplest model to test this hypothesis was

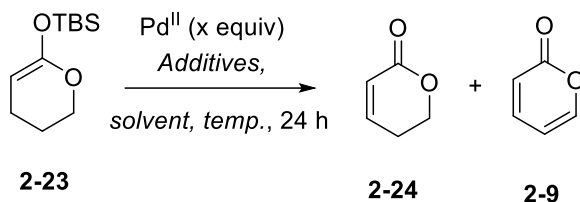


to use  $\delta$ -valerolactone, **2-22**. The initial strategy was to investigate if over-oxidation could be possible on the lactone system. Initial studies by Stahl<sup>7</sup> looked intriguing to help promote the Saegusa-Ito oxidation to produce the desired alpha-pyrone. First, **2-22** was transformed into a silyl enol ether, by using hard enolization with LDA in 65% yield to give compound **2-23**.



**Figure 2.4.** Transformation of  $\delta$ -valerolactone to silyl enol ether lactol.

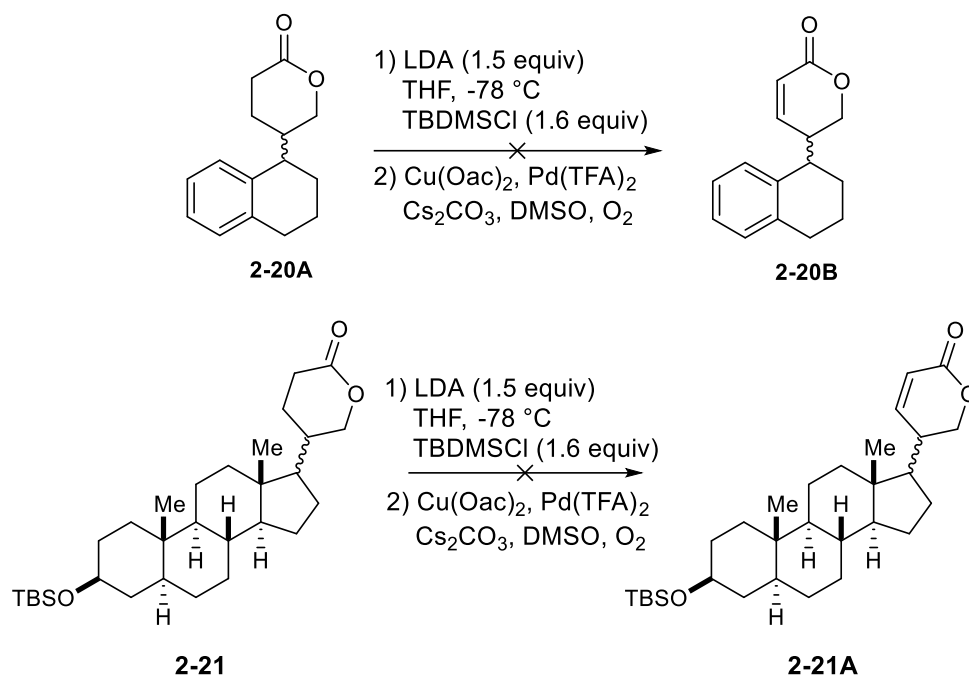
Compound **2-23** was subjected to classic conditions for Saegusa oxidation were tested to find that only very low conversion of the mono-oxidation product **2-24** only was observed (Table 2.2). Stahl and coworkers<sup>7</sup>, recently established a procedure for oxidizing cyclohexanone to phenol by using 2-dimethylamino, pyridine in the presence of *p*-TsOH to achieve their desired transformation. However, when these conditions were attempted with **2-23**, the reaction yielded no product. Since Saegusa-Ito or Stahl oxidation was not successful, we turned to using external oxidant of copper (II) acetate was introduced to mimic Wacker oxidation conditions. Similarly to what is observed for the Wacker oxidation, it was anticipated the Cu(II) would re-oxidize Pd(0) back to Pd(II), which would re-enter the catalytic cycle.

**Table 2.2.** Oxidation conditions screening of **2-23**.

Entry	Pd <sup>II</sup> Reagent	Solvent	Additives	Temp. (°C)	Yield <sup>b</sup>	Ratio (2-24:2-9) <sup>a</sup>
1	Pd(OAc) <sub>2</sub>	DMSO	-	25	20%	2-24 only
2	Pd(TFA) <sub>2</sub>	DMSO	2-dimethylamino pyridine, TsOH, O <sub>2</sub>	80	0%	-
3	Pd(TFA) <sub>2</sub>	DMSO	Cs <sub>2</sub> CO <sub>3</sub> , O <sub>2</sub>	80	5%	2-9 only
4	Pd(TFA) <sub>2</sub>	DMSO	Cu(OAc) <sub>2</sub> , Cs <sub>2</sub> CO <sub>3</sub> , O <sub>2</sub>	80	55%	2-9 only
5	Pd(TFA) <sub>2</sub>	THF/1,4-dioxane	Cu(OAc) <sub>2</sub> , Cs <sub>2</sub> CO <sub>3</sub> , O <sub>2</sub>	65	0%	-
6	Pd(TFA) <sub>2</sub>	DMF	Cu(OAc) <sub>2</sub> , Cs <sub>2</sub> CO <sub>3</sub> , O <sub>2</sub>	80	0%	-
7	Pd(TFA) <sub>2</sub>	2-butanone	Cu(OAc) <sub>2</sub> , Cs <sub>2</sub> CO <sub>3</sub> , O <sub>2</sub>	80	7%	2-24 only
8	Pd(TFA) <sub>2</sub>	1,4-dioxane	Cu(OAc) <sub>2</sub> , Cs <sub>2</sub> CO <sub>3</sub> , O <sub>2</sub>	80	20%	2-24 only
9	Pd(TFA) <sub>2</sub>	NMP	Cu(OAc) <sub>2</sub> , Cs <sub>2</sub> CO <sub>3</sub> , O <sub>2</sub>	80	10%	2-9 only
10	Pd(TFA) <sub>2</sub>	<i>t</i> BuOH	Cu(OAc) <sub>2</sub> , Cs <sub>2</sub> CO <sub>3</sub> , O <sub>2</sub>	80	0	-

<sup>a</sup>Ratios were determined by <sup>1</sup>HNMR analysis. <sup>b</sup>Isolated yields

For Entry 1 (Table 2.2), under standard Saegusa oxidation conditions, only the mono-oxidation product **2-24** was observed. Stahl conditions (Entry 2) gave no productive reaction. Entry 3 investigated introducing exogenous oxygen atmosphere, showed **2-9** being formed in 5% yield. With this finding, Wacker conditions were utilized with Cu(OAc)<sub>2</sub> to produce the product **2-9** in 55% yield. Changing solvents from DMSO seemed to mainly generate either no productive reaction or generated only the mono-oxidized **2-24**.



**Scheme 2.10.** Attempted formation of silyl enol ether on model substrates **2-20A** and **2-21**.

With the optimized oxidation conditions from Table 2.2, model substrates **2-20A** and **2-21** were used to make their silyl enol ether intermediates. The silyl enol ethers were moved forward without further purification or analysis beyond crude HRMS and <sup>1</sup>H NMR to observe characteristic peaks. The *in situ* silyl enol ethers were then subjected to the optimized oxidation conditions, but no productive reaction was observed (*cf.* Scheme 2.10). The main issue with these silyl enol ether intermediates, they are not stable to silica gel, and are readily decomposed by HRMS analysis, so observing their presence is difficult. Further trying to optimize the reaction to be a single-pot operation with silyl enol ether formation and subsequent oxidation resulted in no product formation.

Since the start of this Wacker oxidation investigation, another literature report was published by the Dong lab by using CuTc, an alkyldiphenylphosphine and ditertbutylperoxide in refluxing benzene to achieve mono-oxidation of various cyclic lactone substrates to generate  $\alpha,\beta$ -unsaturated lactones.<sup>8</sup> The mechanism of action for this transformation utilizes a radical copper enolate along

with a terminal oxidant to avoid over oxidation of lactone species. A representative example is shown in Figure 2.5.

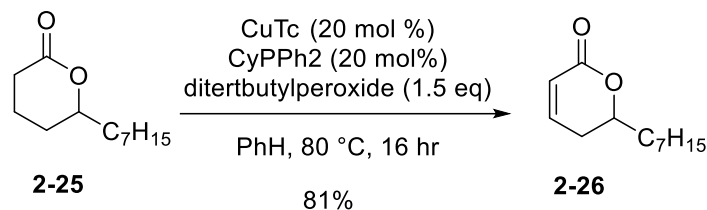


**Figure 2.5.** Dong's Cu(I) oxidation of lactone.

A recent paper by Baran<sup>9</sup> showed that the oxidation can be achieved electrochemically for the six-membered lactones. The proposal for their strategy was to use diphenylphosphate-ketene acetals for the esters instead of silyl enol ethers. They also compared some other oxidation techniques like Newhouse<sup>10</sup>, Ito<sup>11</sup>, and Nicolaou<sup>12</sup>, to show that their methods perform poorly compared to the method from Dong.

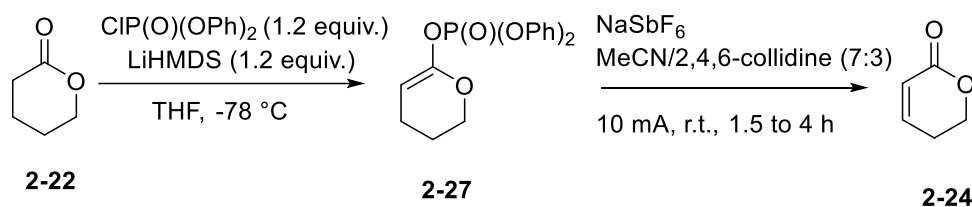


**Figure 2.6.** Baran's electrochemically driven desaturation method.

Several models were tested for proof of concept of the method. In the replicative experiments, although the yield in these cases were lower than the those reported by Dong<sup>8</sup>, they showed consistency and reproducibility for the oxidation of cyclic lactones (Figure 2.7). With these results in hand, oxidation was then carried out on the model bufadienolide compounds that were reduced in previous discussions.

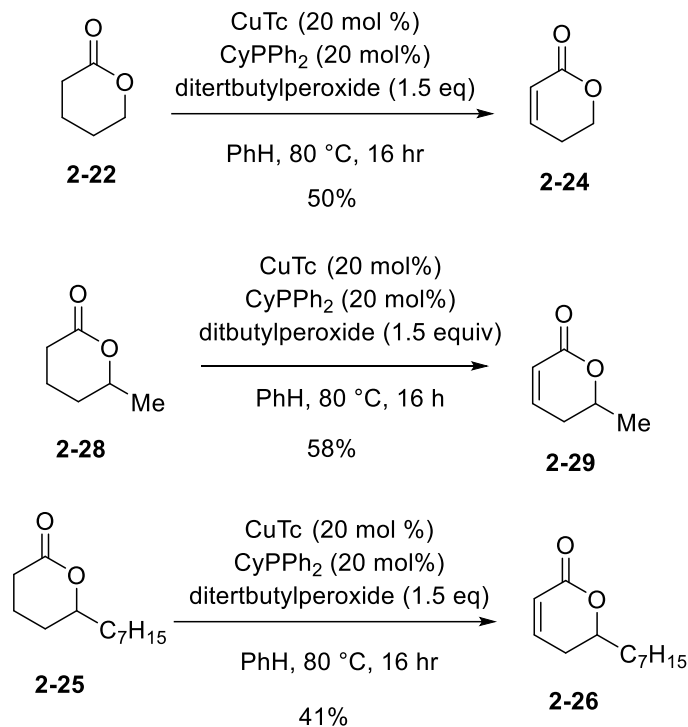


**Figure 2.7.** Replicative experiments of Dong's Cu(I) oxidation of lactone **2-24**.

With the indene pyrone reduced product, Dong's reaction procedure did not show any of the mono-oxidation compound **2-30**.

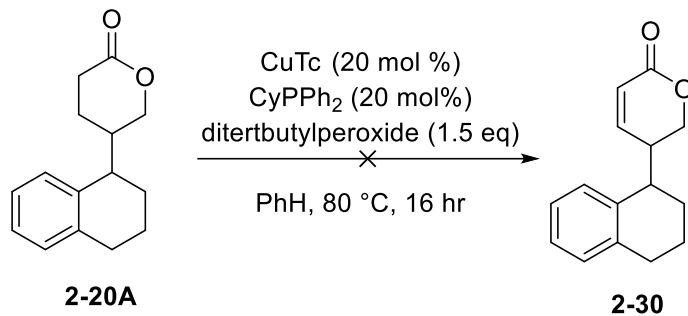


**Figure 2.8.** Replicative experiments of Dong's Cu(I) oxidation of lactone **2-20A**.

With the 5 $\alpha$ -bufadienolide, the reaction also resulted in an unsuccessful reaction. While the precise reasons for the unsuccessful reaction could be attributed to the scale of the reactions. Typically, the oxidation procedure listed by Dong, a precise number of equivalents for the CuTc, CyPPh<sub>2</sub> reagents, and peroxide species are crucial for a successful reaction. It appears that due to

the complex mixture from the previous hydrogenation studies may cause issues with accurately introducing the correct reagent equivalents.

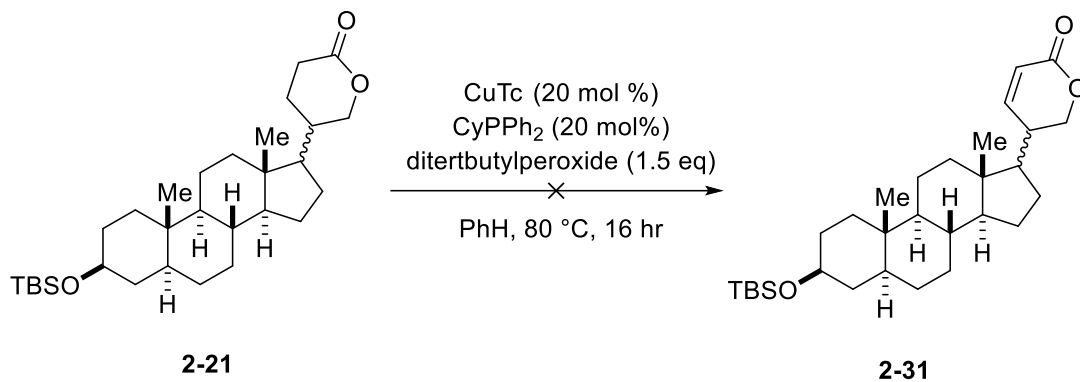


**Figure 2.9.** Attempted Cu(I) oxidation of 5 $\alpha$ -bufadienolide model **2-21**.

This could also be attributed to sensitivity of this transformation to the reaction scale, which limits the applicability of such oxidations to sub-millimole scale reactions. Since the precision of molar equivalents is necessary, this can be difficult to achieve on small scale, which is typical for natural product synthesis. Even with these challenges, this remains a promising method that may still prove useful for synthesizing bufadienolides.

## 2.5 Attempts of pyrone olefin masking for selective hydrogenation studies

Considering the difficulties involved with direct hydrogenation of Stille-coupled  $\alpha$ -pyrone systems, we explored the use of masking groups to drive the desired reduction. Masking groups of diene systems have been shown to be a good option to help prevent the undesired reactivity of sensitive olefin systems.<sup>13</sup> Iron(tricarbonyl) (Fe(CO)<sub>3</sub>) has been used in various chemical syntheses<sup>14</sup> for the masking of pyrone systems, with the first reports coming from DePuy<sup>15</sup>. The reaction of 2-pyrone with Fe<sub>2</sub>(CO)<sub>9</sub> in dry benzene under reflux conditions gave the light-stable iron-masked pyrone **2-32** in 89% yield. Rosenblum<sup>16</sup> showed that another reaction with the same iron and pyrone species under photochemical conditions can be transformed into an iron-masked

cyclobutadiene **2-33**, albeit in poor yield (Figure 2.10). The iron masking group can be removed via oxidation with CAN or Me<sub>3</sub>NO.<sup>13</sup>

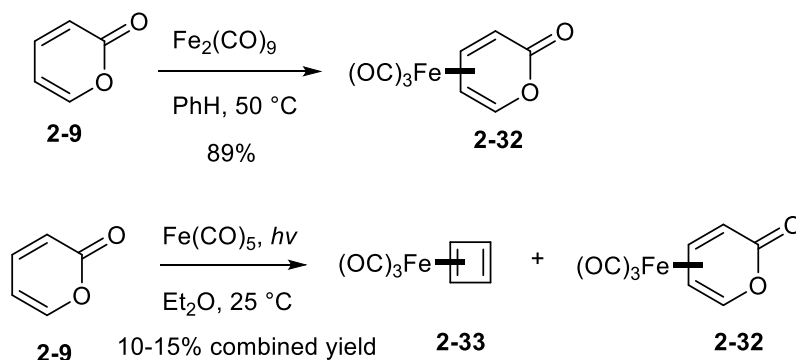


**Figure 2.10.** Prior art towards iron-masking of pyrones.

Fairlamb<sup>14</sup> performed an investigation into furthering the utility of Fe(CO)<sub>3</sub> complexes of brominated pyrones. They were successful with screening multiple solvent conditions and reagents which lead to the selected examples being shown in Figure 2.11. 4-Bromo pyrone **2-34** under the most optimal conditions showed a mixture of the desired iron tricarbonyl masked compound **2-35** and a small amount of the reduced parent compound **2-36** with the iron mask attached. It has been shown that this iron species can reduce these Csp<sup>2</sup>-X bonds. They further showed that a 3,5-dibrominated pyrone **2-37** can be complexed to give exclusively the 5-bromo-iron masked substrate **2-38**. More interestingly, the 5-bromopyrone **2-10** itself is much more stable to reduction than the 3-bromo position and can be synthesized almost exclusively with minor reduction. They stated however that the complex **2-39**, is very sensitive to light and acid.<sup>14</sup>

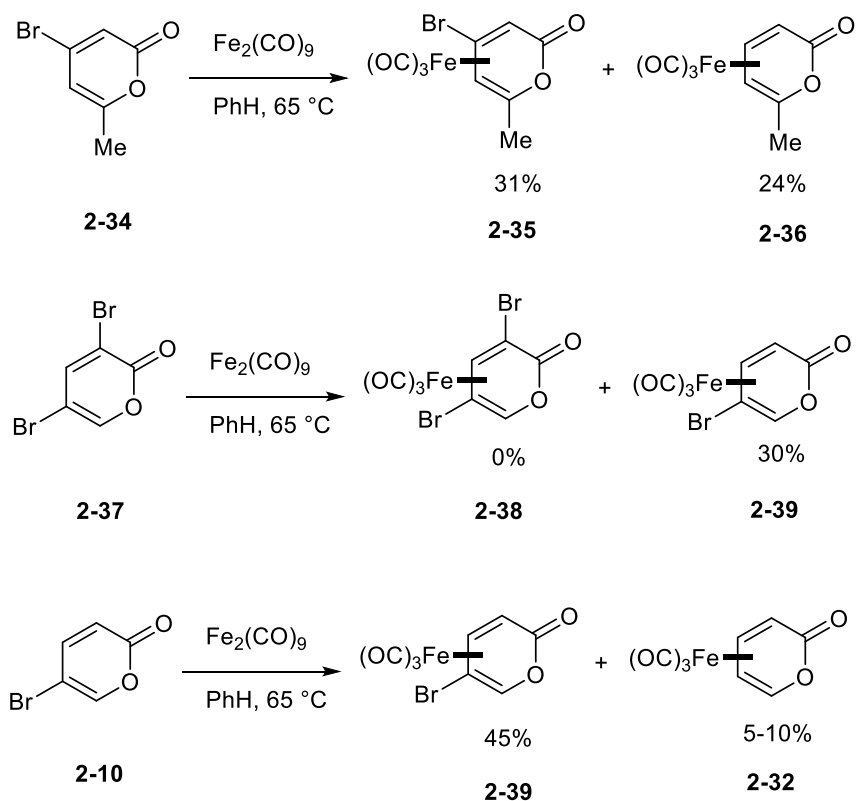


**Figure 2.11.** Complexation of various bromo-substituted 2-pyrones with  $\text{Fe}_2(\text{CO})_9$  via Fairlamb's method.

With this literature precedent in hand, we set out to determine the utility of these iron carbonyl masked complexes for utility with selective hydrogenations, an area which has previously been unexplored. First, 2-pyrone **2-9** was subjected to the reported literature conditions for iron masking and in this case only yielded 44% of the desired product but, the starting material could be recovered via chromatography (brsm 75%). Gratifyingly, when the product was subjected to various common heterogenous hydrogenation catalysts (Pd, Pt, Rh), no reaction was observed, even with a high-pressure atmosphere of hydrogen.



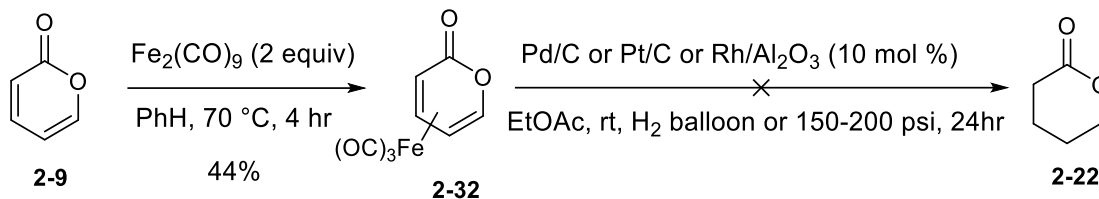


**Figure 2.12.** Hydrogenation of iron-carbonyl masked pyrone.

This prompted an investigation into the ability and selectivity of the  $\text{Fe}(\text{CO})_3$  complex to be installed on a steroid system. With the previously synthesized **2-14** (Figure 2.13),  $\text{Fe}_2(\text{CO})_9$  was introduced, and iron-masking appeared to be successful however, not all the starting material was consumed (brsm 50%). It was also not easily separable by column chromatography but could be seen as a complex mixture by  $^1\text{H}$  NMR and by HRMS. **2-40** was then moved forward as a crude mixture to observe if the optimized hydrogenation conditions in Table 2-2 (*cf.* Figure 2.14) could still be useful.

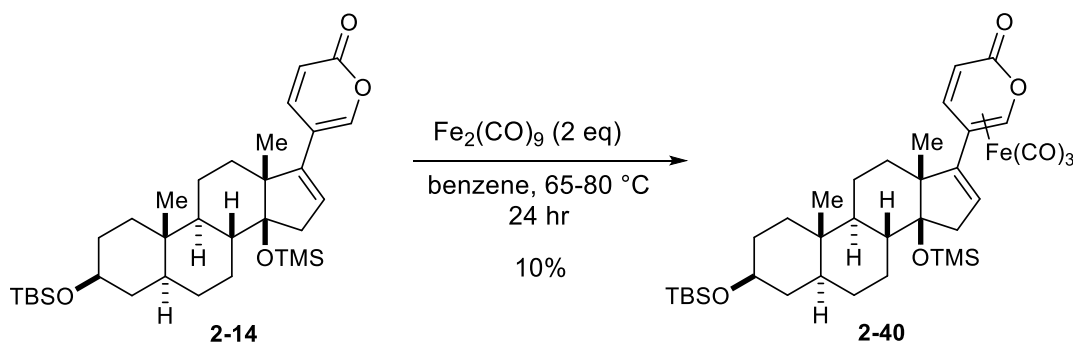


**Figure 2.13.** Iron-carbonyl masking on  $5\alpha$ -bufadienolide.

Unfortunately, the hydrogenation did not yield any product (*cf.* Figure 2.14). While it is not clear why no reduction product was observed, this result might be attributed to the deactivation of the  $\Delta^{16}$ -alkene. Such a situation may arise if the iron(0) tricarbonyl protection is not selective to just the pyrone itself but could also be complexing between the *cis*-diene double bond system of the pyrone and the steroid  $\Delta^{16}$ -alkene. Although no detection of a multi-iron masked steroid could be observed, it could be a possibility for the failure of the hydrogenation reaction.

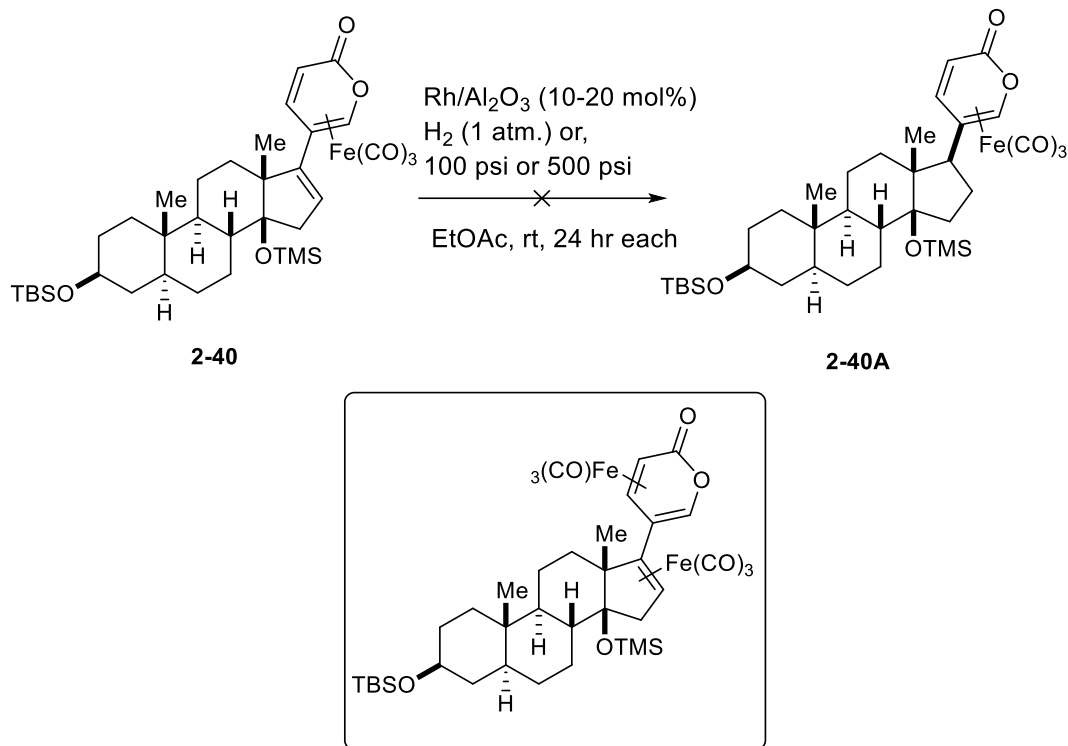


**Figure 2.14.** Hydrogenation of iron-masked 5 $\alpha$ -bufadienolide and proposed iron(0) complexes.

## 2.6 Modifications for furan-amide $^1\text{O}_2$ cycloaddition

Along with the investigation towards regioselective hydrogenation of bufadienolides being an important investigation, Wiesner<sup>17</sup> developed a novel synthetic method for transforming furans into pyrones via an endo-peroxide, singlet-oxygen Diels-Alder rearrangement. This method allowed for one of the first total syntheses of bufalin and related derivatives from a common starting intermediate in testosterone. The synthesis by Wiesner and co-workers started from intermediate **2-41**. They have proposed two separate routes, either by the condensation of a testosterone-derived unsaturated ketone<sup>17</sup> with a lithiated derivative, or directly from digitoxigenin<sup>18</sup> (Figure 2.15). Then, the C-17 hydroxyl group was acetylated and removed via rearrangement to give compound **2-44**. This was followed by hydrogenation and then elimination

to give compound **2-46**. The endoperoxide, formed by irradiation of **2-46** in the presence of a sensitizer (specifically, 5,10,15,20-tetraphenylporphyrin) while O<sub>2</sub> was bubbled through the solution. This was then cleaved *in situ* with an excess of Me<sub>2</sub>S and the resultant unsaturated dialdehyde **2-47** was immediately reduced with an excess of NaBH<sub>4</sub> to yield **2-48** in 82% yield over three steps. Hydrolysis of the acetal gave lactol **2-49** that was oxidized to the lactone with silver carbonate to give **2-50**. Then, methanesulfonyl chloride was used to cap the hydroxyl group on the pyrone and base-mediated elimination gave the fully oxidized pyrone **2-51** in 85% yield. This was followed by hydrobromination/debromination sequence to provide the C-14β-OH-containing intermediate **2-52**. The synthesis of bufalin was then completed by hydrogenolysis of **2-52** using Pd(OH)<sub>2</sub>/C (70% yield).

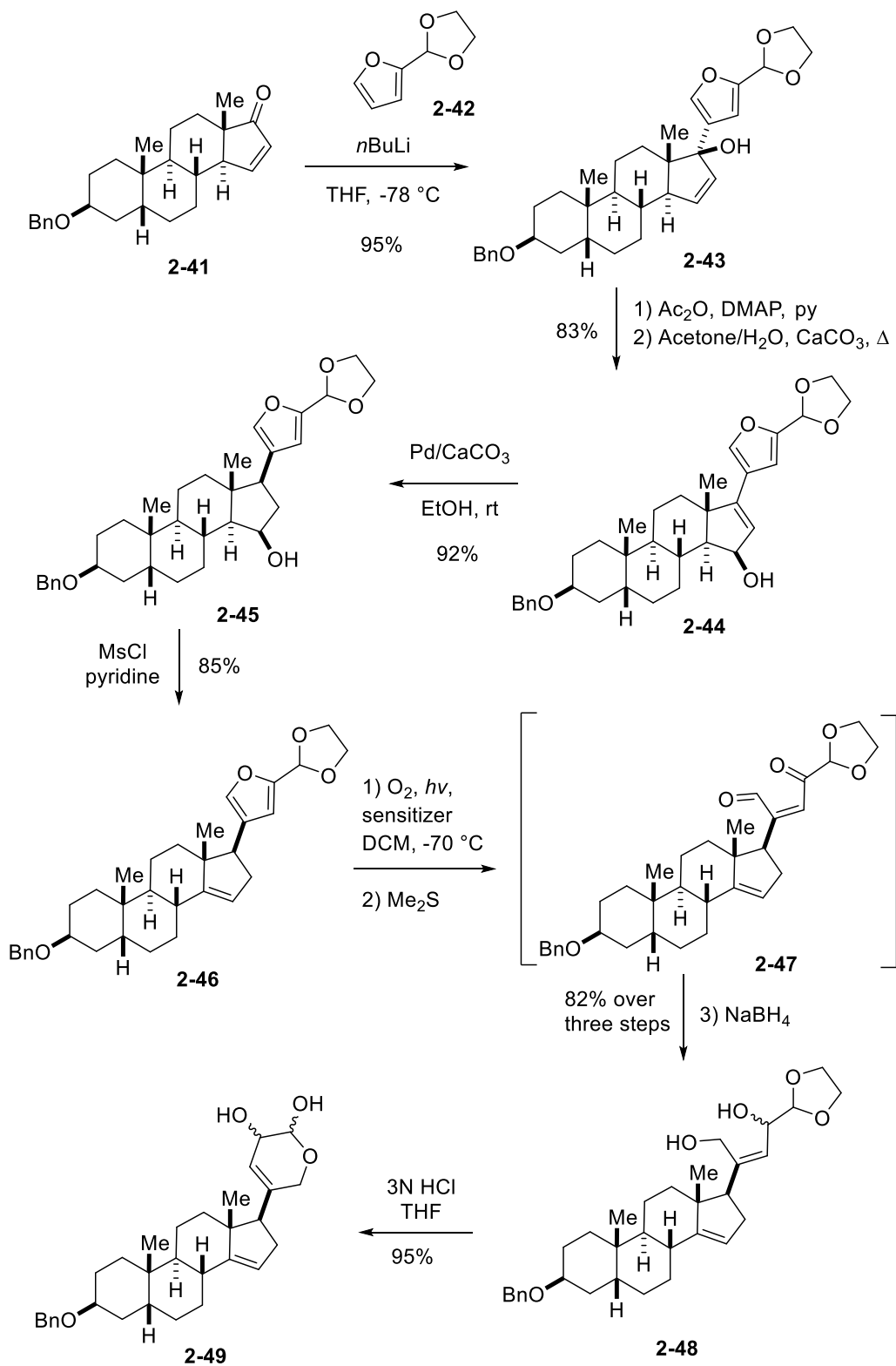


**Figure 2.15.** Wiesner's route for making intermediate 2-49.

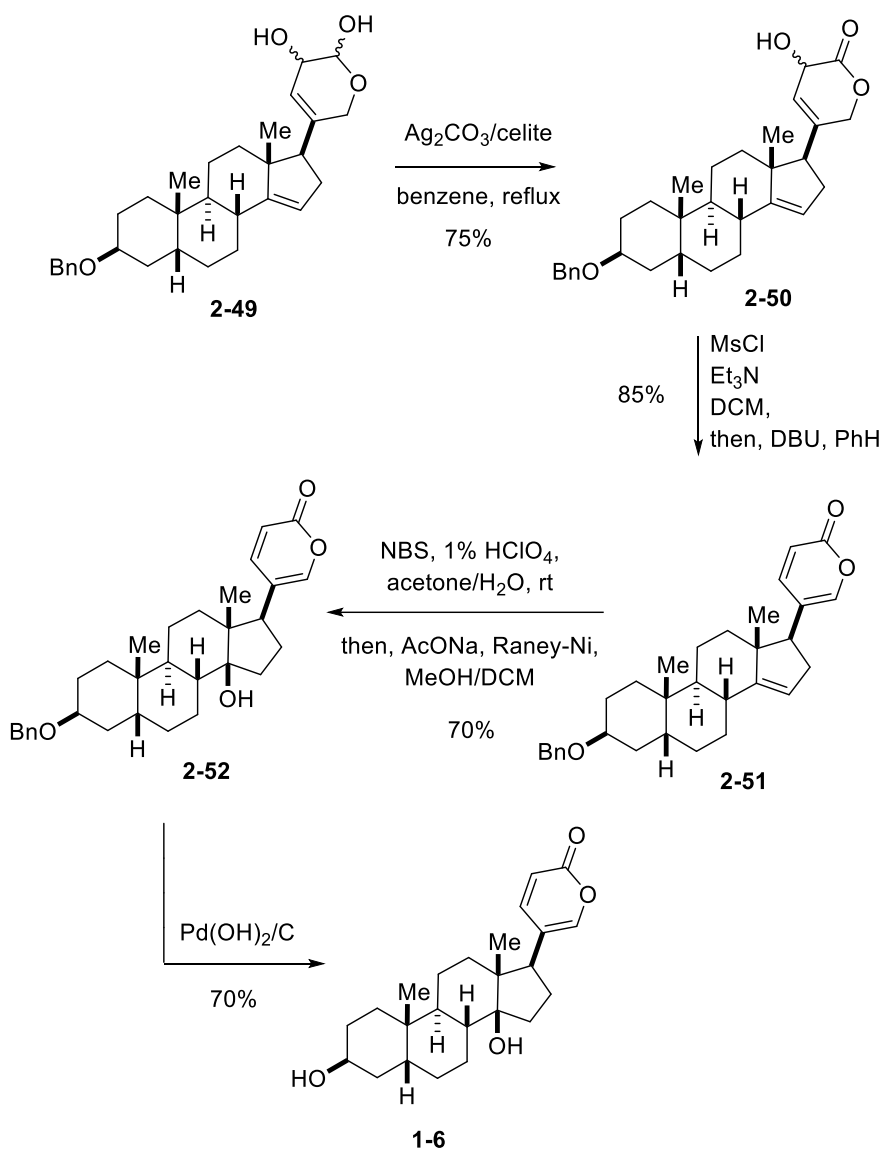


**Figure 2.16.** Wiesner's complete synthesis of bufalin from intermediate **2-49**.

Wiesner's route featured a unique strategy for the installation of the  $\alpha$ -pyrone ring via a  $^1\text{O}_2$  Diels-Alder reaction with an acetal-containing furan. However, the practicality of this approach was significantly diminished by the extended 14-step linear sequence required to convert **2-46** into bufalin and resulting in 15% overall yield. In addition to the lithiated furan addition step for the installation of the C-17-substitution, and the hydrogenolysis step to remove the C3 benzyl

protecting group, these synthetic studies required 5 steps to convert the acetal-containing furan moiety into butenolide and 6 steps to install the correct oxidation states/stereochemistry at the C14- and C17-positions of the D-ring. We envisioned that with our route for making a pre-installed C-14 $\beta$  hydroxyl group, while also having a vinyl iodide moiety at C-17, significant improvements can be made to the overall step count. We also anticipate further improvements in the conciseness of this route if the furan-to-pyrone interconversion is executed as a single-pot operation. We conceived that this could be achieved by using a higher oxidation level carboxylic acid derivative instead of a furan-aldehyde to further lessen the step count and to remove the oxidation step for transforming a lactol to a lactone (*cf.* Figure 2.16). The latter description will be described in the next section.

#### 2.6.1 Initial optimization of endoperoxide rearrangement

Inspired by the Wiesner's original studies (*vide supra*), our new approach was based on the coupling of vinyl iodide **2-8** with the furan moiety pre-installed carboxylic acid derivative, and subsequent hydrogenation to establish the  $\beta$ 17-stereochemistry. This would allow to achieve a more convergent and direct installation of the furan in only 2-3 steps (LLS). In addition, the use of the furan substituent in carboxylic acid (rather than aldehyde) oxidation steps state allows to eliminate extra steps for the redox (and deprotection) manipulations.

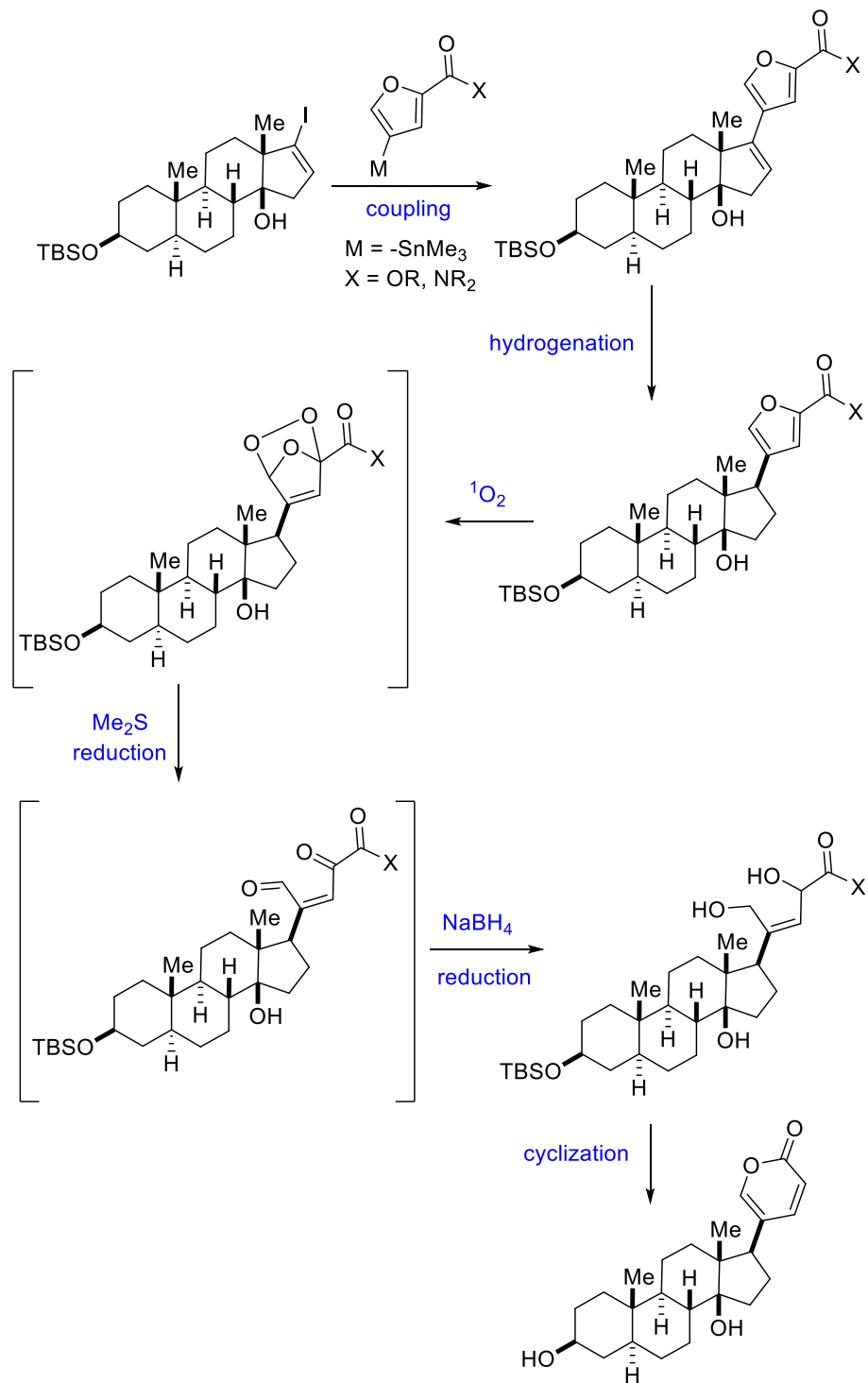


**Figure 2.17.** Proposed route of furan to pyrone with the pre-installed C-14 $\beta$ -OH.

The initial studies executed by Dr. Hem Raj Khatri commenced with the model studies depicted in Figure 2.18. These studies relied on using a model **2-19** to test if esters could be used as a carboxylic acid derivative. Tetralone **2-53** was converted into the vinyl iodide **2-19**, which was subjected to Suzuki coupling and hydrogenation to produce compound **2-54** in 45% yield. This compound was subjected to photooxidation with  $^1\text{O}_2$  (500 W flood lamp, meso-tetraphenylporphine) to produce an endoperoxide that was cleaved over the course of 2 h by adding a large excess of DMS. Unfortunately, the resultant intermediate **2-55** could not be isolated due to the partial isomerization to hemiacetal form on a silica gel, and the crude oil containing **2-55** was directly subjected to the subsequent reduction step. The treatment of **2-55** with  $\text{NaBH}_4$  as the reducing agent led to a complex mixture of products that contained minor quantities of the desired product **2-56** and overreduction byproducts **2-56a-c** (*cf.* Figure 2.18). It appeared that by TLC analysis after column chromatography that the product would decompose to a hemi-acetal product **2-56a** from an incomplete reduction with  $\text{NaBH}_4$ , or overreduction represented by **2-56b** and **2-56c**. These side products were postulated from HRMS and  $^1\text{HNMR}$  analysis. Further efforts to optimize this reaction by controlling the reaction parameters did not lead to significant improvements.



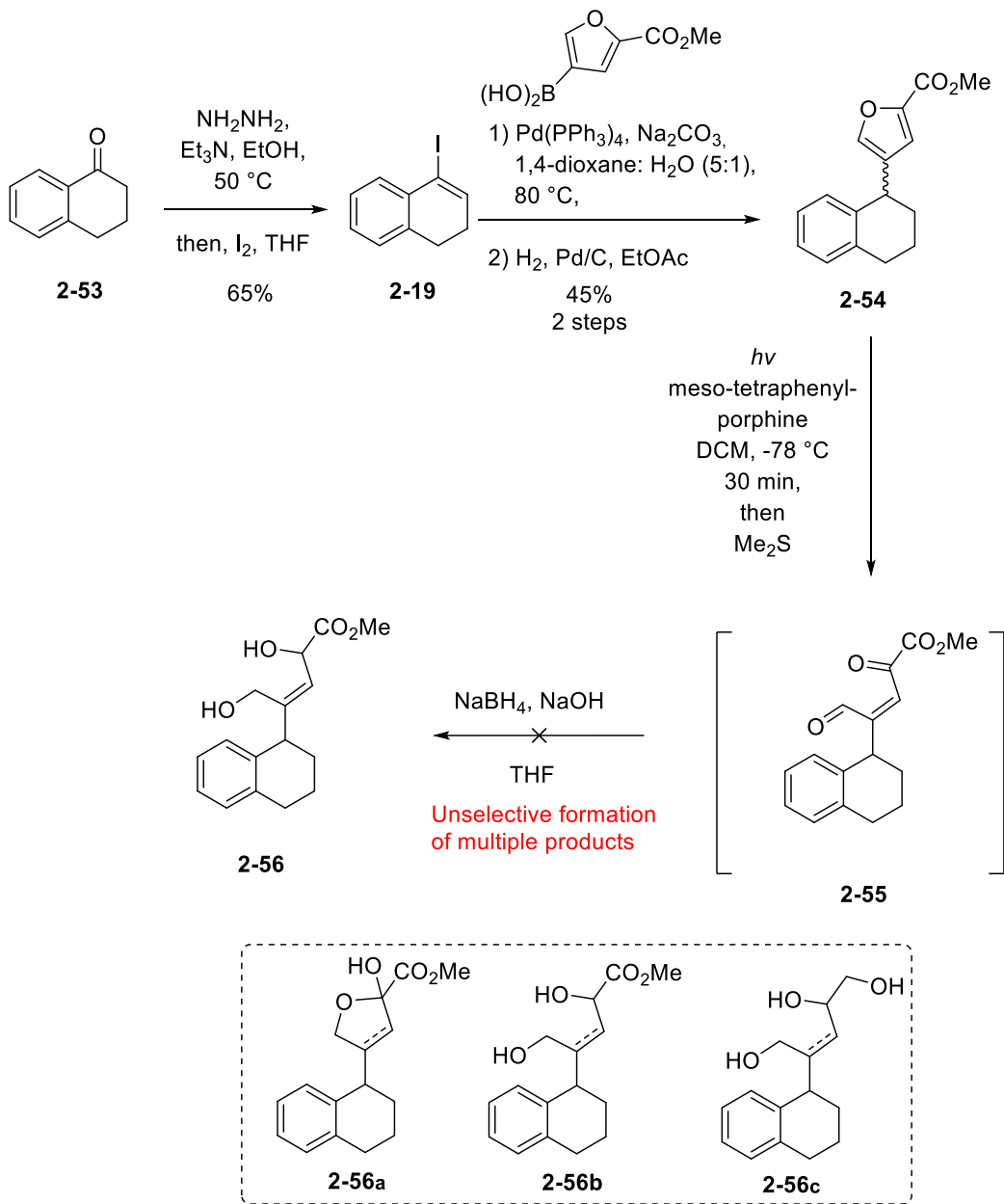


**Figure 2.18.** Model studies with C5' ester containing furan (by Dr. Khatri).

To provide a more stable intermediate for the reduction after the  $^1\text{O}_2$  cycloaddition, we surmised the use of an ortho-ester protecting group to hopefully sustain the reduction conditions. This compound was synthesized and investigated by Dr. Khatri using the **2-57** and forming an acid chloride to esterify with 3-methyl-3-oxetanemethanol, followed by  $\text{BF}_3 \cdot \text{OEt}_2$  to give compound

**2-58** in 52% yield over 3 steps. Stannylation provided **2-59** in 90% and Stille cross-coupling gave compound **2-60** in 85% yield. However, when this compound was subjected to hydrogenation conditions led to opening of the ortho-ester and yielded no productive reaction. Further efforts to optimize this reaction by controlling the reaction parameters did not lead to significant improvements.

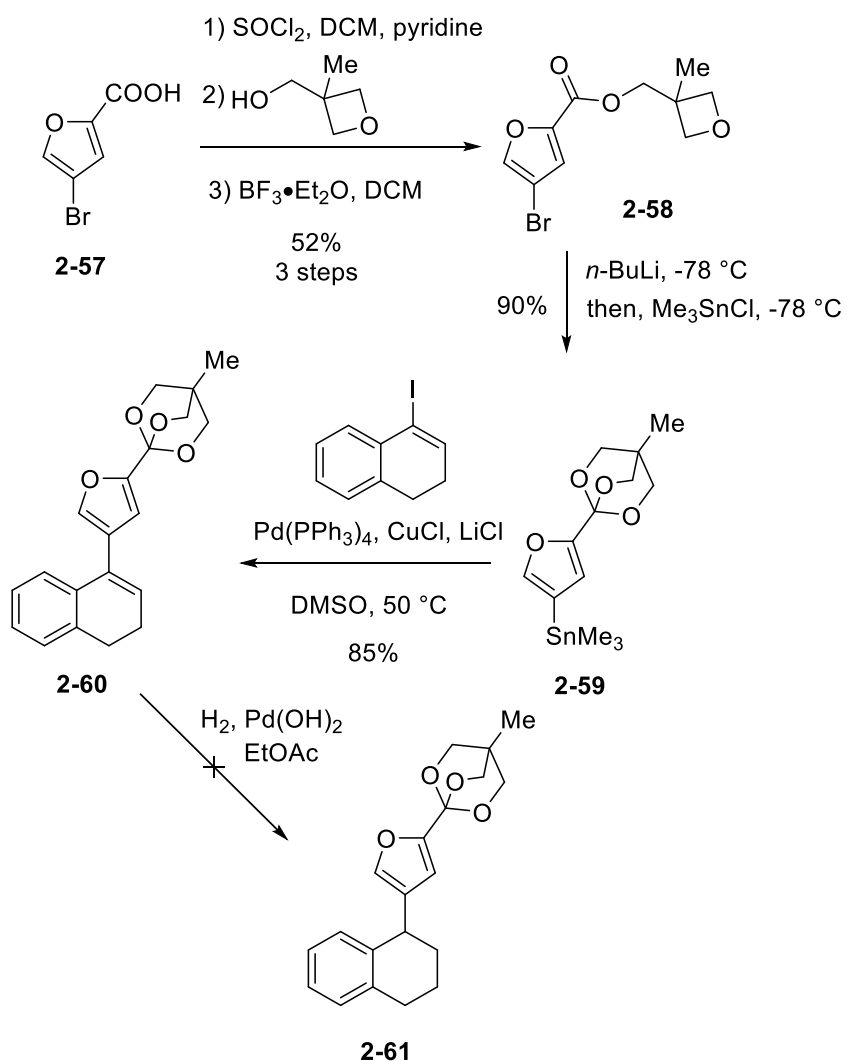


**Figure 2.19.** Model studies with C5' ortho-ester containing furan (by Dr. Khatri).

We surmised that the conversion of the methyl ester into more sterically hindered and electronrich triisopropylsilyl (TIPS)-ester would prevent the overreduction for the NaBH<sub>4</sub> reduction process, and our subsequent studies focused on exploring this modified route (*cf.* Figure 2.20). Using **2-57**, Suzuki coupling was performed giving **2-62** in 80% yield. Next, **2-62** was dissolved in anhydrous THF and protected using triisopropylchlorosilane and triethylamine to provide **2-63** in 69% yield after chromatography. When compound **2-63** was subjected to photooxidation with <sup>1</sup>O<sub>2</sub>, the consumption of starting material was observed by TLC analysis and confirmed by HRMS analysis. However, in the subsequent reduction step with sodium borohydride, the reaction yielded no desired product **2-64**. TLC showed that some side products had been formed that were much more polar than the starting material. When the crude material was analyzed by <sup>1</sup>HNMR and HRMS, the major observable product appeared to be overreduction product **2-64a**. Further efforts to optimize this reaction by controlling the reaction parameters did not lead to significant improvements.

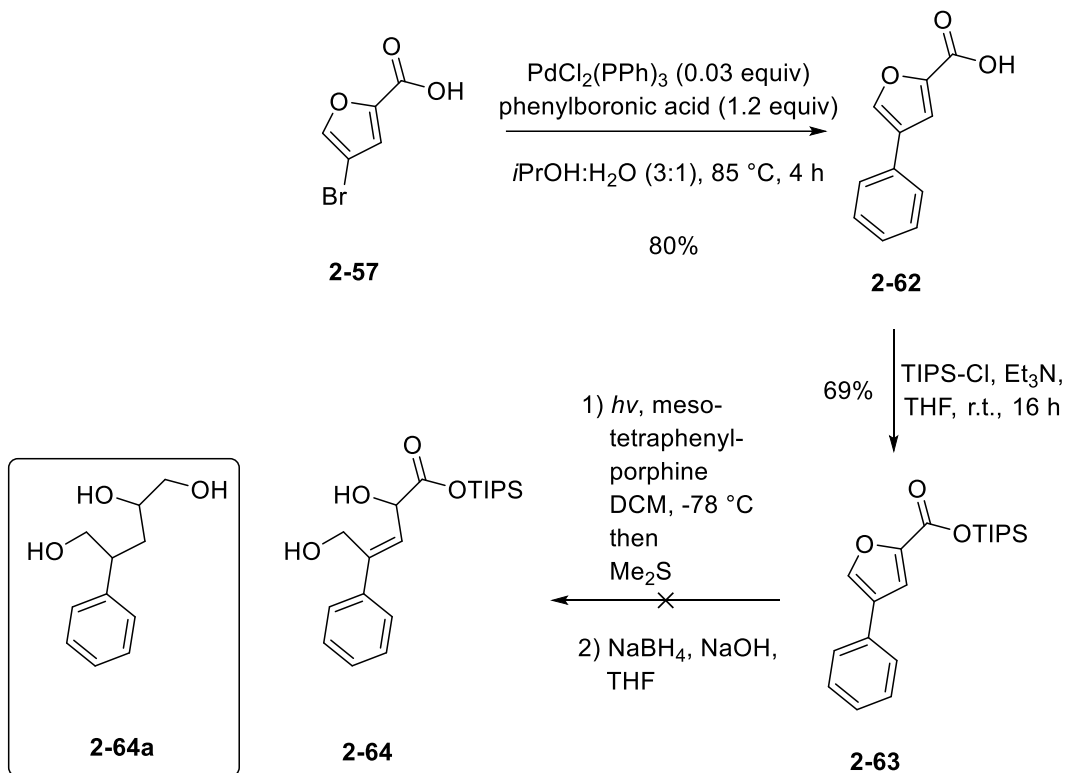


**Figure 2.20.** Model studies with C5'-OTIPS furan ester.

With the evidence that using esters as the C5'-protecting groups was not productive, we subsequently explored amides as more robust alternatives (*cf.* Figure 2.21). Therefore, our studies commenced with exploring the oxidation/reduction/rearrangement sequence with furan amide **2-66** as the model. This substrate was conveniently generated via a 3-step sequence. These steps involved forming an acid chloride from **2-57**, followed by substitution with diisopropylamine to form **2-65** (60% yield, 2 steps). This substrate was then subjected to a Suzuki coupling with phenylboronic acid to provide substrate **2-66** in 65% yield. This was carried on performing the photosensitized singlet oxygen Diels-Alder cycloaddition to give intermediate **2-67**, which was directly subjected to the previously attempted reduction conditions to provide the isolatable intermediate **2-68** in 75% yield. Gratifyingly, subjecting **2-68** to *p*-TsOH (30 mol%) in toluene at 50 °C for 16 h resulted in the formation of the cyclized product **2-69**. Considering that this

compound was stable to the reaction conditions, additionally, only **2-69** was observed, *p*-TsOH (2 equiv in total) was added to finally produce the desired product **2-70** in 50% yield after additional 16 h of stirring at 50 °C.

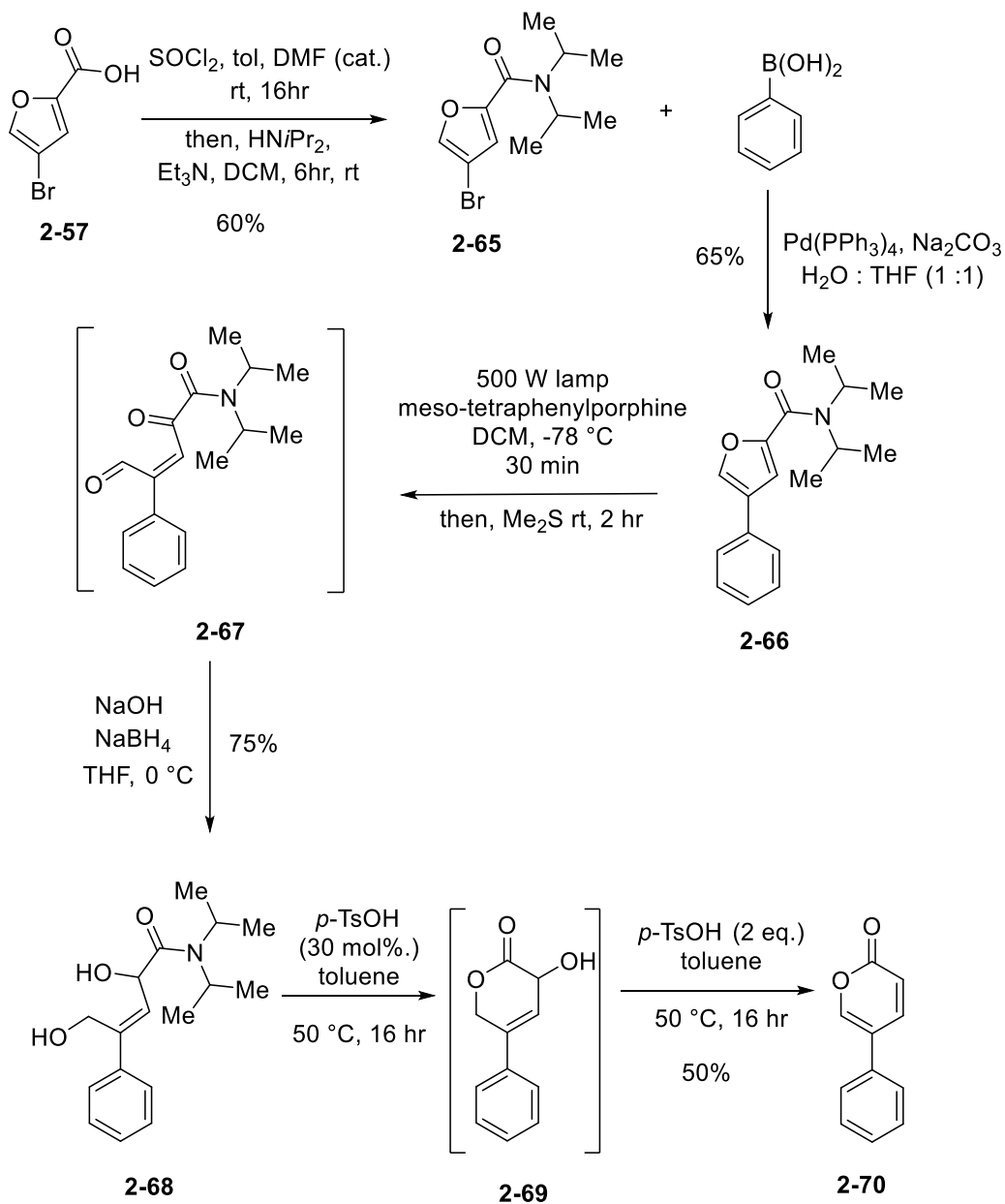
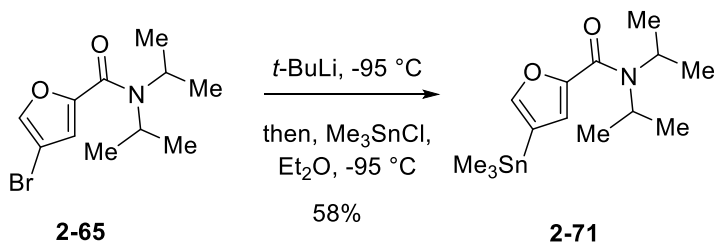


**Figure 2.21.** Initial diisopropyl furan amide test reactions (by Dr. Khatri).

With these encouraging results in hand, we wanted to further explore this transformation by

using a steroid-derived vinyl-iodide model containing pre-installed  $\beta$ 14-hydroxyl group protected as a trimethylsilyl ether. First, compound **2-65** was transformed into the stannane **2-71** in 58% yield.



**Scheme 2-11** Synthesis of **2-76** (by Dr. Khatri).

As before, we used a Stille reaction to conduct the cross-coupling of **2-72** and furfurylstannane **2-71** that resulted in product **2-73** (65% yield), which was subjected to hydrogenation over Pd/C to produce **2-74** as a single diastereomer (70% yield). This product was subjected to the singlet oxygen photooxidation the desired intermediate **2-75** which was observed via HRMS analysis. Next, the solvent was removed *in vacuo* and then redissolved in THF while being kept at 0 °C in an ice bath to which 2M NaOH and NaBH<sub>4</sub> were added, and the reaction was stirred at 0 °C while being monitored HRMS and TLC analysis to detect the consumption of starting material. Once conversion of starting material was completed, the reaction was quenched, and chromatography was performed to isolate compound **2-76**. The desired product **2-76** was detected by HRMS, however, there was also a complex mixture of other compounds present that could not be effectively separated from **2-76**. This complex mixture was then subjected to cyclization with *p*-TsOH. Catalytic amounts of *p*-TsOH were chosen for this reaction to better control the reaction and to suppress side reactivity, like  $\beta$ C14-OTMS elimination due to the acidic and high temperature conditions.

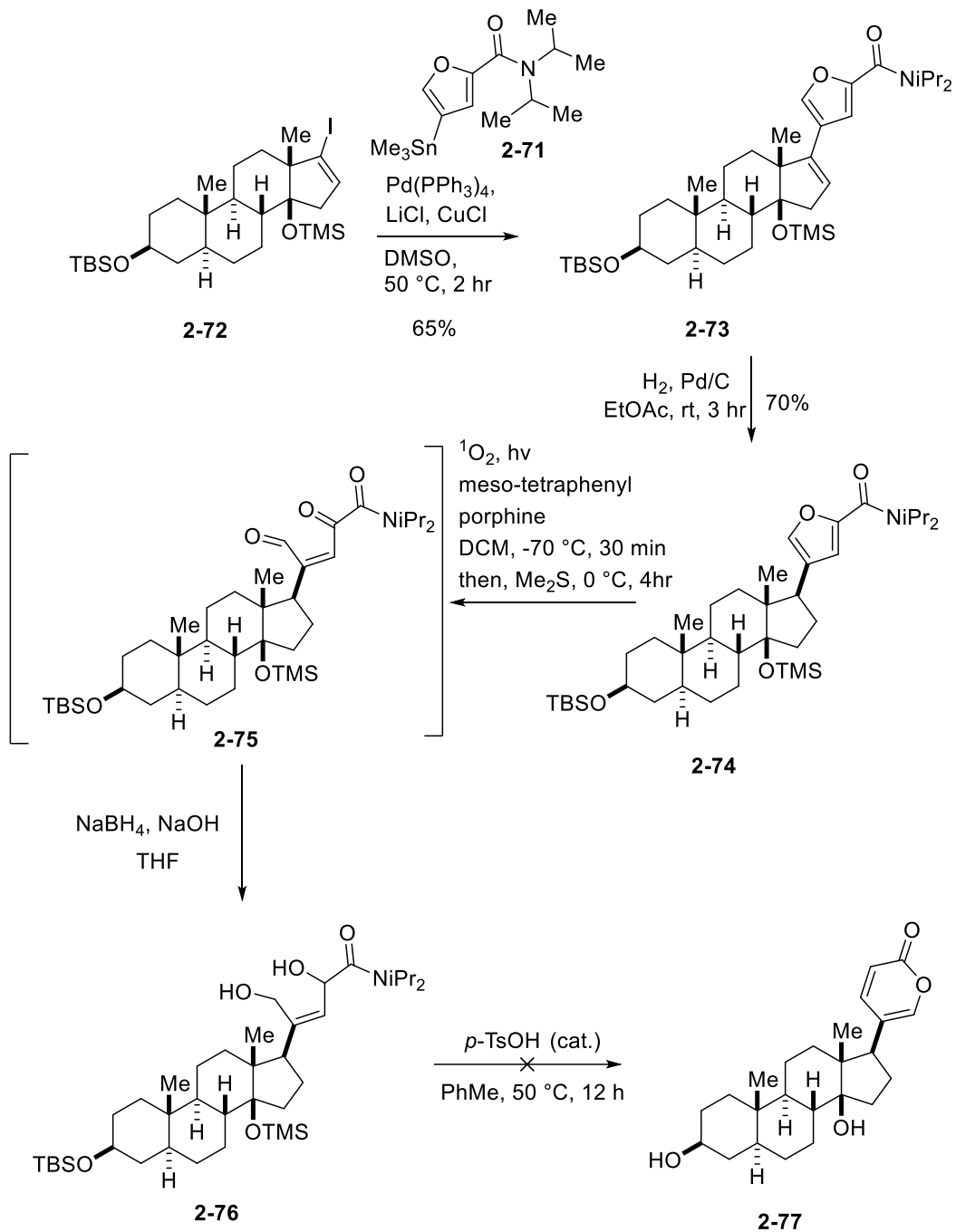


**Figure 2.22.** Diisopropylfuran amide on model steroid (with Dr. Khatri)

While monitoring the reaction, it was observed by TLC analysis that a more polar spot was forming over time, however no desired cyclization product could be detected by HRMS analysis. The reaction was allowed to progress to completion and then quenched and extracted.

Crude  $^1\text{H}$ NMR analysis of the residue revealed that no pyrone  $^1\text{H}$ NMR characteristic peaks were observed, rather, butenolide peaks could be identified. While initially puzzling, the formation of **2-74** is not completely unexpected, and its formation could be explained by the mechanism depicted in Figure 2.23. A hypothesis for the side product formation during the initial Diels-Alder cycloaddition product, intermediate **2-74a** could be envisioned as the initial transition state but, instead could proceed to an anhydride-like intermediate **2-74b** via oxygen insertion between the amide and furan ring system. **2-74b** under basic reductive conditions, would then form a primary alcohol which could then attack the 5-membered position due to the proximity of the two electrophilic sites of the anhydride system.

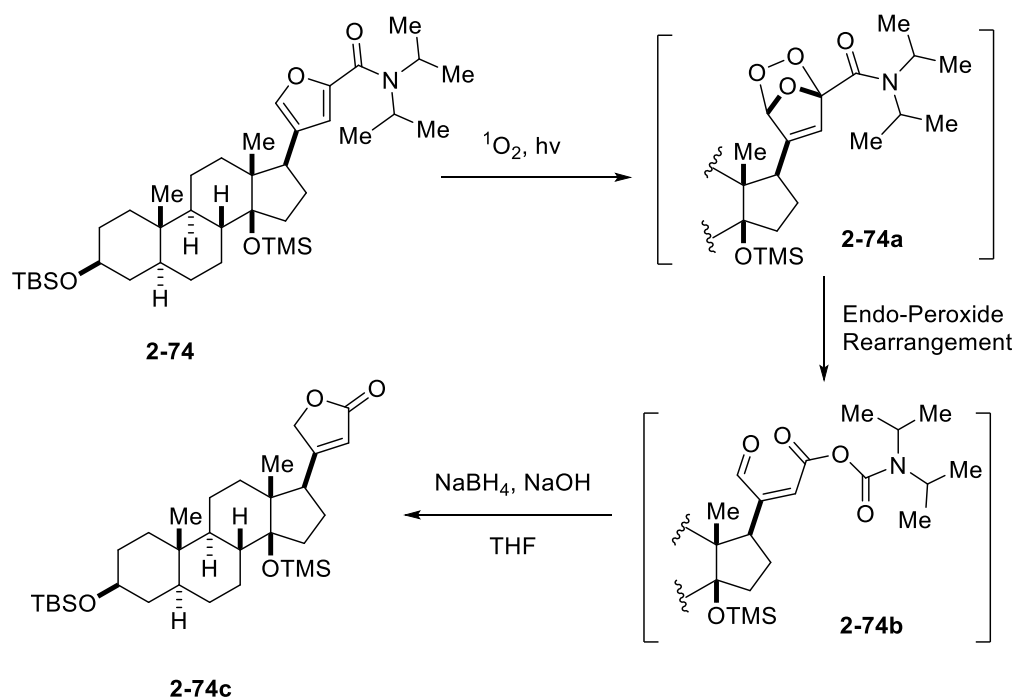


**Figure 2.23.** Proposed side product formation mechanism (by Dr. Khatri).

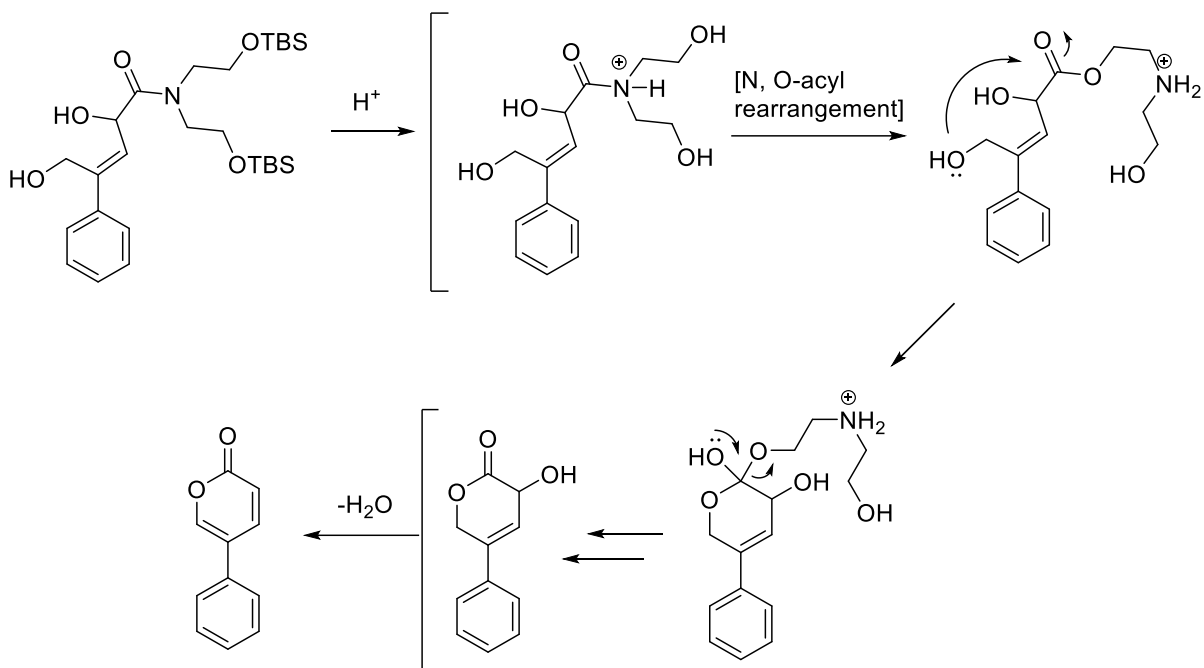
The issue involved from this side product formation could be attributed to the  $\text{NaBH}_4$  reduction step. If the reaction solution was permitted to warm to a higher temperature, more complex decomposition products could be observed since the aldehyde moiety is more susceptible to



reduction and allow this to prematurely cyclize to form a 5-membered ring progressing to the butanolide side product. We approached this issue by keeping the reduction at a low temperature and instead of concentrating to dryness, THF and NaBH<sub>4</sub> were added immediately to increase the formation of **2-76** which could be detected by HRMS analysis. However, during the acid cyclization step, only C3-deprotected steroid could be observed with no cyclization product, even with higher temperatures or by adding more *p*-TsOH equivalents.

### 2.6.2 Furan-endoperoxide rearrangement toward forming alpha-pyrones: Generation 2

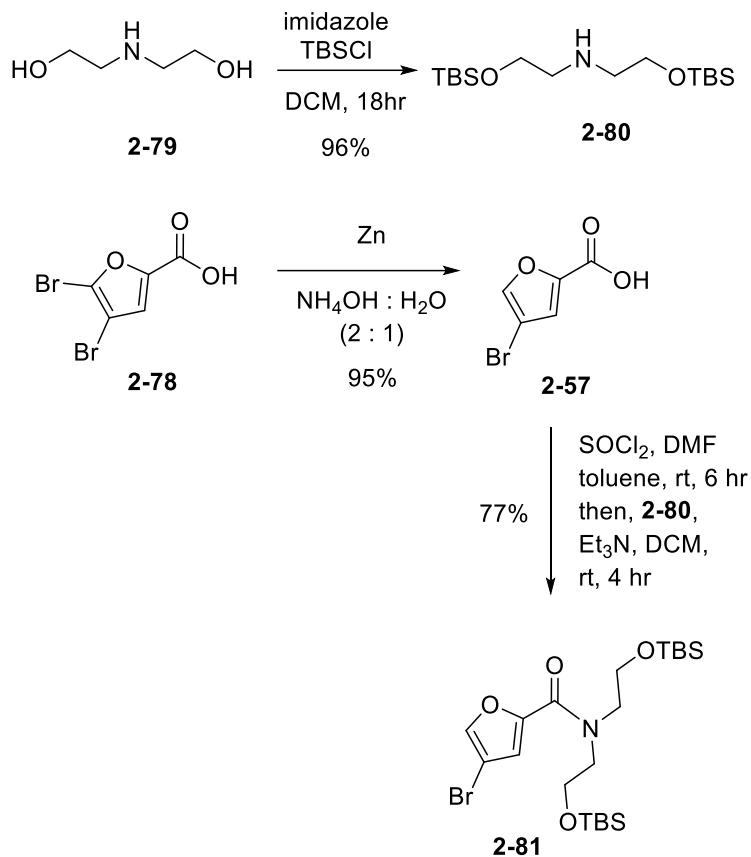
With the issues encountered with the previously mentioned design with the diisopropylamide moiety, we wanted to see if there could be a way to speed up the 6-membered lactone formation by potentially transposing the amide to an ester *in situ* to allow for faster cyclization. To improve upon the issues encountered during the cyclization this original design, we envisioned changing the appendage of the amide system to include a diethanolamine substituent to behave in future acid-catalyzed cyclization reactions like an ester via a *N,O*-acyl rearrangement mechanism (*cf.* Figure 2.24).



**Figure 2.24.** Proposed mechanism for N,O- acyl rearrangement.

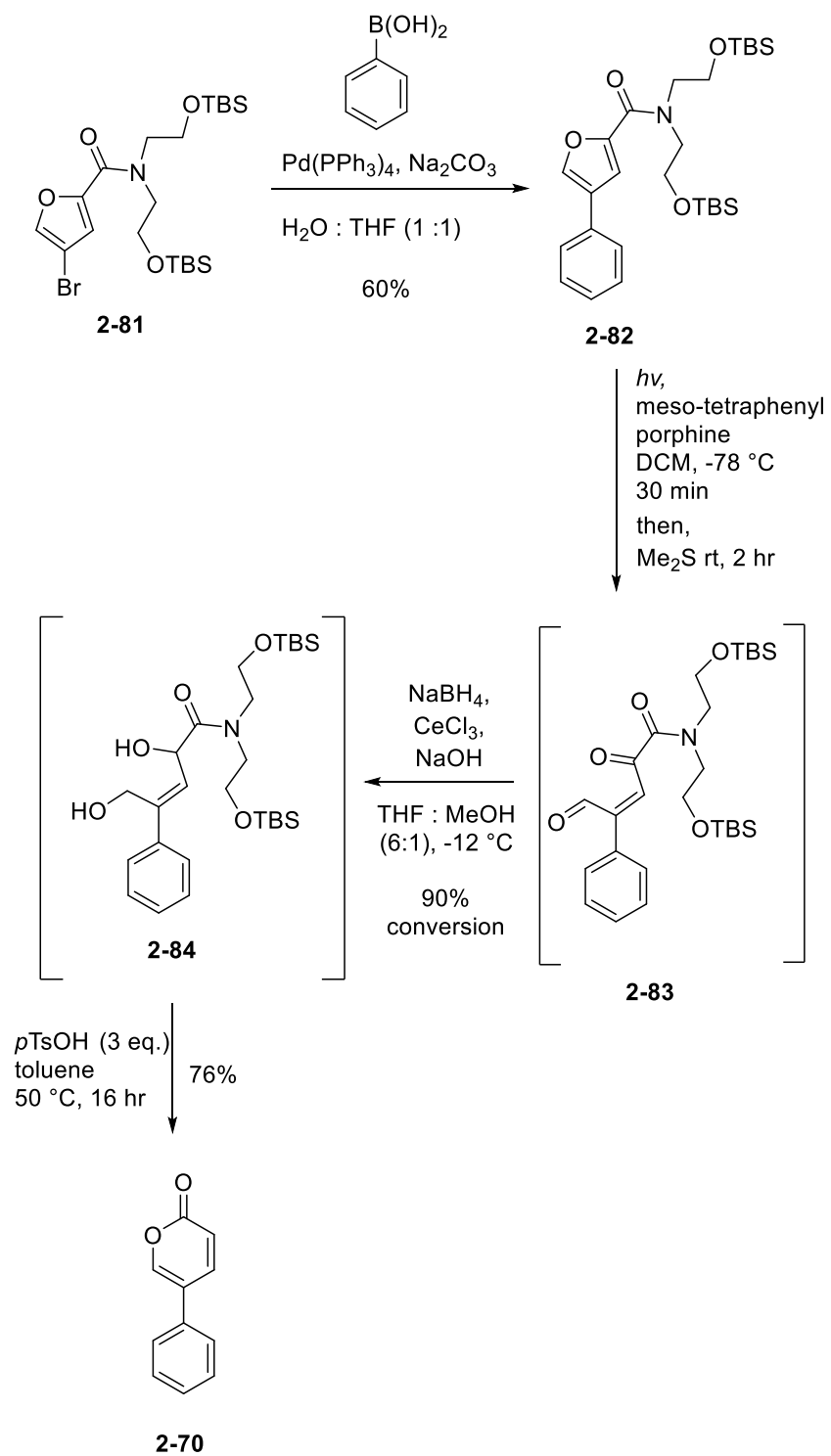
The mechanism proposes that during the acid cyclization stage, due to the acidic environment, the *tert*-butylsilyl protecting groups would be cleaved allowing for an *N,O*-acyl rearrangement, providing an ester in place of the more stable amide. This would potentially allow for a more reactive intermediate to give the 6-membered cyclic lactone and subsequent dehydration to allow pyrone formation.

To begin the synthesis, the dibromofuran acid **2-78** was reduced via aqueous-Zn conditions to yield compound **2-57** in 95% yield and a tangential synthetic step of changing **2-79** into **2-80** via TBS-protection in 96% yield. These products were then combined by first forming an acid chloride of **2-57** and then performing a nucleophilic attack with the amine **2-80** to obtain **2-81** in 77% yield.



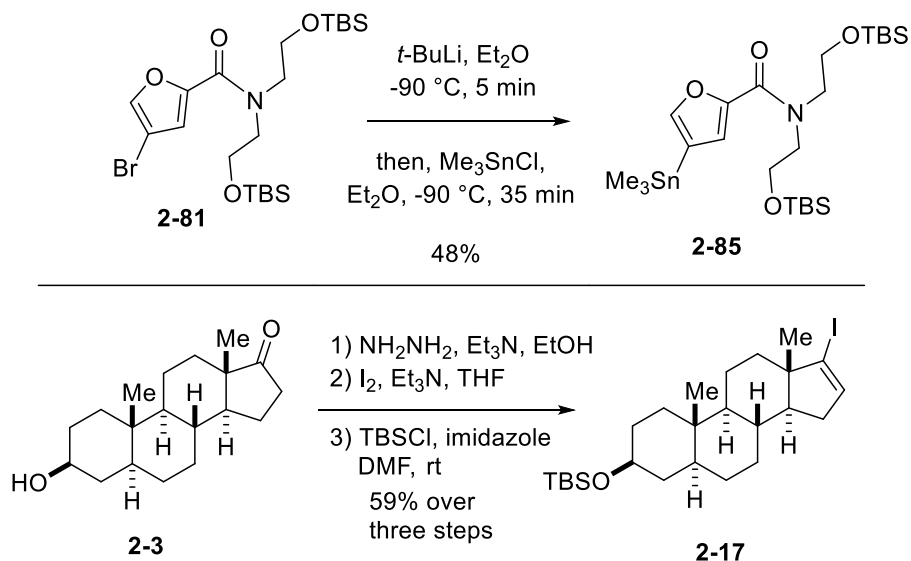
**Figure 2.25.** Synthesis of **2-81**.

**2-81** was then subjected to a Suzuki reaction to obtain model compound **2-82** in 60% yield. This product was subjected to the previously developed singlet oxygen photooxidation of furan (*cf.* Figure 2.21) followed by DMS-promoted cleavage of the resultant endoperoxide. To further improve this protocol and eliminate conjugate reduction side-products, the resultant aldehyde **2-83** was subjected to Luche reduction conditions to obtain intermediate **2-84** in 90% conversion. This allowed for suppression of 1,4-reduction of the allylic alcohol double bond. With this intermediate, the cyclization leading to pyrone product **2-70** was tested next using the acidic conditions previously developed. Gratifyingly, the exposure of **2-84** to *p*-TsOH (3 equiv.) in toluene at 50 °C, led to a significantly faster formation of  $\alpha$ -pyrone **2-70**, which was formed in 76% yield over the course of 16 hours.



**Figure 2.26.** Further optimization of furan amide cyclization

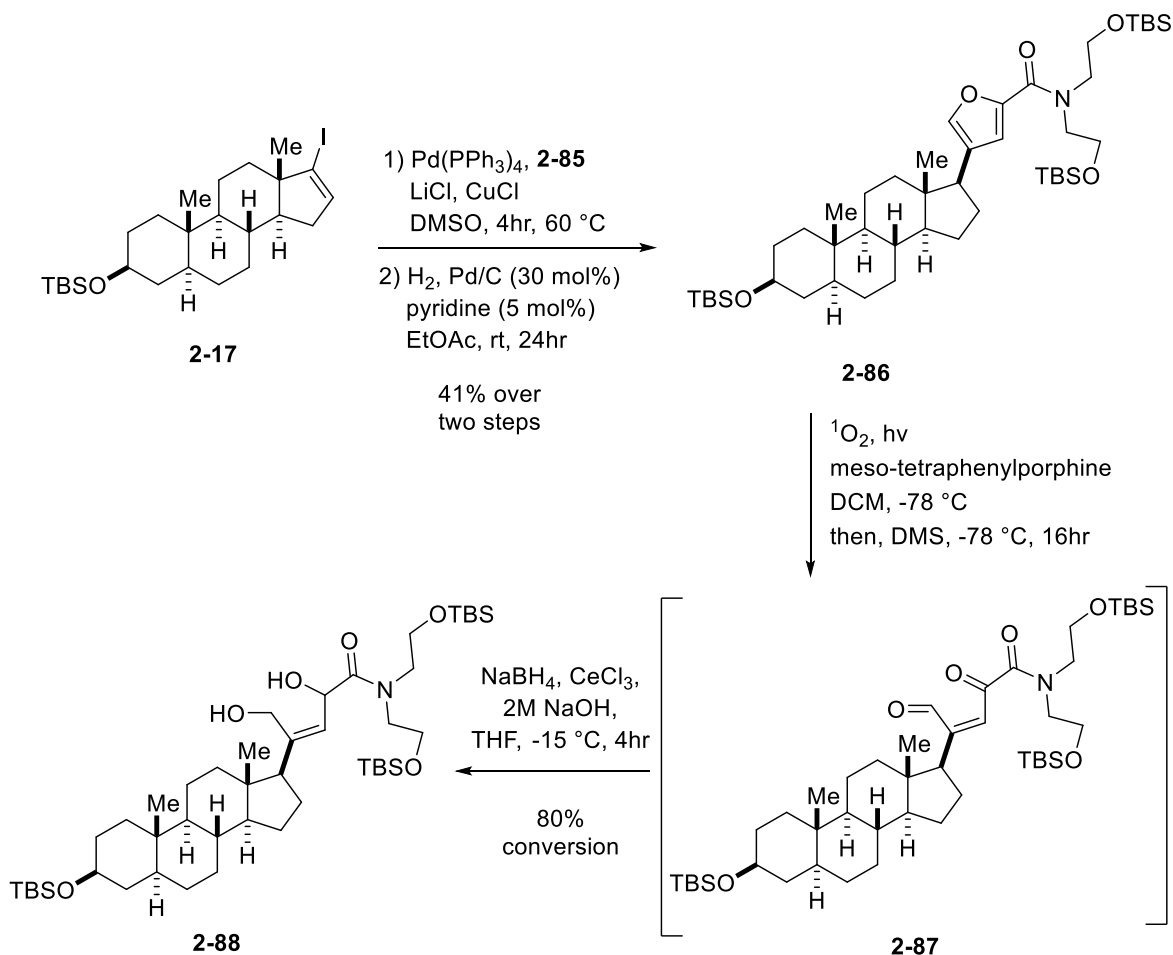
With the viable strategy for interconverting the furan-to- $\alpha$ -pyrone interconversion in hand, our subsequent studies focused on applying this strategy to the more complex steroidal system.



**Figure 2.27.** Synthesis of **2-85** and **2-17** for model steroid studies.

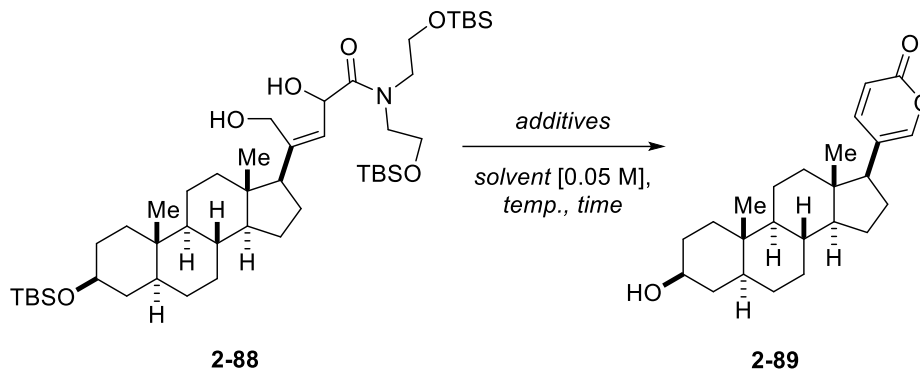
These studies commenced with stannylation of **2-81** leading to **2-85** in 48% yield, which was accomplished by subjecting **2-81** to lithium/halogen exchange with  $t\text{-BuLi}$  ( $-90\text{ }^\circ\text{C}$ ,  $\text{Et}_2\text{O}$ ) and subsequent reaction of the resultant lithiated furan with  $\text{Me}_3\text{SnCl}$ . Compound **2-85** then underwent a Stille reaction with vinyl iodide **2-17**, which was produced from **2-3** in 3 steps and 59% overall yield. The resultant cross coupling product was subjected to hydrogenation reaction using  $\text{Pd/C}$  deactivated by pyridine to obtain compound **2-86** as a single diastereomer in 41% yield (2 steps). This product was subjected to previously developed singlet oxygen photooxidation conditions. The resultant endoperoxide was reduced with a large excess of DMS for 16 h in a cryo-cool bath until the starting material peaks had disappeared by NMR. Thus, producing crude product **2-87** was then submitted to Luche reduction conditions ( $\text{NaBH}_4$ ,  $\text{CeCl}_3 \cdot 7\text{H}_2\text{O}$ , 2M  $\text{NaOH}$ ,  $\text{THF}$ ,  $-15\text{ }^\circ\text{C}$ ) to access diol **2-88** which was confirmed by HRMS analysis. Compound **2-88** was stable to

chromatography but prolonged exposure to silica gel caused decomposition of the product which was isolated as a complex mixture of diastereomers and reduction side-products. This was advanced forward regardless.



**Figure 2.28.** Synthetic route for building intermediate **2-88**.

Initial attempts to cyclize **2-88** were to first investigate *p*-TsOH (Entry 1, Table 2.3). The reaction was monitored by TLC and HRMS to observe the consumption of starting material. After starting material was consumed, the reaction was quenched with sat. aq.  $\text{NaHCO}_3$  and the reaction was extracted with EtOAc. Crude  $^1\text{H}$ NMR and HRMS analysis showed that instead of the desired

**Table 2.3.** Attempts of cyclizing furan amide **2-88** to pyrone.

Entry	Additive	Equiv.	Solvent	Temp (°C)	Time	Conversion <sup>a</sup>	Results <sup>b</sup>
1	<i>p</i> -TsOH	2	PhH	50	12 h	>90%	decomposition
2	<i>p</i> -TsOH	2	PhMe	70	12 h	>90%	decomposition
3	TFA	2	PhMe	25	6 h	>90%	amide cleavage
4	<i>p</i> -TsOH	3	MeCN	75	12 h	>90%	decomposition
5	HF•H <sub>2</sub> O	3	MeCN	25	1 h	>90%	deprotection
6	<i>p</i> -TsOH	0.3	PhMe	75	3 d	<20%	complex mixture
7	Zn(OTf) <sub>2</sub> , DEC	0.05	PhMe	100	18 h	>90%	amide cleavage
8	Zn(OTf) <sub>2</sub> , DEC	0.5	MeOH	75	12 h	>90%	amide cleavage

<sup>a</sup> Monitored by TLC and HRMS analysis for consumption of starting material. <sup>b</sup> Based on the <sup>1</sup>H NMR analysis of the crude reaction mixture.

product, it appeared that the C3-OTBS protecting group had been cleaved and that no characteristic signal peaks for compound **2-89** were present by <sup>1</sup>H NMR or HRMS analysis. It appeared as though the reaction simply decomposed the pyrone moiety altogether. Next, we wanted to investigate if the temperature or solvent change to toluene could influence the reaction (Entry 2), but the results were similar to Entry 1. It seems that *p*-TsOH was too harsh to promote the desired cyclization. We attempted to use a milder acid with trifluoroacetic acid (TFA). We also wanted to suppress any decomposition pathway, so the reaction was run at room temperature. The reaction was

monitored by TLC and the reaction seemed to consume all the starting material. However, HRMS analysis of the crude reaction revealed that free amide **2-80** was observable, with what appeared to be amide cleavage side product **2-90** was observed by HRMS analysis (HRMS (ESI-TOF): calculated for chemical formula:  $C_{30}H_{52}O_5SiNa$ : 553.3919; Found: 553.3890). Interestingly, the C3 protecting group remained under the acidic conditions.

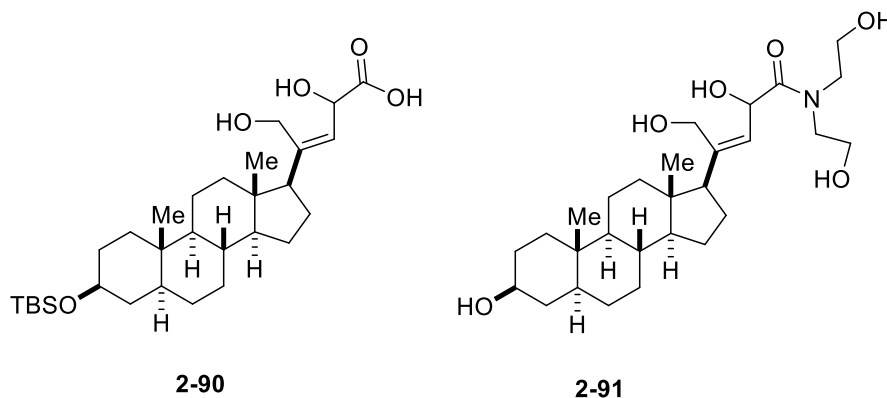


**Figure 2.29.** Proposed observed side products from crude HRMS analysis of experiments in Table 2-3.

We decided to investigate  $HF \cdot H_2O$  to help with faster removal of the silyl protecting groups. Unfortunately, only full deprotection of the compound was observed without any cyclization products **2-91** (*cf.* Figure 2.29). Even with catalytic amounts of *p*-TsOH were used, only a complex mixture of products was observed with no evidence of the partial or fully cyclized products by  $^1H$  NMR or HRMS analysis. Since the cyclization of **2-88** to product **2-89** did not prove to be a trivial transformation, we looked through the literature to find inspiration and discovered a report from Nishii<sup>19</sup> where they used catalytic  $Zn(OTf)_2$  in presence of diethyl carbonate an exogeneous alcohol to achieve amide cleavage through a proposed *N,O*-acyl rearrangement. Nishii's conditions were applied in Entry 7 of Table 2.3. The results of the reaction only led to an amide cleavage product **2-90**, which was observed by HRMS analysis. When the reaction conditions were adjusted to be



used in MeOH (Entry 8), the same result was obtained. Although it was gratifying to see that the reaction was removing the amine, it appears that the desired cyclization for the 6-membered ring system will need further optimization.

## 2.7 Conclusions

In summary, the work described in this chapter shows the importance of bufadienolides while also showcasing how fragile they are to work with due to the duality of the pyrone being both a sensitive conjugate carbonyl that can coexist between two *cis*-alkene systems, with one being within the pyrone ring itself, and the other between the pyrone ring and the  $\Delta^{16}$ -steroid alkene. Pyrones also share characteristics with aromatic compounds, where conditions that can reduce them, can be sometimes engage with the pyrone moiety. All in all, discoveries towards the development of synthetic methods for making bufadienolides is a worthy development. There is still a considerable vacancy for methods describing how to make bufadienolides efficiently, with or without any complex functional groups present. This makes the development of methods for making bufadienolides a worthy endeavor, especially for medicinal chemistry studies. Since most bufadienolides are isolated from extracts of natural sources, their inherent scarcity leads to a limited amount of isolatable compounds. This limits scientific knowledge and understanding of therapeutic potential and interactions. Together with their side effects and adverse drug interactions, this class of therapeutics would require more investigations before they are included among standard medicines.

This chapter described multiple methods and investigations into each one to develop a deeper understanding of the overall reactivity and developing novel strategies for synthesizing bufadienolides.

The first method described in Section 2.2, deals with the most direct approach, selective hydrogenation of the  $\Delta^{16}$ -steroid alkene in the presence of the pyrone. While literature precedent is known for selective hydrogenation of pyrone-steroid compounds, no reports have been established with a  $\beta$ -C14 hydroxyl substituent. During our investigations, it was found that even with an additional protecting  $\beta$ -C14-OTMS group, the extra conjugation within the molecule's structure gives an unusual system that behaves as two *cis*-diene olefin systems. This in turn proved challenging to overcome via direct methods, which sheds some light on why this direct method has not been fully elucidated. With the direct route not being as facile a process, this led us to investigate if the olefins have inherent reactivity differences. When comparing the model substrate to a protected bufalin comparison model in identical bomb-reactor conditions, it was discovered that as the hydrogenation reaction proceeds, the least hindered alkene that is also in  $\alpha,\beta$ -conjugation with the lactone, appears to react first. Even with optimizations for hydrogen pressure, catalyst loading, or time, the reaction appeared uncontrollable. This at least gives us insight that we can use with future developments of enhancing or suppressing the reactivity of the different alkenes.

The second method investigated was with the full hydrogenation strategy. Moreover, the general sensitivity of the pyrone moiety itself introduces other challenges for what catalysts can be used without destroying the cyclic lactone. With our catalyst screening, we have found optimized catalyst loading conditions for reducing the pyrone alkenes with minimal cyclic lactone opening loss. Along with the indene model, the method appears to work on the steroid model as well. This method allows for a bench and air stable protocol with Rh/Al<sub>2</sub>O<sub>3</sub> under elevated hydrogen pressures. Adjustments will need to be made due to complex mixture of over and under

reduced side products, and the loss of product due to pyrone ring opening. Further developments will need to be investigated

The third method, which correlates with the second method described previously, was to investigate re-oxidizing the cyclic lactone. Initially, we investigated developing a single-pot oxidation procedure that utilizes the enhanced reactivity of the silyl enol ether form of the cyclic lactone. From there, model studies and optimizations found a reasonable conversion ratio for promoting  $\delta$ -valerolactone to be turned into an  $\alpha$ -pyrone. However, when trying to form the silyl enol ether on the model steroid system, the transformation was not successful. This could be due to the silyl enol ether in this case not being stable under the established reaction conditions on the steroid system compared to the model. It had been noted that the silyl enol ether of the  $\delta$ -valerolactone would degrade over time automatically. We also utilized the recently published work from the Dong group to observe if the mono-oxidation could at least be possible. Minimal success was found with the indene-lactone model but not on the steroid-lactone model. Further optimizations need to be investigated to improve upon this initial hit.

With the difficulties surrounding the selective hydrogenation of the pyrone-  $\Delta^{16}$ -steroid, we took inspiration from Wiesner's method of novel synthetic method for transforming furans-carbonyls into pyrones via an endo-peroxide, singlet-oxygen Diels-Alder rearrangement. This method allowed for one of the first total syntheses of bufalin and related derivatives from a common starting intermediate in testosterone or digitoxigenin. The limitations of their method includes the total step count of their route and how different stereocenters are incorporated and manipulated. We aimed to create a more efficient process of making pyrones from furan amides which could eliminate the additional oxidation operation that Wiesner's needs to recognize. For our route, instead of performing nucleophilic attack on a C17 ketone, Barton iodination was

utilized to bypass any selectivity issues from substitution and can be cross-coupled to install a furan amide efficiently. This can then be hydrogenated to give one diastereomer at the C17 positions exclusively. The process for singlet oxygen developed by Wiesner was followed to good success, along with the reduction phase. On a model phenyl substrate, our furan amide substrates were worked well with acid cyclization with *p*-TsOH. The issue came when applying the method on a steroid model system. Even with changing temperatures, solvents, or acidic reagents, only complex or decomposition pathways were observed.

With these challenges, we look to the future by focusing on other mild conditions for promoting the cyclization of the bis-allylic alcohol toward making pyrones by looking at other examples of transition metal-assisted lactonization of amides with CeO<sub>2</sub><sup>20</sup>, Sc(OTf)<sub>3</sub><sup>21</sup>, and TiCl<sub>4</sub><sup>22</sup> as potential methods that can be utilized in future studies of bis-allylic alcohol lactonization.

## **2.8 Experimental information**

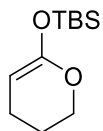
### **Methods and Reagents:**

Unless otherwise stated, all reagents were purchased from commercial suppliers and used without further purification. Tetrahydrofuran (THF), dichloromethane (DCM), toluene (PhMe), dimethylformamide (DMF) and diethyl ether (Et<sub>2</sub>O) were filtered through a column (Innovative Technology PS-MD-5) of activated alumina under nitrogen atmosphere. All reactions were carried out under an atmosphere of nitrogen in flame- or oven-dried glassware with magnetic stirring, unless otherwise noted. Reactions were cooled using Neslab Cryocool CB-80 immersion cooler (0 to -60 °C) and Neslab Cryocool immersion cooler CC-100 II, or via external cooling baths: ice water (0 °C), sodium chloride/ ice water (-10 °C), or dry ice/acetone (-78 °C). Heating was achieved by use of a silicone bath with heating controlled by electronic contact thermometer.

Deionized water was used in the preparation of all aqueous solutions and for all aqueous extractions. Solvents used for extraction and chromatography were ACS or HPLC grade. Purification of reactions mixtures was performed by flash column chromatography on SiO<sub>2</sub> using SiliCycle SiliaFlash P60 (230-400 mesh). Diastereomeric ratios were determined by <sup>1</sup>H NMR analysis. Enantiomeric excess was determined by HPLC analysis using a Waters e2695 Separations Module with a Waters 2998 photodiode array detector.

### Instrumentation:

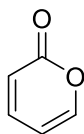
All spectra were recorded on Varian vnmrs 700 (700 MHz), Varian vnmrs 500 (500 MHz), Varian MR400 (400 MHz), Varian Inova 500 (500 MHz) spectrometers and chemical shifts ( $\delta$ ) are reported in parts per million (ppm) and referenced to the <sup>1</sup>H signal of the internal tetramethylsilane according to IUPAC recommendations. Data are reported as (br = broad, s = singlet, d = doublet, t = triplet, q = quartet, qn = quintet, sext = sextet, m = multiplet; coupling constant(*S*) in Hz; integration). High resolution mass spectra (HRMS) were recorded on MicromassAutoSpecUltima or VG (Micromass) 70-250-S Magnetic sector mass spectrometers in the University of Michigan mass spectrometry laboratory. Infrared (IR) spectra were recorded as thin films on NaCl plates on a Perkin Elmer Spectrum BX FT-IR spectrometer. Absorption peaks were reported in wavenumbers (cm<sup>-1</sup>).



**Compound 2-23:** *N,N*-diisopropylamine (1.05 mL, 7.5 mmol, 1.5 equiv.) was added to anhydrous THF (7.2 mL) and chilled to -78 °C. Then, *n*-BuLi (3.34 mL, 7.5 mmol, 1.5 equiv.) was added to the reaction solution, and warmed to 0 °C for 15 mins, and then cooled back down to -78 °C. Then,  $\delta$ -valerolactone (500 mg, 4.9 mmol), was added to the reaction solution dropwise and the solution

was stirred for 1 h at -78 °C. Next, a solution of TBSCl (1.3 g, 7.5 mmol, 1.5 equiv.) in THF (7 mL) was added to the reaction solution and left to stir for 1 h at -78 °C. The reaction was then left to warm to room temperature where then the volatiles were removed *in vacuo*. The crude material was then dissolved in pentane (7 mL), filtered through a syringe filter, then concentrated *in vacuo*. The residue was used without further purification as a yellow sticky oil (700 mg, 3.26 mmol, 65% yield). Characterization data was taken with crude <sup>1</sup>H NMR analysis.

<sup>1</sup>H NMR (500 MHz, C<sub>6</sub>D<sub>6</sub>): δ 4.01 (t, *J* = 3.7 Hz, 1H), 3.75 – 3.69 (m, 2H), 1.87 (td, *J* = 6.4, 3.6 Hz, 2H), 1.40 – 1.36 (m, 2H), 1.01 (s, 9H), 0.23 (s, 6H).



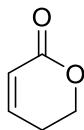
**Compounds 2-9:** Silyl enol ether **2-23** (20 mg, 0.09 mmol), Cs<sub>2</sub>CO<sub>3</sub> (91 mg, 0.28 mmol, 3.0 equiv) were added to a 4 mL flame-dried vial. The contents were transferred to a nitrogen filled glovebox. Then, Pd(TFA)<sub>2</sub> (46 mg, 0.14 mmol, 1.5 eq), and Cu(OAc)<sub>2</sub> (16.5 mg, 0.06 mmol, 1.0 equiv) were added to the reaction vial. Then, anhydrous DMSO (6 mL) was added and the reaction was sparged with O<sub>2</sub> from a balloon for 15 mins and the balloon was left in to provide an O<sub>2</sub> atmosphere. The reaction was then heated to 80 °C for 18 h under an O<sub>2</sub> atmosphere. Then, the solvents were removed *in vacuo* and the crude was purified by SiO<sub>2</sub> (20% EtOAc/hexanes, R<sub>f</sub> = 0.35) to provide **2-9** in 55% yield (11 mg, 0.055 mmol) and 45% of δ-valerolactone (8 mg, 0.035 mmol, 90% brsm).

Spectral data matches reported literature <sup>23</sup>

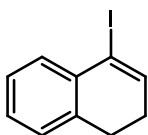
Corresponding <sup>1</sup>H NMR data to **2-9**:

<sup>1</sup>H NMR (500 MHz, CDCl<sub>3</sub>) δ 7.50 (dt, *J* = 5.2, 1.7 Hz, 1H), 7.33 (ddd, *J* = 9.1, 6.3, 2.2 Hz, 1H), 6.35 (dt, *J* = 9.5, 1.3 Hz, 1H), 6.22 (ddd, *J* = 6.3, 5.2, 1.1 Hz, 1H).

Corresponding  $^1\text{H}$  NMR data to **2-24**:<sup>24</sup>



$^1\text{H}$  NMR (500 MHz,  $\text{CDCl}_3$ )  $\delta$  6.93 (dt,  $J = 9.8, 4.2$  Hz, 1H), 6.01 (dt,  $J = 9.8, 1.9$  Hz, 1H), 4.40 (t,  $J = 6.2$  Hz, 2H), 2.44 (tdd,  $J = 6.1, 4.2, 1.8$  Hz, 2H).

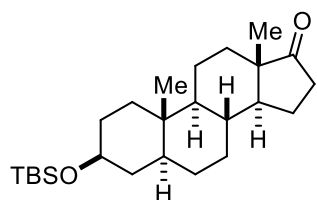


**Compound 2-19:** Hydrazine monohydrate ( $\text{N}_2\text{H}_4 \cdot \text{H}_2\text{O}$ , 10 equiv., 3.4 mL, 68 mmol) was added to a solution of tetralone **2-53** (1 g, 6.8 mmol) and  $\text{Et}_3\text{N}$  (10 equiv., 9.5 mL, 68 mmol) in absolute ethanol (120 mL). The reaction flask was flushed with  $\text{N}_2$  and heated to  $50^\circ\text{C}$  for 6 h then concentrated *in vacuo* to a black residue. The flask was removed from high vacuum and flushed with  $\text{N}_2$  before adding  $\text{Et}_3\text{N}$  (10.0 equiv., 9.5 mL, 68 mmol) and dissolving in THF (120 mL). The reaction was stirred vigorously at room temperature as a solution of  $\text{I}_2$  (4 equiv., 6.9 g, 27.2 mmol) dissolved in THF (20 mL) was added dropwise until the solution turned brown. The reaction was stirred for 10 min until the solution returned to a yellow color before adding more of the  $\text{I}_2$  solution until the brown color persisted. The reaction was stirred for 1 h at room temperature then quenched with 10 w/v%  $\text{Na}_2\text{S}_2\text{O}_3$  (100 mL). The mixture was diluted with deionized water (500 mL) then extracted with  $\text{CH}_2\text{Cl}_2$  (200 mL x 3). The combined organic layers were dried over  $\text{Na}_2\text{SO}_4$ , filtered, and concentrated *in vacuo*. The residue was purified by flash column chromatography on silica gel (Hexanes/ $\text{EtOAc} = 49/1$  to  $24/1$  to  $9/1$ ) to afford vinyl iodide **2-19** (1.13 g, 4.4 mmol) in 65% yield over 2 steps as a dark oil. TLC: 5%  $\text{EtOAc}/\text{Hexane}$ :  $0.75 = R_f$

Spectral data matches reported literature<sup>25</sup>

**<sup>1</sup>H NMR** (600 MHz, CDCl<sub>3</sub>) δ 7.52 (dd, *J* = 7.8, 2.8 Hz, 1H), 7.31 (t, *J* = 7.5 Hz, 1H), 7.24 (tq, *J* = 7.5, 1.4 Hz, 1H), 7.08 (d, *J* = 7.3 Hz, 1H), 6.89 (td, *J* = 4.9, 1.7 Hz, 1H), 2.90 (t, *J* = 8.1 Hz, 2H), 2.40 (td, *J* = 8.1, 4.9 Hz, 2H).

**<sup>13</sup>C NMR** (151 MHz, CDCl<sub>3</sub>) δ 140.2, 135.9, 134.4, 130.9, 128.4, 127.4, 127.1, 98.3, 27.9, 27.3,



**Compound 2-4:** *Trans*-androsterone **2-3** (1 g, 3.44 mmol, 1.0 equiv) and imidazole (117 mg, 1.72 mmol, 0.5 equiv.) was dissolved in anhydrous DMF (35 mL) under an atmosphere of nitrogen. Then, Et<sub>3</sub>N (1.45 mL, 10.3 mmol, 3.0 equiv), was added to the reaction flask. The reaction mixture was left to stir at room temperature for 24 h. The reaction was quenched with dI H<sub>2</sub>O and extracted with EtOAc (2x 150 mL). The organic phase was washed with a 1:1 solution of dI H<sub>2</sub>O: brine that was previously chilled on ice. The organic phase was then combined, dried over Na<sub>2</sub>SO<sub>4</sub>, filtered and concentrated *in vacuo*. The crude was purified with 15% EtOAc/hexanes →33% EtOAc/hexanes. (50% EtOAc/hexanes; R<sub>f</sub> = 0.8) 1.4 g, 3.4 mmol, 95%

**<sup>1</sup>H NMR** (600 MHz, CDCl<sub>3</sub>) δ 3.57 – 3.50 (m, 1H), 2.43 (dd, *J* = 19.2, 8.9 Hz, 1H), 2.05 (dt, *J* = 19.7, 9.1 Hz, 1H), 1.92 (ddd, *J* = 12.8, 8.8, 5.9 Hz, 1H), 1.78 (dt, *J* = 12.8, 3.4 Hz, 2H), 1.71 – 1.61 (m, 3H), 1.56 – 1.39 (m, 4H), 1.38 – 1.18 (m, 5H), 1.12 – 1.03 (m, 1H), 0.99 – 0.90 (m, 2H), 0.88 (d, *J* = 1.1 Hz, 9H), 0.85 (s, 3H), 0.82 (s, 3H), 0.66 (ddd, *J* = 12.6, 10.5, 4.1 Hz, 1H), 0.04 (d, *J* = 1.0 Hz, 5H).

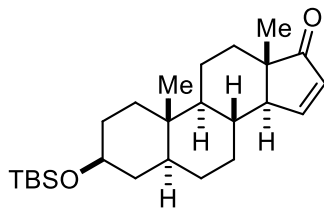
**<sup>13</sup>C NMR** (151 MHz, CDCl<sub>3</sub>) δ 221.4, 71.9, 54.5, 51.5, 47.8, 45.0, 38.6, 37.1, 35.8, 35.7, 35.1, 31.9, 31.6, 30.9, 28.5, 25.9, 21.8, 20.5, 18.3, 13.8, 12.4, -4.6, -4.6.

**HRMS** (ESI-TOF): [M+Na]<sup>+</sup>: Calcd for C<sub>25</sub>H<sub>44</sub>O<sub>2</sub>SiNa 427.3003; Found 427.2995



$[\alpha]_{\text{D}}^{25} = +59.4$  ( $c = 0.22$ ,  $\text{CHCl}_3$ ).

**IR** (film,  $\text{cm}^{-1}$ ): 2929, 2857, 1747, 1716, 1376, 1251, 1091, 838, 772



**Compound 2-5:** In a flame dried 100 mL round bottom flask, **2-4** was added to DCM (70 mL) then cooled to 0 °C under an  $\text{N}_2$  atmosphere. Then,  $\text{Et}_3\text{N}$  (4.9 mL, 34.6 mmol, 5 equiv) was added to the reaction flask, and the flask was cooled to 0 °C, and flushed with dry nitrogen. The flask was charged with TMSOTf (3.0 equiv., 3.5 mL, 20.7 mmol) and stirred for 2 h as the reaction warmed to room temperature. The reaction was diluted with EtOAc, washed with dI  $\text{H}_2\text{O}$ , then, brine. The organic layer was dried over  $\text{Na}_2\text{SO}_4$ , filtered, and concentrated to afford the crude silyl enol ether which was used in the next reaction without further purification.  $\text{Pd}(\text{OAc})_2$  (1.2 equiv., 1.86 g, 8.3 mmol) was added to a solution of the above crude silyl enol ether in  $\text{CH}_3\text{CN}$  (70 mL) at room temperature. After the reaction mixture was stirred at room temperature for 12 h, the suspension was filtered through a pad of Celite with EtOAc (100 mL) and concentrated *in vacuo*. The residue was purified by flash column chromatography on silica gel (Hexanes/EtOAc = 24/1) to afford enone **2-5** (2.8 g, 6.9 mmol) in 71% yield as a white solid. (0.57  $R_f$  = 10% EtOAc/hexanes)

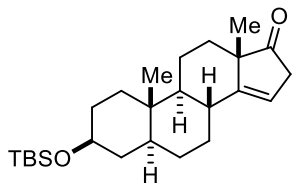
**$^1\text{H}$  NMR** (600 MHz, Chloroform-*d*)  $\delta$  7.53 – 7.49 (m, 1H), 6.01 (dd,  $J = 6.0, 3.1$  Hz, 1H), 3.55 (tt,  $J = 10.5, 4.8$  Hz, 1H), 2.26 (dt,  $J = 11.4, 2.4$  Hz, 1H), 1.97 (dq,  $J = 12.6, 3.5$  Hz, 1H), 1.86 – 1.83 (m, 1H), 1.76 (qd,  $J = 11.4, 4.0$  Hz, 1H), 1.72 – 1.64 (m, 3H), 1.51 – 1.42 (m, 4H), 1.39 – 1.30 (m, 3H), 1.13 (tt,  $J = 14.1, 2.7$  Hz, 1H), 1.10 – 1.06 (m, 1H), 1.05 (s, 3H), 0.96 (td,  $J = 13.3, 3.6$  Hz, 1H), 0.88 (s, 8H), 0.86 (s, 4H), 0.77 (ddd,  $J = 21.5, 10.0, 6.4$  Hz, 2H), 0.05 (s, 6H).

$^{13}\text{C}$  NMR (151 MHz,  $\text{CDCl}_3$ )  $\delta$  213.4, 158.7, 131.6, 71.9, 56.9, 55.8, 51.2, 45.3, 38.5, 36.8, 35.9, 32.4, 31.8, 30.8, 29.2, 28.3, 25.9, 25.6, 20.7, 20.2, 18.3, 12.4, -4.6, -4.6.

HRMS (ESI-TOF):  $[\text{M}+\text{H}]^+$ : Calcd for  $\text{C}_{25}\text{H}_{43}\text{O}_2\text{Si}$  403.3027; Found 403.3017

$[\alpha]_{\text{D}}^{25} = -9.3$  ( $c = 0.14$ ,  $\text{CHCl}_3$ ).

IR (film,  $\text{cm}^{-1}$ ): 3346, 2928, 2855, 1710, 1561



**Compound 2-6:** *i*-Pr<sub>2</sub>EtN (10.0 equiv., 8.7 mL, 49.6 mmol) was added to a suspension of enone **2-5** (2 g, 4.9 mmol) and SiO<sub>2</sub> (3.0 equiv., 895 mg, 14.9 mmol) in toluene (50 mL) at room temperature. The reaction was warmed to 60 °C and stirred for 7 h. The reaction was diluted with EtOAc (100 mL) filtered then washed with 1N HCl (30 mL). The organic layer was dried over Na<sub>2</sub>SO<sub>4</sub>, filtered, and concentrated *in vacuo*. The crude material was purified by flash column chromatography on silica gel (Hexanes/EtOAc = 1/0 to 24/1 to 9/1) to afford **2-6** (1.17 g, 3.35 mmol) and enone **2-5** (715 mg, 1.28 mmol) in 59% yield and 91% brsm, respectively as white solids. R<sub>f</sub>: 0.85, 10%EtOAc/hexanes.

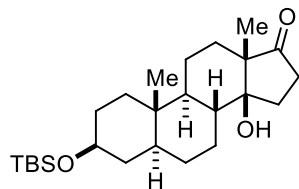
$^1\text{H}$  NMR (600 MHz,  $\text{CDCl}_3$ )  $\delta$  5.47 (d,  $J = 2.2$  Hz, 1H), 3.54 (tt,  $J = 10.9, 4.8$  Hz, 1H), 2.99 (ddd,  $J = 23.0, 3.9, 1.8$  Hz, 1H), 2.82 (dt,  $J = 23.0, 2.3$  Hz, 1H), 2.17 – 2.11 (m, 0H), 1.86 (dt,  $J = 9.5, 3.2$  Hz, 1H), 1.76 (dt,  $J = 12.9, 3.3$  Hz, 1H), 1.69 (ddt,  $J = 15.0, 10.2, 3.4$  Hz, 4H), 1.47 (dtt,  $J = 12.3, 4.8, 2.8$  Hz, 2H), 1.42 (ddd,  $J = 13.4, 3.9, 2.0$  Hz, 1H), 1.39 (dt,  $J = 3.0, 1.5$  Hz, 1H), 1.37 – 1.31 (m, 5H), 1.23 – 1.18 (m, 2H), 1.10 (s, 4H), 1.08 – 1.04 (m, 1H), 0.88 (s, 9H), 0.87 (s, 3H), 0.85 (s, 4H), 0.68 (td,  $J = 11.8, 3.3$  Hz, 1H), 0.05 (s, 6H).

$^{13}\text{C}$  NMR (126 MHz,  $\text{CDCl}_3$ )  $\delta$  222.7, 153.7, 112.8, 71.9, 54.9, 50.9, 44.7, 41.4, 38.5, 36.9, 35.9, 35.5, 33.3, 31.8, 28.9, 28.2, 25.9, 20.8, 19.9, 18.2, 12.1, -4.6.

HRMS (ESI-TOF):  $[\text{M}+\text{H}]^+$  Calcd for  $\text{C}_{25}\text{H}_{43}\text{O}_2\text{Si}$  403.3027; Found 403.3025

$[\alpha]_{\text{D}}^{25} = +40.6$  ( $c = 0.1$ ,  $\text{CHCl}_3$ ).

IR (film,  $\text{cm}^{-1}$ ): 2925, 2882, 2859, 1738, 1639



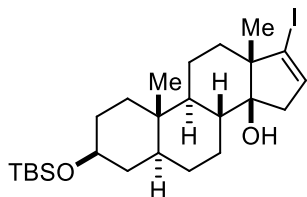
**Compound 2-7:** (103 mg, 0.25 mmol), cobalt (II) acetylacetonate ( $\text{Co}(\text{acac})_2$ , 0.2 equiv., 14.3 mg, 0.05 mmol) in 1,4-dioxane (2.5 mL) was bubbled with  $\text{O}_2$  for 10 min at room temperature. A solution of  $\text{PhSiH}_3$  (3.1 equiv., 0.92 mL, 0.74 mmol) in 1,4-dioxane (5.5 mL) was added to the mixture at room temperature over 2 h via a syringe pump under  $\text{O}_2$  atmosphere (1 atm). After the reaction mixture was stirred under  $\text{O}_2$  atmosphere (1 atm) at room temperature for 3 hours, saturated aqueous  $\text{NaHCO}_3$  (10 mL) and 10 w/v%  $\text{Na}_2\text{S}_2\text{O}_3$  were added to the mixture. The resultant mixture was extracted with  $\text{CH}_2\text{Cl}_2$  (50 mL x 4). The combined organic layers were dried over  $\text{Na}_2\text{SO}_4$ , filtered, and concentrated *in vacuo*. The residue was passed through a silica gel plug (hexane/EtOAc = 1/1) to afford a 1.5:1 ( $\beta$ : $\alpha$ ) mixture of two C14-epimeric alcohols **2-7**. The spectra shown below is representative of the  $\beta$ C-14 epimer. The mixture was carried forward without further purification.

$^1\text{H}$  NMR (700 MHz,  $\text{CDCl}_3$ ):  $\delta$  3.56 (d,  $J = 8.4$  Hz, 1H), 2.39 (td,  $J = 6.7, 3.2$  Hz, 2H), 2.12 (dt,  $J = 13.8, 9.9$  Hz, 1H), 1.97 (dd,  $J = 12.7, 3.5$  Hz, 1H), 1.83 – 1.77 (m, 1H), 1.70 (dq,  $J = 14.3, 4.8, 4.1$  Hz, 2H), 1.57 (ddd,  $J = 25.3, 12.6, 3.6$  Hz, 2H), 1.51 – 1.41 (m, 2H), 1.40 – 1.31 (m,

3H), 1.29 – 1.24 (m, 4H), 1.18 (ddd,  $J = 19.1, 12.5, 4.0$  Hz, 1H), 1.09 (td,  $J = 12.5, 10.9, 6.2$  Hz, 1H), 1.04 (s, 3H), 0.99 – 0.92 (m, 1H), 0.88 (s, 11H), 0.81 (s, 3H), 0.05 (s, 7H).

$^{13}\text{C}$  NMR (176 MHz,  $\text{CDCl}_3$ ):  $\delta$  221.3, 82.5, 71.9, 53.5, 50.1, 44.5, 41.3, 38.4, 37.3, 35.8, 33.0, 31.9, 31.8, 28.3, 27.3, 25.9, 25.6, 19.8, 18.2, 12.7, 12.2, -4.5.

IR (film,  $\text{cm}^{-1}$ ): 3366, 2927, 1636, 1132



**Compound 2-8.** Hydrazine monohydrate ( $\text{N}_2\text{H}_4\cdot\text{H}_2\text{O}$ , 20 equiv., 0.21 mL, 4.3 mmol) was added to a solution of the alcohols  $\beta$ -**2-7** and  $\alpha$ -**2-7** from above and  $\text{Et}_3\text{N}$  (20 equiv., 0.6 mL, 4.2 mmol) in absolute ethanol (11 mL). The reaction flask was flushed with  $\text{N}_2$  and heated to  $50^\circ\text{C}$  for 12 h then concentrated *in vacuo* to white crystals. The flask was removed from high vacuum and flushed with  $\text{N}_2$  before adding  $\text{Et}_3\text{N}$  (20.0 equiv., 0.6 mL, 4.2 mmol) and dissolving in THF (11 mL). The reaction was stirred vigorously at room temperature as a solution of  $\text{I}_2$  (3.5 equiv., 2.16 mg, 0.86 mmol) dissolved in THF (5 mL) was added dropwise until the solution turned brown. The reaction was stirred for 10 min until the solution returned to a yellow color before adding more of the  $\text{I}_2$  solution until the brown color persisted. The reaction was stirred for 1 h at room temperature then quenched with 10 w/v%  $\text{Na}_2\text{S}_2\text{O}_3$  (100 mL). The mixture was diluted with deionized water (500 mL) then extracted with  $\text{CH}_2\text{Cl}_2$  (200 mL x 3). The combined organic layers were dried over  $\text{Na}_2\text{SO}_4$ , filtered, and concentrated *in vacuo*. The residue was purified by flash column chromatography on silica gel (Hexanes/ $\text{EtOAc} = 49/1$  to  $24/1$  to  $9/1$ ) to afford vinyl **2-8** (58.8 mg, 0.11 mmol) in 43% yield over 2 steps as a white solid.

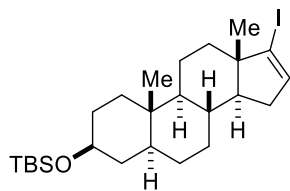
**<sup>1</sup>H NMR** (700 MHz, CDCl<sub>3</sub>): δ 6.10 (d, *J* = 2.6 Hz, 1H), 3.55 (tt, *J* = 10.6, 4.8 Hz, 1H), 2.51 (dd, *J* = 16.4, 1.9 Hz, 1H), 2.19 (dd, *J* = 16.4, 3.2 Hz, 1H), 2.06 (dd, *J* = 6.7, 3.1 Hz, 1H), 1.74 (ddt, *J* = 13.9, 7.5, 3.5 Hz, 3H), 1.71 – 1.67 (m, 1H), 1.64 – 1.57 (m, 6H), 1.53 (dd, *J* = 13.2, 3.5 Hz, 1H), 1.45 (tdd, *J* = 13.8, 9.2, 4.5 Hz, 2H), 1.38 – 1.30 (m, 2H), 1.07 (ddd, *J* = 14.1, 10.3, 4.0 Hz, 4H), 1.04 (s, 4H), 0.96 (ddd, *J* = 14.0, 10.7, 3.6 Hz, 3H), 0.88 (s, 9H), 0.80 (s, 3H), 0.78 – 0.75 (m, 1H), 0.05 (s, 6H).

**<sup>13</sup>C NMR** (176 MHz, CDCl<sub>3</sub>) δ 133.7, 111.3, 82.5, 72.0, 60.4, 54.7, 50.6, 44.5, 42.5, 41.1, 38.4, 37.3, 37.2, 35.7, 31.7, 28.3, 27.2, 25.9, 21.0, 19.6, 18.2, 17.8, 14.1, 12.3, -4.5.

**HRMS** (ESI-TOF) [M-H<sub>2</sub>O-OTBS]<sup>+</sup> *m/z*: calcd for C<sub>19</sub>H<sub>26</sub>I 381.1074; Found 381.1068.

[α]<sub>D</sub><sup>25</sup> = +8.8 (c = 0.28, CHCl<sub>3</sub>).

**IR** (film, cm<sup>-1</sup>): 3444, 2928, 2884, 2857



**Compound 2-17.** Hydrazine monohydrate (N<sub>2</sub>H<sub>4</sub>·H<sub>2</sub>O, 20 equiv., 1.1 mL, 23.3 mmol) was added to a solution of the *trans*-androsterone and Et<sub>3</sub>N (20 equiv., 3.3 mL, 23.3 mmol) in absolute ethanol (58 mL). The reaction flask was flushed with N<sub>2</sub> and heated to 50 °C for 12 h then concentrated *in vacuo* to white crystals. The flask was removed from high vacuum and flushed with N<sub>2</sub> before adding Et<sub>3</sub>N (20.0 equiv., 3.3 mL, 23.3 mmol) and dissolving in THF (58 mL). The reaction was stirred vigorously at room temperature as a solution of I<sub>2</sub> (3.5 equiv., 1.2 g, 4.7 mmol) dissolved in THF (5 mL) was added dropwise until the solution turned brown. The reaction was stirred for 10 min until the solution returned to a yellow color before adding more of the I<sub>2</sub> solution until the brown color persisted. The reaction was stirred for 1 h at room temperature then quenched with 10

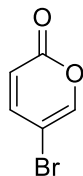
w/v% Na<sub>2</sub>S<sub>2</sub>O<sub>3</sub> (100 mL). The mixture was diluted with deionized water (500 mL) then extracted with CH<sub>2</sub>Cl<sub>2</sub> (200 mL x 3). The combined organic layers were dried over Na<sub>2</sub>SO<sub>4</sub>, filtered, and concentrated *in vacuo*. The residue was purified by flash column chromatography on silica gel (Hexanes/EtOAc = 49/1 to 24/1 to 9/1) to afford vinyl iodide **2-17** (542 mg, 1.05 mmol) in 38% yield over 2 steps as a white solid.

<sup>1</sup>H NMR (600 MHz, C<sub>6</sub>D<sub>6</sub>) δ 6.00 (dd, *J* = 3.3, 1.7 Hz, 1H), 3.58 (tt, *J* = 10.5, 4.9 Hz, 1H), 1.83 (ddd, *J* = 14.8, 5.8, 3.2 Hz, 1H), 1.76 – 1.71 (m, 1H), 1.68 – 1.60 (m, 2H), 1.58 – 1.52 (m, 2H), 1.44 (ddt, *J* = 16.6, 11.1, 3.0 Hz, 4H), 1.28 (dt, *J* = 9.6, 3.8 Hz, 2H), 1.21 – 1.09 (m, 4H), 1.05 (s, 11H), 0.66 (s, 3H), 0.62 (s, 3H), 0.15 (s, 7H).

<sup>13</sup>C NMR (176 MHz, C<sub>6</sub>D<sub>6</sub>) δ 137.3, 112.8, 71.8, 54.5, 54.4, 50.0, 44.8, 38.8, 36.6, 36.3, 35.3, 34.2, 33.3, 32.0, 31.3, 28.5, 25.8, 25.7, 20.9, 17.9, 15.1, 11.8, -4.6, -4.6.

[α]<sub>D</sub><sup>25</sup> = +6.09 (c = 0.28, CHCl<sub>3</sub>).

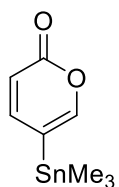
IR (film, cm<sup>-1</sup>): 2925, 2853, 2360, 2340



**Compound 2-10:** In a dry flask under N<sub>2</sub> was placed DCM (10 ml) and 2H-pyran-2-one (500 mg, 5.2 mmol). The flask was cooled to -78 °C (dry-ice – acetone). Bromine (831 mg, 5.2 mmol, 1.0 equiv.) was diluted in DCM (10 ml), taken into a syringe and chilled using dry-ice pellet around the syringe. The cold solution was added to the reaction mixture over 1 h whilst shining light on the flask (500W floodlight). The irradiation was continued for about 5 h (TLC:SiO<sub>2</sub>, EtOAc/hexane 3:7, UV detection, R<sub>f</sub>(-pyrone) = 0.20, R<sub>f</sub>(photodibromide) = 0.54) with stirring, maintaining the temperature at -78 °C. The light source was then removed, and the contents of the flask were allowed to warm to room temperature. The solvent was removed under reduced pressure to afford

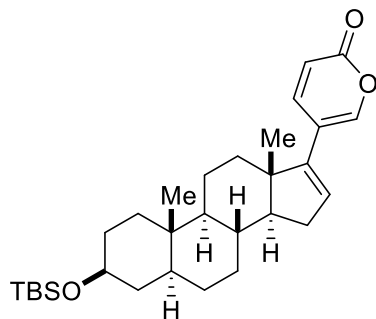
a light-orange oil The photodibromide readily loses HBr at room temperature and was used without further purification. A magnetically stirred solution of the crude residue in 10 mL of DCM was treated dropwise with triethylamine (0.73 ml, 5.3 mmol, 1.1 eq). After 5 min, the solvent was evaporated and the residue extracted with ether, leaving behind most of the triethylamine hydrobromide. After evaporation of the solvent, the residue was chromatographed on silica gel with DCM. **2-10** was isolated (774 mg, 4.42 mmol, 86% yield) as a white solid.

Spectral information matches previously reported literature<sup>26,27</sup>



**Compound 2-11:** **2-10** (400 mg, 2.29 mmol), was placed in a 10 mL flame-dried rbf, with a stir bar and taken into a glovebox. Then, Pd(PPh<sub>3</sub>)<sub>4</sub> (633 mg, 0.548 mmol, 0.2 equiv.) and (Me<sub>3</sub>Sn)<sub>2</sub> (900 mg, 2.74 mmol, 1.2 equiv.) were added. The flask was then taken out of the glovebox, and the contents were dissolved in 1,4-dioxane (5 mL). After being stirred at 70 °C for 12 h, the reaction mixture was concentrated. The residue was purified by flash column chromatography on silica gel hexane/Et<sub>2</sub>O = 1/0 to 20/1 to 10/1, R<sub>f</sub> = 0.5 in 10% EtOAc/hexane) to afford stannane **2-10** (249 mg, 1.02 mmol) in 42% yield as a colorless oil.

Spectral information matches previously reported literature<sup>27</sup>



**Compound 2-18:** Stannane **2-11** (39 mg, 0.1 mmol, 1.3 equiv.) was and vinyl iodide **2-17** (40 mg, 0.078 mmol) were added to a 5 mL round-bottom flask and taken into a glovebox. Then, Pd(PPh<sub>3</sub>)<sub>4</sub> (5 mg, 0.0039 mmol, 0.05 eq), CuCl (152 mg, 1.56 mmol) and LiCl (50 mg, 1.17 mmol, 15 eq), were added to the reaction flask. The round bottom flask was then taken out of the glovebox and the contents were dissolved in anhydrous DMSO (1 mL) and the reaction flask heated to 70 °C for 24 h. Then the reaction was cooled to room temperature, quenched with pH 7 phosphate buffer (2 mL), extracted with Et<sub>2</sub>O (3x 5 mL), dried over Na<sub>2</sub>SO<sub>4</sub>, filtered, and concentrated *in vacuo*. Purified by column chromatography with 5% to 20% EtOAc/hexanes. (36.2 mg, 0.074 mmol, 75%) R<sub>f</sub> = 0.35 20% EtOAc/hexanes

**<sup>1</sup>H NMR** (700 MHz, C<sub>6</sub>D<sub>6</sub>) δ 7.05 (t, *J* = 4.0 Hz, 1H), 6.67 (dd, *J* = 9.7, 2.6 Hz, 1H), 5.95 (dd, *J* = 9.7, 1.2 Hz, 1H), 5.36 (dd, *J* = 3.3, 1.7 Hz, 1H), 3.63 (tt, *J* = 10.5, 4.9 Hz, 1H), 1.98 (ddd, *J* = 15.6, 6.6, 3.3 Hz, 1H), 1.82 – 1.76 (m, 1H), 1.73 – 1.65 (m, 1H), 1.62 – 1.45 (m, 5H), 1.43 – 1.39 (m, 3H), 1.28 (dt, *J* = 11.4, 5.7 Hz, 1H), 1.24 – 1.19 (m, 1H), 1.19 – 1.13 (m, 1H), 1.13 – 1.07 (m, 1H), 1.06 (s, 9H), 0.99 – 0.89 (m, 3H), 0.85 (tt, *J* = 12.2, 5.8 Hz, 1H), 0.78 (td, *J* = 13.6, 4.0 Hz, 1H), 0.72 (s, 3H), 0.62 (s, 3H), 0.17 (s, 6H).

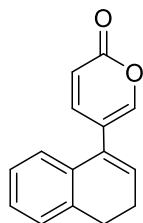
**<sup>13</sup>C NMR** (151 MHz, C<sub>6</sub>D<sub>6</sub>) δ 160.1, 147.5, 147.0, 142.9, 128.3, 127.6, 116.5, 72.2, 57.4, 54.7, 47.1, 45.3, 39.2, 37.1, 35.8, 35.5, 33.9, 32.4, 32.1, 31.4, 28.9, 26.1, 21.3, 18.1, 16.2, 12.3, -4.3.

**HRMS** (ESI-TOF) [M+H]<sup>+</sup> *m/z*: calcd for C<sub>30</sub>H<sub>47</sub>O<sub>3</sub>Si 483.3288; Found 483.3281

[α]<sub>D</sub><sup>25</sup> = -1.2 (c = 0.2, CHCl<sub>3</sub>).



**IR** (film,  $\text{cm}^{-1}$ ): 2922, 1733, 1717, 1558, 1540, 670



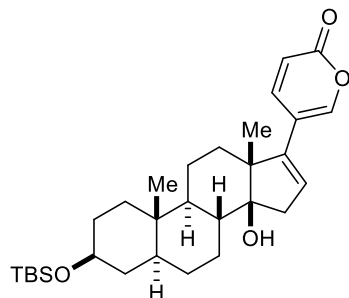
**Compound 2-20:** Stannane **2-11** (202 mg, 0.78 mmol) was and vinyl iodide (176 mg, 0.78 mmol) were added to a 10 mL round-bottom flask and taken into a glovebox. Then,  $\text{Pd}(\text{PPh}_3)_4$  (18 mg, 0.016 mmol, 0.03 eq),  $\text{CuCl}$  (530 mg, x mmol) and  $\text{LiCl}$  (236 mg, 5.62 mmol, 7 eq), were added to the reaction flask. The round bottom flask was then taken out of the glovebox and the contents were dissolved in anhydrous DMSO (2 mL) and the reaction flask heated to 70 °C for 24 h. Then the reaction was cooled to room temperature, quenched with pH 7 phosphate buffer (10 mL), extracted with  $\text{Et}_2\text{O}$  (3x 10 mL), dried over  $\text{Na}_2\text{SO}_4$ , filtered, and concentrated *in vacuo*. Purified by column chromatography with 5% to 20%  $\text{EtOAc}$ /hexanes. (120.7 mg, 69%)  $R_f = 0.35$  20%  $\text{EtOAc}$ /hexanes.

**$^1\text{H NMR}$**  (500 MHz,  $\text{C}_6\text{D}_6$ )  $\delta$  7.02 – 6.96 (m, 1H), 6.94 (d,  $J = 7.7$  Hz, 1H), 6.78 – 6.75 (m, 1H), 6.64 (d,  $J = 7.5$  Hz, 1H), 6.39 (dt,  $J = 9.5, 2.0$  Hz, 1H), 5.82 (d,  $J = 9.6$  Hz, 1H), 5.38 (t,  $J = 4.7$  Hz, 1H), 2.44 (t,  $J = 8.0$  Hz, 1H), 1.84 (td,  $J = 8.0, 4.7$  Hz, 2H), 0.97 – 0.85 (m, 2H).

**$^{13}\text{C NMR}$**  (126 MHz,  $\text{C}_6\text{D}_6$ )  $\delta$  160.4, 149.3, 144.1, 136.7, 133.4, 132.7, 128.3, 127.9, 126.9, 124.9, 119.0, 115.7, 27.9, 23.2.

**HRMS** (ESI-TOF):  $m/z$ :  $[\text{M} + \text{Na}]^+$  calcd for  $\text{C}_{15}\text{H}_{12}\text{O}_2\text{Na}$  225.0909; found 225.0914

**IR** (thin film,  $\text{cm}^{-1}$ ): 2925, 1737, 1721, 1534, 1223, 1120, 956.



**Compound 2-12:** Stannane **2-11** (28 mg, 0.11 mmol, 2 equiv.) and vinyl iodide **2-8** (28.5 mg, 0.78 mmol) were added to a 10 mL round-bottom flask and taken into a glovebox. Then, Pd(PPh<sub>3</sub>)<sub>4</sub> (3 mg, 0.03 mmol, 0.05 eq), CuCl (79.4 mg, 0.8 mmol, 15 equiv) and LiCl (45.4 mg, 1.08 mmol, 20 equiv), were added to the reaction flask. The round bottom flask was then taken out of the glovebox and the contents were dissolved in anhydrous DMSO (5.5 mL) and the reaction flask heated to 70 °C for 24 h. Then the reaction was cooled to room temperature, quenched with pH 7 phosphate buffer (10 mL), extracted with Et<sub>2</sub>O (3x 10 mL), dried over Na<sub>2</sub>SO<sub>4</sub>, filtered, and concentrated *in vacuo*. Purified by column chromatography with 5% to 20% EtOAc/hexanes to give a solid (23 mg, 0.046 mmol, 85%) R<sub>f</sub> = 0.35, 20% EtOAc/hexanes

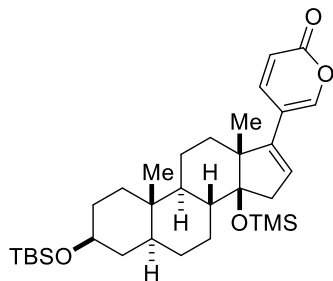
**<sup>1</sup>H NMR** (500 MHz, C<sub>6</sub>D<sub>6</sub>) δ 6.87 (d, *J* = 2.6 Hz, 1H), 6.55 (dd, *J* = 9.7, 2.7 Hz, 1H), 5.91 (dd, *J* = 9.7, 1.2 Hz, 1H), 5.15 (t, *J* = 2.7 Hz, 1H), 3.65 – 3.59 (m, 1H), 2.29 (d, *J* = 17.0 Hz, 1H), 2.09 (d, *J* = 11.6 Hz, 1H), 1.95 (d, *J* = 3.4 Hz, 1H), 1.92 (d, *J* = 3.2 Hz, 1H), 1.49 – 1.36 (m, 2H), 1.33 (d, *J* = 13.1 Hz, 3H), 1.30 – 1.12 (m, 10H), 1.04 (s, 9H), 0.79 (s, 3H), 0.64 (s, 3H), 0.14 (d, *J* = 1.2 Hz, 6H).

**<sup>13</sup>C NMR** (126 MHz, CDCl<sub>3</sub>) δ 161.3, 147.7, 145.2, 144.3, 125.2, 116.1, 85.9, 72.2, 52.5, 50.4, 44.6, 40.7, 39.9, 38.5, 37.5, 35.9, 31.9, 29.9, 28.6, 27.6, 26.1, 20.8, 19.9, 18.4, 16.3, 12.6, -4.4.

**HRMS** (ESI-TOF) *m/z*: [M + H]<sup>+</sup> calcd for C<sub>30</sub>H<sub>47</sub>O<sub>4</sub>Si 499.3237; found. 499.3238

[α]<sub>D</sub><sup>25</sup> = +8.5 (c = 0.25, CHCl<sub>3</sub>).

**IR** (thin film, cm<sup>-1</sup>): 3750, 2927, 2849, 1733, 1717, 668



**Compound 2-13:** In a flame-dried 4 mL vial, **2-12** (50 mg, 0.10 mmol) was dissolved in anhydrous DCM (2 mL). Imidazole (102 mg, 1.5 mmol, 15 eq) was then added, and then TMSCl (63  $\mu$ L, 0.50 mmol, 5 eq) and the reaction was stirred at room temperature for 24 h. At the 12 h time point, an additional 5 eq of TMSCl and 15 eq of imidazole was added to the reaction vessel to push the reaction to completion, while being monitoring by TLC analysis. The reaction was quenched with dI water (1 mL) and sat. aq. NaHCO<sub>3</sub> (1 mL), extracted with DCM (3 x 5 mL). The organic phase was washed with brine (5 mL), dried over Na<sub>2</sub>SO<sub>4</sub>, filtered, and concentrated *in vacuo* to give a colorless semi-solid. Compound was purified by chromatography (SiO<sub>2</sub>, 10% EtOAc/hexanes). (53 mg, 93  $\mu$ mol, 93%). TLC: 20% EtOAc/hexanes; R<sub>f</sub>: 0.5

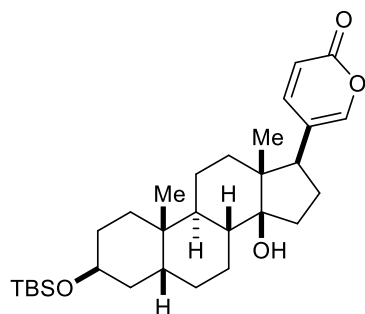
**<sup>1</sup>H NMR** (600 MHz, C<sub>6</sub>D<sub>6</sub>)  $\delta$  7.09 – 7.07 (m, 1H), 6.77 (dd,  $J$  = 9.7, 2.7 Hz, 1H), 5.98 (dd,  $J$  = 9.7, 1.1 Hz, 1H), 5.25 – 5.21 (m, 1H), 3.64 (tt,  $J$  = 10.1, 4.8 Hz, 1H), 2.29 (dd,  $J$  = 17.5, 1.9 Hz, 1H), 2.15 (dd,  $J$  = 17.3, 3.2 Hz, 1H), 2.05 (dt,  $J$  = 12.6, 3.4 Hz, 1H), 1.81 – 1.74 (m, 1H), 1.63 – 1.54 (m, 4H), 1.51 – 1.43 (m, 2H), 1.30 – 1.15 (m, 3H), 1.05 (s, 9H), 1.00 – 0.93 (m, 2H), 0.92 (s, 3H), 0.89 – 0.77 (m, 3H), 0.63 (s, 3H), 0.62 – 0.56 (m, 1H), 0.16 (s, 6H), 0.07 (s, 9H).

**<sup>13</sup>C NMR** (151 MHz, C<sub>6</sub>D<sub>6</sub>)  $\delta$  160.1, 147.9, 145.9, 143.2, 128.6, 124.1, 116.5, 115.7, 90.6, 72.3, 52.9, 50.7, 44.7, 42.5, 39.1, 38.7, 38.6, 37.6, 35.8, 32.4, 28.9, 28.1, 26.2, 20.1, 18.4, 16.7, 12.5, 2.9, -4.2.

**HRMS** (ESI-TOF)  $m/z$ : [M + H]<sup>+</sup> calcd for C<sub>33</sub>H<sub>55</sub>O<sub>4</sub>Si<sub>2</sub>; 571.3633 found 571.3639

[ $\alpha$ ]<sub>D</sub><sup>25</sup> = -0.037 (c = 0.5, CHCl<sub>3</sub>).

IR (thin film,  $\text{cm}^{-1}$ ): 2926, 2856, 1740



**Compound 2-15a:** In a flame dried 4 mL reaction vial, **2-15** (50 mg, 0.13 mmol) was dissolved in anhydrous DMF (1 mL). While stirring, imidazole (26 mg, 0.39 mmol, 3 eq) and then TBSCl (29 mg, 0.19 mmol, 1.5 eq) were added to the reaction vessel, and this was allowed to stir at room temperature for 24 h. At the 12 h time point, add an additional 1.5 eq of TBSCl and 3 eq of imidazole was added to to push the reaction to completion, while monitoring the reaction by TLC analysis. The reaction was quenched with dI water (1 mL) and sat. aq.  $\text{NaHCO}_3$  (1 mL), and then extracted with DCM (3 x 3 mL). The organic phase was washed with brine (5 mL), dried over  $\text{Na}_2\text{SO}_4$ , filtered, and concentrated *in vacuo* to give a colorless semi-solid. Compound was purified by chromatography ( $\text{SiO}_2$ , 20% EtOAc/hexanes) (56 mg, 0.11 mmol, 87%). TLC: 50% EtOAc/hexanes;  $R_f$ : 0.75

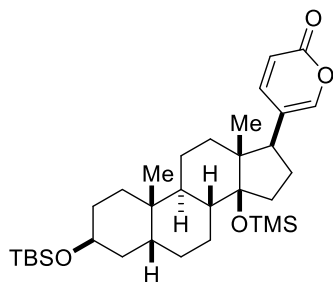
$^1\text{H NMR}$  (700 MHz,  $\text{C}_6\text{D}_6$ )  $\delta$  7.45 (dd,  $J = 9.7, 2.6$  Hz, 1H), 6.60 (d,  $J = 2.6$  Hz, 1H), 6.08 (d,  $J = 9.8$  Hz, 1H), 3.96 (d,  $J = 3.4$  Hz, 1H), 1.94 – 1.86 (m, 2H), 1.81 – 1.71 (m, 2H), 1.70 – 1.62 (m, 6H), 1.60 (d,  $J = 9.5$  Hz, 1H), 1.57 – 1.52 (m, 1H), 1.50 – 1.45 (m, 1H), 1.39 – 1.34 (m, 1H), 1.32 – 1.21 (m, 4H), 1.20 – 1.16 (m, 2H), 1.09 (dddd,  $J = 30.2, 25.8, 12.7, 3.7$  Hz, 2H), 0.99 (s, 9H), 0.84 (s, 3H), 0.40 (s, 3H), 0.07 (s, 6H).

$^{13}\text{C NMR}$  (126 MHz,  $\text{CDCl}_3$ )  $\delta$  162.6, 148.6, 147.0, 122.9, 115.4, 85.6, 67.3, 51.4, 48.5, 46.0, 42.6, 41.1, 36.1, 35.9, 35.4, 34.3, 32.9, 29.9, 28.9, 26.9, 26.0, 23.9, 21.7, 21.6, 18.2, 16.7, -4.72.

**HRMS** (ESI-TOF)  $m/z$ :  $[\text{M} + \text{Na}]^+$  calcd for  $\text{C}_{30}\text{H}_{48}\text{O}_4\text{SiNa}$ ; 523.7842 found 523.7846

$[\alpha]_{\text{D}}^{25} = +1.17$  ( $c = 0.25$ ,  $\text{CHCl}_3$ ).

**IR** (thin film,  $\text{cm}^{-1}$ ): 2934, 2851, 1740



**Compound 2-16:** In a flame-dried 4 mL vial, **2-15a** (50 mg, 0.13 mmol) was dissolved in anhydrous DMF (1 mL) while stirring. Then, imidazole (26 mg, 0.39 mmol, 3 eq) and then TMSCl (29 mg, 0.19 mmol, 1.5 eq) were added to the reaction via sequentially and stir at room temperature for 24 h. At the 12 h time point, add an additional 1.5 eq of TMSCl and 3 eq of imidazole to push the reaction to completion, while being monitored by TLC analysis. The reaction was quenched with dI water (1 mL) and sat. aq.  $\text{NaHCO}_3$  (1 mL), extracted with DCM (3 x 3 mL). The organic phase was washed with brine (5 mL), dried over  $\text{Na}_2\text{SO}_4$ , filtered, and concentrated *in vacuo* to give a colorless semi-solid. Compound was purified by chromatography ( $\text{SiO}_2$ , 5% to 10% EtOAc/hexanes) (56 mg, 0.11 mmol, 87%). TLC: 50% EtOAc/hexanes;  $R_f$ : 0.75

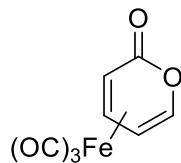
**$^1\text{H}$  NMR** (500 MHz,  $\text{C}_6\text{D}_6$ )  $\delta$  7.10 (dd,  $J = 9.7, 2.7$  Hz, 1H), 6.73 – 6.72 (m, 1H), 6.10 (dd,  $J = 9.6, 1.1$  Hz, 1H), 4.04 (t,  $J = 2.9$  Hz, 1H), 2.03 – 1.93 (m, 2H), 1.87 (ddt,  $J = 13.7, 9.1, 4.8$  Hz, 1H), 1.81 – 1.69 (m, 3H), 1.69 – 1.58 (m, 2H), 1.58 – 1.53 (m, 2H), 1.50 – 1.44 (m, 2H), 1.43 – 1.28 (m, 13H), 1.27 – 1.16 (m, 3H), 1.03 (s, 9H), 0.92 (s, 3H), 0.58 (s, 3H), 0.11 (s, 9H).

$[\alpha]_{\text{D}}^{25} = -0.37$  ( $c = 0.5$ ,  $\text{CHCl}_3$ ).

**$^{13}\text{C}$  NMR** (126 MHz,  $\text{C}_6\text{D}_6$ )  $\delta$  160.2, 148.3, 144.9, 120.1, 114.5, 90.9, 66.9, 50.9, 48.6, 41.5, 40.32, 36.6, 35.5, 35.2, 33.9, 33.3, 29.4, 28.1, 27.7, 26.1, 25.3, 23.3, 22.9, 20.3, 17.8, 17.5, 0.5, -5.5.

**HRMS** (ESI-TOF)  $m/z$ :  $[\text{M} + \text{H}]^+$  calcd for  $\text{C}_{33}\text{H}_{57}\text{O}_4\text{Si}_2$ ; 573.3789 found 573.3783

IR (thin film,  $\text{cm}^{-1}$ ): 2935, 2852, 1742.

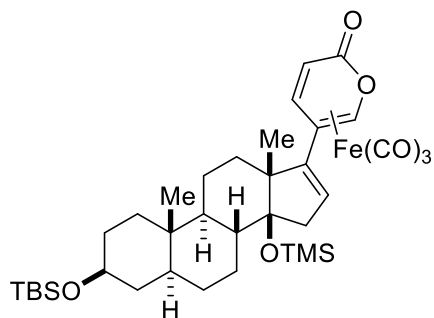


*Caution:  $\text{Fe}(\text{CO})_5$  and  $\text{Fe}_2(\text{CO})_9$  are highly toxic;  $\text{Fe}(\text{CO})_5$  is volatile.*

**Compound 2-32:** To a dried Schlenk tube under  $\text{N}_2$  was added  $\text{Fe}_2(\text{CO})_9$  (24.2 mg, 1 mmol, 1.5 equiv) and 2-pyrone **2-9** (50 mg, 0.5 mmol). Degassed anhydrous  $n\text{-Bu}_2\text{O}$  (2 mL) was added via cannula and the mixture stirred at  $65\text{ }^\circ\text{C}$  for 0.5 h while  $\text{N}_2$  was bubbled through slowly. Two further portions of  $\text{Fe}_2(\text{CO})_9$  (0.5 equiv) were added at 0.5 h intervals. After 2 h, the mixture was allowed to cool to r.t. and the solvent removed in vacuo. Purification by column chromatography using hexanes/EtOAc (9:1), which was increased to 3:1 after 10 fractions. The expected order of elution is  $\text{Fe}_3(\text{CO})_{12}$  (dark green) in small quantities from the reactions (elutes first), then the expected pyrone complex, followed by starting material. Chromatography was used to purify the compound ( $\text{SiO}_2$ ) 55 mg, 0.23 mmol, 44% yield, as a yellow solid.

Spectral data matches previously reported literature<sup>15</sup>

**$^1\text{H NMR}$**  (500 MHz,  $\text{CDCl}_3$ ):  $\delta$  6.31 (m, 1H), 5.63 (m, 2H), 3.00 (m, 1H).



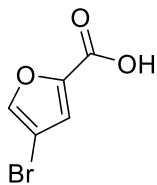
**Compound 2-40:** To a dried Schlenk tube under  $\text{N}_2$  was added  $\text{Fe}_2(\text{CO})_9$  (10 mg, 0.02 mmol, 1.5 equiv) and **2-14** (8 mg, 0.018 mmol). Degassed anhydrous  $n\text{-Bu}_2\text{O}$  (0.2 mL) was added via cannula and the mixture stirred at  $65\text{ }^\circ\text{C}$  for 0.5 h while  $\text{N}_2$  was bubbled through slowly. Two

further portions of  $\text{Fe}_2(\text{CO})_9$  (0.5 equiv) were added at 0.5 h intervals. After 2 h, the mixture was allowed to cool to r.t. and the solvent removed in vacuo. Purification by column chromatography using hexanes/EtOAc (9:1), which was increased to 3:1 after 10 fractions. The expected order of elution is  $\text{Fe}_3(\text{CO})_{12}$  (dark green) in small quantities from the reactions (elutes first), then the expected pyrone complex, followed by starting material. Chromatography was used to purify the mixture of compounds ( $\text{SiO}_2$ ) 3 mg, 0.004 mmol, 24% yield, as a white solid. Column chromatography resulted in a complex mixture.

The spectral data below is best associated to the desired product from crude analysis of a complex mixture of products. HRMS of the crude showed a significant amount of starting material, which was present in the  $^1\text{H}$  NMR sample as well.

**$^1\text{H}$  NMR** (600 MHz,  $\text{C}_6\text{D}_6$ )  $\delta$  7.00 (s, 1H), 5.55 (dd,  $J = 6.1, 2.7$  Hz, 1H), 5.36 (t,  $J = 2.6$  Hz, 1H), 5.32 (d,  $J = 2.7$  Hz, 1H), 3.65 (dq,  $J = 11.0, 6.3, 5.9$  Hz, 1H), 2.63 (d,  $J = 6.1$  Hz, 1H), 2.59 (d,  $J = 6.0$  Hz, 1H), 2.15 (dd,  $J = 17.3, 3.2$  Hz, 1H), 2.05 (dt,  $J = 12.6, 3.4$  Hz, 1H), 1.81 – 1.74 (m, 1H), 1.63 – 1.54 (m, 3H), 1.51 – 1.43 (m, 2H), 1.30 – 1.15 (m, 3H), 1.05 (s, 9H), 1.00 – 0.93 (m, 2H), 0.92 (s, 3H), 0.89 – 0.77 (m, 3H), 0.63 (s, 3H), 0.62 – 0.56 (m, 1H), 0.16 (s, 6H), 0.07 (s, 9H).

**HRMS** (ESI-TOF):  $m/z$ :  $[\text{M} + \text{H}]^+$  calcd for  $\text{C}_{36}\text{H}_{54}\text{O}_7\text{FeSi}_2$  711.2829, found, 711.2837

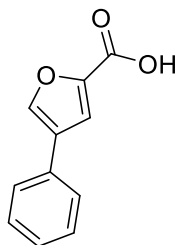


**Compound 2-57: 2-78** (2 g, 7.4 mmol) was suspended in  $\text{H}_2\text{O}$  (23 mL) in a round bottom flask while cooling in an ice bath. Then,  $\text{NH}_4\text{OH}$  (6.6 mL, 7 M) was added to the reaction flask with vigorous stirring. Then, powdered zinc dust (485 mg, 7.4 mmol) was added in small portions. After

final addition of zinc, the reaction was stirred at room temperature for 3 hours. Then the reaction was filtered through a celite plug. The mother liquor was acidified with 2 N HCl until a pH of 2 was reached. Then the aqueous solution was extracted with ethyl acetate (4x 30mL). The organic phase was then dried over Na<sub>2</sub>SO<sub>4</sub>, filtered and concentrated *in vacuo* to give an off-white solid (1.3 g, 6.8 mmol, 94%)

Spectral data matches reported literature <sup>28</sup>

<sup>1</sup>H NMR (500 MHz, DMSO-*d*<sub>6</sub>): δ 6.13.40 (br s, 1H), 8.19 (d, *J* = 1.0 Hz, 1H), 7.37 (d, *J* = 1.0 Hz, 1H).

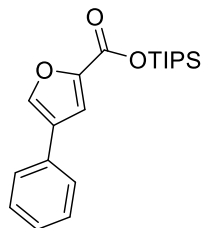


**Compound 2-62: 2-57** (50 mg, 262 μmol), phenylboronic acid (38 mg, 314 μmol, 1.2 eq), Na<sub>2</sub>CO<sub>3</sub> (49 mg, 462 μmol, 1.8 eq) were added to a vial. The reaction vial was then transferred to a glovebox where, Pd(Cl)<sub>2</sub>(PPh<sub>3</sub>)<sub>2</sub> (5.5 mg, 8 μmol, 0.03 eq) was added. Then, the reaction vial was capped, transferred from the glovebox and suspended in a mixture of *i*PrOH : H<sub>2</sub>O (1.2 mL:0.5 mL) and the sealed vial was heated to 85 °C for 18 h. The reaction was then cooled to room temperature, quenched with 1N HCl to a pH of 2 and then extracted with EtOAc (3 x 2 mL). The organic phase was then dried with Na<sub>2</sub>SO<sub>4</sub> and then filtered through a silica plug and concentrated *in vacuo* to give the product as a solid. (49 mg, 260 μmol, 98%).

Spectral data matches reported literature <sup>29</sup>

<sup>1</sup>H NMR (500 MHz, CDCl<sub>3</sub>) δ 7.91 (s, 1H), 7.62 – 7.58 (m, 2H), 7.51 (d, *J* = 7.6 Hz, 2H), 7.43 (dt, *J* = 14.9, 7.7 Hz, 1H), 7.34 (q, *J* = 6.8 Hz, 1H).





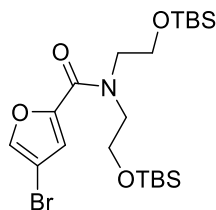
**Compound 2-63: 2-62** (49 mg, 260  $\mu\text{mol}$ ) was dissolved in THF (1 mL). Then, TIPS-Cl (59  $\mu\text{L}$ , 275  $\mu\text{mol}$ , 1.1 eq),  $\text{Et}_3\text{N}$  (55  $\mu\text{L}$ , 393  $\mu\text{mol}$ , 1.5 eq) and the reaction was monitored by TLC for completion. At such time, the reaction was quenched with  $\text{H}_2\text{O}$ , washed with  $\text{NH}_4\text{Cl}$ , then extracted with DCM (3x 1 mL) and the organic phase was quickly filtered through a silica plug. (62 mg, 179  $\mu\text{mol}$ , 69%)

**$^1\text{H NMR}$**  (401 MHz,  $\text{CDCl}_3$ )  $\delta$  7.83 (d,  $J = 1.0$  Hz, 1H), 7.60 – 7.55 (m, 2H), 7.50 – 7.46 (m, 2H), 7.45 – 7.36 (m, 1H), 7.36 – 7.29 (m, 1H), 1.44 – 1.35 (m, 3H), 1.03 (s, 18H).

**$^{13}\text{C NMR}$**  (126 MHz,  $\text{CDCl}_3$ )  $\delta$  157.3, 146.8, 141.8, 141.3, 131.1, 128.7, 127.1, 125.8, 116.5, 17.4, 12.5

**HRMS** (ESI-TOF):  $m/z$ :  $[\text{M} - \text{H}_2\text{O} - \text{H}]$  calcd for  $\text{C}_{20}\text{H}_{28}\text{O}_3\text{Si}$ ; 325.1624 found 325.1640

**IR** (thin film,  $\text{cm}^{-1}$ ): 2943, 2866, 1701, 1523, 1463, 1263, 1120, 1014



**Compound 2-81:** Add compound **2-57** (1.8 g, 9.42 mmol) to a 100 mL round-bottom flask and dissolve in toluene (50 mL) under  $\text{N}_2$  atmosphere. Then, add  $\text{SOCl}_2$  (1.6 mL, 22.62 mmol) and a few drops of anhydrous DMF. Then stir at room temperature for 4 h. Concentrate by azeotroping with toluene via rotovap (4x 10 mL), then redissolve residue in DCM (50 mL) and chill to 0  $^\circ\text{C}$ . Afterwards, add  $\text{Et}_3\text{N}$  (1.96 mL, 14.13 mmol, 1.5 equiv.) and then amine **2-80** (3.77 g, 11.3 mmol,

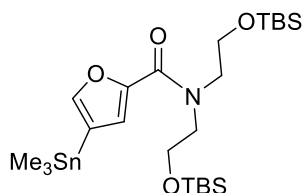
1.2 equiv.) and stir for 1 h while warming to room temperature. Then, concentrate *in vacuo* and immediately perform a column with 20% to 33% EtOAc/hexanes. (3.67 g, 7.25 mmol 77%).  $R_f = 0.7$ ; 20%EtOAc/hexanes.

$^1\text{H NMR}$  (500 MHz,  $\text{CDCl}_3$ )  $\delta$  7.47 (s, 1H), 7.12 (s, 1H), 3.84 (s, 4H), 3.65 (s, 4H), 0.89 (s, 18H), 0.05 (s, 12H).

$^{13}\text{C NMR}$  (126 MHz,  $\text{CDCl}_3$ )  $\delta$  159.2, 148.9, 141.7, 119.0, 100.9, 61.7, 61.2, 51.9, 50.3, 25.9, 18.2, 18.2, -5.4, -5.4.

**HRMS** (ESI-TOF):  $m/z$ :  $[\text{M} + \text{H}]^+$  calcd for  $\text{C}_{21}\text{H}_{40}\text{O}_4\text{BrNSi}_2$ ; 506.1751 found 506.1755

**IR** (thin film,  $\text{cm}^{-1}$ ): 2953, 2926, 2884, 1633, 1495, 1101



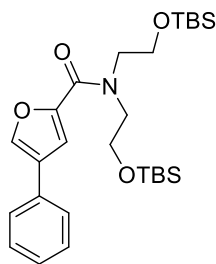
**Compound 2-85:** Dissolve compound **2-81** (500 mg, 0.98 mmol) in  $\text{Et}_2\text{O}$  (5 mL), and chill to  $-95^\circ\text{C}$  in a liquid nitrogen/methanol bath. Then, dropwise addition of *t*-BuLi (1.51 mL, 2.17 mmol, 2.2 equiv.) and stir for 5 minutes. Add a separate solution of  $\text{Me}_3\text{SnCl}$  (600 mg, 2.9 mmol, 3 equiv.) in  $\text{Et}_2\text{O}$  (5 mL) and stir for an additional 10 mins at  $-95^\circ\text{C}$ . Quench the reaction with  $\text{H}_2\text{O}$  and extract with  $\text{Et}_2\text{O}$ . Dry organic phase over  $\text{Na}_2\text{SO}_4$ . Perform column chromatography with 3%  $\text{Et}_3\text{N}$ /hexane treated silica gel and an eluent of 33% EtOAc/hexanes ( $R_f = 0.5$ ). (65 mg, 0.11 mmol, 48%)

$^1\text{H NMR}$  (700 MHz,  $\text{C}_6\text{D}_6$ )  $\delta$  7.08 (s, 1H), 6.71 (s, 1H), 3.78 (m, 4H), 3.58 (m, 4H), 0.91 (s, 9H), 0.88 (s, 18H), 0.05 (s, 12H).

$^{13}\text{C NMR}$  (151 MHz,  $\text{C}_6\text{D}_6$ )  $\delta$  159.9, 148.8, 147.5, 123.3, 62.8, 51.8, 26.3, 25.7, 18.1, -5.6.

**HRMS** (ESI-TOF):  $m/z$ :  $[\text{M} + \text{H}]^+$  calcd for  $\text{C}_{24}\text{H}_{49}\text{O}_4\text{BrNSi}_2\text{Sn}$ ; 592.2294 found 592.2306

**IR** (thin film,  $\text{cm}^{-1}$ ): 2926, 2857, 1665, 1640, 1462, 1255, 1102, 926, 837



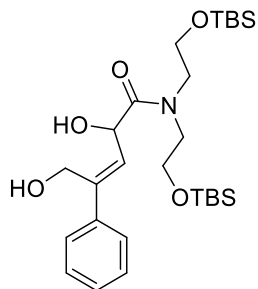
**Compound 2-82:** In a 10 mL rbf, compound **2-81** (236 mg, 0.854 mmol), phenyl boronic acid (124 mg, 1.03 mmol, 1.2 equiv), and  $\text{Na}_2\text{CO}_3$  (451 mg, 4.3 mmol, 5 equiv.) were added and the reaction vessel was transferred to a glovebox. Then,  $\text{Pd}(\text{PPh}_3)_4$  (49 mg, 0.04 mmol, 0.05 equiv) was added to the reaction flask. The reaction flask was taken out of the glovebox and to it was added  $\text{H}_2\text{O}$  (750  $\mu\text{L}$ ) and toluene (3 mL). The reaction was then set 85  $^\circ\text{C}$  and stirred for 20 h. Then, the reaction was cooled to room temperature, quenched with saturated, aqueous  $\text{NH}_4\text{Cl}$  (3 mL) and extracted with  $\text{Et}_2\text{O}$  and  $\text{EtOAc}$  (3x for 10 mL each). The organic phase was dried over  $\text{Na}_2\text{SO}_4$ , filtered and concentrated *in vacuo*. Chromatography was performed with 33%  $\text{EtOAc}$ /hexanes. (258 mg, 0.51 mmol, 60%) TLC:  $R_f = 0.2$  in 1:9 ( $\text{EtOAc}$ :hexanes)

**$^1\text{H}$  NMR** (500 MHz,  $\text{CDCl}_3$ )  $\delta$  7.74 (d,  $J = 1.0$  Hz, 1H), 7.52 – 7.48 (m, 2H), 7.43 – 7.38 (m, 3H), 7.33 – 7.29 (m, 1H), 3.89-3.70 (m, 8H), 0.91 (s, 18H), 0.07 (s, 12H).

**$^{13}\text{C}$  NMR** (126 MHz,  $\text{CDCl}_3$ )  $\delta$  160.1, 149.3, 139.3, 131.4, 128.9, 127.6, 125.9, 115.4, 61.3, 52.0, 25.9, 18.2, -5.4.

**HRMS** (ESI-TOF):  $m/z$ :  $[\text{M} + \text{H}]^+$  calcd for  $\text{C}_{27}\text{H}_{46}\text{O}_4\text{NSi}_2$ ; 504.8372 found 504.8375

**IR** (thin film,  $\text{cm}^{-1}$ ): 2953, 2928, 2884, 1626, 1104

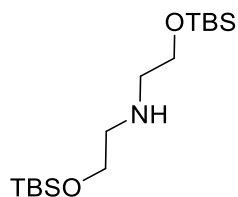


**Compound 2-84: 2-82** (6 mg, 0.012 mmol), was dissolved in DCM (1 mL), and transferred to an 8 mL flame-dried borosilicate test tube and purged with nitrogen. Then, meso-tetraphenylporphine (0.2 mg,  $2.9 \times 10^{-4}$ , 0.004 equiv.) was added to the reaction. The reaction test tube was chilled to  $-78\text{ }^{\circ}\text{C}$  and then  $\text{O}_2$  was bubbled through the solution via a syringe. Then, light was irradiated into the reaction via a 500 W floodlamp. While keeping the reaction at  $-78\text{ }^{\circ}\text{C}$ , the light was shined and the disappearance of starting material was monitored by TLC analysis (Hexanes/EtOAc (5:1),  $R_f = 0.55$ ). After approximately 30 mins, a large excess of  $\text{Me}_2\text{S}$  (0.5 mL) was added to the reaction and the light was turned off and the oxygen was replaced with nitrogen. The reaction was left to stir at  $-78\text{ }^{\circ}\text{C}$  for 24 h. After this time, DCM was removed via nitrogen stream, then the crude residue was dissolved in THF (1 mL) and chilled to  $-40\text{ }^{\circ}\text{C}$ . Then, the reaction was warmed to  $-10\text{ }^{\circ}\text{C}$ . Then, a solution of 2M NaOH (30  $\mu\text{L}$ ) was added to the reaction solution, then  $\text{NaBH}_4$  (1 mg, 0.026 mmol, 2 equiv.) and then  $\text{CeCl}_3$  (3 mg, 0.013 mmol, 1 equiv.). The reaction was left to stir at  $-10\text{ }^{\circ}\text{C}$  until analysis by HRMS showed that the *bis*-reduced product was observed, and the *mono*-reduced product had disappeared. After 4-5 h, the reaction was quenched sat. aq.  $\text{NH}_4\text{Cl}$  (0.5 mL), extracted with DCM (3x 1 mL), then EtOAc (3x 1 mL), dried over  $\text{Na}_2\text{SO}_4$ , filtered, and concentrated *in vacuo*. The complex mixture was carried forward without chromatography due to the *mono*- and *tri*-reduced substrates were inseparable. (5.8 mg, 0.011 mmol, 90% conversion).

*Spectra is for peaks pertaining to the desired product:*

**<sup>1</sup>H NMR** (500 MHz, CDCl<sub>3</sub>) δ 7.50 – 7.46 (m, 1H), 7.43 – 7.30 (m, 4H), 5.82 (d, *J* = 8.7 Hz, 1H), 5.43 (d, *J* = 8.8 Hz, 1H), 4.68 (s, 1H), 3.86 – 3.70 (m, 8H), 0.90 (m, 18H), 0.07 (m, 12H).

**HRMS** (ESI-TOF): *m/z*: [M +Na]<sup>+</sup> calcd for C<sub>27</sub>H<sub>49</sub>O<sub>5</sub>NSi<sub>2</sub>Na; 546.3041 found 546.3046

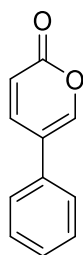


**Compound 2-80:** 2,2'-iminodiethanol **2-79** (2 g, 18.7 mmol) and imidazole (5.7 g, 37.9 mmol, 2.2 equiv.), was dissolved in DCM (40 mL), then TBSCl (4.4 g, 75.9 mmol, 4 equiv.) was then added. The reaction mixture was stirred for 3 h at room temperature, and then diluted with ethyl acetate. The organic layers were then washed with water, then, brine, dried over Na<sub>2</sub>SO<sub>4</sub>, and concentrated *in vacuo*. Chromatography purified (SiO<sub>2</sub>, 5% EtOAc/hexanes) to afford the *bis*-TBS-protected 2,2'-iminodiethanol (6.1 g, 18.3 mmol, 96%) as a colorless oil.

Spectral data matches previously reported literature<sup>30</sup>

**<sup>1</sup>H NMR** (500 MHz, CDCl<sub>3</sub>) δ 3.73 (t, *J* = 5.3 Hz, 4H), 2.74 (t, *J* = 5.4 Hz, 4H), 0.88 (d, *J* = 2.1 Hz, 18H), 0.05 (d, *J* = 2.0 Hz, 16H).

**<sup>13</sup>C NMR** (126 MHz, CDCl<sub>3</sub>) δ 62.3, 51.6, 25.9, 18.2, -5.4.



**Compound 2-70:** Dissolve crude compound mixture **2-84** (10 mg, 0.02 mmol) in toluene (1 mL) then add pTsOH (10 mg, 0.05 mmol, 3.0 equiv.) and stir at 50 °C for 6 h. The reaction was then allowed to cool to room temperature. Concentrate *in vacuo*, and directly perform column

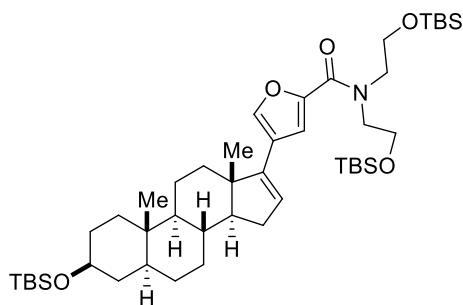
chromatography with SiO<sub>2</sub>, 100% hexanes to 100% EtOAc to afford the product as a white solid (2 mg, 70%). 1:1 EtOAc: Hex, (x2 runs), R<sub>f</sub> = 0.85

<sup>1</sup>H NMR (500 MHz, CDCl<sub>3</sub>) δ 7.72 (d, *J* = 2.8 Hz, 1H), 7.66 (dd, *J* = 9.7, 2.7 Hz, 1H), 7.47 (t, *J* = 7.3 Hz, 2H), 7.44 – 7.37 (m, 3H), 6.47 (d, *J* = 9.7 Hz, 1H).

<sup>13</sup>C NMR (126 MHz, CDCl<sub>3</sub>) δ 148.3, 143.9, 133.5, 129.3, 128.4, 128.4, 125.9, 120.7, 116.5.

HRMS (ESI-TOF): *m/z*: [M + H]<sup>+</sup> calcd for C<sub>11</sub>H<sub>9</sub>O<sub>2</sub>; 173.0596 found 173.0601.

IR (thin film, cm<sup>-1</sup>): 2916, 2848, 1707, 1463



**Compound 2-86a:** **2-17** (29 mg, 0.06 mmol), stannane **2-85** (50 mg, 0.08 mmol, 1.5 equiv.) were added to a flame-dried 10 mL rbf and these contents were transferred to a glovebox. Then, Pd(PPh<sub>3</sub>)<sub>4</sub> (3.25 mg, 0.003 mmol, 0.05 equiv), LiCl (17.7 mg, 0.42 mmol, 7.5 equiv.), and CuCl (27.5 mg, 0.28 mmol, 5 equiv.) were added to the reaction flask. The flask was then taken out of the glovebox and the contents were dissolved in anhydrous DMSO (1 mL) and heated to 70 °C for 16 h. After this time, the reaction was allowed to cool to room temperature and then quenched with pH 7 phosphate buffer (10 mL), then extracted with Et<sub>2</sub>O (4x 5 mL). The organic phase was then washed with dI H<sub>2</sub>O (10 mL), then brine (10 mL), dried over Na<sub>2</sub>SO<sub>4</sub>, filtered, and concentrated *in vacuo*. The residue was purified by column chromatography (SiO<sub>2</sub>, 5% to 33% EtOAc/hexanes) to give compound **2-86a** as a yellow oil. (20 mg, 0.02 mmol, 41%). 20% EtOAc/hexanes; R<sub>f</sub> = 0.5.

<sup>1</sup>H NMR (500 MHz, CDCl<sub>3</sub>) δ 7.47 (d, *J* = 0.9 Hz, 1H), 7.15 (d, *J* = 0.9 Hz, 1H), 5.86 (d, *J* = 1.5 Hz, 1H), 3.85 (m, 8H), 3.60 – 3.54 (m, 1H), 2.22 (dd, *J* = 6.5, 3.3 Hz, 1H), 2.19 (dd, *J* = 6.4, 3.3

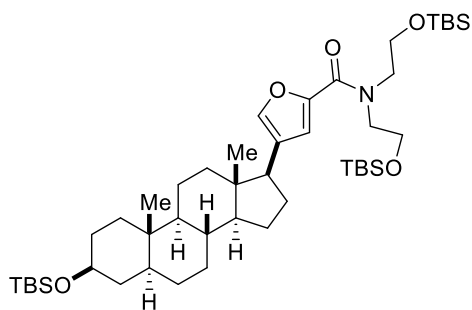
Hz, 1H), 1.99 – 1.92 (m, 2H), 1.77 – 1.64 (m, 3H), 1.62 (dd,  $J = 11.1, 4.0$  Hz, 1H), 1.55 (s, 2H), 1.53 – 1.42 (m, 4H), 1.40 – 1.34 (m, 1H), 1.31 (q,  $J = 5.2, 4.5$  Hz, 1H), 1.15 – 1.07 (m, 1H), 1.04 – 0.94 (m, 3H), 0.92 (s, 3H), 0.89 (s, 27H), 0.86 (s, 3H), 0.06 (s, 18H).

$^{13}\text{C}$  NMR (126 MHz,  $\text{CDCl}_3$ )  $\delta$  160.2, 148.2, 145.5, 141.7, 138.4, 126.5, 122.9, 119.1, 116.1, 72.1, 57.0, 54.8, 47.1, 45.2, 38.7, 37.0, 35.7, 35.6, 33.9, 31.9, 31.5, 29.7, 28.7, 25.9, 21.3, 18.3, 18.2, 16.3, 12.4, -4.6, -5.4.

**HRMS** (ESI-TOF):  $m/z$ :  $[\text{M} + \text{H}]^+$  calcd for  $\text{C}_{46}\text{H}_{84}\text{NO}_5\text{Si}_3$ ; 814.5651; found 814.5658.

$[\alpha]_{\text{D}}^{25} = +8.7$  ( $c = 0.9$ ,  $\text{CHCl}_3$ ).

**IR** (thin film,  $\text{cm}^{-1}$ ): 3649, 2922, 2850, 1653, 1096



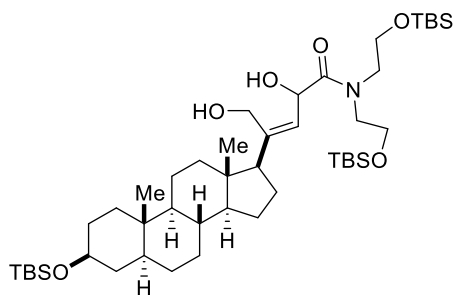
**Compound 2-86:** Compound **2-86a** (20 mg, 0.02 mmol) was dissolved in EtOAc (1 mL), and added to previously flame-dried vial. Then, pyridine (83  $\mu\text{L}$ , 0.001 mmol, 0.05 equiv.) was added, then the vial was then flushed with hydrogen gas. Then, Pd/C (2.3 mg, 0.002 mmol, 0.1 eq.) was added slowly to the reaction vial. The reaction was monitored by TLC for the consumption of starting material. When the reaction was done, the hydrogen balloon was removed, and the reaction was filtered through Celite and concentrated *in vacuo*. The crude residue was then purified by column chromatography to provide the compound as a yellow solid. (15.8 mg, 0.019 mmol, 97%)  $R_f = 0.4$ , 33% EtOAc/hexanes.

$^1\text{H}$  NMR (700 MHz,  $\text{CDCl}_3$ )  $\delta$  7.21 – 7.19 (m, 1H), 6.98 (s, 1H), 3.83 (s, 8H), 3.55 (dq,  $J = 11.0, 5.6, 5.0$  Hz, 1H), 2.44 (t,  $J = 9.7$  Hz, 1H), 1.99 – 1.91 (m, 1H), 1.79 – 1.62 (m, 8H), 1.55 (s, 4H),

1.47 – 1.42 (m, 2H), 1.38 – 1.30 (m, 2H), 1.22 – 1.03 (m, 4H), 0.95 – 0.92 (m, 1H), 0.87 – 0.84 (m, 27H), 0.80 (s, 3H), 0.48 (s, 3H), 0.01 (d,  $J = 0.8$  Hz, 18H).

$^{13}\text{C}$  NMR (151 MHz,  $\text{CDCl}_3$ )  $\delta$  160.3, 148.0, 140.4, 127.0, 118.1, 72.1, 55.7, 54.6, 47.2, 45.1, 43.5, 38.6, 37.2, 35.9, 35.6, 32.2, 31.9, 29.7, 26.9, 25.9, 25.8, 24.4, 20.9, 18.3, 18.2, 12.9, 12.4, 1.0, -4.6, -5.4.

**HRMS** (ESI-TOF):  $[\text{M} + \text{H}]^+$  calcd for  $\text{C}_{46}\text{H}_{86}\text{NO}_5\text{Si}_3$ ; 816.5808; found 816.5815.



**Compound 2-88:** Compound **2-86** (5 mg, 0.006 mmol), was dissolved in DCM (1 mL), and transferred to a 8 mL flame-dried borosilicate test tube and purged with nitrogen. Then, meso-tetraphenylporphine (0.2 mg,  $2.9 \times 10^{-4}$ , 0.004 equiv.) was added to the reaction. The reaction test tube was chilled to  $-78$  °C and then  $\text{O}_2$  was bubbled through the solution via a syringe. Then, light was irradiated into the reaction via a 500 W floodlamp. While keeping the reaction at  $-78$  °C, the light was shined and the disappearance of starting material was monitored by TLC analysis (Hexanes/EtOAc (5:1),  $R_f = 0.55$ ). After approximately 30 mins, a large excess of  $\text{Me}_2\text{S}$  (1 mL) was added to the reaction and the light was turned off and the oxygen was replaced with nitrogen. The reaction was left to stir at  $-78$  °C for 24 h. After this time, DCM was dissolved in THF (100  $\mu\text{L}$ ) and chilled to  $-40$  °C. Then, the reaction was warmed to  $-10$  °C. Then, a solution of 2M NaOH (25  $\mu\text{L}$ ) was added to the reaction solution, then  $\text{NaBH}_4$  (0.25 mg, 0.006 mmol, 1 equiv.) and then  $\text{CeCl}_3$  (1 mg, 0.003 mmol, 1 equiv.). The reaction was left to stir at  $-10$  °C until analysis by HRMS showed that the *bis*-reduced product was observed. After 4-5 h, the reaction was quenched sat. aq.



NH<sub>4</sub>Cl (0.5 mL), extracted with DCM (3x 1 mL), then EtOAc (3x 1 mL), dried over Na<sub>2</sub>SO<sub>4</sub>, filtered and concentrated *in vacuo*. The complex mixture was carried forward without chromatography due to the *mono*- and *tri*-reduced substrates were inseparable complex mixture. (4 mg, 0.005 mmol, 80% conversion).

*<sup>1</sup>H NMR peaks correlate to characteristic peaks for the reduction product aldehyde and alkene peaks for analysis of reaction progression:*

**<sup>1</sup>H NMR** (700 MHz, CDCl<sub>3</sub>) δ *Aldehyde peaks*: 10.58 (s, 1H) [undesired], 10.55 (s, 1H) [desired],

*Alkene characteristic peak for allylic alcohol*: 5.48 (m, 1H)

*HRMS peak correlates to the desired mass peak:*

**HRMS** (ESI-TOF): [M +Na]<sup>+</sup> calcd for C<sub>46</sub>H<sub>89</sub>NO<sub>6</sub>Si<sub>3</sub>Na; 858.5890; found 858.5895.

## 2.9 References

- (1) (a) Kamboj, A.; Rathour, A.; Kaur, M. *International Journal of Pharmacy and Pharmaceutical Sciences*, **2013**, 5 (4), 8. (b) Heasley, B., *Chem. Eur. J.* **2012**, 18, 3092 – 3120.
- (2) Bagrov, A. Y.; Shapiro, J. I, Fedorova, O. V.; *Pharmacol Rev*, **2009**, 61, 9–38.
- (3) (a) Mukai, K.; Kasuya, S.; Nakagawa, Y.; Urabe, D.; Inoue, M. *Chem. Sci.* **2015**, 6, 3383–3387. (b) Zhang, H.; Reddy, M. S.; Phoenix, S.; Deslongchamps, P. *Angew. Chem., Int. Ed.* **2008**, 47, 1272–1275. (c) Renata, H.; Zhou, Q.; Baran, P. S. *Science* **2013**, 339, 59–63. (d) Khatri, H. R.; Bhattarai, B.; Kaplan, W.; Li, Z.; Long, M. J. C.; Aye, Y.; Nagorny, P. *J. Am. Chem. Soc.* **2019**, 141, 4849–4860.
- (4) (a) Sondheimer, F.; McCrae, W.; Salmond, W. G. Synthesis of Bufadienolides. *J. Am. Chem. Soc.* **1969**, 91, 1228–1230. (b) Pettit, G. R.; Houghton, L. E.; Knight, J. C.; Bruschweiler, F. *J. Org. Chem.* **1970**, 35, 2895–2898. (c) Yoshii, E.; Oribe, T.; Koizumi, T.; Hayashi, I.; Tumura, K. *Chem. Pharm. Bull.* **1977**, 25, 2249–2256. (d) Hoppe, H.- W.; Stammen, B.; Werner, U.; Stein, H.; Welzel, P. *Tetrahedron* **1989**, 45, 3695–3710. (e) Kamano, Y.; Pettit, G. R.; Inoue, M. *J. Org. Chem.* **1974**, 39, 3007–3010. (f) Pettit, G. R.; Kamano, Y.; Drasar, P.; Inoue, M.; Knight, J. C. *J. Org. Chem.* **1987**, 52, 3573– 3578.
- (5) Zhong, Y.; Zhao, C.; Wu, W.-Y.; Fan, T.-Y.; Li, N.-G.; Chen, M.; Duan, J.-A.; Shi, Z.-H. *Eur. J. Med. Chem.* **2020**, 189, 112038.
- (6) Hilton, P.; Hilton, J., Novel Beta-Steroid Compounds. U.S. Patent WO 2006120472, November 16<sup>th</sup>, 2006.
- (7) Diao, T.; Stahl, S. S., *J. Am. Chem. Soc.* 2011, 133, 14566–14569.
- (8) Chen, M.; Dong, G., *J. Am. Chem. Soc.* **2019**, 141, 14889–14897.
- (9) Gnaim, S.; Takahira, Y.; Wilke, H. R.; Yao, Z.; Li, J.; Delbrayelle, D.; Echeverria, P. G.; Vantourout, J. C.; Baran, P. S., *Nature Chemistry*, **2021**, 13, 367–372.
- (10) Chen, Y.; Romaine, J. P; Newhouse, T. R., *J. Am. Chem. Soc.* **2015**, 137, 5875–5878.
- (11) Ito, Y.; Hirao, T.; Saegusa, T., *J. Org. Chem.* 1978, 43, 1011–1013.
- (12) Nicolaou, K. C.; Zhong, Y. L.; Baran, P. S., *J. Am. Chem. Soc.*, **2000**, 122, 7596–7597.
- (13) Ley, S. V.; Cox, L. R.; Meek, G., *Chem. Rev.* **1996**, 96, 423-442.
- (14) Fairlamb, I. J. S; Syvanne, S. M. ; Whitwood, A. C. , *Synlett.* **2003**, 11, 1693-1697
- (15) DePuy, C. H.; Parton, R. L.; Jones, T. *J. Am. Chem. Soc.* **1977**, 99, 4070.

- (16) Rosenblum, M.; Gatsonis, C. *J. Am. Chem. Soc.* **1967**, *89*, 5074
- (17) Wiesner, K.; Tsai, T. Y. R.; Sen, A.; Kumar, R.; Tsubuki, M. *Helv. Chim. Acta.* **1983**, *66*, 2632–2640
- (18) Jäggi, F. J.; Tsai, T. Y. R.; Wiesner, K., *Heterocycles*, **1982** *19* (4), 647-652
- (19) Nishii, Y.; Hirai, T.; Fernandez, S.; Knochel, P.; Mashima, K. *Eur. J. Org. Chem.* **2017**, *34*, 5010-5014
- (20) Siddiki, S. M. A. H.; Touchy, A. S.; Tamura, M.; Shimizu, K-I., *RSC Adv.*, **2014**, *4*, 35803
- (21) Kita, Y.; Nishii, Y, Onoue, A.; Mashima, K., Atkinson, B., N.; Williams, J. M. J., *Adv. Synth. Catal.* **2013**, *355*, 3391-3395; *Tet. Lett.* **2014**, *55*, 6935-6938
- (22) Fisher, L. E.; Caroon, J. M.; Stabler, S. R.; Lundberg, S.; Zaidi, S.; Sorensen, C. M.; Sparacino, M. L.; Muchowski, J. M., *Can. J. Chem.* **1994**, *72*, 142
- (23) Turner, W. V.; *J Org Chem.* **1974**, *39*(13), 1935-1937 Amit, B.; Zehavi, U.; and Patchornik, A., *J. Org. Chem.* **1974**, *39*, 2, 192–196.
- (24) D'Annibale, A.; Ciaralli, L.; Bassetti, M.; Pasquini, C., *J Org Chem* **2007**, *72*(16), 6067-6074
- (25) Ojha, D. P.; Prabhu, K. R., *Org Lett*, **2015** *17*(1), 18-21
- (26) Pirkle, W. H.; Dines, M., *J Org Chem* **1969** *34*, 2239–4224
- (27) Pettit, G. R.; Moser, B. R.; Mendonça, R. F.; Knight, J. C.; Hogan, F. *J. Nat. Prod.* **2012**, *75*, 1063–1069.
- (28) Marron, B., E, *Journal of Medicinal Chemistry*, **2008**, *51*(3), 407-416
- (29) Alonso, M. E.; Jano, P.; Hernandez, M. I., Greenberg, R. S.; Wenkert, E., *J. Org. Chem.* **1983**, *48*, 3047-3050.
- (30) Wang, W.; Li, R.; Gokel, G. W., *Chem. Eur. J.* **2009**, *15*, 10543– 10553

## Chapter 3

### Total Synthesis of Cardiotonic Steroid Family: Synthesis of Cardiotonic Steroids

#### Oleandrigenin and Rhodexin B

(This chapter was partially published in: Fejedelem, Z.; Carney, N.; Nagorny, P. *J. Org. Chem.*

2021, <https://doi.org/10.1021/acs.joc.1c00985> Preprint.

<https://doi.org/10.26434/chemrxiv.14496015.v1>)

#### 3.1 Introduction

Cardiotonic steroids represent a broad family of natural steroids found in various plant and animal sources and they feature cis-AB and cis-CD ring junctions with  $\beta$ 14-hydroxylation and a 5- or 6-membered oxygenated heterocycles at the C-17 position of the steroidal skeleton. These uniquely shaped steroids serve as potent inhibitors of  $\text{Na}^+/\text{K}^+$ -ATPase, and, as a result, exhibit great range of valuable physiological effects on humans and animals.<sup>1</sup> These effects include a medley of activities including, cardiotonic,<sup>1</sup> anticancer,<sup>2</sup> antiviral,<sup>3</sup> immunomodulatory,<sup>4</sup> and anti-inflammatory.<sup>5</sup> Among the various cardiotonic steroids, cardenolide oleandrin (**3-1**) has received significant attention due to its extensive biological profile.<sup>6-8</sup> This compound is isolated from the ornate shrub *Nerium Oleander*, which is used in traditional medicine to treat various conditions including hemorrhoids, ulcers, and leprosy. The shrub can be used to create medicinal extracts for therapeutic value with the hot (Anvirzel®) and cold (Breastin®) extracts of *Nerium Oleander* and these extract concoctions have been developed for the treatment of different cancers.<sup>7</sup> Similarly, the supercritical  $\text{CO}_2$  *Nerium Oleander* extract PBI-05204 has been recently investigated in Phase

I and II clinical trials of patients with cancer in the US, and demonstrated in vitro and in vivo efficacy against various viruses including SARS-Cov-2.<sup>8</sup>

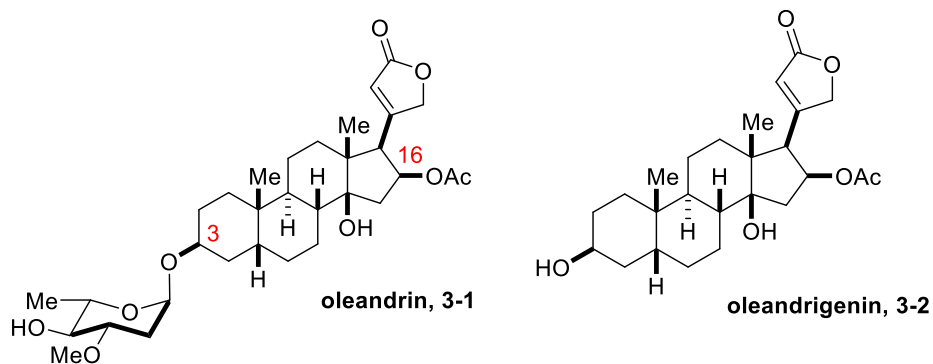


**Figure 3.1.** Structural representation of oleandrin, oleandrigenin.

The primary active ingredient of these extracts, oleandrin (**3-1**), features a  $\beta$ 16-acetoxy-substitution and C-3-glycosylation-pendant along with an unusual 2-deoxysugar, *L*-oleandrose (Figure 3.1). Its aglycone, oleandrigenin (**3-2**) is another primary bioactive agent also found in the natural extracts. Oleandrigenin is found as a core feature amongst various other bioactive natural products such as rhodexin B/tupichinolide (**3-3**)<sup>9</sup>.

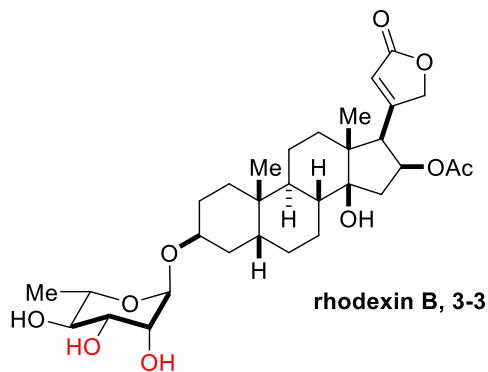


**Figure 3.2.** Structural representation of rhodexin B (tupichinolide).

Rhodexin B (**3-3**) goes by many names due to several reports where it has been isolated from several plant sources including, *Tupistra chinensis*, *Cryptostegia grandiflora*, and *Adonis*

multiflora.<sup>9</sup> It most notably possesses cytotoxicity towards multiple cancer cell lines including: HL-60 (acute leukemia), SMMC-7721 (liver cancer), A-549 (lung cancer) MCF-7 (breast cancer), with IC<sub>50</sub> values as low as ~60 nM. <sup>10</sup> The commercial availability of the  $\beta$ 16-oxygenated cardenolides for medicinal chemistry exploration has been significantly limited due to a lack of the reliable synthetic routes to these types of steroids. While there are many recent studies which have focused on developing concise approaches to cardiotonic steroids,<sup>11-12</sup> to date there is only one reported synthesis of oleandrigenin (**3-2**) by Wicha and co-workers (Figure 3.3).<sup>13</sup> They begin their synthesis of oleandrigenin commenced from testosterone propionate in five steps. **3-4** was hydrogenated to give **3-5** which was subsequently reduced with *L*-Selectride to provide compound **3-6** in 83% in 2 steps. Then, **3-6** was saponified with potassium hydroxide to provide **3-8** and then oxidized with CrO<sub>3</sub> to give compound **3-9**. Ketone **3-9** was converted to vinyl iodide **3-10** via Barton iodination in 89% yield. Suzuki-Miyaura cross-coupling reaction of **3-10** and (3-furyl)boronic acid afforded **3-11** in 74% yield. Hydroboration of **3-11** using borane-THF complex in THF following by oxidation in the presence of alkaline hydrogen peroxide afforded **3-12** in 87%. **3-12** was subsequently oxidized with Dess-Martin periodinane to provide ketone **3-13** in 86% yield.

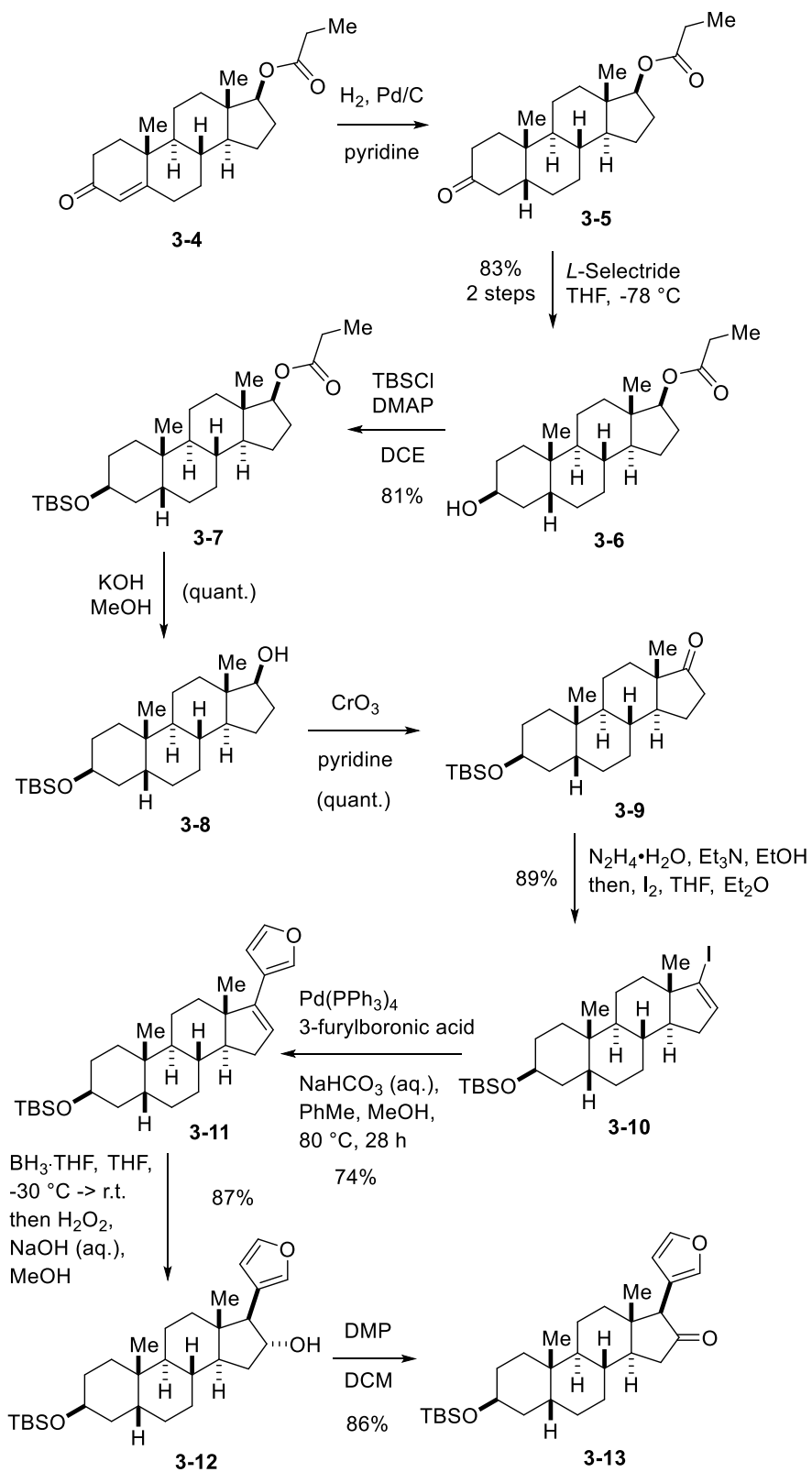
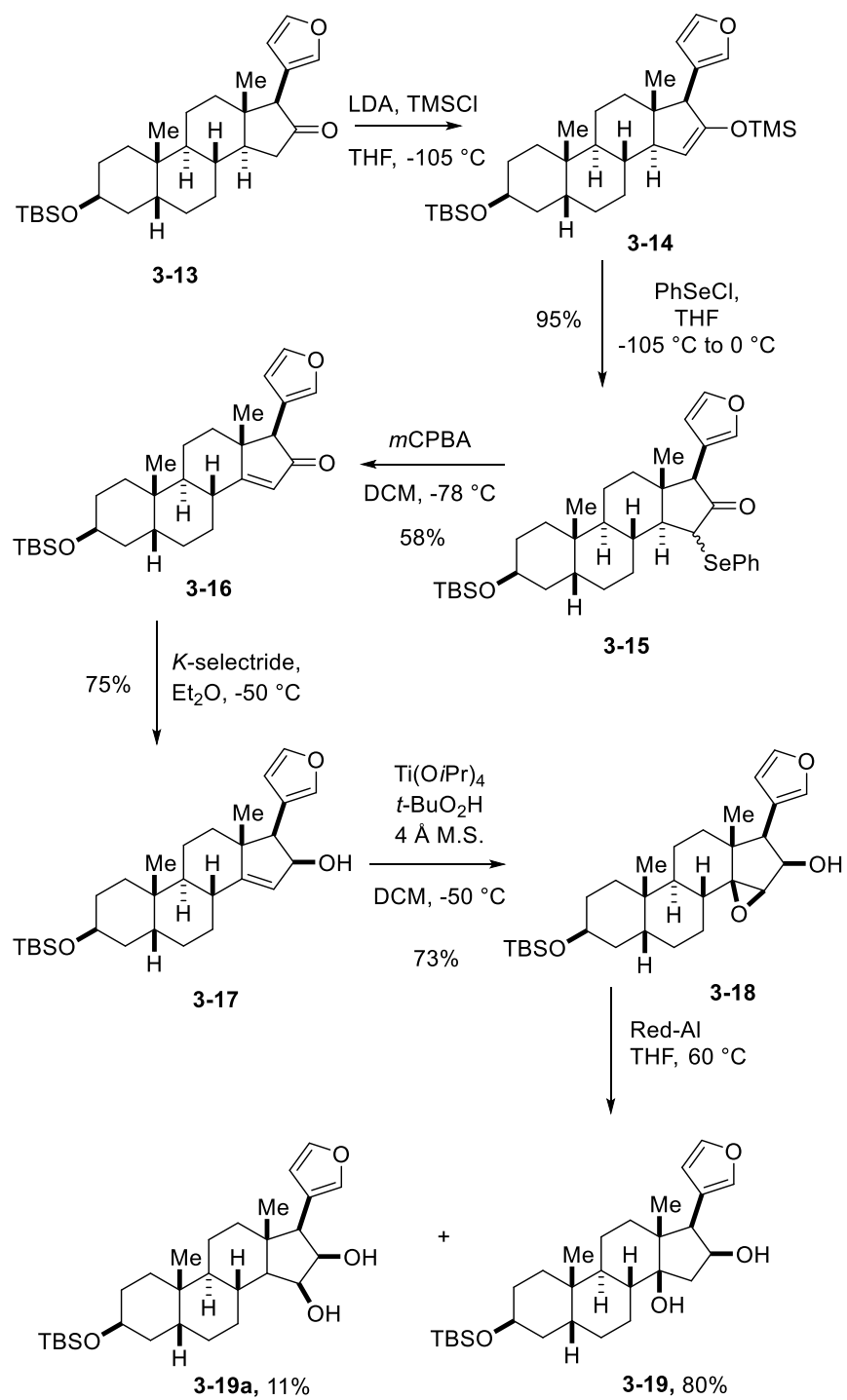


Figure 3.3. Wicha's synthesis ketone **3-13** from **3-4**.

**3-13** was then treated with LDA in THF to form enolate which was then trapped with TMSCl to provide silyl enol ether **3-14**, which was subsequently reacted with phenylselenium chloride to give **3-15** in 95% overall yield. **3-15** was then treated with *m*-CPBA, furnishing  $\alpha,\beta$ -unsaturated ketone **3-16**, which was isolated in a 58% yield. Reduction of **3-16** was carried out using *K*-Selectride to provide **3-17** in a 75% yield. Sharpless epoxidation of **3-17** using titanium(IV) isopropoxide and tert-butylhydroperoxide in DCM in the presence of 4 Å molecular sieves at -50 °C gave epoxide **3-18** in 73% yield. Reduction of **3-18** with Red-Al in THF at 60 °C afforded a mixture of two products that were separable by chromatography (**3-19**, 80% yield and side product **3-19a**, 11% yield)





**Figure 3.4.** Wicha's synthesis **3-19** from **3-13**

The diol **3-19** was then acetylated using acetic anhydride and DMAP in DCM at 0 °C to provide **3-20**. To transform the furanyl-derivative to a butanolide, photochemical oxidation of **3-20** in the presence of diethyl(isopropyl)amine, which was followed by NaBH<sub>4</sub> reduction after an incubation period, followed by acidification, afforded **3-21** in 66% yield. The TBS protective group was then removed using [Py·(HF)<sub>n</sub>] in THF provided oleandrigenin **3-2** (91% yield). Wicha was able to complete the synthesis of oleandrigenin from **3-4** in 18 steps and 5% overall yield.

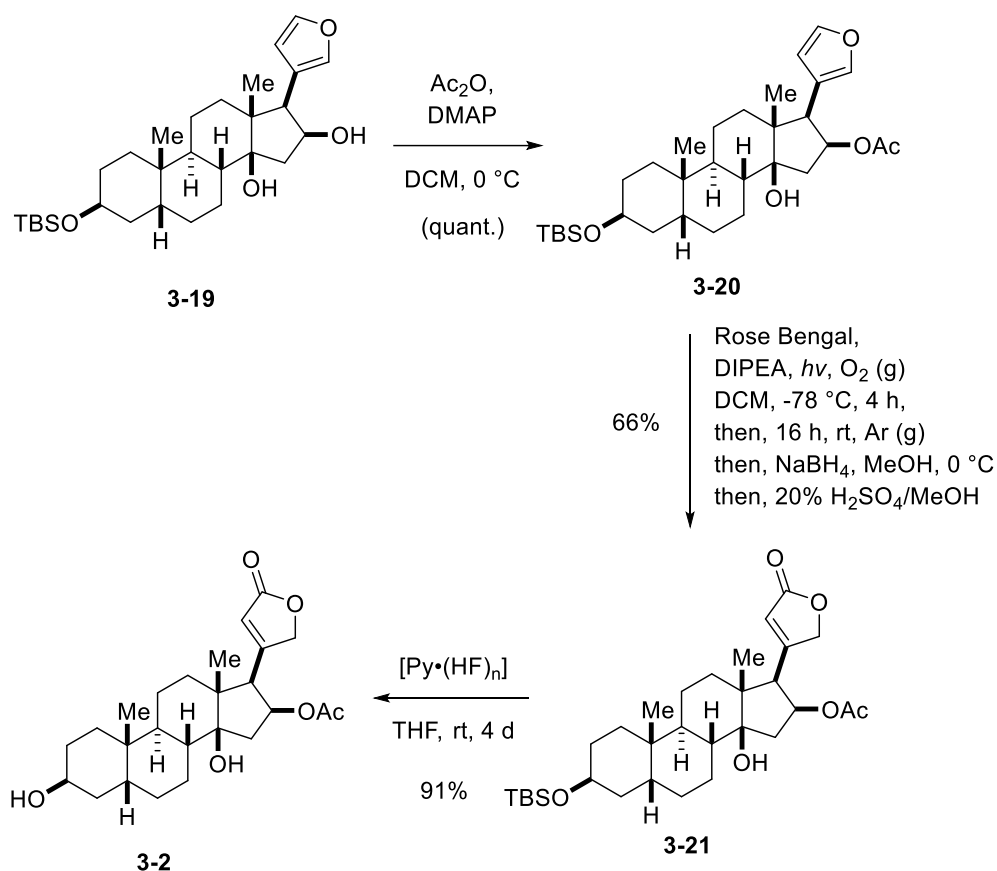


**Figure 3.5.** Wicha's completed synthesis of oleandrigenin (**3-2**).

Wicha's mechanistic proposal (Figure 3.6) for photooxidation of the furan ring in **3-20** leads to intermediate peroxide **3-20a**, that in the presence of a bulky base (B) undergoes rearrangement to acid-aldehyde salt **3-20b** to give the cyclic closure product **3-20c**. NaBH<sub>4</sub> reduction then affords **3-21** as the product.

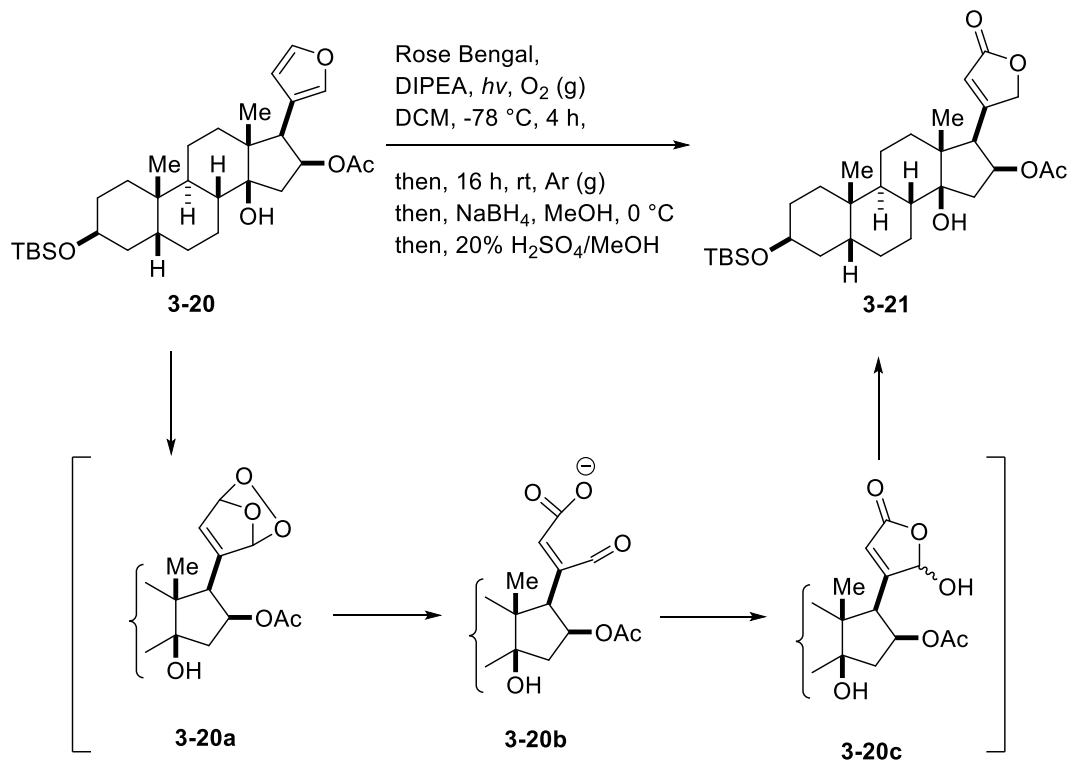
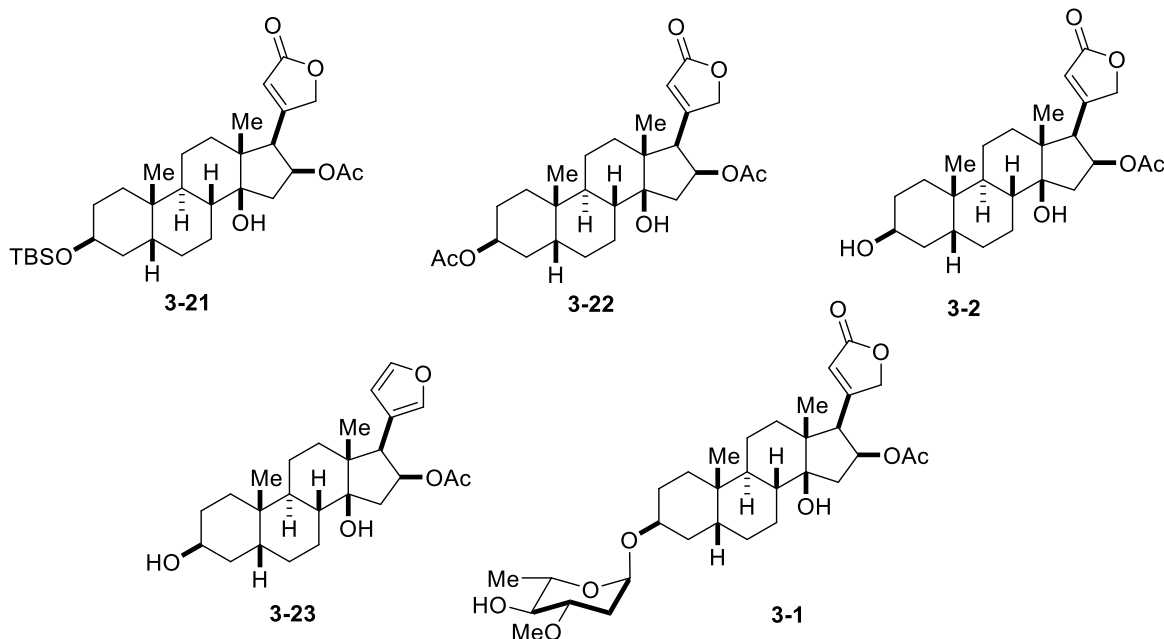


**Figure 3.6.** Wicha's mechanistic proposal for photooxidation endo-peroxide rearrangement for transformation of **3-20** to **3-21**.

After successfully completing oleandrigenin, Wicha and co-workers conducted cytotoxicity studies on oleandrigenin and compared its activity against the other synthetic derivatives they synthesized as well. They looked at cytotoxicity against human cancer, noncancerous cells and ATPase inhibiting activities. Cytotoxic activity was tested in three cancer cell lines: human chronic lymphoblastic leukemia (CEM), human breast adenocarcinoma (MCF7), human cervical adenocarcinoma (HeLa) and on human normal fibroblasts (BJ) (Table 3.1).

**Table 3.1.** Select examples from Wicha's cytotoxic ( $IC_{50}$ ;  $\mu M$ ; 72 h) assay study against cancer cell lines.<sup>13</sup>



Compound	CEM*	MCF7*	HeLa*	BJ*
<b>3-1</b>	$0.019 \pm 0.002$	$0.033 \pm 0.008$	$0.062 \pm 0.002$	$0.026 \pm 0.006$
<b>3-2</b>	$0.2 \pm 0.0$	$0.8 \pm 0.3$	$0.2 \pm 0.0$	$0.1 \pm 0.0$
<b>3-21</b>	$17.3 \pm 1.7$	$20.3 \pm 3.5$	$34.1 \pm 3.3$	$10.6 \pm 1.8$
<b>3-22</b>	$0.4 \pm 0.0$	$1.7 \pm 0.7$	$1.1 \pm 0.1$	$0.2 \pm 0.1$
<b>3-23</b>	$9.4 \pm 1.7$	$16.1 \pm 0.4$	$14.2 \pm 0.4$	$4.0 \pm 0.7$

\* $IC_{50}$  values are listed in  $\mu M$  concentrations; investigating cytotoxicity in human cancer and noncancerous cells and ATPase inhibiting activities to observe induction of apoptosis and influence the cell cycle in human cancer cells.

Oleandrigenin 3-OAc (**3-22**) surprisingly had similar activity to oleandrigenin **3-2** across all the cancer cell lines tested. However, oleandrin possessed the strongest effects (**3-1**) When these compounds were tested for their interaction with isolated  $Na^+/K^+$ -ATPase enzymes, it was found that compound **3-22** was not able to inhibit enzyme ATPase activity. Whereas, the furyl derivative

**3-23** were more potent inhibitors than oleandrin **3-1** and oleandrogenin **3-2**.<sup>13</sup> In addition, they showed that **3-21**, while bearing a bulky and group, was able to exhibit strong Na<sup>+</sup>/K<sup>+</sup>-ATP-ase inhibitory and cytotoxic activities.

Our group has had a long-standing interest in developing concise total syntheses of cardiotonic steroids and their analogues for the subsequent medicinal chemistry and chemical biology explorations.<sup>14</sup> Due to the intriguing biological profile exhibited by oleandrin (**3-1**) and other cardiotonic steroids derived from oleandrogenin (**3-2**), we became interested in developing our own strategy for the total synthesis of **3-2** and its related glycosides. For the medicinal chemistry exploration of this compound, we targeted a synthetic route that would minimize the D-ring manipulations after the installation of the  $\beta$ 17-substituent. From Wicha's reports, the manipulations necessary to install the  $\beta$ C16 and C14 oxygen stereocenters required hydroboration-oxidation of the C-16/C-17 double bond to acquire an  $\alpha$ C16 alkoxy group that needs to be oxidized to a ketone, which is then used to introduce the  $\beta$ C-14 alkoxy group.

Fernandez-Mateos<sup>15</sup> reported a clever route for stereo specific epoxide ring opening for their approach for synthesizing limonoids.

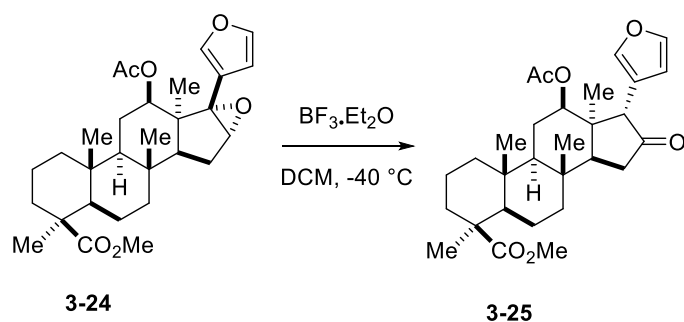


**Figure 3.7.** Fernandez-Mateos selected example of stereospecific epoxide ring opening with Lewis acid.

By installing a specific regioisomer of the epoxide, the furan stereocenter will be inverted via a House-Meinwald rearrangement to facially move the hydrogen and subsequently inverts the furan substituent. Taking inspiration from this example, we surmised a scheme for making oleandrigenin that could be accomplished if the vinyl iodide **3-12** containing a preinstalled  $\beta$ 14-OH group is used as the advanced intermediate (*cf.* Figure 3.8). The pre-installed  $\beta$ 14 alcohol can then act a directing group to selectively install the epoxide in the desired orientation.

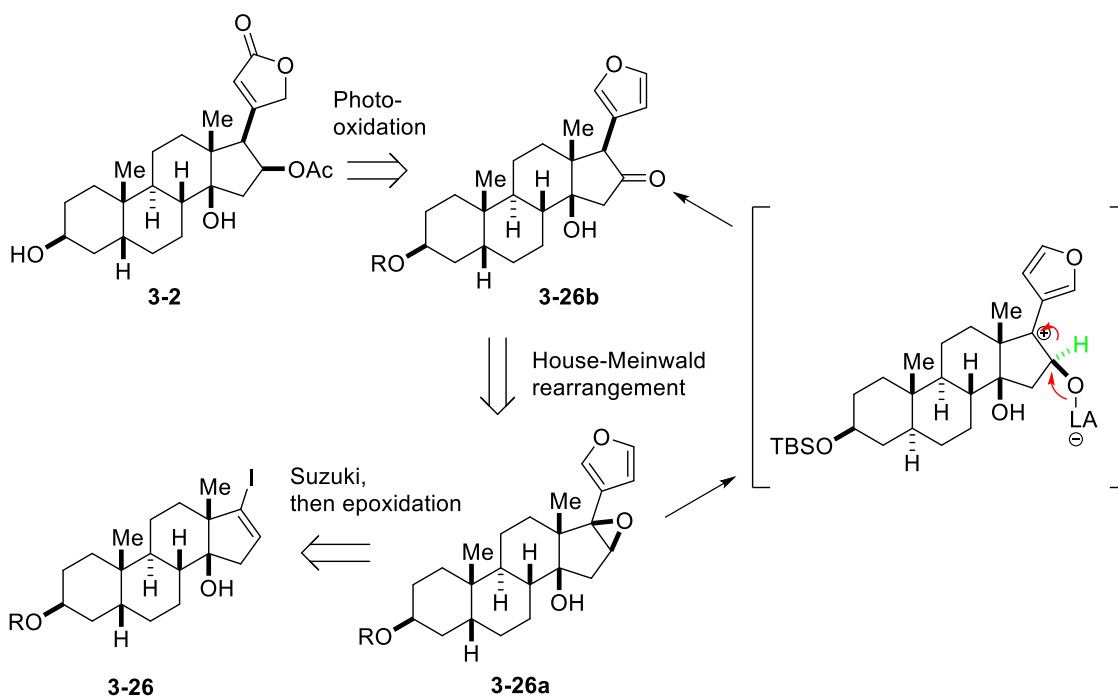


**Figure 3.8.** Retrosynthetic proposal for C-16 oxidation and mechanistic proposal for C-16 oxidation via House-Meinwald rearrangement.

This compound could be conveniently converted to epoxide **3-26a**, which, when subjected to a Lewis acid, will undergo an epoxide rearrangement to install the desired  $\beta$ 17 stereochemistry

and oxygenation at the C16 position (**3-26b**).<sup>15</sup> After this transformation, established synthetic techniques would be used to obtain the natural product oleandrigenin.<sup>13</sup>

It is important to note that during the preparation of this document and related publication, Inoue and co-workers applied a similar rearrangement strategy of an epoxide towards the synthesis of bufadienolides.<sup>16</sup> They started by stereoselectively hydrogenating testosterone **3-27** at the C5-double bond by using Pd/C in pyridine, providing the cis-fused AB ring **3-28** as a major diastereomer in 96% yield ( $\beta\text{-H}:\alpha\text{-H}$  at C5 = 9.3:1). The C3-ketone of **3-28** was stereoselectively reduced in the presence of the C17-ketone by using the bulky reductant  $\text{KBH}(s\text{-Bu})_3$  in 94% yield. The resultant C3-OH was protected as its *tert*-butyldimethylsilyl (TBS) ether to generate **3-29** after separating the diastereomers in 87% yield. Subsequent Saegusa-Ito oxidation with  $\text{Pd}(\text{OAc})_2$  transformed **3-29** to the  $\alpha,\beta$ -unsaturated ketone **3-30**. This was isomerized to the more substituted nonconjugated C14-olefin of **3-31** by employing *i*Pr<sub>2</sub>NEt and SiO<sub>2</sub> in C<sub>6</sub>F<sub>5</sub>CF<sub>3</sub>. A Co(acac)<sub>2</sub>-catalyzed Mukaiyama hydration of olefin **3-31** using O<sub>2</sub> and PhSiH<sub>3</sub> stereoselectively introduced the requisite  $\beta$ -configured C14 tertiary alcohol of **3-32** in 82% yield ( $\beta\text{-OH}:\alpha\text{-OH}$  at C14 = 2.3:1). To prepare for the Stille coupling reaction, the C17-ketone of **3-32** was changed to the corresponding vinyl iodide **3-33** through sequential treatment with NH<sub>2</sub>NH<sub>2</sub> and then with I<sub>2</sub> and Et<sub>3</sub>N in 50% yield. Stille coupling was then conducted to provide **3-34** in 67% yield.

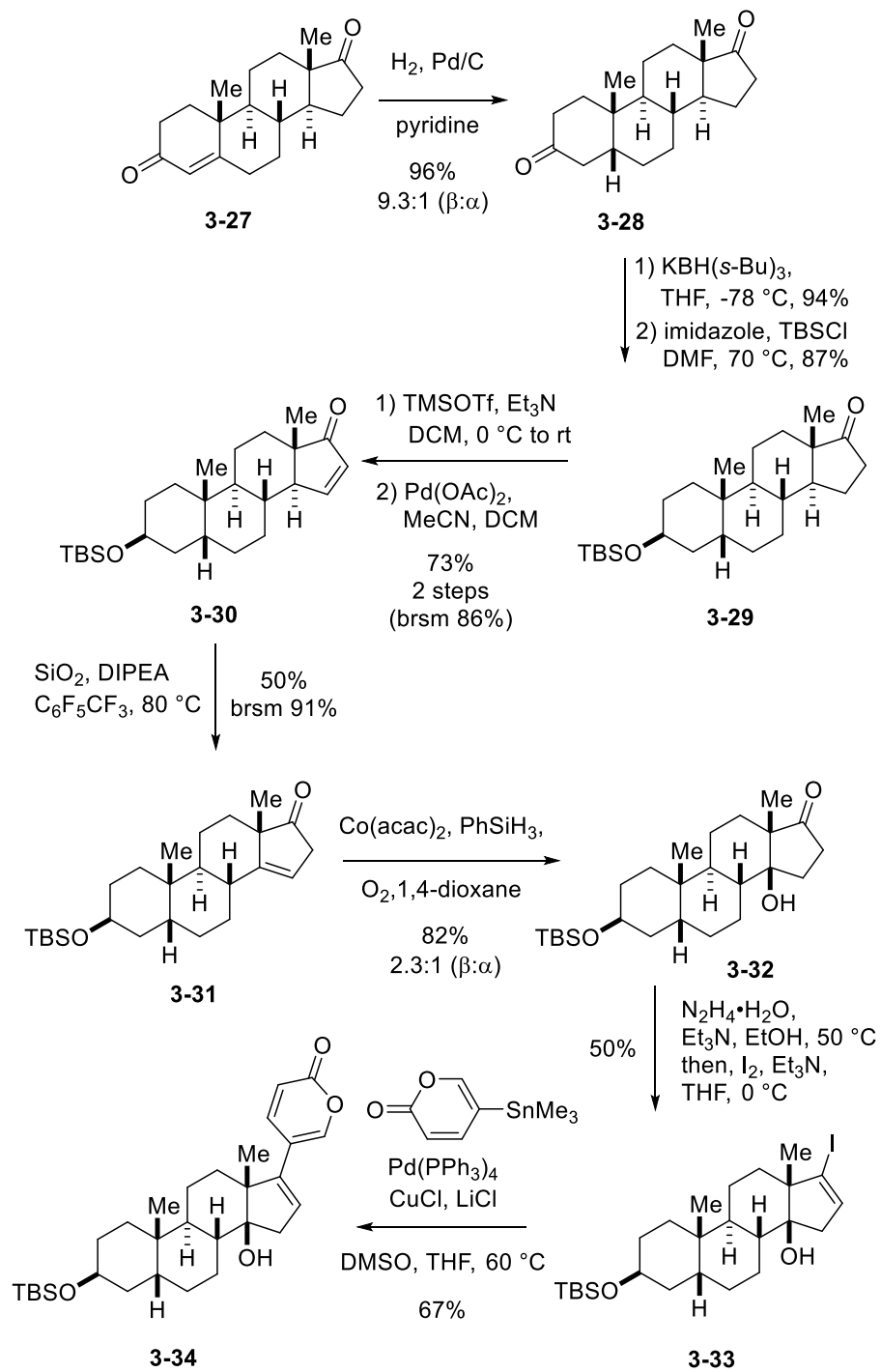


**Figure 3.9.** Inoue's synthesis of bufadienolide precursor **3-34**.



From there, compound **3-34** was then epoxidized in a surprisingly selective manner at the C-16/17 position of the steroid without touching the pyrone moiety. They observed that the epoxide rearrangement of **3-35** via Lewis acid mediated ring opening was not as facile of a transformation due to the unusual reactivity of 2-pyrone. For example, by using  $\text{InCl}_3$  to activate the epoxide, the desired product **3-37** was not detected. The major compound they obtained was instead a fused hexacycle product **3-36**, which was isolated in 60% yield, and the structure was confirmed by X-ray crystallographic analysis. They commenced screening several reagents and finally landed on a combination of trimethylsilyl trifluoromethanesulfonate (TMSOTf) and 2,6-lutidine to induce the desired rearrangement product **3-37** in 68% yield.

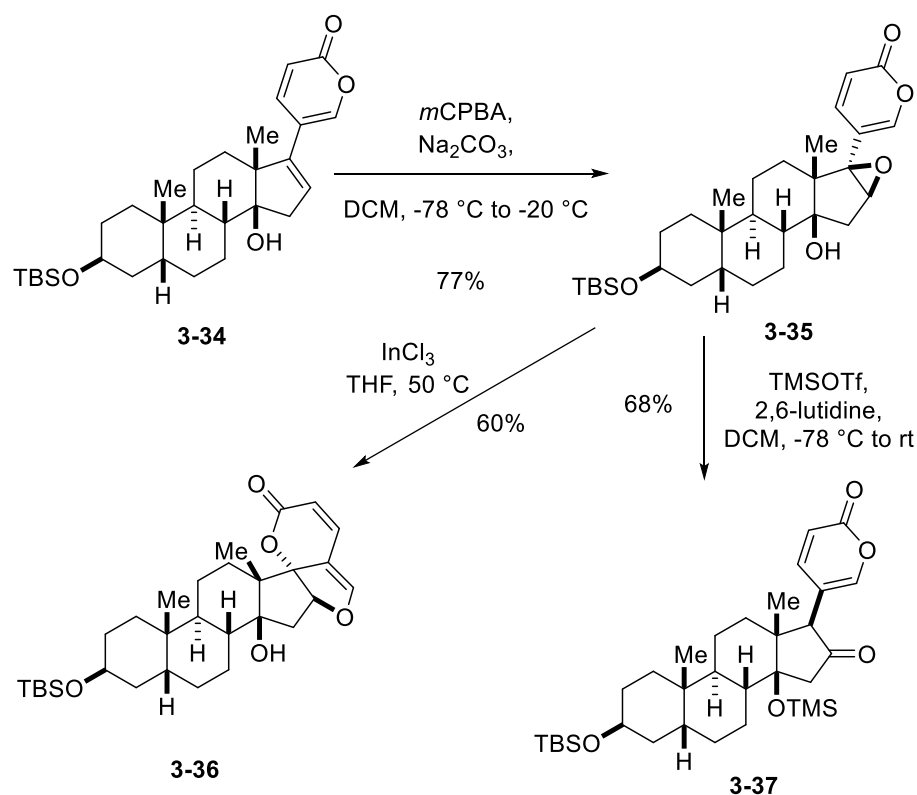


**Figure 3.10.** Inoue's synthesis of **3-37**.

They proposed plausible mechanisms for each respective transformation. With  $\text{TMSOTf}$  and 2,6-lutidine in  $\text{DCM}$  (*cf.* Figure 3.12, Path A), this promoted the C14O-TMS ether formation along

with the 1,2-hydride shift. The  $\beta$ -orientation of all the were confirmed by nuclear Overhauser effect (NOE) correlations. TMSOTf and 2,6-lutidine activate the oxirane ring and cap both C14- and C16-alcohols with TMS groups. The added bulk and electron donating nature of the newly formed C16O-TMS group decelerates the nucleophilic attack on the oxocarbenium ion and accelerates the 1,2-hydride shift.

To rationalize the  $\text{InCl}_3$ -induced opening of the oxirane ring (*cf.* Figure 3.12, Path B) is assisted by electron donation from the oxygen lone pair of the 2-pyrone ring, producing a cation. The nucleophilic indium alkoxide then attacks the electrophilic oxocarbenium ion to afford an unstable acetal. Further activation with  $\text{InCl}_3$  cleaves the acetal, and the liberated carboxylate adds to the C17 position from the opposite face of the C13-methyl group, providing the rigid hexacycle.

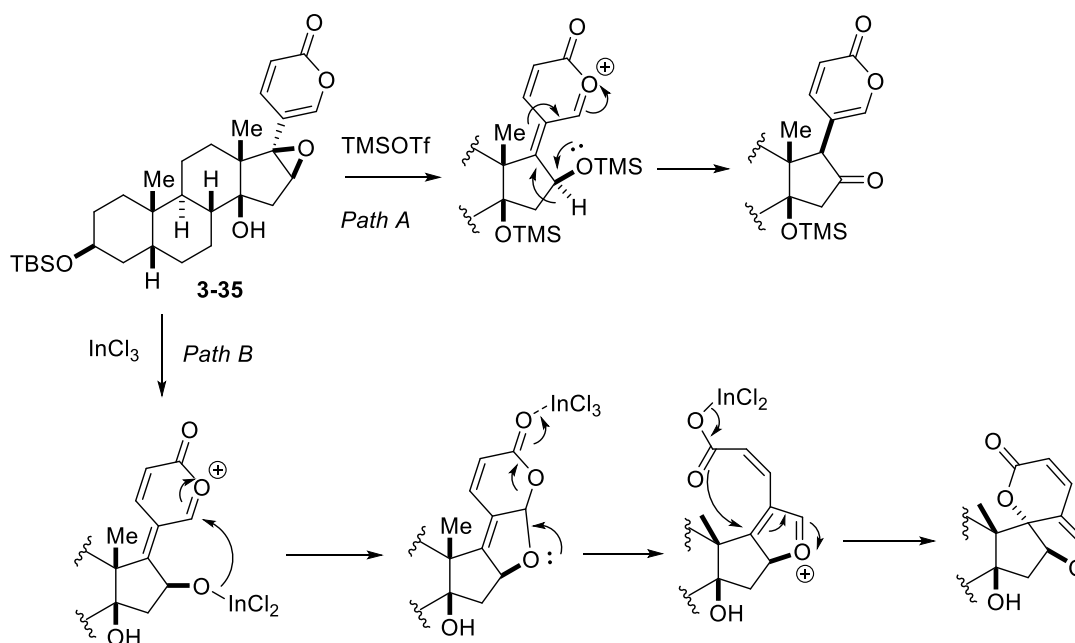


**Figure 3.11.** Mechanistic proposal by Inoue for the observed transformations with **3-35** and TMSOTf (path A), and  $\text{InCl}_3$  (path B).

Carrying forward with their synthesis, the C14O-TMS group of **3-37** helps to further shield the  $\beta$ -face, and with that,  $\text{NaBH}_4$  reduction occurred from the opposite side, stereo-selectively giving

C16 $\beta$ -alcohol **3-38** in 93% yield. As a brief representative example of their further modifications, Inoue's group made bufotalin **3-40** by acetylating the C16-alcohol **3-39** and removed the two silyl protecting groups with HF in pyridine. To produce bufalin (**1-6**), reductive removal of the C16-alcohol of **3-38** was necessary. They found that direct application of the typical Barton–McCombie-type deoxygenation to **3-38** was unsuccessful, presumably due to the unwanted participation of 2-pyrone in the reaction. To remedy this, **3-38** was subjected to a neutral halogenation/dehalogenation process. CBr<sub>4</sub>, PPh<sub>3</sub>, and imidazole, to transform **3-38** into the desired bromide **3-41** and the undesired olefin **3-42** via an S<sub>N</sub>2 reaction and an E2 elimination, respectively.

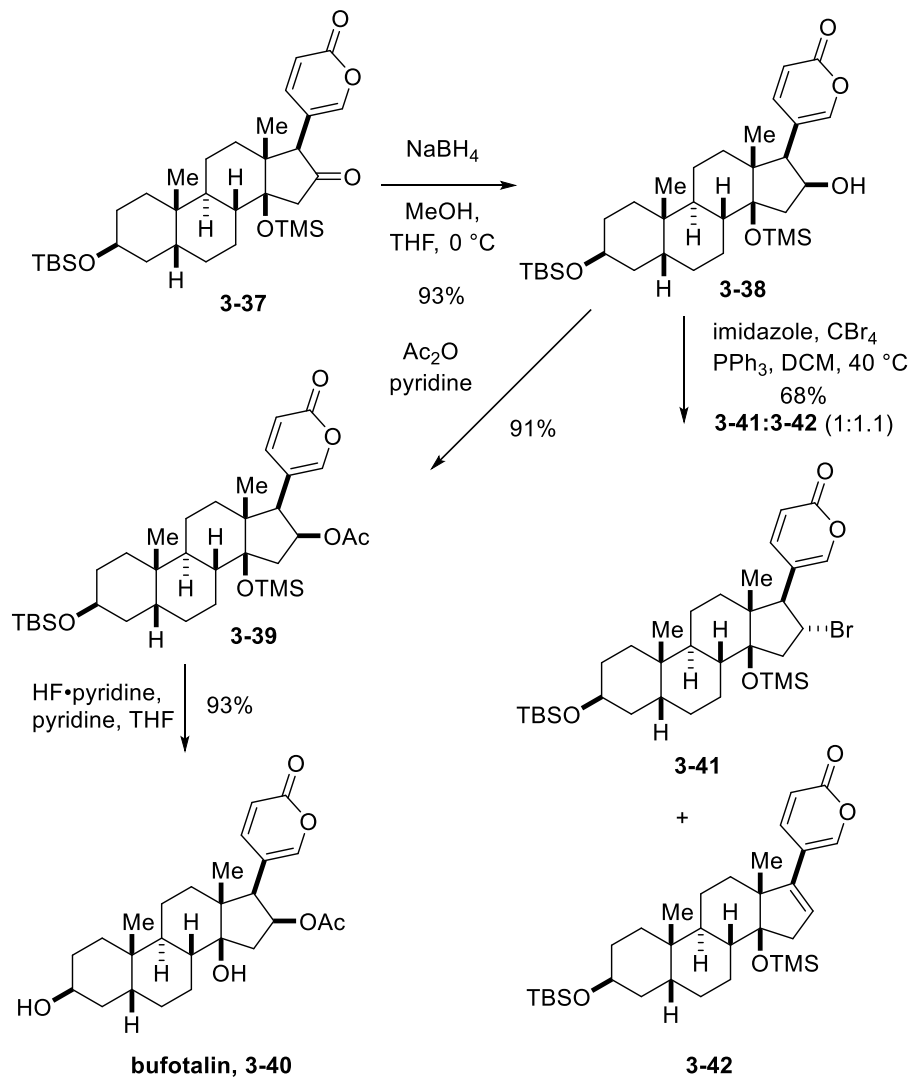


**Figure 3.12.** Inoue's synthesis of bufotalin and scheme leading to bufalin.

Compounds **3-41** and **3-42** could not be separated and were together subjected to radical deoxygenation conditions using Et<sub>3</sub>B and *n*-Bu<sub>3</sub>SnH under an O<sub>2</sub> atmosphere. Then, in one pot, aqueous HCl and MeOH were added for deprotection to afford bufalin along with the **3-43**.

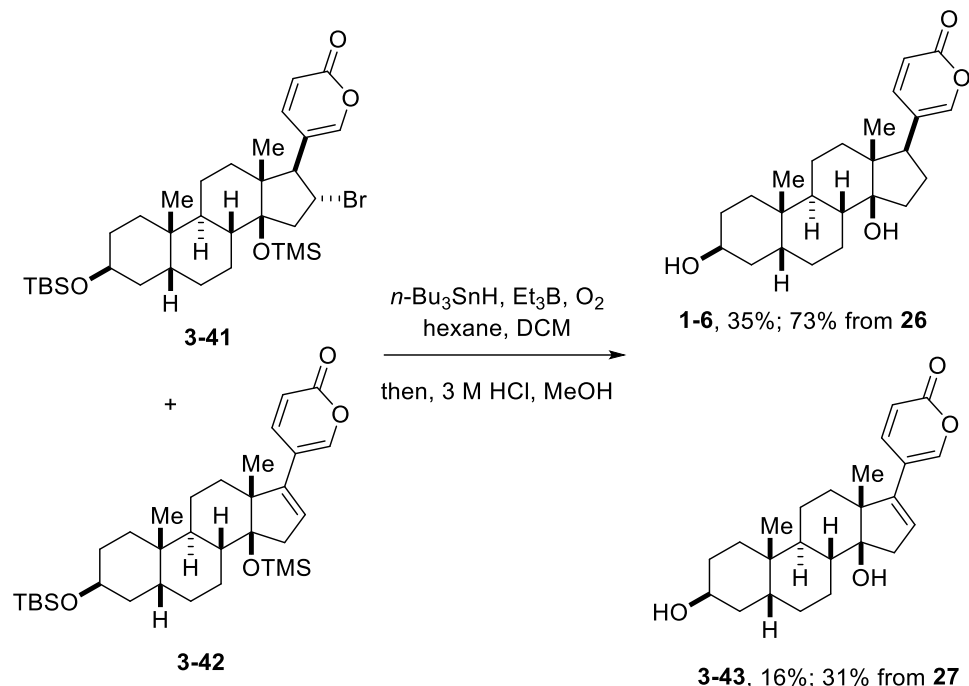


**Figure 3.13.** Inoue's completed synthesis of bufalin.

This synthesis is very impressive and important for the field of total synthesis of bufadienolides. However, with the major struggles surrounding the undesired sensitivity of the 2-pyrone moiety, as was also recognized with our studies in Chapter 2, it can be observed that the feats accomplished are noteworthy. To this end, no applications of House-Meinwald Lewis acid directed epoxide ring opening have been utilized towards the synthesis of cardenolides. And with only one report for the total synthesis of oleandrigenin, the proposed retrosynthetic route (*cf.* Figure 3.8), provides novelty to this method. In the following sections of this chapter, we describe the development of the studies towards the synthesis of oleandrigenin (**3-2**) from testosterone, and the subsequent glycosylation of **3-2** into the natural product rhodexin B (**3-3**) also known as tupichinolide. To the best of our knowledge, this is the first successful example of the C3 sugar installation in the presence of the  $\beta$ 16-acetoxy group, as well as the first reported synthesis of

rhodexin B, and we believe that the studies described in this manuscript will be instrumental for the future medicinal chemistry exploration of glycosylated oleandrigenin (**3-2**) derivatives.

### 3.2 Direct installation of $\beta$ C-16 oxygenation

#### 3.2.1 Direct C-16 oxidation of butanolide containing steroid

To begin our studies, oxidation of a butanolide containing steroid was first investigated. Using the previously synthesized  $5\alpha$ -vinyl iodide **2-8** (cf. Figure 2.3), Stille cross-coupling was carried out to make compound **3-43**.

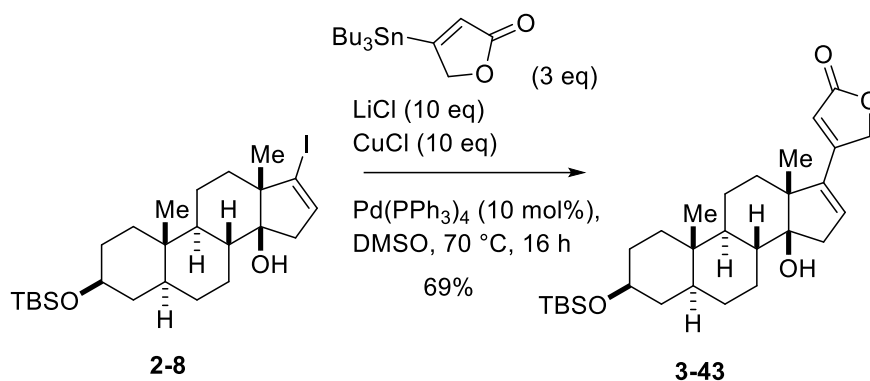


**Figure 3.14.** Stille cross-coupling for making model butenolide **3-43**.

To elucidate the capability of this compound for direct epoxide installation, a method developed for masking butenolides as silyloxy furans was used first to then be followed by hydroboration oxidation. Unfortunately, the process described in Figure 3.15 yielded no desired compound. Even when no preemptive protection of the butenolide was used prior to hydroboration oxidation, the butenolide did not survive the reaction conditions.

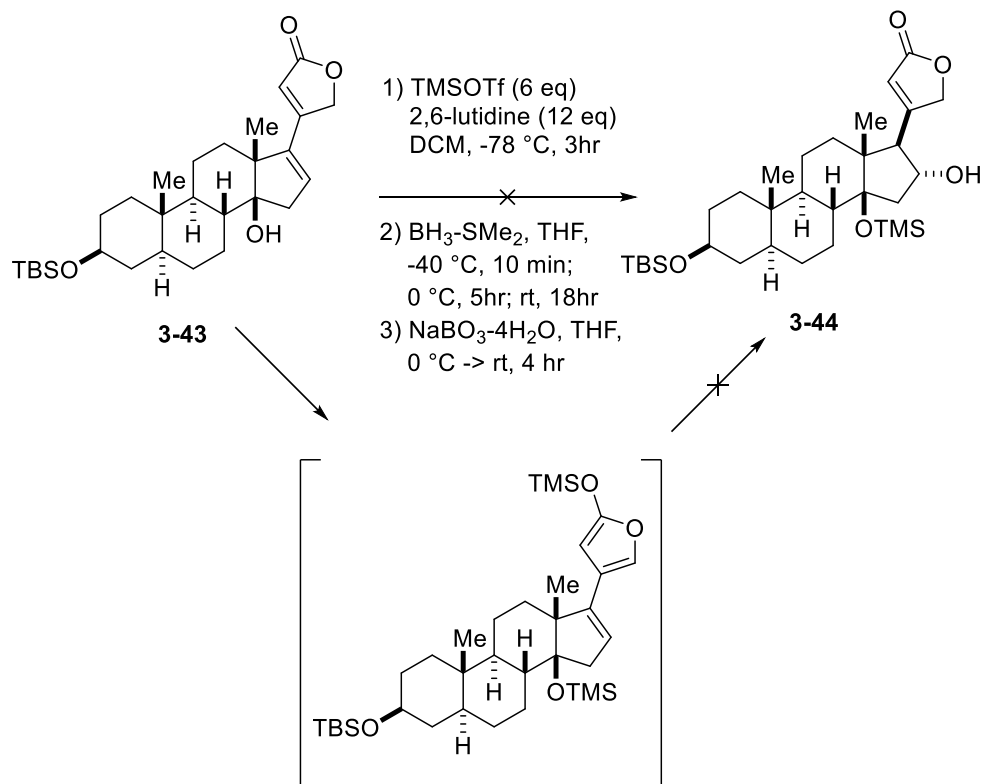


**Figure 3.15.** Hydroboration oxidation on model butanolide **3-43**.

With the hydroboration operation being unsuccessful, we decided to employ the report by Rubio<sup>15</sup> describing a method of installing an epoxide at the correct orientation can induce facial regioselectivity for forcing the C-17 substituent to be in the  $\beta$ -orientation. To begin this study, the model **3-43** was first used to install the epoxide via  $\beta$ 14-hydroxyl directed epoxidation under the Sharpless conditions provided epoxide **3-44** (70% yield, >20:1 dr).

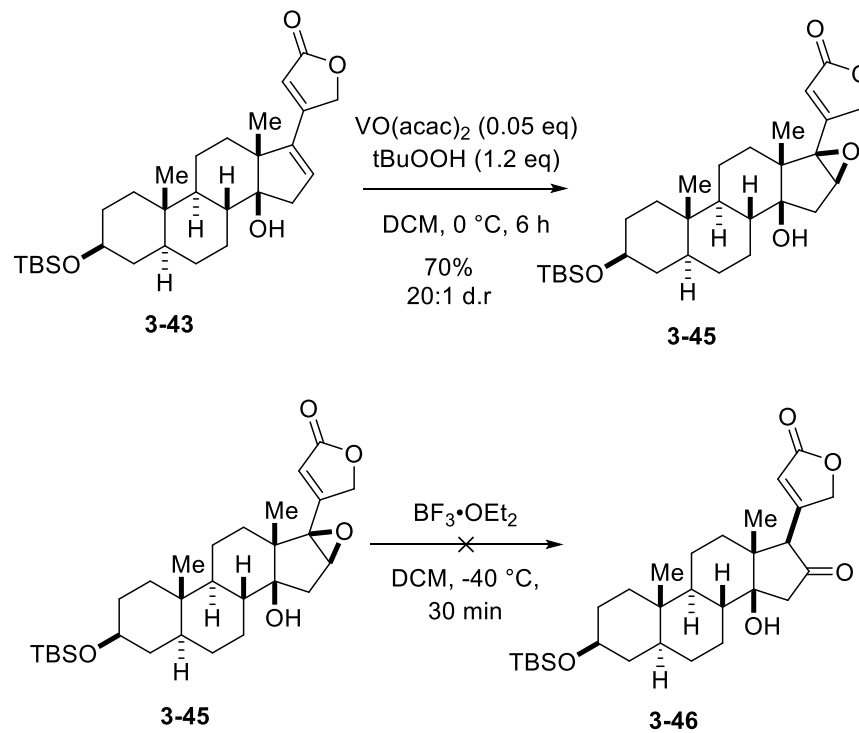


**Figure 3.16.** Attempted Lewis acid epoxide ring opening on model butanolide **3-43**.

From there, the literature conditions<sup>15</sup> described for using the Lewis acid mediated epoxide ring opening, found that no productive reaction was observed. Even when sub-stoichiometric amounts of  $\text{BF}_3 \cdot \text{OEt}_2$  were used, no productive reaction was observed, only decomposition by HRMS, crude NMR analysis.

Upon searching through the literature, a report was discovered from Asakawa<sup>17</sup> proposing an unusual pathway involving a rearrangement resulting in the formation of a novel spirocyclic product or a C-14/15 and C-16/17 eliminated triene product. They claim that with their studies of using  $\text{BF}_3 \cdot \text{OEt}_2$  catalyzed reaction conditions for opening their epoxide compound, undergoes 1,2-migration of a methylene group in the  $\gamma$ -position of the steroid to give a spirocyclic derivative **3-48**. They were able to confirm the spiro-cyclic product via mass spectrometry, chemical analysis, UV-Vis,  $^1\text{H}$  NMR and  $^{13}\text{C}$  NMR to confirm the tetraene moiety **3-49**. They also showed that if the ketone butanolide product was made separately and subjected to the same reaction conditions, the



same outcome was observed for the 1,2-alkyl shift leading to the spiro-cycled product in 93% overall.

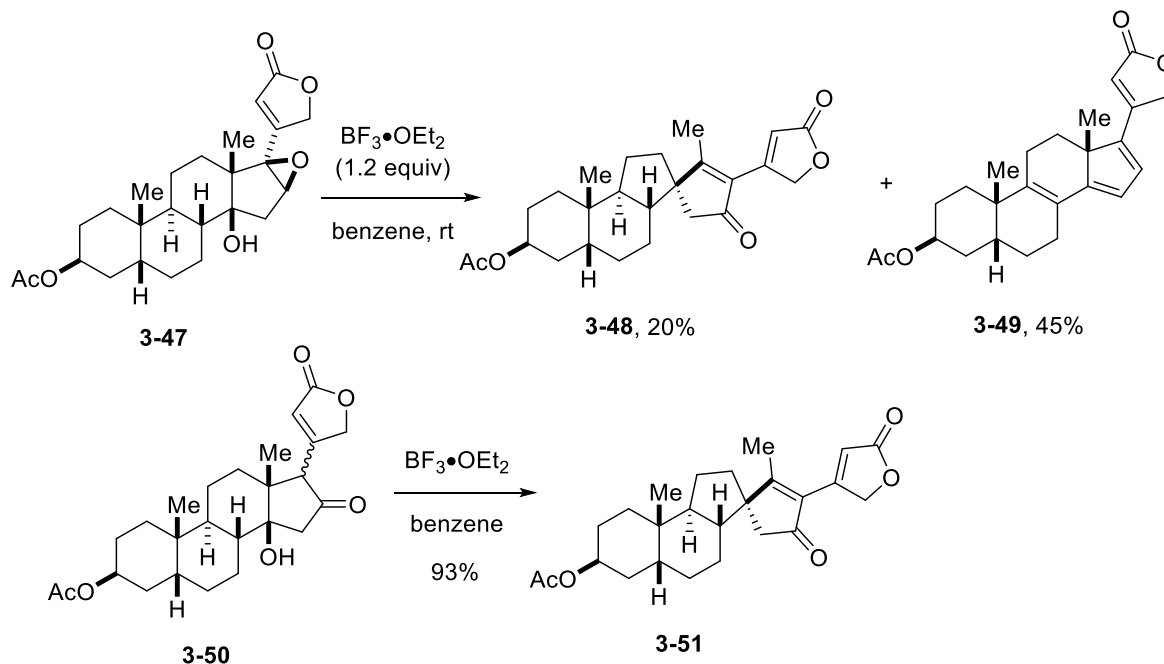


**Figure 3.17.** Asakawa's  $\text{BF}_3 \cdot \text{OEt}_2$ , Lewis acid ring opening with pre-installed C16-ketone.<sup>17</sup>

They propose two possible mechanistic routes for the formation of the spirocyclic product which was reproduced to be modeled with the starting substrate used in this described study (Figure 3.18). The epoxide ring opening to the C-16 position, can follow two individual paths, with one leading to initial elimination of the C-14 hydroxyl group (Path 1) which then instigates the alkyl shift. Or Path 2, which shows alkyl shift propagating the C-14 elimination followed by ketone formation after quench.

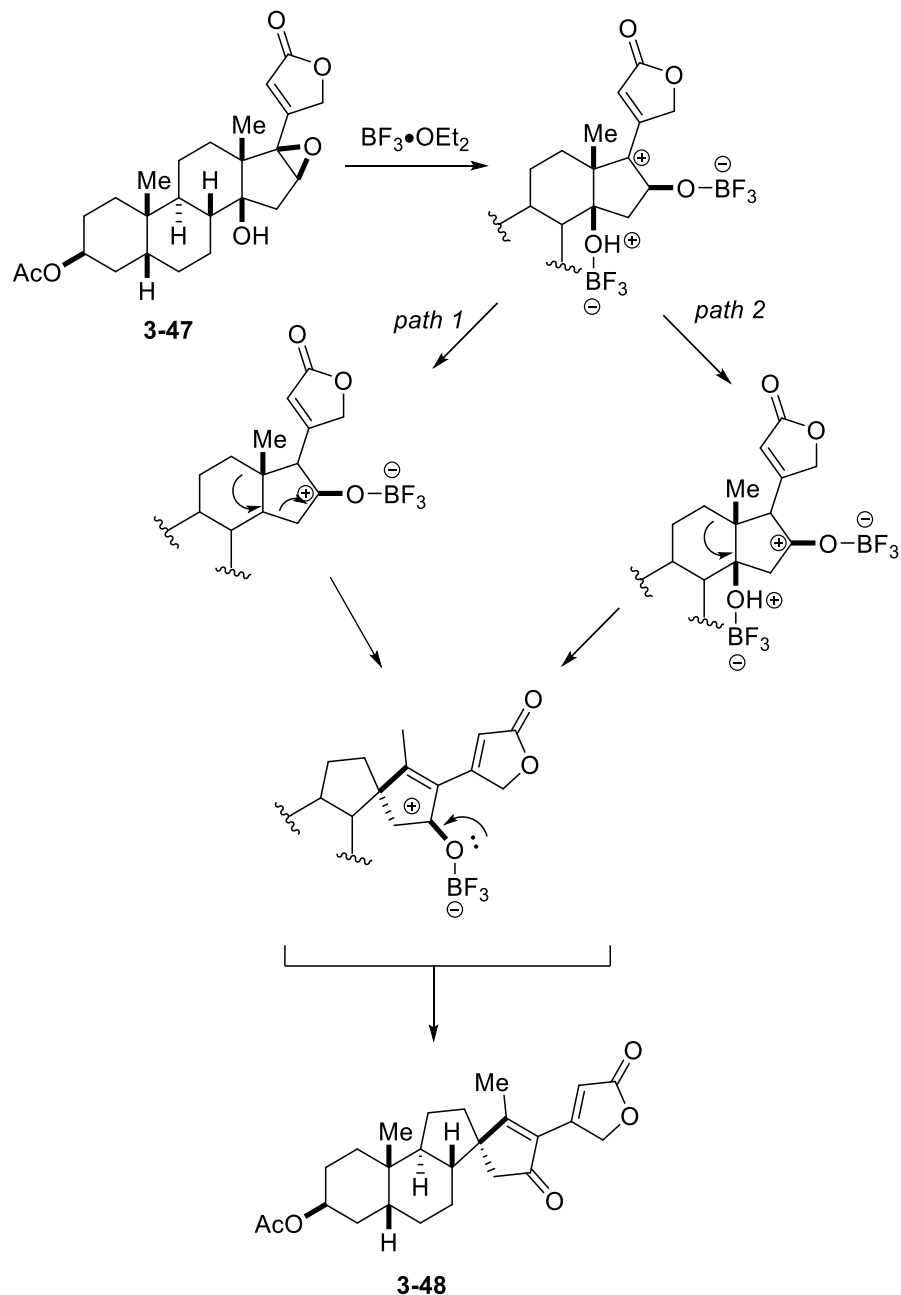


**Figure 3.18.** Mechanistic proposal for transformation of epoxide **3-47** to spirocyclic intermediate **3-48**.

The other mechanism they propose for the elimination product **3-49** (*cf.* Figure 3-19) follows epoxide ring opening to the C-17 position which promotes multiple downstream hydride elimination sequences to yield the tetraene side product with no alkyl shift.

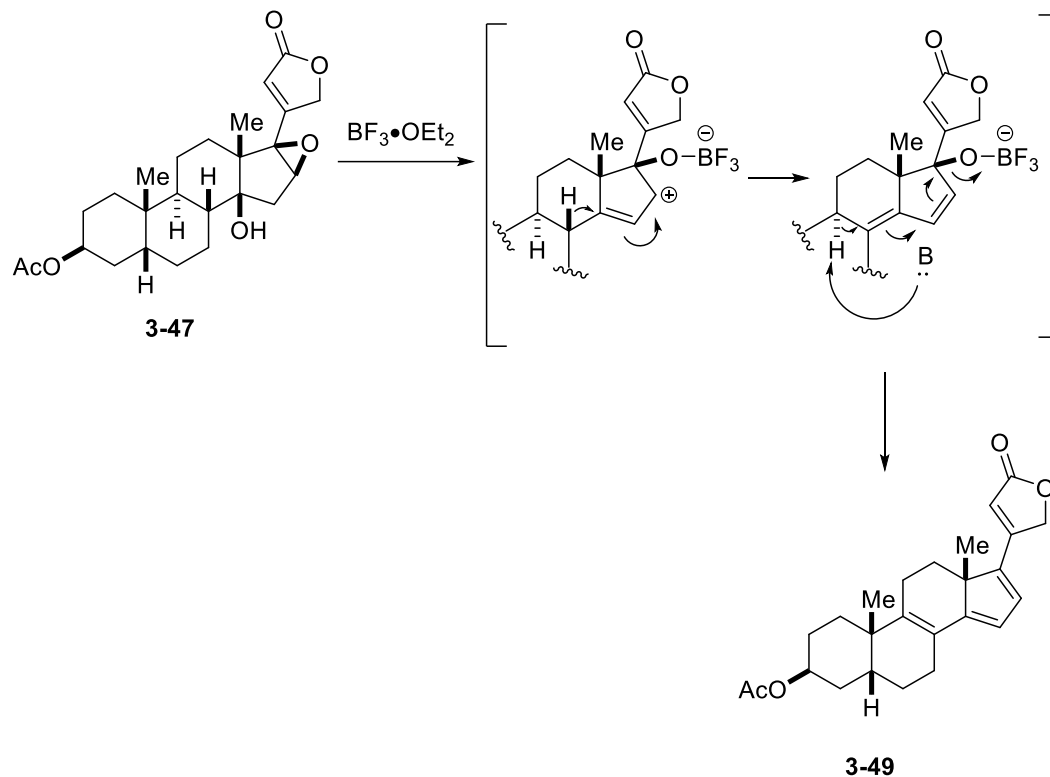
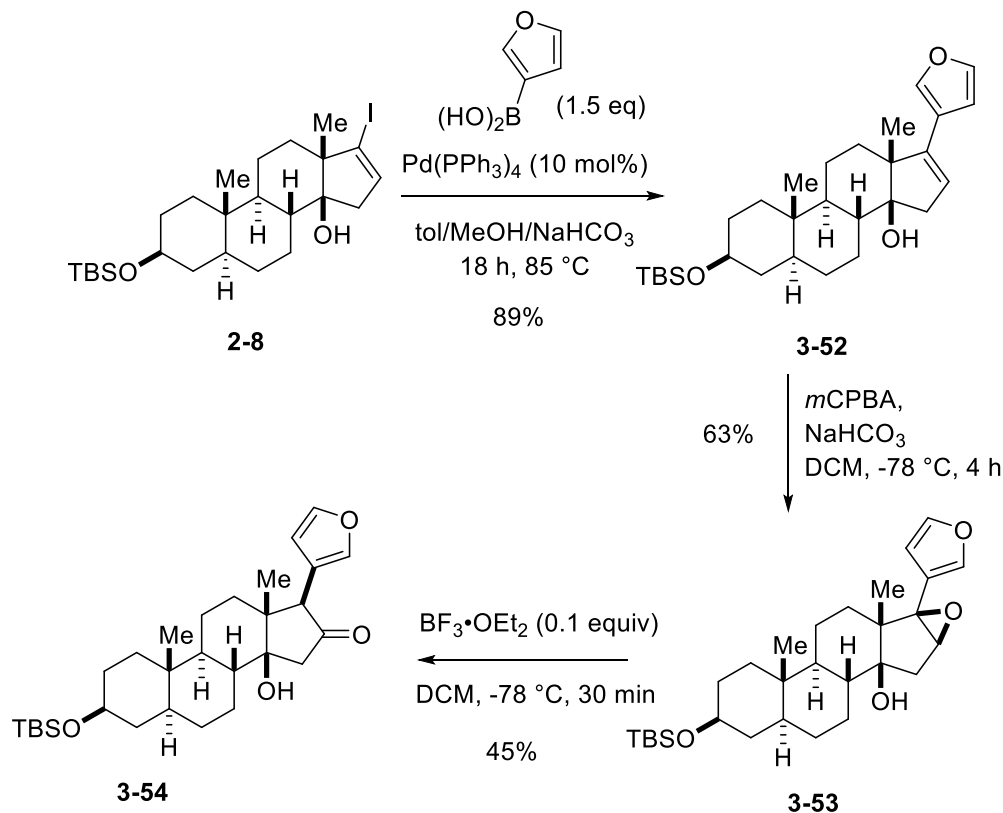


**Figure 3.19.** Asakawa's proposed decomposition pathways with **3-47**.

This outcome led us to believe that even if productive formation of the desired compound were achieved, it would be consumed at a competitive rate to the starting material.

### 3.3 Directed C16 oxidation of furan-containing steroid

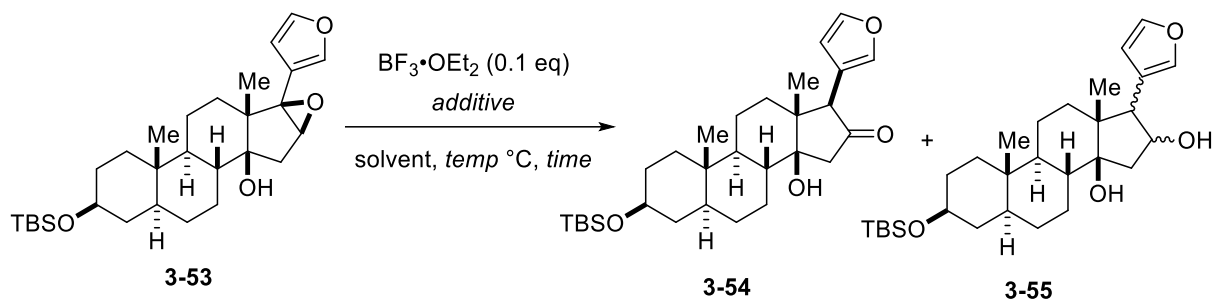
Since the butenolide studies did not prove to be fruitful due to the unexpected sensitivity of the butenolide, we decided to switch our strategy toward furan-based steroids to understand if these substrates would be useful for the Lewis acid mediated epoxide ring opening strategy.



**Figure 3.20.** Suzuki coupling to make model substrate **3-54**.

The studies began by subjecting model vinyl iodide substrate **2-8** to be Suzuki coupled with 3-furylboronic acid to generate model furan **3-52** in 89% yield. With this, epoxidation was carried out with *m*-CPBA and  $\text{NaHCO}_3$  to afford **3-53** in 63% yield. **3-53** was then subjected to the literature conditions ( $\text{BF}_3 \cdot \text{Et}_2\text{O}$ ,  $\text{DCM}$ ,  $-78\text{ }^\circ\text{C}$ , 30 min<sup>15</sup> that gratifyingly resulted in the formation of the desired rearrangement ketone product **3-54** (45% yield) along with multiple decomposition products. There was a minor spot that appeared by TLC and after further elucidation, it was discovered that the compound appeared to resemble a C-16 alcohol **3-55**. Further analysis of the alcohol product revealed that instead of the desired  $\beta\text{C}16$  alcohol, the stereochemical orientation ambiguous which could be a mixture of stereoisomers. Surmising that **3-54** might not be stable to the reaction conditions for a long enough time, we investigated the possibility of single step rearrangement followed by the C-16 ketone reduction to observe the selectivity of the reaction

(Table 3.2) and to find more mild reaction conditions to limit product degradation and to see if external reductants could be used to influence the reduction of the ketone into the alcohol product **3-55** or could influence the stereochemical outcome. The strongest indicator of positive change was that time and Lewis-basic solvents led to the most optimized conditions for the formation of the ketone product **3-54**. The inclusion of triethylsilane as a terminal reductant, provided the corresponding ketone product **3-54** (19% yield) in addition to the reduction product **3-55** (38% yield). Our subsequent attempts to improve the formation of the alcohol product **3-55** by varying the temperature, Lewis acids or silane source, led to really no improvement in dictating the regioselectivity of the reduction. The formation of ketone **3-54** was significantly increased (entry 4, 93% yield) by altering the solvent, temperature, and reaction time ( $\text{BF}_3 \cdot \text{Et}_2\text{O}$ , dioxane, rt, 1 min). The major change for the temperature was due to the freezing point of 1,4-dioxane being 10 °C so room temperature was recognized as a sufficient starting point. This along with the high Lewis acid stabilizing effects, and from previous reactions testing time effects on reaction progression, the most optimized conditions were confirmed (Table 3.2).

**Table 3.2.** Initial optimization of epoxide ring opening.

Entry	Solvent	Additive	Temperature	Time	Conversion <sup>a</sup>	Yield <sup>b</sup>
1	DCM	-	-40	5 min	100%	10% ( <b>3-54</b> )
2	THF	-	-10	5 min	20%	50% ( <b>3-54</b> )
3	1,4-dioxane	-	25	5 min	100%	90% ( <b>3-54</b> )
4	1,4-dioxane	-	25	1 min	100%	95% ( <b>3-54</b> )
6	DCM	$\text{Et}_3\text{SiH}$ (5 eq)	-78	1 h	100%	19% ( <b>3-54</b> ) + 38% ( <b>3-55</b> )
7	DCM	$\text{Et}_3\text{SiH}$ (50 eq)	-78	1 h	100%	19% ( <b>3-54</b> ) + 38% ( <b>3-55</b> )
8	DCM	$\text{Et}_3\text{SiH}$ (50 eq)	-90	1 h	100%	63% ( <b>3-54</b> ) + 18% ( <b>3-55</b> )

<sup>a</sup> Monitored by TLC analysis. <sup>b</sup> Isolated yield.

With these optimized conditions in hand from the model studies, we deduced that building the natural core was the next logical step since the novelty of the isomerization was established. The natural steroid core synthetic studies commenced with testosterone **3-56**. Selective hydrogenation with pyridine and Pd/C yielded **3-27** in a 10:1 d.r. but the isomers were not separable. To remedy

this, further transformations were carried out to reduce the C3-ketone into the desired  $\beta$ C3-alcohol with *in situ* protection with TBSCl to yield **3-29** in 76% yield over three steps. This derivative was subjected to D-ring modification by first installing an enone through Saegusa-Ito's two step oxidation in 65% yield. Taking advantage of the torsional strain of the C/D ring junction, due to the unsaturation at  $\Delta^{15}$ -alkene, the deconjugation of **3-30** was accomplished using our group's previously developed conditions (PhMe, SiO<sub>2</sub>, DIEA, 60 °C) to produce the  $\beta,\gamma$ -unsaturated ketone **3-31** in 69% yield (93% bsm). The subsequent experiments were focused on installing the  $\beta$ 14-hydroxyl group via Mukaiyama hydration<sup>18</sup> Using Co(acac)<sub>2</sub>/PhSiH<sub>3</sub>/O<sub>2</sub> conditions developed above and the hydration of **3-31** was carried on a 1.2 g scale providing a mixture of epimers at the C14 position (14 $\beta$ :14 $\alpha$  = 2.9:1). The resultant product was subjected to the Barton iodination procedure to provide the known vinyl iodide **3-33** in 38% yield.

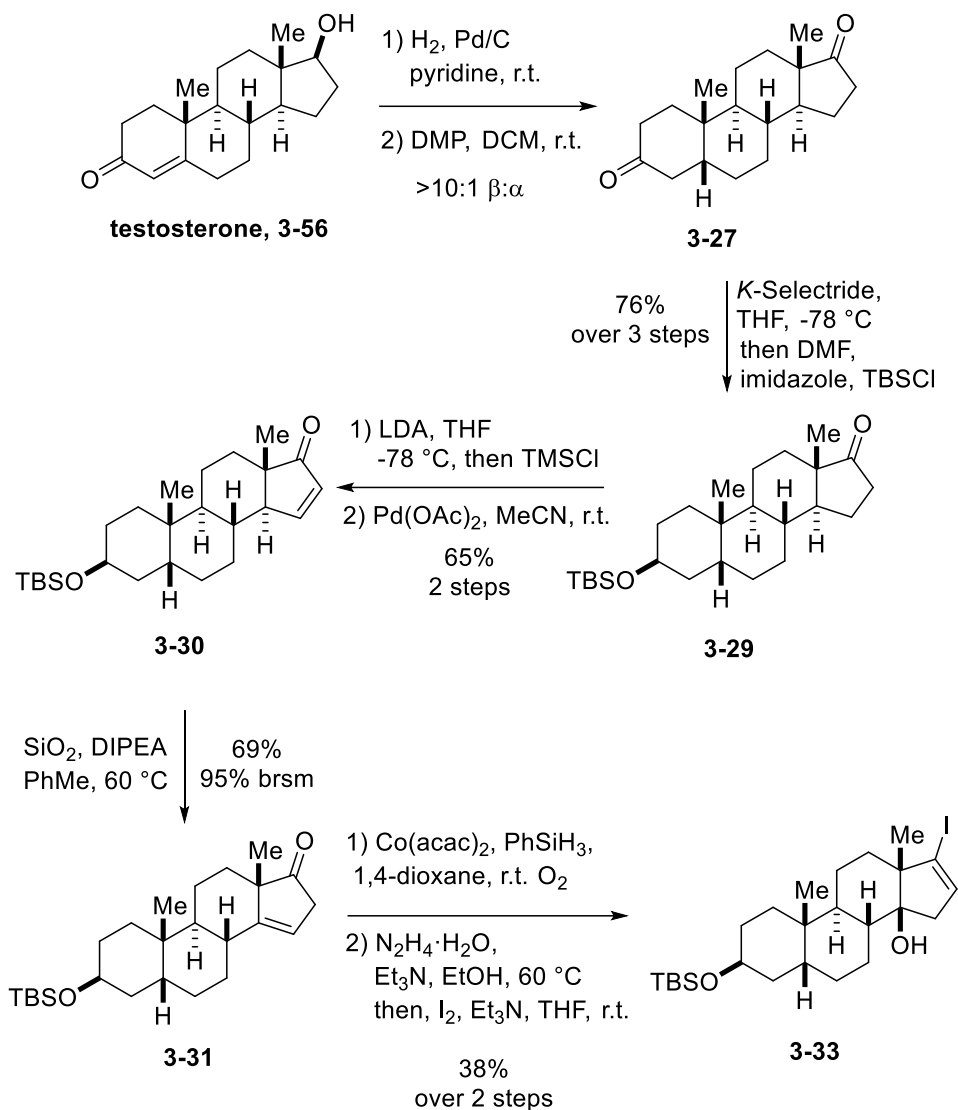


**Figure 3.21.** Synthetic route for building steroid core of oleandrigenin.

Vinyl iodide **3-33** represents an important intermediate for the further functionalization of the C17 position and was utilized for Suzuki cross-coupling with the 3-furylboronic acid, which proceeded in 76% yield. The resultant intermediate was subjected to β14-hydroxyl directed epoxidation with *m*-CPBA to afford epoxide **3-57** in good yield and excellent diastereoselectivity (83%, >20:1 dr). The optimized conditions used for the model studies (Table 3.1, entry 4) were



subsequently used to promote the House-Meinwald isomerization of epoxide **3-57** containing the desired 5 $\beta$ -configuration allowing this transformation to proceed in 95% yield and provided **3-58** as a single diastereomer. The analysis of this compound as well as the subsequent intermediates were consistent with the stereoselective hydrogen migration to establish the desired  $\beta$ 17-stereocenter. Ketone **3-58** was subjected to reduction with NaBH<sub>4</sub> to provide the desired  $\beta$ 16-product **3-19** in 76% yield and 9.6:1 d.r.. The resultant diastereomeric mixture was separated by normal phase column chromatography, and the desired diastereomer was acylated (Ac<sub>2</sub>O, DMAP, Py) to provide the known intermediate **3-20** as a single diastereomer after purification. The conversion of **3-20** into oleandrigenin **3-2** was subsequently carried out using the previously published protocol from the Wicha<sup>13</sup> group, that involved singlet oxygen to oxidize the furan moiety, followed by the reductive rearrangement and acidic work up leading to the formation of  $\beta$ 17-butenolide (52% yield) along with deprotected oleandrigenin (12% yield). The subsequent HF•Py mediated deprotection of the TBS group completed the formation of oleandrigenin **3-2** from **3-20** in 58% over 2 steps (15 steps and 3% yield from testosterone). The spectroscopic data obtained for **3-2** matched well with the corresponding characterization data previously disclosed by the Wicha group<sup>13</sup> thus confirming the identity of synthetic oleandrigenin **3-2**.

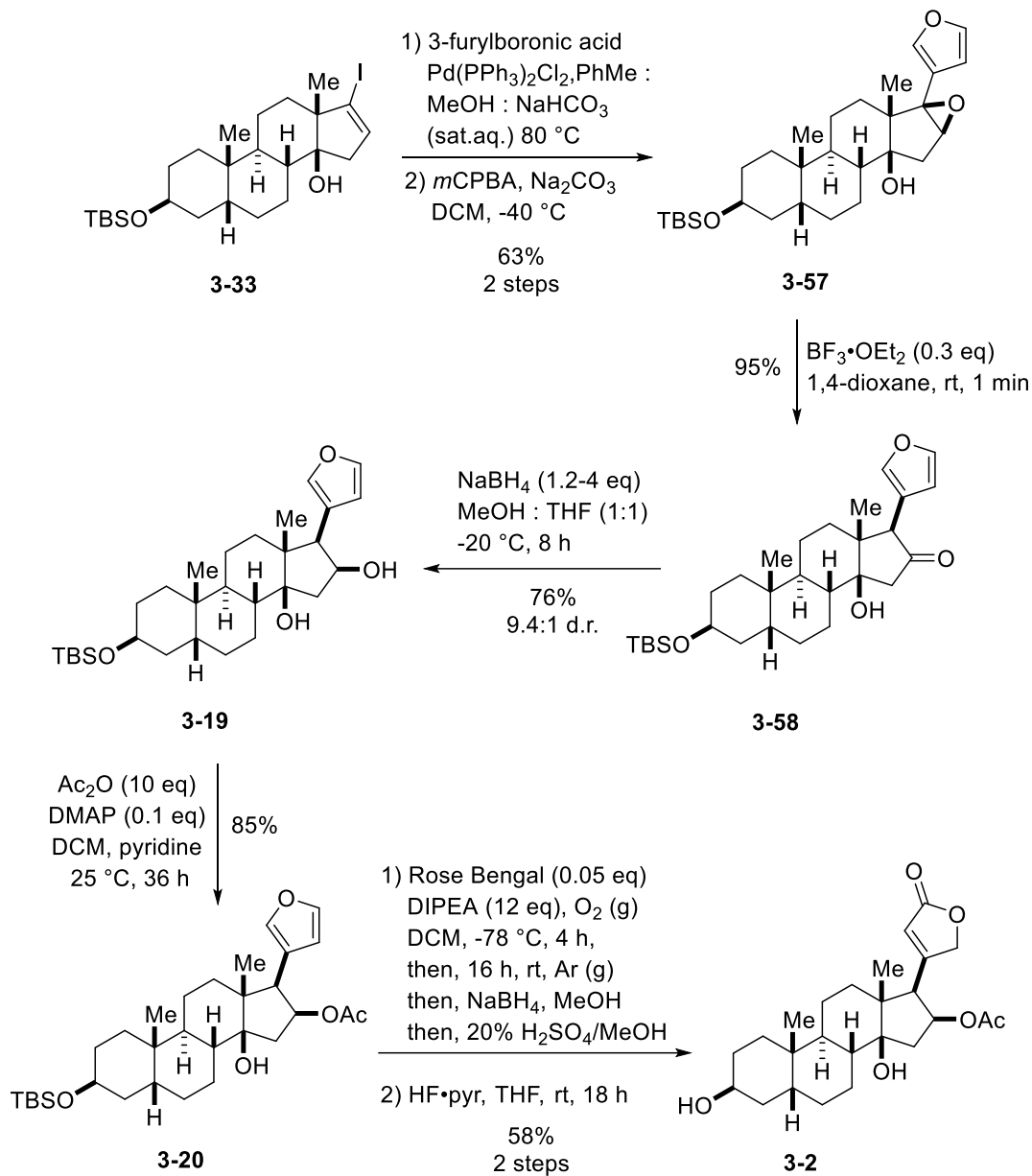


**Figure 3.22.** Synthetic route for completion of the synthesis of oleandrigenin.

With the concise approach to oleandrigenin **3-2** in hand, our subsequent studies focused on developing a strategy for the C3 glycosylation leading to rhodexin B **3-3** containing  $\alpha$ -L-rhamnose at the C3 position of the steroid (*cf.* Figure 3.1). While the chemical glycosylation of cardiotonic steroids has been previously accomplished in various contexts<sup>12</sup> including our own studies,<sup>14</sup>

to the best of our knowledge, the glycosylation of **3-2** has not been previously investigated. The  $\beta$ 16-acetate moiety presents additional challenges for the introduction of sugar due to many common protecting groups on the sugar moiety being acetates themselves, other mild deprotection strategies needed to be considered for developing orthogonal deprotection strategies. When aglycone **3-2** was subjected to the standard glycosylation conditions with the known donor **3-59**,<sup>14</sup> which was graciously donated by Ryan Rutkoski, glycosylated product **3-61** was indeed obtained in good yield and selectivity (60%, 10:1 dr) along with the minor quantities of a C14-elimination side-product (~ 5% yield), which was observed by HRMS analysis and crude <sup>1</sup>H NMR.

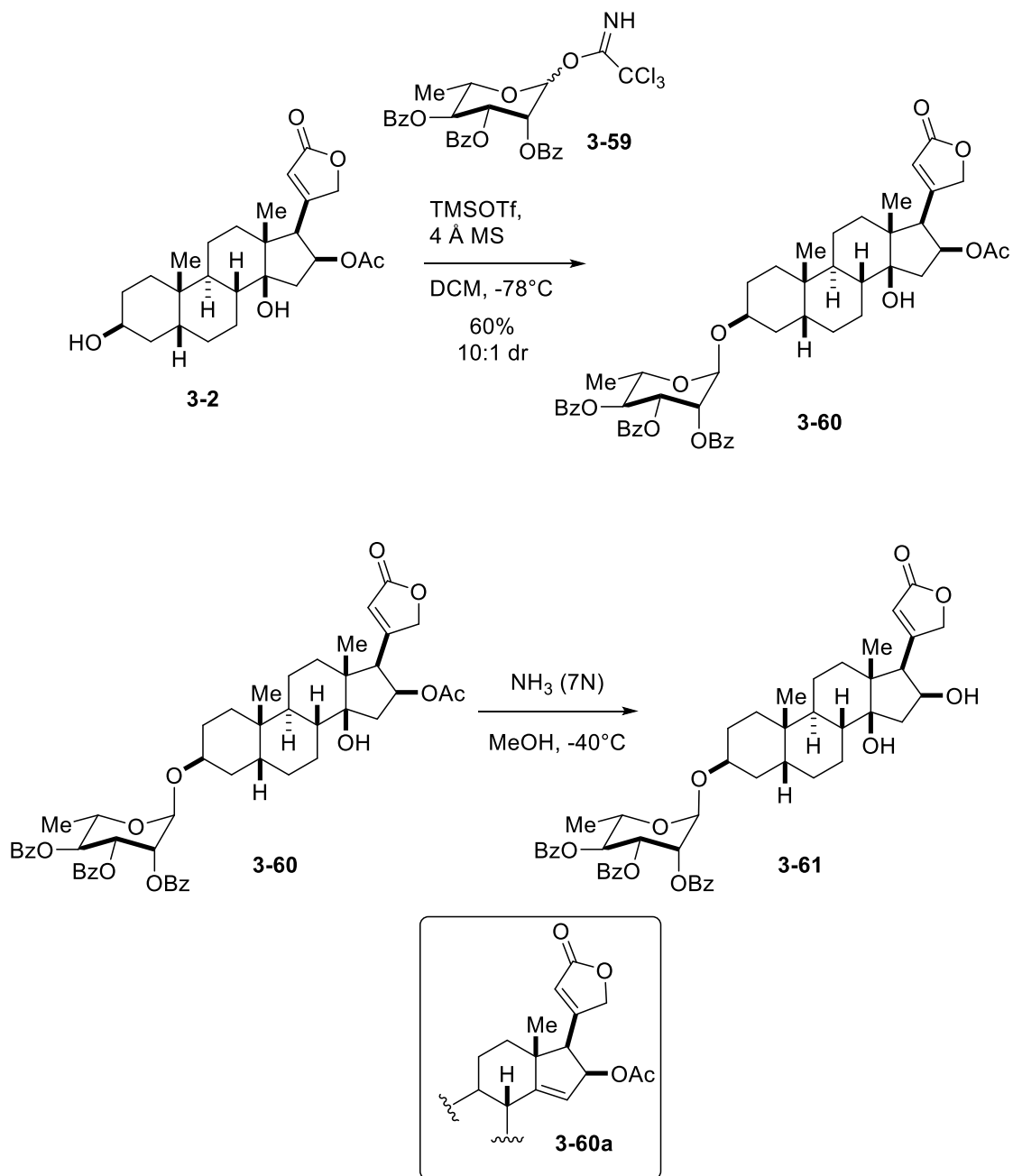


**Figure 3.23.** First attempt of glycosylation towards rhodexin B. (donor **3-59** was graciously donated by Ryan Rutkoski)

However, accomplishing a selective deprotection of the benzoates on *L*-rhamnose moiety of **3-60** represented a major challenge as the use of various basic conditions invariably lead to the

deprotection of the  $\beta$ 16-acetate group before the benzoate moieties were completely removed (**3-61**). These structures were confirmed by crude  $^1\text{H}$  NMR analysis and HRMS analysis. Previously, our group encountered a related problem in the context of accomplishing a selective deprotection of the C19 position of cannogenol- $\alpha$ -*L*-rhamnoside,<sup>19</sup> and the challenges associated with the selective deprotection of the C19-position in the presence of butenolide were solved by employing 2-methoxyacetate (MAc) protecting group that is significantly more labile than benzoate under both acidic and basic conditions.<sup>20</sup> The 2-methoxyacetate rhamnoside donor **3-65** (synthesized by Nolan Carney), was prepared by starting with *L*-rhamnose **3-62** and the protecting groups were installed to generate **3-63** in 81% yield. This was followed by anomeric deprotection with benzylamine to make compound **3-64** and then completion of the sugar donor with trichloroacetonitrile yielded **3-65**<sup>20</sup> in 78% yield. Glycosylation with oleandrigenin gave **3-66** in 87% yield with minor amounts of C14-eliminated side product (**3-66a**), which was observed by HRMS and crude  $^1\text{H}$  NMR.

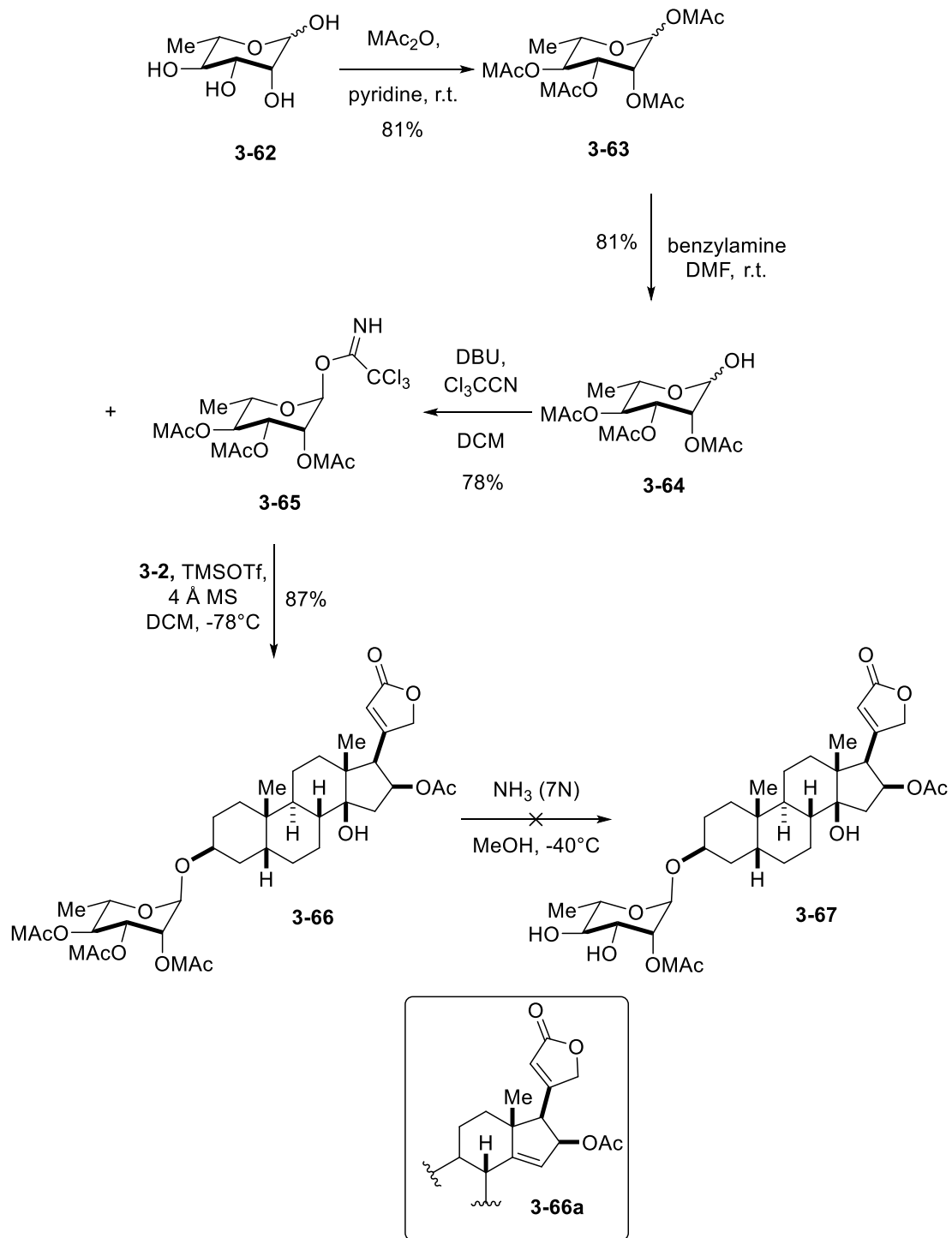


**Figure 3.24.** Second attempt of glycosylation towards rhodexin B. (Donor **3-65** was graciously donated by Nolan Carney)

The treatment of **3-66** with the saturated solution of NH<sub>3</sub> in MeOH led to the selective formation of the monoprotected glycoside **3-67** still containing MAc protection at the 2'-position of the *L*-rhamnose moiety, which was confirmed by COSY analysis of the substrate. Further exposure of **3-66** to the ammonia in methanol led to the competitive cleavage of the β16-acetate and subsequent degradation of butenolide and did not result in providing rhodexin B. Similarly, exposure of **3-66** to Yb(OTf)<sub>3</sub> (50 mol%) in methanol, the conditions previously used to effectively cleave MAc groups,<sup>20</sup> resulted in the cleavage of the glycosidic linkage and β14-hydroxide elimination.

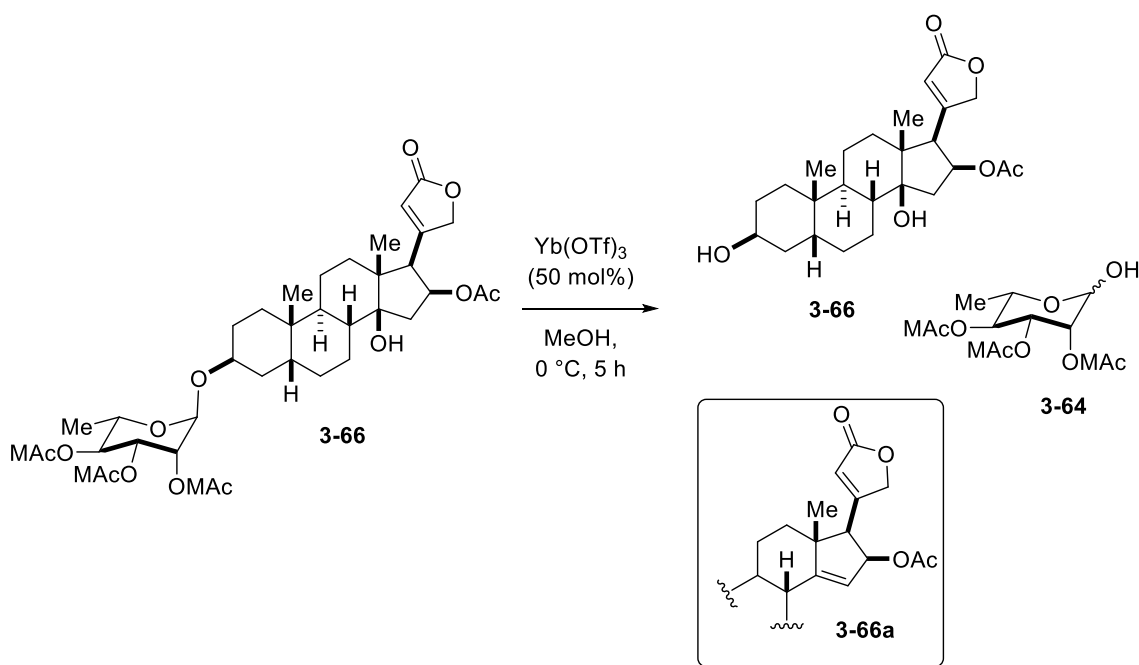


**Figure 3.25.** Yb(OTf)<sub>3</sub> mediated deprotection attempt on **3-66** and proposed products based on crude <sup>1</sup>H NMR and HRMS analysis.

Based on these observations, a different trichloroacetimidate donor needed to be discovered that would provide more facile orthogonal deprotection in the presence of a sensitive C16-OAc. We found in the literature that donor **3-73**, previously developed by Nguyen and co-workers was investigated next.<sup>21</sup>

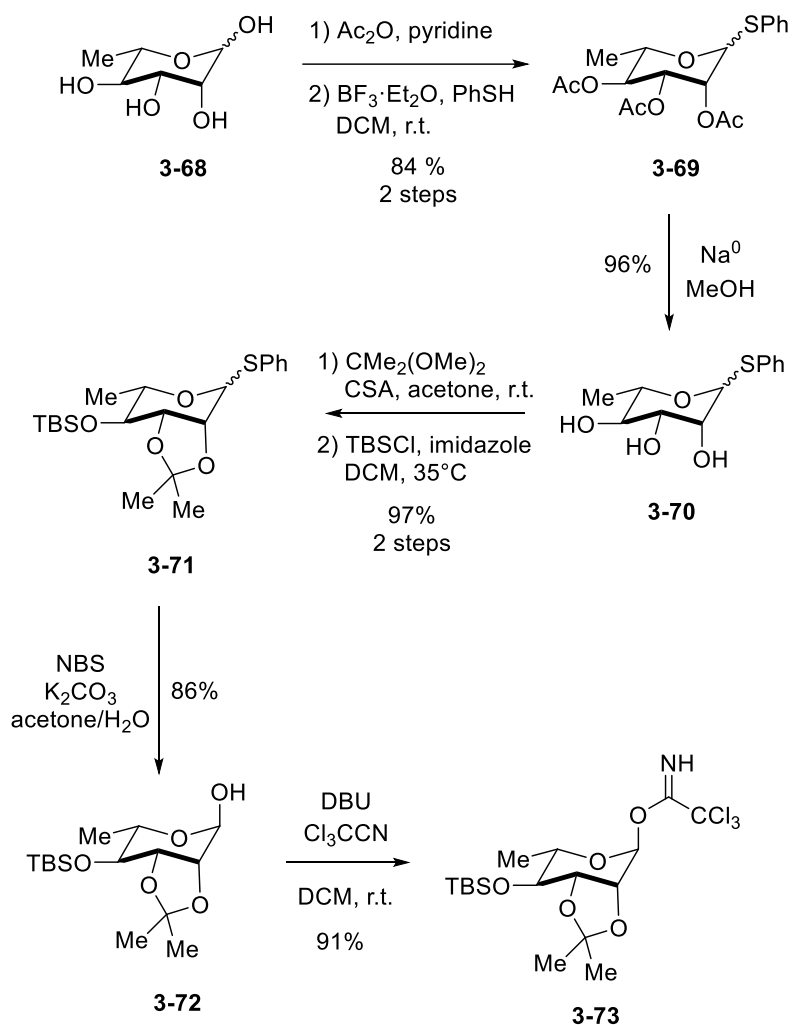


**Figure 3.26.** Synthesis of rhamnoside donor **3-73** from Nguyen<sup>21</sup> (synthesized by Nolan Carney).

To investigate this method by Nguyen, the supply of oleandrigenin was limited, and due to observing significant C14 elimination side product formation (**3-76a**), we decided to first test their conditions on a related compound digitoxigenin (**3-74**).



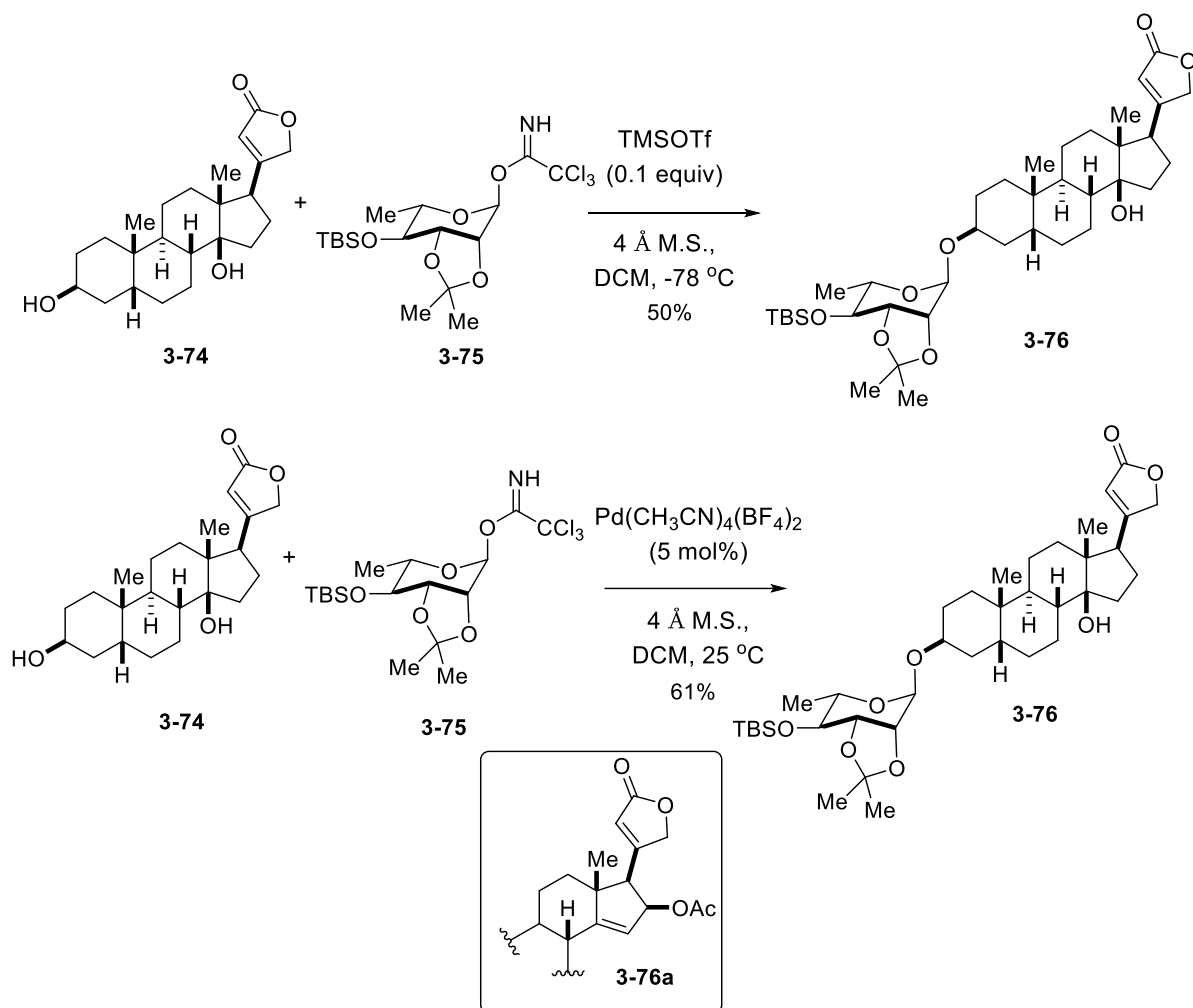


**Figure 3.27.** Optimization of Nguyen’s glycosylation method with digitoxigenin.

The reaction of **3-75** and digitoxigenin **3-74** was first attempted using classical glycosylation conditions with TMSOTf (10 mol%) as the catalyst. However, a only 50% of the desired glycoside **3-76** and the  $\beta$ 14-hydroxide elimination side-product was observed under these conditions. Applying the conditions developed by the Nguyen group<sup>21</sup> for the glycosylation with **3-74** and employing Pd(CH<sub>3</sub>CN)<sub>4</sub>(BF<sub>4</sub>)<sub>2</sub> (10 mol%) as the catalyst. While at room temperature, this reaction led to a significant formation of the C14 eliminated side product, as well as **3-76**.

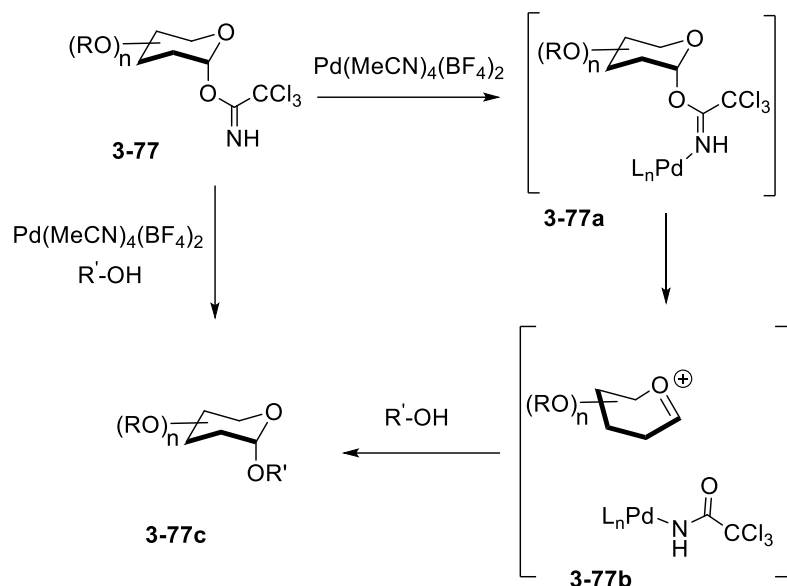


**Figure 3.28.** Nguyen's proposed mechanism for cationic Pd(II)-catalyzed stereoselective formation of  $\alpha$ -glycosides<sup>21</sup>

Nguyen proposes a possible mechanism for the cationic Pd(II)-catalyzed stereoselective formation glycosides (*cf.* Figure 3-28). Cationic palladium(II), reversibly coordinates to the imidate nitrogen of **3-77** to form complex **3-77a** which subsequently undergoes ionization to generate oxocarbenium intermediate **3-77b**. Along with the steric and anomeric effects that are *L*-rhamnose substrates, axial addition of nucleophiles to **3-77c** are more favored.

Since the reaction was successful under Nguyen's conditions, we decided that to minimize the elimination side product was to adjust the reaction conditions to be cooled to  $-78$  °C. This reaction adjustment resulted in **3-76** (76% yield, >20:1 dr) along with **3-76a** (ca. 15% yield, >20:1 dr). Desired product **3-76** was successfully separated from **3-76a** and subjected to the deprotection using HCl in methanol. These conditions provided a synthetic sample of rhodexin B **3-3** (90% yield). The subsequent comparison of the spectroscopic characteristics of the synthetic sample provided a good match with the published  $^1\text{H}$ ,  $^{13}\text{C}$  NMR and optical rotation data<sup>10</sup>

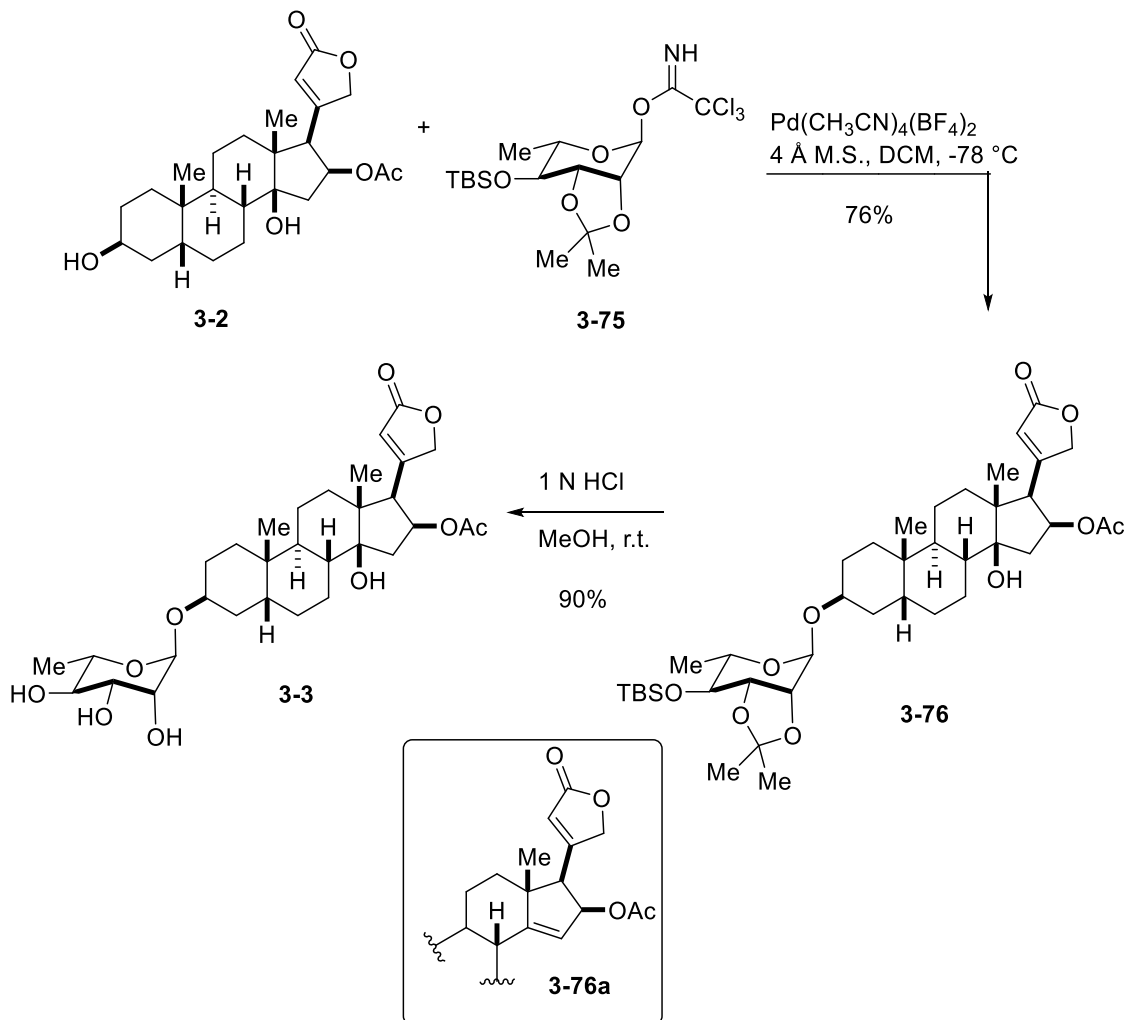


**Figure 3.29.** Successful glycosylation and deprotection towards rhodexin B.

### 3.4 Conclusions

In conclusion, this chapter describes a new concise synthesis of valuable cardiotoxic steroid oleandrigenin (**3-2**) from a readily available derivative of DHEA or testosterone (**3-56**), and its subsequent elaboration into natural product rhodexin B/tupichinolide (**3-3**). This synthesis features a Lewis acid-catalyzed epoxide rearrangement of a precursor with pre-installed  $\beta$ 14-hydroxylation. This strategy allowed to achieve a more concise reaction sequence leading to oleandrigenin and avoids extra synthetic manipulations on the late-stage intermediates containing the  $\beta$ 17-substitution. We have evaluated various protecting group strategies for the installation of

the  $\alpha$ -L-rhamnoside and established a viable route that could be used to produce natural product rhodexin B (**3-3**) and its analogs for the biological evaluation. We believe that these studies are instrumental for the synthesis of oleandrin (**3-2**) and other steroids bearing the  $\beta$ 16-oxidation.

### 3.5 Future Directions

We have accomplished an expedient synthesis for oleandrigenin and have developed a robust method for glycosylating the C3-position of C16-OAc containing steroid cores. We aim our future studies of this system to provide a modifiable structure for potential medicinal chemistry analogues. These include preliminary targets of introducing different heterocycles modifications at the C3 and C17 positions of the steroid, while also looking toward glycoside modifications, as well as various acetate site modifications. With these modifications, there is opportunity to make a library of compounds with natural substituents, or synthetic derivatives. The importance of each site could then be elucidated as it pertains to biological activity and could assist to broaden the knowledge of medicinal chemistry investigations.

### 3.6 Experimental

#### Methods and Reagents :

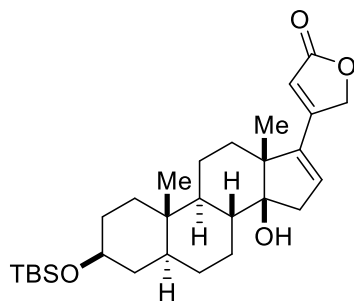
Unless otherwise stated, all reagents and solvents were purchased from commercial sources and were used as received without further purification unless otherwise specified. DCM, DMF, Et<sub>2</sub>O, THF, PhMe, were purified by Innovative Technology's Pure-Solve System using basic alumina. All reactions were carried out under a positive pressure of nitrogen in flame- or oven-dried glassware with magnetic stirring. Reactions were cooled using a cryocooler or external cooling baths (ice water (0 °C), sodium chloride/ice water (-20 °C), dry ice/acetonitrile (-40 °C), or dry ice/acetone (-78 °C)). Heating was achieved by use of a silicone oil bath with heating controlled by an electronic contact thermometer. Deionized water was used in the preparation of

all aqueous solutions and for all aqueous extractions. Solvents used for extraction and chromatography were ACS or HPLC grade. Purification of reaction mixtures was performed by flash chromatography using SiliCycle SiliaFlash P60 (230-400 mesh). Yields indicate the isolated yield of the title compound with  $\geq 95\%$  purity as determined by  $^1\text{H}$  NMR analysis. Diastereomeric ratios were determined by  $^1\text{H}$  NMR analysis.  $^1\text{H}$  NMR spectra were recorded on a Varian vnmrs 700 (700 MHz), 600 (600 MHz), 500 (500 MHz), 400 (400 MHz), Varian Inova 500 (500 MHz), or a Bruker Avance Neo 500 (500 MHz) spectrometer and chemical shifts ( $\delta$ ) are reported in parts per million (ppm) with solvent resonance as the internal standard ( $\text{CDCl}_3$  at  $\delta$  7.26,  $\text{D}_3\text{COD}$  at  $\delta$  3.31,  $\text{C}_6\text{D}_6$  at  $\delta$  7.16). Tabulated  $^1\text{H}$  NMR Data are reported as s = singlet, d = doublet, t = triplet, q = quartet, qn = quintet, sext = sextet, m = multiplet, ovrlp = overlap, and coupling constants in Hz. Proton-decoupled  $^{13}\text{C}$  NMR spectra were recorded on Varian vnmrs 700 (700 MHz) spectrometer and chemical shifts ( $\delta$ ) are reported in ppm with solvent resonance as the internal standard ( $\text{CDCl}_3$  at  $\delta$  77.16,  $\text{D}_3\text{COD}$  at  $\delta$  49.0,  $\text{C}_6\text{D}_6$  at  $\delta$  128.06). High resolution mass spectra (HRMS) were performed and recorded on Micromass AutoSpec Ultima or VG (Micromass) 70-250-S Magnetic sector mass spectrometers in the University of Michigan mass spectrometry laboratory. Infrared (IR) spectra were recorded as thin films a Perkin Elmer Spectrum BX FT-IR spectrometer. Absorption peaks are reported in wavenumbers ( $\text{cm}^{-1}$ ). Optical rotations were measured at room temperature in  $\text{CHCl}_3$  or  $\text{H}_3\text{COH}$  on a Jasco P-2000 polarimeter.

**Instrumentation:**

All spectra were recorded on Varian vnmrs 700 (700 MHz), Varian vnmrs 500 (500 MHz), Varian MR400 (400 MHz), Varian Inova 500 (500 MHz) spectrometers and chemical shifts ( $\delta$ ) are reported in parts per million (ppm) and referenced to the  $^1\text{H}$  signal of the internal tetramethylsilane according to IUPAC recommendations. Data are reported as (br = broad, s =

singlet, d = doublet, t = triplet, q = quartet, qn = quintet, sext = sextet, m = multiplet; coupling constant(*S*) in Hz; integration). High resolution mass spectra (HRMS) were recorded on MicromassAutoSpecUltima or VG (Micromass) 70-250-S Magnetic sector mass spectrometers in the University of Michigan mass spectrometry laboratory. Infrared (IR) spectra were recorded as thin films on NaCl plates on a Perkin Elmer Spectrum BX FT-IR spectrometer. Absorption peaks were reported in wavenumbers (cm<sup>-1</sup>).



**Compound 3-43:** To a flame-dried round bottom flask was added, compound **2-8** (63.8 mg, 0.12 mmol, 1.0 equiv.), and then the contents were transferred to a glovebox. There, Pd(PPh<sub>3</sub>)<sub>4</sub> (7 mg, 0.006 mmol, 0.05 equiv.), CuCl (177 mg, 1.8 mmol, 15 equiv.), and LiCl (100 mg, 2.4 mmol, 20 equiv.). The flask was capped, taken out of the glovebox and the contents were dissolved in anhydrous DMSO (12 mL). Then tributylstannyl butenolide (134 mg, 0.36 mmol, 3.0 equiv.) was added to the reaction flask. The contents were left to stir at 70 °C for 16 h. After this time, the heating was removed, and the reaction was left to cool to room temperature. The reaction was then quenched with pH 7 phosphate buffer (10 mL), extracted with Et<sub>2</sub>O (3x 20 mL), dried over Na<sub>2</sub>SO<sub>4</sub>, filtered and concentrated *in vacuo*. Purified by column chromatography with 10% to 33% EtOAc/hexanes. (40 mg, 0.08 mmol, 69%) R<sub>f</sub> = 0.25 50% EtOAc/hexanes

**<sup>1</sup>H NMR** (700 MHz, C<sub>6</sub>D<sub>6</sub>) δ 5.69 (s, 1H), 4.17 (d, *J* = 16.0 Hz, 1H), 4.12 (d, *J* = 16.0 Hz, 1H), 3.59 (td, *J* = 10.5, 5.1 Hz, 1H), 2.13 (d, *J* = 18.0 Hz, 1H), 1.99 (d, *J* = 12.7 Hz, 1H), 1.88 (dd, *J* =

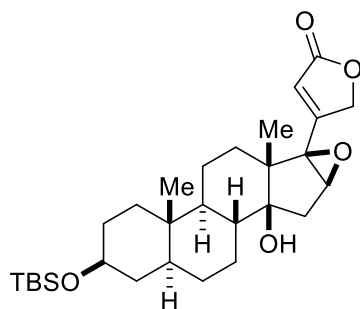
18.2, 3.3 Hz, 1H), 1.74 (d,  $J = 12.4$  Hz, 1H), 1.57 – 1.47 (m, 6H), 1.37 – 1.23 (m, 7H), 1.17 (d,  $J = 11.7$  Hz, 3H), 1.02 (s, 9H), 0.83 (s, 3H), 0.60 (s, 3H), 0.13 (s, 6H).

$^{13}\text{C NMR}$  (151 MHz,  $\text{C}_6\text{D}_6$ )  $\delta$  173.1, 157.4, 143.6, 131.1, 112.5, 84.6, 71.9, 70.6, 51.6, 50.3, 44.3, 40.5, 40.0, 38.8, 37.8, 35.4, 32.0, 29.9, 28.5, 27.3, 25.8, 19.7, 18.1, 15.9, 12.1, -4.6.

**HRMS** (ESI-TOF)  $[\text{M}+\text{H}]^+$   $m/z$ : calcd for  $\text{C}_{29}\text{H}_{47}\text{O}_4\text{Si}$  487.7753; Found 487.7759.

$[\alpha]_{\text{D}}^{25} = +14.1$  ( $c = 0.57$ ,  $\text{CHCl}_3$ ).

**IR** (film,  $\text{cm}^{-1}$ ) 3853, 3734, 3710, 3649, 3628, 2924, 1742.

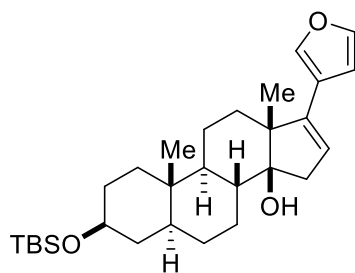


**Compound 3-45:** **3-43** in a flame-dried round bottom flask (5 mg, 0.01 mmol), was dissolved in DCM (0.5 mL) and cooled to  $-10$  °C.  $\text{VO}(\text{acac})_2$  (0.12 mg,  $4.7 \times 10^{-4}$  mmol, 0.05 equiv.) was added and then *tert*-butylhydroperoxide (1.2  $\mu\text{L}$ , 0.012 mmol, 1.2 equiv.) was added and the reaction was left to stir while warming to  $0$  °C and monitored by TLC analysis. After the disappearance of starting material, the reaction was quenched with solid  $\text{Na}_2\text{SO}_3$  and vigorously stirred for 30 mins. Then the contents were filtered through a silica gel plug and the plug was rinsed with EtOAc (3 x 5 mL). The organic phase was dried with  $\text{Na}_2\text{SO}_4$ , filtered, and concentrated *in vacuo*. The crude residue was purified ( $\text{SiO}_2$ , 20% EtOAc/hexanes) via silica plug due to its sensitivity to silica gel, to afford the product as a white solid. (3.5 mg, 0.007 mmol, 70%)  $R_f = 0.6$ ; 50% EtOAc/hexanes.

**<sup>1</sup>H NMR** (500 MHz, C<sub>6</sub>D<sub>6</sub>) δ 5.74 (dd, *J* = 7.4, 2.2 Hz, 1H), 4.16 – 4.09 (m, 1H), 3.95 – 3.92 (m, 1H), 3.62 (dt, *J* = 13.5, 7.0 Hz, 1H), 2.83 (d, *J* = 121.3 Hz, 1H), 2.28 – 2.18 (m, 1H), 1.76 (dt, *J* = 14.7, 7.4 Hz, 2H), 1.62 (m, 7H), 1.54 (dd, *J* = 9.0, 5.5 Hz, 2H), 1.43 (dd, *J* = 15.4, 9.1 Hz, 2H), 1.37 – 1.30 (m, 6H), 1.21 – 1.18 (m, 8H), 1.03 (s, 3H), 0.57 (s, 3H), 0.13 (s, 6H).

**<sup>13</sup>C NMR** (151 MHz, C<sub>6</sub>D<sub>6</sub>) δ 171.3, 160.3, 118.8, 79.5, 71.4, 70.4, 69.1, 62.5, 48.7, 46.2, 43.8, 39.6, 38.1, 36.7, 34.9, 34.2, 32.8, 31.5, 29.3, 26.8, 22.2, 19.2, 13.5, 12.8, -5.1, -5.1.

**HRMS** (ESI-TOF) [M+Na]<sup>+</sup> *m/z*: calcd for C<sub>29</sub>H<sub>46</sub>O<sub>5</sub>SiNa 525.7562; Found 525.7567.



**Compound 3-52: 2-8** (152 mg, 0.28 mmol), and 3-furanylboronic acid (48 mg, 0.43 mmol, 1.5 equiv.) were transferred to a flame-dried round bottom flask with a magnetic stir bar. The flask was then transferred to a glovebox where Pd(PPh<sub>3</sub>)<sub>4</sub> (35 mg, 0.03 mmol, 0.10 equiv.) was weighed out into the reaction flask. Afterwards, the flask was taken out of the glovebox and dry toluene (6 mL) was introduced, followed by MeOH (1.2 mL) and NaHCO<sub>3(sat.)</sub> (0.75 mL). The biphasic suspension was then equipped with a reflux condenser and heated to 80 °C from an oil bath, while stirring for 18 h. After the designated reaction time, the heat was turned off and the flask was allowed to cool to room temperature. Then, the reaction solution was partitioned between dI water (10 mL) and a 1:1 mixture of EtOAc : hexanes (20 mL). The layers were separated, and the organic phase was washed with HCl (1N aq. solution, 10 mL), then H<sub>2</sub>O (10 mL), then brine (10 mL). The organic phase was then dried over Na<sub>2</sub>SO<sub>4</sub>, filtered, and concentrated *in vacuo*. Flash column



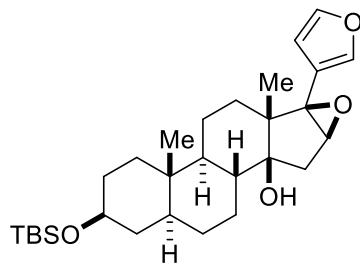
chromatography was performed on the crude residue through silica gel (Hexanes/EtOAc = 9/1) to afford **3-52** (121 mg, 0.26mmol) in 89% yield as a white solid. Rf: 0.4 in 9:1 Hexanes/EtOAc.

$^1\text{H NMR}$  (500 MHz,  $\text{CDCl}_3$ )  $\delta$  7.44 (s, 1H), 7.36 (s, 1H), 6.49 – 6.44 (m, 2H), 5.74 (s, 1H), 3.57 (tt,  $J = 10.5, 4.8$  Hz, 2H), 2.63 (dd,  $J = 17.1, 2.1$  Hz, 2H), 2.22 (dd,  $J = 17.1, 3.2$  Hz, 2H), 2.10 (dd,  $J = 12.8, 3.4$  Hz, 1H), 1.96 (dd,  $J = 10.5, 3.4$  Hz, 1H), 1.79 – 1.72 (m, 1H), 1.67 (dt,  $J = 12.0, 6.0$  Hz, 2H), 1.52 – 1.45 (m, 2H), 1.34 (dd,  $J = 13.0, 2.3$  Hz, 2H), 1.28 (dd,  $J = 10.1, 6.4$  Hz, 1H), 1.22 (s, 3H), 1.18 – 1.08 (m, 2H), 0.98 (td,  $J = 13.5, 3.8$  Hz, 2H), 0.89 (d,  $J = 2.1$  Hz, 9H), 0.83 (s, 3H), 0.06 (s, 6H).

$^{13}\text{C NMR}$  (126 MHz,  $\text{C}_6\text{D}_6$ )  $\delta$  145.1, 142.9, 138.5, 121.9, 121.5, 110.2, 90.7, 72.3, 52.8, 50.9, 44.6, 42.4, 39.2, 39.0, 38.7, 37.5, 35.7, 32.3, 29.0, 28.0, 26.1, 20.2, 18.3, 17.2, 12.4, 2.9, -4.3, -4.3.

**HRMS** (ESI-TOF)  $[\text{M}+\text{Na}]^+$   $m/z$ : calcd for  $\text{C}_{29}\text{H}_{46}\text{O}_3\text{Si}$  493.3108; Found 493.3111.

**IR** (film,  $\text{cm}^{-1}$ ) 3446, 2942, 2855, 2361, 2339.



**Compound 3-53: 3-52** (18 mg, 0.038 mmol) was dissolved in dry DCM (1 mL) in a flame-dried round bottom flask with a magnetic stirring bar and the reaction vessel was cooled to  $-40$  °C in a dry ice/acetonitrile bath. Then,  $\text{NaHCO}_3$  (2.0 equiv., 6.4 mg, 0.076 mmol) was added to the reaction, followed by *m*CPBA (75% w/w, 1.0 equiv., 6.6 mg, 0.038 mmol) after a 10 min incubation period. The reaction was then stirred for 5 h while warming but not reaching above  $-10$  °C. After the designated reaction time, the reaction was quenched with  $\text{Na}_2\text{S}_2\text{O}_3(\text{sat})$  (2 mL) and

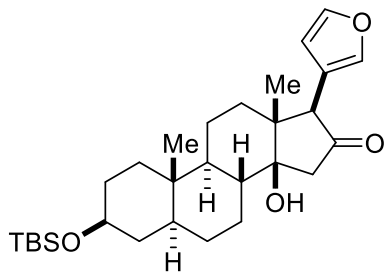
then the cooling bath was removed. The solution was then vigorously stirred for 30 mins at room temperature to create a cloudy mixture. Then, the reaction solution was extracted with DCM (3 x 2 mL) and EtOAc (3 x 2 mL). The organic phase was washed with sat. aq. NaHCO<sub>3</sub> (5 mL), then brine (5 mL). The organic phase was then dried over Na<sub>2</sub>SO<sub>4</sub>, filtered, and concentrated *in vacuo*. Flash column chromatography was performed on the crude solid through silica gel (Hexanes/EtOAc = 19/1 to 9/1 to 4/1) to afford **3-53** (11.7 mg, 0.02 mmol) in 63% yield as a white solid. Rf: 0.69 in 4:1 Hexanes/EtOAc

**<sup>1</sup>H NMR** (500 MHz, C<sub>6</sub>D<sub>6</sub>) δ 7.22 (t, *J* = 1.2 Hz, 1H), 7.05 (t, *J* = 1.8 Hz, 1H), 6.22 (dd, *J* = 1.8, 0.9 Hz, 1H), 3.64 (tt, *J* = 10.5, 5.0 Hz, 1H), 2.37 (dq, *J* = 12.9, 3.5 Hz, 1H), 1.80 (d, *J* = 14.6 Hz, 1H), 1.67 (dd, *J* = 14.7, 1.2 Hz, 1H), 1.61 – 1.54 (m, 4H), 1.45 (td, *J* = 12.7, 10.7 Hz, 1H), 1.34 (dt, *J* = 13.2, 3.2 Hz, 2H), 1.24 (ddt, *J* = 16.4, 12.3, 4.0 Hz, 2H), 1.16 (s, 4H), 1.05 (s, 9H), 0.97 – 0.86 (m, 4H), 0.84 – 0.77 (m, 1H), 0.73 (dd, *J* = 13.6, 3.4 Hz, 1H), 0.62 (s, 3H), 0.49 – 0.42 (m, 1H), 0.15 (s, 6H).

**<sup>13</sup>C NMR** (126 MHz, C<sub>6</sub>D<sub>6</sub>) δ 142.85, 141.56, 120.04, 110.87, 80.67, 72.30, 69.59, 62.13, 49.97, 46.51, 44.69, 40.60, 39.05, 37.57, 35.78, 35.27, 34.73, 32.33, 30.17, 28.90, 27.70, 26.12, 20.22, 18.34, 14.13, 12.30, 1.36, -4.27, -4.29.

**HRMS** (ESI-TOF) [M+Na]<sup>+</sup> *m/z*: calcd for C<sub>29</sub>H<sub>46</sub>O<sub>3</sub>Si 509.3058; Found 509.3055.

**IR** (film, cm<sup>-1</sup>) 3345, 2920, 2848, 2355, 2342.



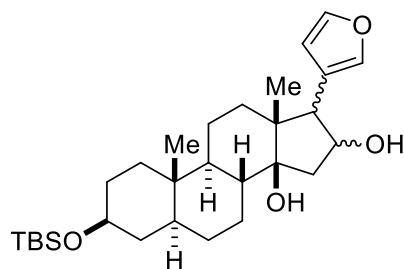
**Compound 3-54.:** Compound **3-53** (11 mg, 0.02 mmol) was dissolved in anhydrous DCM (1 mL) in a flame-dried round-bottom flask. The reaction flask was chilled to -78 °C, and then Et<sub>3</sub>SiH (18 μL, 0.1 mmol, 5 equiv.) was added. Then, a solution of BF<sub>3</sub>•OEt<sub>2</sub> (2 μL of a solution of 200 μL of BF<sub>3</sub>•OEt<sub>2</sub> in 3 mL of dry Et<sub>2</sub>O) was added to the reaction in quick drops. The reaction was left to stir for 30 mins and the solution changed from opaque to orange-brown, and then transparent over the course of the reaction. After such time, the solution was diluted with Et<sub>2</sub>O (1 mL) and then quenched with NaHCO<sub>3(sat.)</sub> (1 mL). The aqueous phase was extracted with DCM (4 x 2 mL). The organic layer was then washed with brine (3 mL), dried over Na<sub>2</sub>SO<sub>4</sub>, filtered, and concentrated *in vacuo*. The residue was purified by flash column chromatography on silica gel (Hexanes/EtOAc = 19/1 to 9/1) to afford **54** (1.8 mg, 0.004 mmol) in 19% yield as a white solid. Along with alcohol product **3-55** (3.7 mg, 0.008 mmol, 38% yield). Rf: 0.5 in 4 :1 Hexanes:EtOAc.

**<sup>1</sup>H NMR** (500 MHz, C<sub>6</sub>D<sub>6</sub>) δ 7.39 (d, *J* = 1.6 Hz, 1H), 6.31 (d, *J* = 1.8 Hz, 1H), 5.12 (s, 1H), 3.65 (dq, *J* = 10.8, 5.2 Hz, 2H), 3.18 (s, 1H), 2.42 (dd, *J* = 15.4, 10.0 Hz, 1H), 1.97 (dd, *J* = 12.9, 3.4 Hz, 1H), 1.81 – 1.73 (m, 4H), 1.68 (td, *J* = 10.4, 5.3 Hz, 2H), 1.62 – 1.51 (m, 4H), 1.49 – 1.43 (m, 2H), 1.34 – 1.31 (m, 1H), 1.22 – 1.17 (m, 4H), 1.08 (s, 3H), 1.06 (s, 9H), 0.94 – 0.87 (m, 3H), 0.59 (s, 3H), 0.16 (d, *J* = 1.7 Hz, 6H).

**<sup>13</sup>C NMR** (126 MHz, C<sub>6</sub>D<sub>6</sub>) δ 203.3, 142.2, 140.6, 110.3, 85.2, 74.6, 71.8, 49.3, 44.2, 41.7, 41.1, 37.1, 31.9, 29.8, 29.7, 28.3, 26.1, 25.8, 20.0, 12.4, 11.9, 1.0, -4.6.

**HRMS** (ESI-TOF) [M+Na]<sup>+</sup> m/z: calcd for C<sub>29</sub>H<sub>46</sub>O<sub>4</sub>Si 509.3057; Found 509.3058.

**IR** (film, cm<sup>-1</sup>): 3450, 2925, 2850, 2355, 2332.

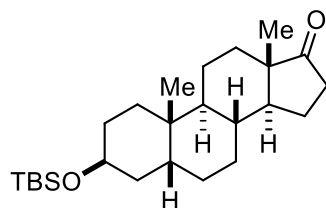


**Compound 3-55:**

<sup>1</sup>H NMR (500 MHz, CDCl<sub>3</sub>) δ 7.41 (dd, *J* = 1.6, 0.9 Hz, 1H), 7.37 (t, *J* = 1.7 Hz, 1H), 6.39 – 6.38 (m, 1H), 4.58 (ddd, *J* = 10.7, 7.2, 4.1 Hz, 1H), 3.55 (dt, *J* = 11.0, 6.0 Hz, 1H), 2.76 (d, *J* = 7.3 Hz, 1H), 2.68 (dd, *J* = 15.7, 10.1 Hz, 1H), 1.95 (dd, *J* = 12.9, 3.4 Hz, 1H), 1.67 (ddd, *J* = 15.3, 7.6, 3.4 Hz, 4H), 1.46 (dt, *J* = 10.1, 3.7 Hz, 2H), 1.37 – 1.28 (m, 3H), 1.25 (s, 2H), 1.21 (dd, *J* = 12.9, 3.8 Hz, 1H), 1.16 – 1.10 (m, 3H), 1.07 (s, 3H), 1.04 – 0.98 (m, 1H), 0.94 (dd, *J* = 14.6, 4.5 Hz, 1H), 0.88 (s, 9H), 0.78 (s, 3H), 0.05 (s, 6H). Rf: 0.2 in 4 :1 Hexanes:EtOAc

**HRMS** (ESI-TOF) [M+Na]<sup>+</sup> *m/z*: calcd for C<sub>29</sub>H<sub>46</sub>O<sub>4</sub>Si 511.3214; Found 511.3217.

**IR** (film, cm<sup>-1</sup>): 2926, 2855, 2360.



**Compound 3-29:** Diketone **3-27** was added to a flame-dried 500 mL round-bottom flask (3.20 g, 11.1 mmol). The flask was flushed with N<sub>2</sub> before dissolving the solid in anhydrous THF (110 mL) and cooled to -78 °C. *K*-Selectride (1.5 equiv, 1.0 M THF solution, 22.1 mL, 22.2 mmol) was added to the solution dropwise and monitored by TLC until starting material was consumed (50% hexane/EtOAc, 30 min). Once the starting material was consumed, dimethylformamide (110 mL) was added to the solution at -78 °C. Imidazole (4.0 equiv, 3.01 g, 44.3 mmol) and then *tert*-

butyldimethylsilyl chloride (3.0 equiv, 5.01 g, 33.2 mmol) were added to the solution. The reaction was warmed to room temperature and stirred for 16 h while concentrating over a stream of N<sub>2</sub>. The reaction was then concentrated in vacuo and brought up in EtOAc (500 mL) and washed with ice-cold 50% brine/ deionized water (300 mL × 4) and then brine (300 mL). The organic layer was dried over Na<sub>2</sub>SO<sub>4</sub>, filtered, and concentrated in vacuo. The residue was purified by flash column chromatography on silica gel (hexane/EtOAc = 1:0 to 24:1 to 9:1) to afford **3-29** (3.97 g, 9.81 mmol) as a single diastereomer in an 88% yield as a white solid. Rf: 0.63 in 9:1 hexane/EtOAc.

**m.p.** 123–125 °C

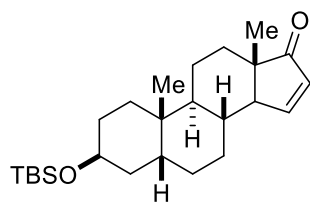
**<sup>1</sup>H NMR** (700 MHz, CDCl<sub>3</sub>): δ 4.03 (t, J = 2.8 Hz, 1H), 2.43 (dd, J = 19.3, 8.9 Hz, 1H), 2.06 (dt, J = 18.8, 9.1 Hz, 1H), 1.91 (dddd, J = 18.1, 13.7, 8.7, 5.1 Hz, 2H), 1.87–1.78 (m, 3H), 1.62–1.15 (m, 16H), 1.11 (qd, J = 13.2, 4.2 Hz, 1H), 0.96 (s, 3H), 0.88 (s, 9H), 0.85 (s, 3H), 0.01 (s, 6H).

**<sup>13</sup>C{<sup>1</sup>H} NMR** (176 MHz, CDCl<sub>3</sub>): δ 221.7, 67.4, 51.8, 48.1, 40.4, 36.7, 36.1, 35.5, 35.4, 34.5, 32.0, 30.2, 28.7, 26.8, 26.0, 25.6, 24.1, 22.0, 20.5, 18.2, 14.0, -4.7.

**[α]<sub>D</sub><sup>27</sup>** = +53.5 (c = 0.31, CHCl<sub>3</sub>).

**HRMS** (ESI-TOF) m/z: [M + Na]<sup>+</sup> calcd for C<sub>25</sub>H<sub>44</sub>O<sub>2</sub>SiNa 427.3008; found 427.3002

**IR** (thin film): 2926, 2856, 1740 cm<sup>-1</sup>.



**Compound 3-30:** In a flame dried 100 mL round bottom flask, diisopropylamine (1.5 equiv., 1.8 mL, 13.1 mmol) was added to THF (0.66 M, 20 mL) then cooled to -78 °C under an N<sub>2</sub> atmosphere. Freshly titrated *n*-BuLi (1.5 equiv., 2.45 M, 13.1 mmol, 5.35 mL) was added to the

solution dropwise. The solution was warmed to 0 °C on an ice bath for 30 min before cooling back down to -78 °C. A solution of **3-29** (1.0 equiv., 3.53 g, 8.72 mmol) in THF (0.67 M, 13.0 mL) was cooled to -78 °C before adding to the solution of LDA dropwise. The reaction mixture was stirred at -78 °C for 30 min. The flask was charged with TMSCl (1.5 equiv., 1.65 mL, 13.1 mmol) and stirred for 1 h as the reaction warmed to room temperature. The reaction was quenched with ice cold NaHCO<sub>3</sub> (sat) then extracted with pentane (35 mL x 4). The organic layer was dried over Na<sub>2</sub>SO<sub>4</sub>, filtered, and concentrated to afford the crude silyl enol ether which was used in the next reaction without further purification. Pd(OAc)<sub>2</sub> (1.1 equiv., 2.16 g, 9.59 mmol) was added to a solution of the above crude silyl enol ether in CH<sub>3</sub>CN (0.2 M, 44 mL) at room temperature. After the reaction mixture was stirred at room temperature for 12 h, the suspension was filtered through a pad of Celite with EtOAc (100 mL) and concentrated *in vacuo*. The residue was purified by flash column chromatography on silica gel (Hexanes/EtOAc = 24/1) to afford enone **3-30** (2.27 g, 5.64 mmol) in 65% yield as a white solid. Rf: 0.40 in 9:1 Hexanes:EtOAc.

**m.p.** 151-154 °C.

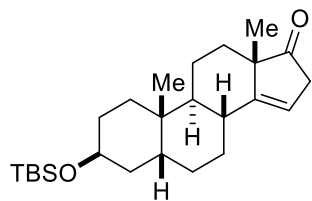
**<sup>1</sup>H NMR** (700 MHz, CDCl<sub>3</sub>) δ 7.53–7.50 (m, 1H), 6.01 (dd, J = 6.0, 3.0 Hz, 1H), 4.04 (s, 1H), 2.33 (dt, J = 11.3, 2.5 Hz, 1H), 1.99–1.92 (m, 1H), 1.90–1.78 (m, 4H), 1.75–1.70 (m, 1H), 1.62–1.35 (m, 10H), 1.28–1.18 (m, 3H), 1.05 (s, 3H), 1.00 (d, J = 1.6 Hz, 3H), 0.89 (d, J = 1.6 Hz, 9H), 0.02 (d, J = 1.6 Hz, 6H).

**<sup>13</sup>C NMR** (176 MHz, CDCl<sub>3</sub>): δ 213.7, 158.9, 131.8, 67.3, 57.4, 51.4, 41.8, 36.7, 35.6, 34.6, 32.9, 30.1, 29.6, 28.7, 26.7, 26.0, 25.6, 24.1, 20.9, 20.2, 18.2, -4.7.

**HRMS** (ESI-TOF): [M+H]<sup>+</sup> m/z: calcd for C<sub>25</sub>H<sub>45</sub>O<sub>2</sub>Si 403.3032; Found 403.3015.

**[α]<sub>D</sub><sup>27</sup>** -24.2 (c = 0.23, CHCl<sub>3</sub>).

**IR** (film, cm<sup>-1</sup>) 3346, 2928, 2855, 1710, 1561 cm<sup>-1</sup>



**Compound 3-31:** *i*-Pr<sub>2</sub>EtN (10.0 equiv., 8.5 mL, 48.9 mmol) was added to a suspension of enone **3-30** (1.97 g, 4.89 mmol) and SiO<sub>2</sub> (6.0 equiv., 1.76 g, 29.4 mmol) in toluene (0.1 M, 50 mL) at room temperature. The reaction was warmed to 60 °C and stirred for 7 h. The reaction was diluted with EtOAc (100 mL) filtered then washed with 1N HCl (30 mL). The organic layer was dried over Na<sub>2</sub>SO<sub>4</sub>, filtered, and concentrated *in vacuo*. The crude material was purified by flash column chromatography on silica gel (Hexanes/EtOAc = 1/0 to 24/1 to 9/1) to afford **3-31** (1.35 g, 3.35 mmol) and enone **3-30** (515 mg, 1.28 mmol) in 69% yield and 95% BRSM, respectively as white solids. Rf: 0.63 in 9:1 Hexanes:EtOAc.

**m.p.** 109-111 °C.

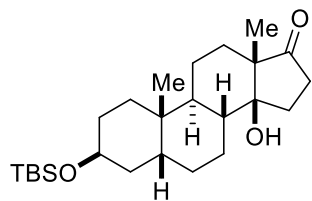
**<sup>1</sup>H NMR** (700 MHz, CDCl<sub>3</sub>) δ 5.48 (d, J = 2.5 Hz, 1H), 4.01 (t, J = 2.6 Hz, 1H), 2.99 (ddd, J = 23.1, 4.1, 1.7 Hz, 1H), 2.83 (dt, J = 23.0, 2.3 Hz, 1H), 2.18 (t, J = 11.1 Hz, 1H), 1.96 (tt, J = 13.9, 4.2 Hz, 1H), 1.86–1.74 (m, 3H), 1.62–1.49 (m, 5H), 1.45–1.32 (m, 5H), 1.23 (ddd, J = 19.5, 9.6, 3.5 Hz, 3H), 1.10 (s, 3H), 0.99 (s, 3H), 0.88 (s, 9H), 0.01 (s, 6H).

**<sup>13</sup>C NMR** (176 MHz, CDCl<sub>3</sub>) δ 223.0, 154.3, 112.7, 67.4, 51.2, 41.6, 41.3, 36.6, 35.8, 35.6, 34.4, 33.7, 29.9, 28.8, 26.5, 26.0, 23.8, 23.2, 21.0, 20.1, 18.2, -4.7, -4.7.

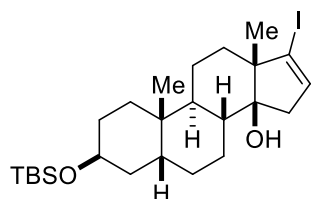
**HRMS** (ESI-TOF) [M+H]<sup>+</sup> m/z: calcd for C<sub>25</sub>H<sub>45</sub>O<sub>2</sub>Si 403.3032; Found 403.3024.

[α]<sub>D</sub><sup>27</sup> +75.4 (c = 0.34, CHCl<sub>3</sub>).

**IR** (film, cm<sup>-1</sup>) 2925, 2882, 2859, 1738, 1639.



**Compound 3-33a.** A solution of **3-31** (1.19 g, 2.95 mmol), cobalt (II) acetylacetonate ( $\text{Co}(\text{acac})_2$ , 0.2 equiv., 152 mg, 0.59 mmol) in 1,4-dioxane (30 mL) was bubbled with  $\text{O}_2$  for 10 min at room temperature. A solution of  $\text{PhSiH}_3$  (3.1 equiv., 1.1 mL, 9.0 mmol) in 1,4-dioxane (5.5 mL) was added to the mixture at room temperature over 2 h via a syringe pump under  $\text{O}_2$  atmosphere (1 atm). After the reaction mixture was stirred under  $\text{O}_2$  atmosphere (1 atm) at room temperature for 3 hours, saturated aqueous  $\text{NaHCO}_3$  (10 mL) and 10 w/v%  $\text{Na}_2\text{S}_2\text{O}_3$  were added to the mixture. The resultant mixture was extracted with  $\text{CH}_2\text{Cl}_2$  (50 mL x 4). The combined organic layers were dried over  $\text{Na}_2\text{SO}_4$ , filtered, and concentrated *in vacuo*. The residue was passed through a silica gel plug (hexane/ $\text{EtOAc}$  = 1/1) to afford a 2.9:1 mixture of two C14-epimeric alcohols  $\beta$ -**3-33a** and  $\alpha$ -**3-33a** as a gel. The gel was used in the next reaction without further purification.



**Compound 3-33:** Hydrazine monohydrate ( $\text{N}_2\text{H}_4 \cdot \text{H}_2\text{O}$ , 17.5 equiv., 2.5 mL, 51.5 mmol) was added to a solution of the alcohols  $\beta$ -**3-33a** and  $\alpha$ -**3-33a** from above and  $\text{Et}_3\text{N}$  (17.6 equiv., 7.3 mL, 52.0 mmol) in absolute ethanol (130 mL). The reaction flask was flushed with  $\text{N}_2$  and heated to  $50^\circ\text{C}$  for 12 h then concentrated *in vacuo* to white crystals. The flask was removed from high vacuum and flushed with  $\text{N}_2$  before adding  $\text{Et}_3\text{N}$  (20.0 equiv., 7.3 mL, 52.0 mmol) and dissolving in THF (130 mL). The reaction was stirred vigorously at room temperature as a solution of  $\text{I}_2$  (3.5



equiv., 2.6 g, 10.3 mmol) dissolved in THF (5 mL) was added dropwise until the solution turned brown. The reaction was stirred for 10 min until the solution returned to a yellow color before adding more of the I<sub>2</sub> solution until the brown color persisted. The reaction was stirred for 1 h at room temperature then quenched with 10 w/v% Na<sub>2</sub>S<sub>2</sub>O<sub>3</sub> (100 mL). The mixture was diluted with deionized water (500 mL) then extracted with CH<sub>2</sub>Cl<sub>2</sub> (200 mL x 3). The combined organic layers were dried over Na<sub>2</sub>SO<sub>4</sub>, filtered, and concentrated *in vacuo*. The residue was purified by flash column chromatography on F60 silica gel (Hexanes/EtOAc = 49/1 to 24/1 to 9/1) to afford vinyl iodide **3-33** (601 mg, 1.13 mmol) in 38% yield over 2 steps as a white solid. The identity was confirmed by comparison to the previously reported variant.<sup>15</sup> Rf: 0.49 in 9:1 Hexanes/EtOAc. **m.p.** 123-125 °C.

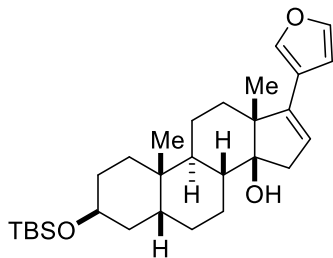
**<sup>1</sup>H NMR** (700 MHz, CDCl<sub>3</sub>) δ 6.11 (t, J = 2.5 Hz, 1H), 4.04 (d, J = 3.7 Hz, 1H), 2.56 (dd, J = 16.4, 1.9 Hz, 1H), 2.21 (dd, J = 16.4, 3.2 Hz, 1H), 1.88 (td, J = 14.5, 7.4 Hz, 1H), 1.84–1.74 (m, 4H), 1.65 (td, J = 11.9, 3.8 Hz, 1H), 1.56–1.40 (m, 5H), 1.37 (dt, J = 13.2, 3.3 Hz, 1H), 1.27–1.15 (m, 4H), 1.04 (s, 3H), 1.04–0.98 (m, 1H), 1.01–0.95 (m, 1H), 0.94 (s, 3H), 0.88 (s, 9H), 0.02 (s, 6H).

**<sup>13</sup>C NMR** (176 MHz, CDCl<sub>3</sub>) δ 133.7, 111.6, 82.7, 67.3, 55.0, 42.8, 41.6, 37.7, 36.7, 36.2, 35.4, 34.4, 29.9, 28.9, 26.7, 26.0, 24.2, 21.3, 19.9, 18.2, 18.1, –4.7, –4.7.

**HRMS** (ESI-TOF) [M-H<sub>2</sub>O-OTBS]<sup>+</sup> m/z: calcd for C<sub>19</sub>H<sub>26</sub>I 381.1074; Found 381.1068.

[α]<sub>D</sub><sup>27</sup> +14.3 (c = 0.29, CHCl<sub>3</sub>).

**IR** (film, cm<sup>-1</sup>): 3444, 2928, 2884, 2857.



**Compound 3-57a:** Substrate **3-33** (862 mg, 1.62 mmol), and 3-furylboronic acid (544 mg, 4.86 mmol, 3.0 equiv.) were transferred to a flame-dried round bottom flask with a magnetic stir bar. The flask was then transferred to a glovebox where PdCl<sub>2</sub>(PPh<sub>3</sub>)<sub>4</sub> (0.10 equiv., 187 mg, 0.16 mmol) was weighed out into the reaction flask. Afterwards, the flask was taken out of the glovebox and dry toluene (20 mL) was introduced, followed by MeOH (4 mL) and NaHCO<sub>3(sat.)</sub> (4 mL). The biphasic suspension was then equipped with a reflux condenser and heated to 80 °C from an oil bath, while stirring for 18 h. After the designated reaction time, the heat was turned off and the flask was allowed to cool to room temperature. Then, the reaction solution was partitioned between dI water (20 mL) and a 1:1 mixture of EtOAc : hexanes (20 mL). The layers were separated, and the organic phase was washed with HCl (1N aq. solution, 30 mL), then H<sub>2</sub>O (30 mL), then brine (30 mL). The organic phase was then dried over Na<sub>2</sub>SO<sub>4</sub>, filtered and concentrated *in vacuo*. Flash column chromatography was performed on the crude residue through silica gel (Hexanes/EtOAc = 9/1) to afford **3-57a** (579 mg, 1.23 mmol) in 76% yield as a white solid. Rf: 0.39 in 9:1 Hexanes/EtOAc.

**m.p.** 125-128 °C.

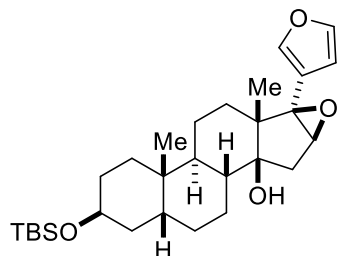
**<sup>1</sup>H NMR** (500 MHz, CDCl<sub>3</sub>) δ 7.44 (s, 1H), 7.36 (t, *J* = 1.6 Hz, 1H), 6.47 (dd, *J* = 1.9, 0.9 Hz, 1H), 5.75 (t, *J* = 2.5 Hz, 1H), 4.05 (t, *J* = 2.8 Hz, 1H), 2.69 (dd, *J* = 17.0, 2.0 Hz, 1H), 2.25 (dd, *J* = 17.1, 3.2 Hz, 1H), 1.97 (dt, *J* = 13.1, 3.0 Hz, 1H), 1.92 (t, *J* = 4.4 Hz, 1H), 1.89 (d, *J* = 2.7 Hz, 1H), 1.86 (d, *J* = 2.4 Hz, 1H), 1.85 – 1.79 (m, 2H), 1.72 (ddd, *J* = 15.6, 9.9, 3.9 Hz, 2H), 1.58 (dd, *J* = 11.6, 3.3 Hz, 1H), 1.55–1.48 (m, 2H), 1.48–1.45 (m, 1H), 1.43 (q, *J* = 3.4 Hz, 1H), 1.41–1.33 (m, 1H), 1.30–1.23 (m, 2H), 1.20 – 1.05 (m, 2H), 0.96 (s, 3H), 0.89 (s, 10H), 0.02 (s, 6H).

**<sup>13</sup>C NMR** (126 MHz, CDCl<sub>3</sub>) δ 143.9, 142.6, 138.1, 121.4, 121.1, 109.8, 85.9, 67.3, 52.1, 40.4, 39.9, 38.6, 36.3, 36.1, 35.2, 34.3, 29.8, 28.8, 26.6, 25.8, 24.1, 21.4, 19.9, 18.1, 16.8, –4.8, –4.9.

**HRMS** (ESI-TOF)  $[M+Na]^+$   $m/z$ : calcd for  $C_{29}H_{46}O_3Si$  493.3108; Found 493.3111.

$[\alpha]_D^{27}$  +41 ( $c=0.05$ ,  $CHCl_3$ ).

**IR** (film,  $cm^{-1}$ ) 3446, 2942, 2855, 2361, 2339.



**Compound 3-57:** The intermediate **3-57a** from above (374 mg, 0.794 mmol) was dissolved in dry DCM (20 mL) in a flame-dried round bottom flask with a magnetic stirring bar and the reaction vessel was cooled to  $-40$  °C in a dry ice/acetonitrile bath. Then,  $NaHCO_3$  (1.20 equiv., 100 mg, 1.19 mmol) was added to the reaction, followed by *m*CPBA (75% w/w, 1.2 equiv., 241 mg, 0.979 mmol) after a 10 min incubation period. The reaction was then stirred for 5 h while warming but not reaching above  $-10$  °C. After the designated reaction time, the reaction was quenched with  $Na_2S_2O_3$ (sat) (20 mL) and then the cooling bath was removed. The solution was then vigorously stirred for 30 mins at room temperature to create a cloudy mixture. Then, the reaction solution was extracted with DCM (3 x 20 mL) and EtOAc (3 x 20 mL). The organic phase was washed with sat. aq.  $NaHCO_3$  (50 mL), then brine (50 mL). The organic phase was then dried over  $Na_2SO_4$ , filtered and concentrated *in vacuo*. Flash column chromatography was performed on the crude solid through silica gel (Hexanes/EtOAc = 19/1 to 9/1 to 4/1) to afford **3-57**(299 mg, 0.615 mmol) in 77% yield as a white solid. Rf: 0.69 in 4:1 Hexanes/EtOAc.

**m.p.** 154-157 °C.

**$^1H$  NMR** (400 MHz,  $C_6D_6$ )  $\delta$ 7.25 (s, 1H), 7.06 (d,  $J = 1.5$  Hz, 1H), 6.24 (d,  $J = 1.8$  Hz, 1H), 4.08 (s, 1H), 3.57 (s, 1H), 3.30 (s, 1H), 2.18 (dd,  $J = 13.8, 3.5$  Hz, 1H), 1.96 – 1.87 (m, 2H), 1.86 – 1.77

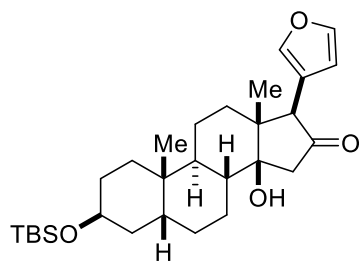
(m, 2H), 1.75 – 1.71 (m, 2H), 1.68 (dt,  $J = 10.9, 4.3$  Hz, 2H), 1.52 – 1.46 (m, 2H), 1.41 (d,  $J = 16.8$  Hz, 1H), 1.36 (t,  $J = 3.2$  Hz, 1H), 1.31 (d,  $J = 3.5$  Hz, 1H), 1.28 – 1.20 (m, 4H), 1.18 (s, 3H), 1.12 (dd,  $J = 13.1, 4.1$  Hz, 1H), 1.02 (s, 9H), 0.94 (d,  $J = 14.6$  Hz, 1H), 0.89 (s, 3H), 0.86 – 0.76 (m, 1H), 0.11 (d,  $J = 2.3$  Hz, 6H).

$^{13}\text{C}$  NMR (126 MHz,  $\text{C}_6\text{D}_6$ )  $\delta$  142.7, 141.4, 119.9, 110.7, 80.7, 69.5, 67.7, 62.1, 46.5, 40.8, 36.4, 35.8, 35.3, 35.2, 34.9, 34.5, 30.1, 30.0, 29.1, 26.9, 25.9, 24.1, 21.4, 20.2, 18.2, 14.1, 1.2, -4.7(5), -4.7(6), -4.8(2).

HRMS (ESI-TOF)  $[\text{M}+\text{Na}]^+$   $m/z$ : calcd for 509.3057. Found: 509.3054.

$[\alpha]_{\text{D}}^{27} +7.6$  ( $c = 0.13$ ,  $\text{CHCl}_3$ ).

IR (film,  $\text{cm}^{-1}$ ): 3357, 2926, 2854, 2361, 2338.



**Compound 3-58.**: Compound **3-57** from above (267 mg, 0.548 mmol) was dissolved in anhydrous 1,4-dioxane (27.5 mL) in a flame-dried round-bottom flask. Then, a solution of  $\text{BF}_3 \cdot \text{OEt}_2$  (750  $\mu\text{L}$  of a solution of 200  $\mu\text{L}$  of  $\text{BF}_3 \cdot \text{OEt}_2$  in 3 mL of dry  $\text{Et}_2\text{O}$ ) was added to the reaction in quick drops. The reaction went from opaque to orange-brown, and then transparent over the course of a minute. After such time, the solution was diluted with  $\text{Et}_2\text{O}$  (15 mL) and then quenched with  $\text{NaHCO}_3(\text{sat.})$  (15 mL). The aqueous phase was extracted with DCM (4 x 20 mL). The organic layer was then washed with brine (30 mL), dried over  $\text{Na}_2\text{SO}_4$ , filtered, and concentrated *in vacuo*. The residue was purified by flash column chromatography on silica gel (Hexanes/ $\text{EtOAc} = 19/1$  to  $9/1$ ) to afford **3-58** (253 mg, 0.519 mmol) in 95% yield as a white solid. Rf: 0.5 in 4 : 1 Hexanes: $\text{EtOAc}$ .

**m.p.** 143-147 °C.

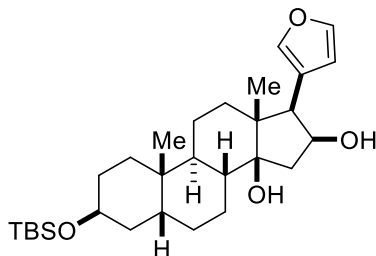
**<sup>1</sup>H NMR** (700 MHz, CDCl<sub>3</sub>) δ 7.33 (d, *J* = 1.9 Hz, 1H), 7.26 (overlapping with CDCl<sub>3</sub> s, 1H), 6.36 (d, *J* = 1.7 Hz, 1H), 4.06 (t, *J* = 2.8 Hz, 1H), 3.05 (s, 1H), 2.83 (d, *J* = 18.2 Hz, 1H), 2.33 (d, *J* = 18.2 Hz, 1H), 1.87 (td, *J* = 13.8, 6.9 Hz, 1H), 1.83 (d, *J* = 14.1 Hz, 1H), 1.79–1.73 (m, 3H), 1.68 (td, *J* = 12.0, 3.7 Hz, 1H), 1.62–1.57 (m, 2H), 1.54 (td, *J* = 14.2, 3.7 Hz, 2H), 1.45 (qd, *J* = 11.4, 9.3, 3.7 Hz, 3H), 1.40 (d, *J* = 9.2 Hz, 2H), 1.31 (qd, *J* = 13.3, 3.5 Hz, 1H), 1.27–1.21 (m, 4H), 1.13 (qd, *J* = 13.1, 4.1 Hz, 1H), 0.96 (s, 3H), 0.91 (s, 3H), 0.89 (s, 9H), 0.04–0.00 (m, 6H).

**<sup>13</sup>C NMR** (176 MHz, CDCl<sub>3</sub>) δ 217.5, 142.5, 141.7, 121.3, 112.0, 82.6, 67.0, 58.2, 46.3, 46.2, 41.6, 40.2, 36.0, 35.9, 35.2, 34.2, 29.6, 28.7, 26.5, 25.8, 23.9, 21.4, 21.1, 18.1, 15.9, –4.8(5), –4.8(8).

**HRMS** (ESI-TOF) [M+Na]<sup>+</sup> *m/z*: calcd for C<sub>29</sub>H<sub>46</sub>O<sub>4</sub>Si 509.3057; Found 509.3058.

**[α]<sub>D</sub><sup>27</sup>** +67.1 (*c* = 0.06, CHCl<sub>3</sub>).

**IR** (film, cm<sup>-1</sup>): 3454, 2930, 2856, 2365, 2341.



**Compound 3-19: 3-58** (300 mg, 0.616 mmol) was dissolved in anhydrous THF (5 mL) and MeOH (5 mL) in a flame-dried round-bottom flask. The reaction vessel was flushed with N<sub>2</sub> for 15 min while being cooled to –20 °C in an ice/salt mixture. NaBH<sub>4</sub> (28 mg, 0.74 mmol, 1.5 equiv.), was added and the reaction was left to stir for 2 h at –20 °C. After the first 1 h, another equivalent of NaBH<sub>4</sub> was added to the reaction. After stirring for another 4 h, checking that all starting material was consumed by TLC, NH<sub>4</sub>Cl<sub>(sat.)</sub> (10 mL) was added to quench the reaction. The aqueous phase

was extracted with EtOAc (15 mL x 3) and DCM (10 mL x 4). The organic layer was then washed with brine (40 mL), dried over Na<sub>2</sub>SO<sub>4</sub>, filtered, and concentrated *in vacuo* to provide 9.6:1 mixture of the desired diastereomer **3-19** and its  $\alpha$ 16-epimer. The residue was purified by flash column chromatography on silica gel (Hexanes/EtOAc = 19/1 to 9/1) to afford **3-19** (207 mg, 0.423 mmol) in 69% yield as a white solid along with the minor diastereomer  $\alpha$ 16 **3-19a** (21.6 mg, 44  $\mu$ mol, 7.1%). Unreacted starting material **3-58** was recovered as well (4 mg, 8  $\mu$ mol 77% brsm). Rf: 0.5 in 4 :1 Hexanes:EtOAc.

**m.p.** 200 °C.

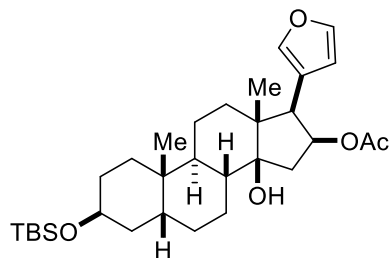
**<sup>1</sup>H NMR** (700 MHz, CDCl<sub>3</sub>)  $\delta$  (*c* = 0. 7.40 (d, *J* = 1.8 Hz, 1H), 7.31 (s, 1H), 6.42 (s, 1H), 4.37 (s, 1H), 4.05 (d, *J* = 3.5 Hz, 1H), 3.03 (d, *J* = 6.9 Hz, 1H), 2.66 (s, 1H), 2.34 (dd, *J* = 14.5, 6.0 Hz, 1H), 2.28 (s, 1H), 1.91 (d, *J* = 14.5 Hz, 1H), 1.88–1.74 (m, 5H), 1.66–1.58 (m, 1H), 1.57–1.54 (m, 2H), 1.52–1.43 (m, 3H), 1.39 (ddt, *J* = 13.0, 9.7, 3.4 Hz, 3H), 1.30–1.13 (m, 8H), 0.92 (s, 3H), 0.88 (s, 9H), 0.81 (s, 3H), 0.02 (s, 6H).

**<sup>13</sup>C NMR** (176 MHz, CDCl<sub>3</sub>)  $\delta$  142.6, 141.4, 121.4, 113.8, 85.9, 73.7, 67.2, 54.8, 48.4, 41.9, 41.4, 40.8, 36.1, 35.7, 35.4, 34.3, 29.7, 29.7, 28.7, 26.9, 25.8, 23.9, 22.7, 22.0, 21.3, 18.1, 17.1, 14.1, 1.0, –4.8(3), –4.8(8).

**HRMS** (ESI-TOF) [M+Na]<sup>+</sup> *m/z*: calcd for C<sub>29</sub>H<sub>46</sub>O<sub>4</sub>Si 511.3214; Found 511.3220.

**[ $\alpha$ ]<sub>D</sub><sup>27</sup>** +9.5 (*c* = 0.07, CHCl<sub>3</sub>).

**IR** (film, cm<sup>-1</sup>): 2926, 2855, 2360.



**Compound 3-20.:** **3-19** from above (145 mg, 0.297 mmol) was dissolved in anhydrous DCM (4.5 mL) and then transferred to an oven-dried round bottom flask. The reaction vessel was flushed with N<sub>2</sub> for 15 mins. Then, DMAP (3.6 mg, 29 μmol, 0.10 equiv.), and then Ac<sub>2</sub>O (283 μL, 2.98 mmol) was added at room temperature. Then, anhydrous pyridine (1.5 mL) was added to the reaction solution and was then left to stir for 16 h at room temperature. After checking that all starting material was consumed by TLC, MeOH (1 mL) and NH<sub>4</sub>Cl<sub>(sat.)</sub> (10 mL) were added in succession to quench the reaction. The aqueous phase was extracted with EtOAc (20 mL x 4). The organic layer was then washed with brine (25 mL), dried over Na<sub>2</sub>SO<sub>4</sub>, filtered, and concentrated *in vacuo*. The residue was purified by flash column chromatography on silica gel (Hexanes/EtOAc = 19/1 to 9/1) to afford **3-20** (134 mg, 0.252 mmol) in 85% yield as a white solid. Rf: 0.54 in 4:1 Hexanes:EtOAc.

**m.p.** 143-145 °C.

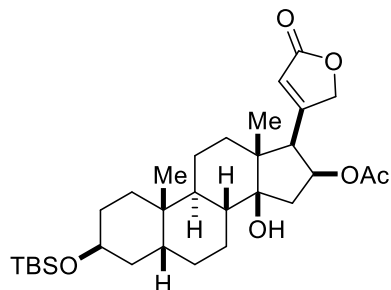
**<sup>1</sup>H NMR** (700 MHz, CDCl<sub>3</sub>): δ 7.28 (s, 1H), 7.19 (s, 1H), 6.51 (s, 1H) 5.53 (td, *J* = 8.7, 1.7 Hz, 1H), 4.05 (s, 1H), 3.23 (d, *J* = 8.5 Hz, 1H), 2.61 (dd, *J* = 15.5, 8.9 Hz, 1H), 1.89–1.82 (m, 2H), 1.81 (s, 3H), 1.59–1.50 (m, 4H), 1.47 (dd, *J* = 14.5, 11.9 Hz, 1H), 1.43–1.36 (m, 3H), 1.30 (td, *J* = 13.8, 3.5 Hz, 1H), 1.27–1.15 (m, 4H), 0.92 (s, 3H), 0.88 (s, 9H), 0.76 (s, 3H), 0.02 (s, 6H).

**<sup>13</sup>C NMR** (176 MHz, CDCl<sub>3</sub>): δ 169.4, 141.1, 140.6, 120.8, 113.5, 83.7, 73.2, 66.3, 52.0, 48.1, 41.1, 39.4, 39.3, 35.2, 34.9, 34.4, 33.4, 28.9, 27.9, 25.9, 25.0, 23.0, 20.5, 20.3, 20.2, 17.3, 15.8, – 5.6(7), –5.7(1).

**HRMS** (ESI-TOF)  $[M+Na]^+$  m/z: calcd for  $C_{31}H_{50}O_5Si$  553.3320; Found 553.3350.

$[\alpha]_D^{27}$   $-5.5$  ( $c=0.2$ ,  $CHCl_3$ ).

**IR** (film,  $cm^{-1}$ ): 2976, 2849, 2890, 2855, 1732.



**Compound 3-2a: 3-20** (63 mg, 0.12 mmol) was dissolved in anhydrous DCM (6.0 mL) and then transferred to a flame-dried 20 mL borosilicate glass test tube, which contained rose bengal (6.0 mg, 6.1  $\mu$ mol, 0.05 equiv.) under an atmosphere of  $N_2$  with a rubber septum cap. Then, DIPEA (250  $\mu$ L, 1.4 mmol, 12 equiv.) was added to the reaction solution. The reaction vessel was then cooled to  $-78$   $^{\circ}C$  for 15 min. The reaction was then irradiated with a 500W Wall Mounted Floodlamp, at a stationary distance of approximately 10 cm for efficient radiation. The nitrogen line was then replaced with a balloon filled with oxygen and the reaction was stirred while being irradiated for 6 h. After the confirmation of no more starting material by TLC, the light source was removed, as well as the oxygen balloon. The reaction was then allowed to stir while warming to room temperature while being flushed with an argon balloon to remove any remaining oxygen. The test tube was then covered with aluminum foil and left to stir for 16 h. Then, the solvent was removed via a nitrogen stream and redissolved in MeOH (6 mL) and cooled in an ice bath to  $0^{\circ}C$ . Then,  $NaBH_4$  (314 mg, 8.3 mmol, 70 equiv.) over 1 h to reduce excessive bubbling. The reaction was then stirred at  $0^{\circ}C$  for 1 h, and then at room temperature for 1 h. After the listed time, the reaction was then chilled to  $0^{\circ}C$  and diluted with EtOAc (15 mL). Then, a solution of 20%  $H_2SO_4/MeOH$  was added dropwise until the pink/red color was dissolved away to leave an off-



yellow solution. The reaction solution was then poured into dI water (20 mL). The aqueous phase was extracted with EtOAc (15 mL x 3). The organic layer was then washed with NaHCO<sub>3</sub>(sat.) (30 mL), brine (30 mL), dried over Na<sub>2</sub>SO<sub>4</sub>, filtered, and concentrated *in vacuo*. The residue was purified by flash column chromatography on silica gel (Hexanes/EtOAc = 9/1 to 1/1, then Hexanes:Acetone 9/1 to 3/2)) to afford **3-2a** (33.2 mg, 60 μmol, 51%) as a viscous clear oil and oleandrogenin (**3-2**) as a white film (5.2 mg, 12 μmol, 10%). Rf: 0.64 1:1 Hexanes: EtOAc.

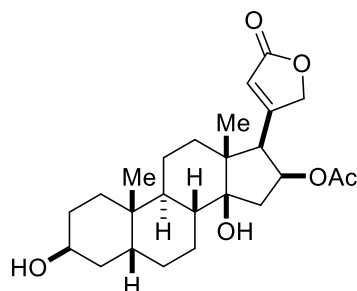
**<sup>1</sup>H NMR** (600 MHz, CDCl<sub>3</sub>) δ 5.96 (t, *J* = 1.9 Hz, 1H), 5.47 (td, *J* = 9.3, 2.6 Hz, 1H), 4.99 (dd, *J* = 18.2, 1.9 Hz, 1H), 4.85 (dd, *J* = 18.1, 1.8 Hz, 1H), 4.04 (t, *J* = 2.8 Hz, 1H), 3.18 (d, *J* = 8.7 Hz, 1H), 2.72 (dd, *J* = 15.6, 9.7 Hz, 1H), 1.96 (s, 3H), 1.85 (ddd, *J* = 13.6, 9.4, 4.3 Hz, 1H), 1.82–1.79 (m, 1H), 1.78–1.72 (m, 2H), 1.71–1.65 (m, 1H), 1.59–1.49 (m, 5H), 1.43 (ddd, *J* = 15.5, 8.3, 2.9 Hz, 2H), 1.40–1.36 (m, 2H), 1.30 (td, *J* = 13.5, 3.5 Hz, 1H), 1.25–1.20 (m, 3H), 1.16 (dd, *J* = 14.8, 11.0 Hz, 1H), 0.92 (s, 3H), 0.91 (s, 3H), 0.87 (s, 9H), 0.01 (d, *J* = 1.8 Hz, 6H).

**<sup>13</sup>C NMR** (151 MHz, CDCl<sub>3</sub>) δ 174.1, 170.4, 167.9, 121.4, 84.3, 75.7, 74, 67.1, 56.2, 50.0, 41.9, 41.2, 39.3, 35.9, 35.6, 35.2, 34.2, 29.7, 28.7, 26.6, 25.9, 23.8, 21.3, 21.1, 20.9, 18.1, 16.0, –4.8(0), –4.8(3).

**HRMS** (ESI-TOF) [M+Na]<sup>+</sup> *m/z*: calcd for C<sub>31</sub>H<sub>50</sub>O<sub>6</sub>Si 569.3269; Found 569.3251.

**[α]<sub>D</sub><sup>27</sup>** –3.03 (*c* = 1.28, CHCl<sub>3</sub>).

**IR** (film, cm<sup>-1</sup>) 2976, 2849, 2890, 2855, 1732.



**Oleandrigenin (3-2): 3-2a** (18.4 mg, 33.7  $\mu\text{mol}$ ) was dissolved in anhydrous THF (1.5 mL) and then transferred to a plastic screw-cap vial. To a second separate plastic screw-cap reaction vial, was added HF $\cdot$ Py (70%, 456  $\mu\text{L}$ , 100 equiv.) and then was diluted with anhydrous pyridine (456  $\mu\text{L}$ , *careful, exotherm!*). After the solution cooled to room temperature, the prepared HF $\cdot$ Py solution was added to the plastic vial containing the starting reagent. The reaction was left to stir for 18 h at room temperature. After the confirmation of no more starting material by TLC, TMSOMe (1.5 mL) was added to quench the reaction, followed by  $\text{NaHCO}_3(\text{sat.})$  (2 mL). After leaving to stir for 20 min, the reaction was extracted with EtOAc (3 x 15 mL). Then, dry the organic phase with brine (20 mL), dried over  $\text{Na}_2\text{SO}_4$ , filtered, and concentrated *in vacuo*. The residue was purified by flash column chromatography on silica gel (Hexanes/EtOAc = 1/1 then, Hexanes Acetone 4/1 to 3/2)) to afford oleandrigenin (**3-2**) (13.2 mg, 30.5  $\mu\text{mol}$ , 91%) as a white solid. R<sub>f</sub>: 0.5 in 3:2 Hexane: Acetone.

**m.p.:** 220 °C (decomposition).

**$^1\text{H}$  NMR** (600 MHz,  $\text{CDCl}_3$ )  $\delta$  5.97 (t,  $J = 1.9$  Hz, 1H), 5.48 (td,  $J = 9.3, 2.7$  Hz, 1H), 4.98 (dd,  $J = 18.1, 1.9$  Hz, 1H), 4.86 (dd,  $J = 18.1, 1.9$  Hz, 1H), 4.14 (t,  $J = 2.9$  Hz, 1H), 3.19 (d,  $J = 8.7$  Hz, 1H), 2.74 (dd,  $J = 15.6, 9.7$  Hz, 1H), 1.97 (s, 3H), 1.92–1.84 (m, 2H), 1.78 (dd,  $J = 15.6, 2.8$  Hz, 2H), 1.74–1.67 (m, 1H), 1.55 (ddt,  $J = 16.5, 7.6, 3.4$  Hz, 5H), 1.51–1.47 (m, 1H), 1.48–1.41 (m, 1H), 1.40–1.33 (m, 1H), 1.33–1.28 (m, 2H), 1.21 (ddd,  $J = 21.8, 11.7, 3.5$  Hz, 1H), 0.95 (s, 3H), 0.94 (s, 3H).

**$^{13}\text{C}$  NMR** (151 MHz,  $\text{CDCl}_3$ )  $\delta$  174.0, 170.4, 167.6, 121.4, 84.3, 75.6, 73.9, 66.7, 56.1, 49.9, 41.8, 41.2, 39.2, 35.8, 35.4, 35.3, 33.3, 29.5, 27.9, 26.3, 23.7, 21.0, 21.0, 20.8, 15.9.

**HRMS** (ESI-TOF)  $[\text{M}+\text{Na}]^+$   $m/z$ : calcd for  $\text{C}_{25}\text{H}_{36}\text{O}_6$  455.2404; Found 455.2403.

**$[\alpha]_D^{23}$**   $-3.25$  ( $c = 0.56$ ,  $\text{CHCl}_3$ ).

IR (film,  $\text{cm}^{-1}$ ): 3511, 2931, 1788, 1745, 1692, 1258.

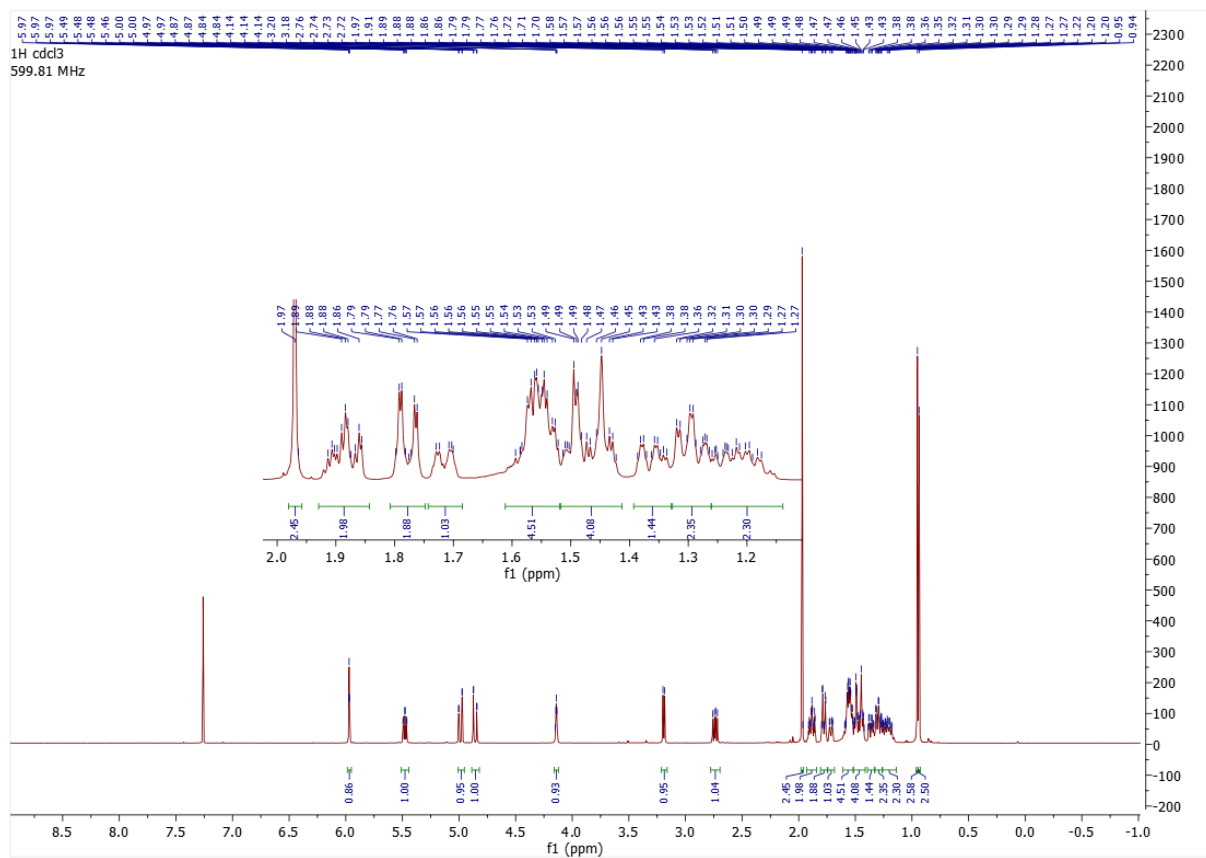
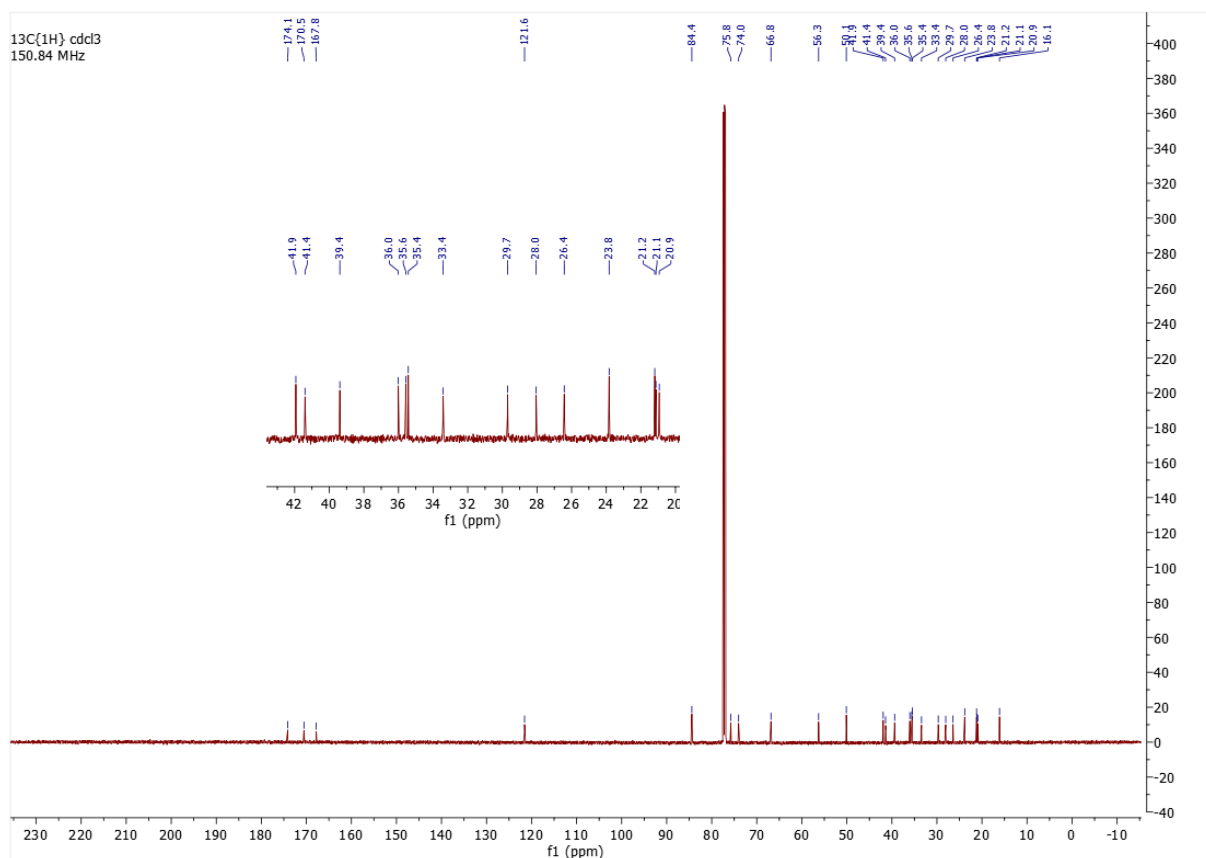


Figure 3.30.  $^1\text{H}$ NMR spectrum corresponding to oleandrigenin (**3-2**).



**Figure 3.31.**  $^{13}\text{C}$  NMR spectrum corresponding to oleandrigenin (**3-2**).

Michalak et. al. <sup>13</sup>	Synthetic ( <b>3-2</b> )
5.96 (br.s, 1H)	5.97 (t, $J = 1.9$ Hz, 1H)
5.47 (td, $J = 9.4, 2.2$ Hz, 1H)	5.48 (td, $J = 9.3, 2.7$ Hz, 1H)
4.99 (d, $J = 18.1$ Hz, 1H)	4.98 (dd, $J = 18.1, 1.9$ Hz, 1H)
4.85 (d, $J = 18.1$ Hz, 1H)	4.86 (dd, $J = 18.1, 1.9$ Hz, 1H)
4.13 (br.s, 1H)	4.14 (t, $J = 2.9$ Hz, 1H)
3.19 (d, $J = 8.7$ Hz, 1H)	3.19 (d, $J = 8.7$ Hz, 1H)
2.73 (dd, $J = 15.6, 9.7$ Hz, 1H)	2.74 (dd, $J = 15.6, 9.7$ Hz, 1H)
1.96 (s, 3H)	1.97 (s, 3H)

1.96-1.09 (m, 20H)	1.92-1.84 (m, 2H)
--	1.78 (dd, $J = 15.6, 2.8$ Hz, 2H)
--	1.74-1.67 (m, 1H)
--	1.55 (ddt, $J = 16.5, 7.6, 3.4$ Hz, 5H)
--	1.51-1.47 (m, 1H)
--	1.48-1.41 (m, 1H)
--	1.40-1.33 (m, 1H)
--	1.33-1.28 (m, 2H)
--	1.21 (ddd, $J = 21.8, 11.7, 3.5$ Hz, 1H)
0.95 (s, 3H)	0.95 (s, 3H)
0.93 (s, 3H)	0.94 (s, 3H)

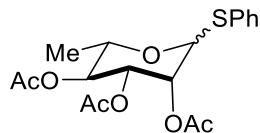
**Table 3.3**  $^1\text{H}$  NMR ( $\text{CDCl}_3$ ) comparison of reported synthetic (left) vs. synthetic (right) oleandrigenin with reported data from the literature.

Michalak et. al. <sup>13</sup>	Synthetic (3-2)
174.0	<b>174.1</b>
170.4	<b>170.5</b>
167.8	<b>167.8</b>
121.4	<b>121.6</b>
84.2	<b>84.4</b>

75.6	<b>75.8</b>
73.9	<b>74.0</b>
66.7	<b>66.8</b>
56.1	<b>56.3</b>
50.0	<b>50.1</b>
41.8	<b>41.9</b>
41.2	<b>41.4</b>
39.2	<b>39.4</b>
35.9	<b>36.0</b>
35.4	<b>35.6</b>
35.3	<b>35.4</b>
33.3	<b>33.4</b>
29.5	<b>29.7</b>
27.9	<b>28.0</b>
26.3	<b>26.4</b>
23.7	<b>23.8</b>
21.0	<b>21.2</b>
21.0	<b>21.1</b>
20.8	<b>20.9</b>
15.9	<b>16.1</b>

---

**Table 3.4**  $^{13}\text{C}$  NMR ( $\text{CDCl}_3$ ) comparison of reported synthetic (left) vs. synthetic (right) oleandrigenin with reported data from the literature.



**Compound 3-69:** *L*-rhamnose monohydrate (2.00 g, 10.98 mmol) and acetic anhydride (5.0 eq, 5.6 g, 54.89 mmol) were added to a flame dried 50 mL round bottom flask. The flask was flushed with nitrogen and anhydrous pyridine (1.0 M, 11 mL) was added to the flask to give a clear solution. The solution was stirred until starting material was consumed by TLC (8 hr). The solution was concentrated *in vacuo*. The crude oil was dissolved in EtOAc (100 mL) and washed with 1 N HCl (20 mL), saturated aqueous NaHCO<sub>3</sub> (50 mL x2), then brine (50 mL). The organic layer was dried over Na<sub>2</sub>SO<sub>4</sub>, filtered, and concentrated *in vacuo*. The per-acetylated crude material was moved forward without further purification. The crude oil was dissolved in anhydrous CH<sub>2</sub>Cl<sub>2</sub> (0.1 M, 110mL) then flushed with N<sub>2</sub> before adding PhSH (1.5 eq, 1.7 mL, 16.47 mmol) then BF<sub>3</sub>·Et<sub>2</sub>O (3.0 eq, 4.1 mL, 32.94 mmol). The solution gradually turned pink and was stirred overnight. The solution was quenched with excess saturated aqueous NaHCO<sub>3</sub> and stirred vigorously until color disappeared (5-10 min). The organic layer was separated, and the aqueous layer extracted with CH<sub>2</sub>Cl<sub>2</sub> (30 mL). The organic layers were concentrated *in vacuo*, and the crude material was brought up in EtOAc (100 mL) and washed with saturated aqueous NaHCO<sub>3</sub> (50 mL) then brine (50 mL). The organic layer was dried over Na<sub>2</sub>SO<sub>4</sub>, filtered, and concentrated *in vacuo*. The residue was purified by flash column chromatography on silica gel (hexanes/EtOAc = 5.7/1 to 3/1) to afford an inseparable 3:1 α:β diastereomeric mixture of **3-69** (3.53 g, 9.22 mmol) in 84% yield over 2 steps as a white solid. Rf: 0.70 in 1:1 Hexane: EtOAc

**m.p.** 100-105 °C.

*Major diastereomer:*

**<sup>1</sup>H NMR** (500 MHz, CDCl<sub>3</sub>): δ 7.49 – 7.44 (m, 2H), 7.35 – 7.27 (m, 3H)(overlapping), 5.50 (dd,  $J = 3.4, 1.6$  Hz, 1H), 5.41 (d,  $J = 1.6$  Hz, 1H), 5.29 (dd,  $J = 10.1, 3.3$  Hz, 1H), 5.14 (t,  $J = 9.9$  Hz, 1H), 5.11 (t,  $J = 9.8$  Hz, 0H), 4.36 (dq,  $J = 9.7, 6.2$  Hz, 1H), 2.21 (s, 1H), 2.14 (s, 3H), 2.08 (s, 3H), 2.01 (s, 3H), 1.25 (d,  $J = 6.2$  Hz, 3H).

**<sup>13</sup>C{<sup>1</sup>H} NMR** (126 MHz, CDCl<sub>3</sub>): δ 170.2, 170.1, 170.1, 133.4, 132.0, 129.3, 128.0, 85.8, 71.5, 71.3, 69.5, 67.9, 21.1, 21.0, 20.8, 20.8, 17.5.

*Minor diastereomer:*

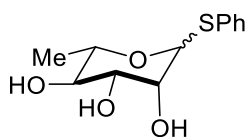
**<sup>1</sup>H NMR** (500 MHz, CDCl<sub>3</sub>): δ 7.52 – 7.49 (m, 2H), 7.35 – 7.27 (m, 3H)(overlapping), 5.65 (dd,  $J = 3.7, 1.2$  Hz, 1H), 5.11 (t,  $J = 9.8$  Hz, 1H) (overlapping), 5.01 (dd,  $J = 10.1, 3.5$  Hz, 1H), 4.90 (d,  $J = 1.4$  Hz, 1H), 3.55 (dq,  $J = 9.7, 6.2$  Hz, 1H), 2.21 (s, 3H), 2.05 (s, 3H), 1.98 (s, 3H), 1.32 (d,  $J = 6.1$  Hz, 3H).

**<sup>13</sup>C{<sup>1</sup>H} NMR** (126 MHz, CDCl<sub>3</sub>): δ 170.4, 170.3, 170.0, 133.5, 132.2, 129.3, 128.2, 85.6, 75.1, 72.0, 71.2, 70.4, 20.9, 20.8, 17.9.

**HRMS** (ESI-TOF): [M+Na]<sup>+</sup>  $m/z$ : calculated for C<sub>18</sub> H<sub>22</sub>O<sub>7</sub>SNa 405.0984; Found 405.0993

$[\alpha]_D^{25} = -68.4$  ( $c = 0.59$ , CHCl<sub>3</sub>).

**IR** (thin film): 2977, 1743, 1583 cm<sup>-1</sup>



**Compound 3-70:** Per-acetylated *L*-rhamnose thioglycoside **3-69** (1.17 g, 4.58 mmol) was added to a flame dried N<sub>2</sub> flushed 50 mL round bottom flask. The flask was charged with anhydrous methanol (0.2 M, 24 mL) until a clear solution was formed. A piece of Na (catalytic quantity) was cut and washed with hexane to remove kerosene then added to the solution. The solution was stirred until starting material was consumed by TLC (30 min) indicated by a color change from



clear to yellow. The reaction was quenched with glacial acetic acid then  $K_2CO_3$ . The solution was concentrated *in vacuo*. The white solid was dissolved in acetone (50 mL) and passed through a silica plug. The organic layer was concentrated *in vacuo* to afford an inseparable 3:1  $\alpha$ : $\beta$  diastereomeric mixture **3-70** (1.17 g, 4.40 mmol) in 96% yield as a white foam of with trace amounts of acetic acid. Rf: 0.58 in acetone

**m.p.** 39.0-43.7 °C

*Major diastereomer:*

$^1H$  NMR (500 MHz,  $CD_3OD$ ):  $\delta$  7.50 – 7.43 (m, 2H)(overlapping), 7.35 – 7.19 (m, 3H)(overlapping), 5.38 (d,  $J = 1.6$  Hz, 1H), 4.10 – 4.00 (m, 2H)(overlapping), 3.65 (dd,  $J = 9.4$ , 3.3 Hz, 1H), 3.50 – 3.42 (m, 1H)(overlapping), 1.27 (d,  $J = 6.2$  Hz, 3H).

$^{13}C\{^1H\}$  NMR (126 MHz,  $CD_3OD$ ):  $\delta$  136.0, 132.6, 130.1, 128.4, 90.2, 74.1, 73.9, 72.9, 71.0, 17.8.

*Minor diastereomer:*

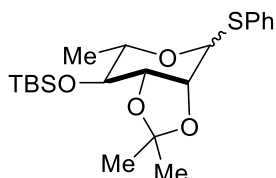
$^1H$  NMR (500 MHz,  $CD_3OD$ ):  $\delta$  7.50 – 7.43 (m, 2H)(overlapping), 7.35 – 7.19 (m, 3H)(overlapping), 4.95 (s, 1H), 4.10 – 4.00 (m, 2H)(overlapping), 3.50 – 3.42 (m, 1H)(overlapping), 3.38 (t,  $J = 9.2$  Hz, 1H), 1.33 (d,  $J = 6.1$  Hz, 3H).

$^{13}C\{^1H\}$  NMR (126 MHz,  $CD_3OD$ ):  $\delta$  137.2, 131.1, 129.9, 127.8, 88.5, 77.9, 75.9, 74.2, 73.6, 71.0, 18.2.

**HRMS** (ESI-TOF):  $[M+Na]^+$  m/z: calculated for  $C_{12}H_{16}O_4SNa$  279.0667; Found 279.0665

$[\alpha]_D^{25} = -206.6$  ( $c = 0.49$ ,  $CHCl_3$ ).

**IR** (thin film): 3371, 2975, 2932, 2870, 1584  $cm^{-1}$ .



**Compound 3-71:** Using a modification of the previously reported method<sup>3</sup>, **3-70** was converted to **3-71** as follows: Triol-*L*-rhamnose thioglycoside **3-70** (1.20 g, 4.71 mmol) and (1*S*)-(+)-10-camphorsulfonic acid (10 mol %, 122 mg, 0.52 mmol) were dissolved in anhydrous acetone in a flame dried, N<sub>2</sub> flushed 50 mL round bottom flask. 2,2-dimethoxypropane (10 eq, 8.0 mL, 65.20 mmol) was then added to the reaction and stirred until all starting material was consumed by TLC (45 min). The yellow reaction was diluted with CH<sub>2</sub>Cl<sub>2</sub> (150 mL) then washed with saturated aqueous NaHCO<sub>3</sub> then water. The clear organic layer was then dried over Na<sub>2</sub>SO<sub>4</sub> and concentrated *in vacuo*. The crude material was pushed forward without further purification. The flask containing the crude material was flushed with N<sub>2</sub> then charged with CH<sub>2</sub>Cl<sub>2</sub> (0.1 M, 47 mL). The flask was then charged with imidazole (1.5 eq, 481 mg, 7.07 mmol) then tert-butyldimethylsilyl chloride (1.2 eq, 852 mg, 5.66 mmol). The solution was warmed to 35°C and stirred overnight under a N<sub>2</sub> atmosphere. The reaction was concentrated *in vacuo* then brought up in EtOAc (100 mL) and washed with water and brine. The organic layer was then dried over Na<sub>2</sub>SO<sub>4</sub> and concentrated *in vacuo*. The residue was purified by flash column chromatography on silica gel (hexanes/EtOAc = 5.7/1) to afford an inseparable 3:1  $\alpha$ : $\beta$  diastereomeric mixture of **3-71** (1.80 g, 4.57 mmol) in 97% yield over 2 steps as a clear oil. Rf: 0.68 in 9:1 Hexane: EtOAc

*Major diastereomer:*

<sup>1</sup>H NMR (500 MHz, CDCl<sub>3</sub>):  $\delta$  7.44 – 7.34 (m, 2H)(overlapping), 7.23 – 7.13 (m, 3H)(overlapping), 5.63 (s, 1H), 4.23 (d,  $J$  = 5.6 Hz, 1H), 3.97 – 3.84 (m, 2H), 3.31 (dd,  $J$  = 9.6, 7.1 Hz, 1H), 3.19 (dq,  $J$  = 8.9, 6.2 Hz, 1H), 1.42 (s, 3H), 1.25 (s, 3H), 1.08 (d,  $J$  = 6.2 Hz, 3H), 0.85 – 0.76 (m, 9H) (overlapping), 0.05 (s, 3H), -0.01 (s, 3H).

<sup>13</sup>C{<sup>1</sup>H} NMR (126 MHz, CDCl<sub>3</sub>):  $\delta$  133.9, 131.9, 129.1, 128.5, 127.6, 109.3, 84.1, 79.0, 76.4, 67.8, 28.3, 26.7, 26.0, 25.8, 18.3, 17.8, -3.8, -4.7.

*Minor diastereomer:*

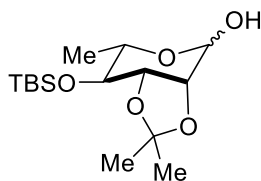
$^1\text{H NMR}$  (500 MHz,  $\text{CDCl}_3$ ):  $\delta$  7.44 – 7.34 (m, 2H)(overlapping), 7.23 – 7.13 (m, 3H)(overlapping), 4.94 (d,  $J = 2.1$  Hz, 1H), 4.30 (dd,  $J = 5.6, 2.2$  Hz, 1H), 3.43 – 3.36 (m, 1H), 1.49 (s, 3H), 1.30 (s, 3H), 1.22 (d,  $J = 6.2$  Hz, 3H), 0.85 – 0.76 (m, 9H)(overlapping), 0.05 (s, 3H), -0.00 (s, 3H).

$^{13}\text{C}\{^1\text{H}\}$  NMR (126 MHz,  $\text{CDCl}_3$ ):  $\delta$  135.6, 130.7, 129.1, 129.1, 127.3, 110.4, 84.1, 80.7, 76.6, 76.2, 75.4, 28.2, 26.6, 26.0, 18.6, 18.2, , -3.4, -3.9.

HRMS (ESI-TOF):  $[\text{M}+\text{Na}]^+$   $m/z$ : calculated for  $\text{C}_{21}\text{H}_{34}\text{O}_4\text{SSiNa}$  433.1845; Found 433.1834

$[\alpha]_{\text{D}}^{25} = -111.2$  ( $c = 0.64$ ,  $\text{CHCl}_3$ ).

IR (thin film): 2955, 2930, 2895, 2856  $\text{cm}^{-1}$ .



**Compound 3-72:** Protected thioglycoside **3-71** (1.46 g, 3.56 mmol) and  $\text{K}_2\text{CO}_3$  (5.0 eq, 2.50 g, 17.78 mmol) were dissolved in a 15:1 acetone: $\text{H}_2\text{O}$  solution (0.1 M, 36 mL). To the vigorously stirring solution, N-bromosuccinimide (1.5 eq, 949 mg, 5.33 mmol) was added in a single portion. The reaction was monitored by TLC until full consumption of starting material (30-60 min) and was quenched with saturated aqueous  $\text{NaHCO}_3$  (30 mL). The mixture was concentrated *in vacuo* until all acetone was removed then extracted with EtOAc (30 mL x3). The pooled organic layers were washed with brine then dried over  $\text{Na}_2\text{SO}_4$  and concentrated *in vacuo*. The residue was purified by flash column chromatography on silica gel (hexanes/EtOAc = 5.7/1) to afford an inseparable 2:1  $\alpha$ : $\beta$  diastereomeric mixture of **3-72** (959 mg, 3.04 mmol) in 86% yield as a white solid. Rf: 0.3 in 4:1 Hexane: EtOAc

**m.p.** 79-82 °C

*Major diastereomer:*

**<sup>1</sup>H NMR** (500 MHz, CDCl<sub>3</sub>): δ 5.31 (s, 1H), 4.16 (d, *J* = 6.0 Hz, 1H), 4.09 (td, *J* = 6.1, 2.7 Hz, 2H)(overlapping), 3.92 – 3.83 (m, 1H), 3.50 – 3.38 (m, 2H)(overlapping), 2.91 (d, *J* = 4.6 Hz, 1H), 1.52 (s, 3H), 1.35 (s, 3H), 1.25 (d, *J* = 6.4 Hz, 3H), 0.89 (s, 9H), 0.15 (s, 3H), 0.09 (s, 3H).

**<sup>13</sup>C{<sup>1</sup>H} NMR** (126 MHz, CDCl<sub>3</sub>): δ 109.3, 92.5, 78.3, 76.1, 75.0, 67.4, 28.0, 26.3, 26.0, 18.4, 18.2, -4.0, -4.8.

*Minor Diastereomer:*

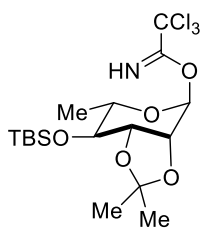
**<sup>1</sup>H NMR** (500 MHz, CDCl<sub>3</sub>): δ 4.98 (d, *J* = 9.8 Hz, 1H), 4.21 (dd, *J* = 6.1, 2.3 Hz, 1H), 3.92 – 3.83 (m, 1H), 3.55 (d, *J* = 11.6 Hz, 1H), 1.53 (s, 3H), 1.37 (s, 3H), 1.29 (d, *J* = 6.0 Hz, 3H), 0.88 (s, 9H), 0.12 (s, 3H), 0.08 (s, 3H).

**<sup>13</sup>C{<sup>1</sup>H} NMR** (126 MHz, CDCl<sub>3</sub>): δ 110.3, 92.4, 80.0, 75.0, 74.4, 73.3, 27.7, 26.5, 25.9, 18.8, 18.1, -4.1, -4.7.

**HRMS** (ESI-TOF): [M+Na]<sup>+</sup> *m/z*: calculated for C<sub>15</sub> H<sub>30</sub>O<sub>5</sub>SiNa 341.1760; Found 341.1748

[α]<sub>D</sub><sup>25</sup> = -2.8 (*c* = 0.15, CHCl<sub>3</sub>).

**IR** (thin film): 3429, 2986, 2955, 2931, 2903, 2857 cm<sup>-1</sup>



**Compound 3-73:** **3-72** (969 mg, 3.04 mmol) and trichloroacetonitrile (12.0 eq, 3.66 mL, 36.51 mmol) were dissolved in anhydrous CH<sub>2</sub>Cl<sub>2</sub> (0.1 M, 30 mL) in a flame dried, N<sub>2</sub> flushed 100 mL round bottom flask. To the vigorously stirring solution, 1,8-diazabicyclo[5.4.0]undec-7-ene (0.3 eq, 136 μL, 0.91 mmol) was added in a single portion. The reaction was monitor by TLC until

full consumption of starting material (30min) as indicated by a gradual color change from clear to dark red. The reaction was concentrated *in vacuo* and immediately purified by flash column chromatography on silica gel (hexanes/Et<sub>3</sub>N = 49/1) to afford **3-73** (1.28 g, 2.77 mmol) as a single diastereomer in 91% yield as a white solid. Rf: 0.51 in 9:1 Hexane: EtOAc

**m.p.** 98-101 °C

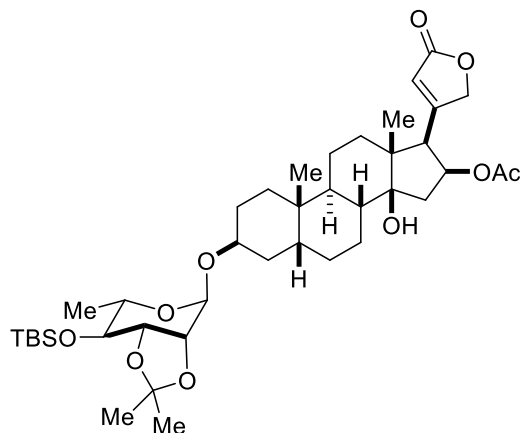
**<sup>1</sup>H NMR** (500 MHz, C<sub>6</sub>D<sub>6</sub>): δ 8.53 (s, 1H), 6.85 (s, 1H), 4.29 (d, *J* = 5.8 Hz, 1H), 4.15 (dd, *J* = 7.2, 5.8 Hz, 1H), 4.03 (dq, *J* = 9.9, 6.3 Hz, 1H), 3.57 (dd, *J* = 9.7, 7.2 Hz, 1H), 1.43 (s, 3H), 1.33 (d, *J* = 6.2 Hz, 3H), 1.15 (s, 3H), 0.99 (s, 8H), 0.28 (s, 3H), 0.12 (s, 3H).

**<sup>13</sup>C{<sup>1</sup>H} NMR** (126 MHz, C<sub>6</sub>D<sub>6</sub>): δ 160.4, 109.6, 96.2, 79.3, 76.3, 75.5, 69.5, 28.2, 26.3, 26.2, 18.4, 18.0, -3.7, -4.7.

**HRMS** (ESI-TOF): [M-CONHCCl<sub>3</sub>]<sup>+</sup> *m/z*: calculated for C<sub>15</sub>H<sub>29</sub>O<sub>4</sub>Si<sup>+</sup> 301.1830; Found 301.1823

[α]<sub>D</sub><sup>25</sup> = -28.7 (*c* = 0.54, CHCl<sub>3</sub>).

**IR** (thin film): 3348, 2986, 2955, 2934, 2902, 2857, 1671 cm<sup>-1</sup>



**Compound 3-76:** **3-2** (13.2 mg, 0.03 mmol) was added to a oven-dried 1 dram vial and transferred to a glovebox, where Pd(ACN)<sub>4</sub>(BF<sub>4</sub>)<sub>2</sub> (1.4 mg, 0.003 mmol, 0.1 equiv.), was added. Then, the vial was removed from the glovebox and flame-dried 4 Å M.S. (30 mg) was added to the reaction vial and then flushed with N<sub>2</sub> for 15 min. Subsequently, the reaction mixture was dissolved in DCM

and chilled to  $-78\text{ }^{\circ}\text{C}$ . **7** was dissolved in anhydrous DCM (1.3 g/10 mL = 0.28 M) in a separate flame-dried 1 dram vial and 1 equiv. of donor **3-75** was added to the reaction vial, and an additional 0.5 eq of **3-75** was added every 45 min until 3.0 equiv. was added in total. The resulting mixture was stirred for an additional 1 h at  $-78\text{ }^{\circ}\text{C}$ . Subsequently, the reaction was diluted with benzene (1 mL) and filtered through celite, concentrated *in vacuo* and then purified by silica gel chromatography (5% EA/Hexanes to 20% EA/Hexanes) to yield **3-76** (17 mg, 0.023 mmol, 76%) as a clear semi-solid oil. Rf: 0.59, 20% EA/Hexanes.

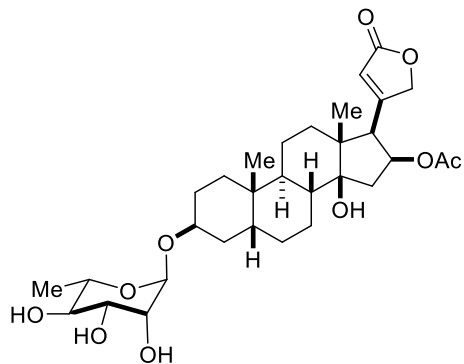
**$^1\text{H}$  NMR** (700 MHz,  $\text{CDCl}_3$ )  $\delta$  5.97 (d,  $J = 1.9$  Hz, 1H), 5.48 (td,  $J = 9.2, 2.6$  Hz, 1H), 5.02 (s, 1H), 4.98 (dd,  $J = 18.1, 1.9$  Hz, 1H), 4.85 (dd,  $J = 18.0, 1.8$  Hz, 1H), 4.08 (d,  $J = 5.7$  Hz, 1H), 4.00 (t,  $J = 6.4$  Hz, 1H), 3.97 (d,  $J = 3.2$  Hz, 1H), 3.60 (dq,  $J = 9.7, 6.3$  Hz, 1H), 3.32 (dd,  $J = 9.7, 7.1$  Hz, 1H), 3.19 (d,  $J = 8.7$  Hz, 1H), 2.73 (dd,  $J = 15.7, 9.6$  Hz, 1H), 1.97 (s, 3H), 1.86 (ddt,  $J = 13.9, 9.6, 4.3$  Hz, 1H), 1.77 (dd,  $J = 15.8, 2.6$  Hz, 1H), 1.71 (dd,  $J = 13.1, 3.0$  Hz, 2H), 1.68–1.66 (m, 2H), 1.60–1.53 (m, 4H), 1.52 (s, 3H), 1.50–1.47 (m, 1H), 1.44 (dd,  $J = 14.1, 3.7$  Hz, 2H), 1.38 (s, 1H), 1.36 (s, 3H), 1.31 (dd,  $J = 13.0, 3.8$  Hz, 1H), 1.27–1.24 (s, 8H), 1.19 (d,  $J = 6.2$  Hz, 4H), 0.94 (s, 3H), 0.93 (s, 3H), 0.90 (s, 9H), 0.15 (s, 3H), 0.09 (s, 3H).

**$^{13}\text{C}$  NMR** (176 MHz,  $\text{CDCl}_3$ )  $\delta$  174.0, 170.4, 167.6, 121.4, 108.8, 94.8, 84.3, 79.2, 76.1, 75.6, 73.9, 70.9, 65.9, 56.1, 49.9, 41.8, 41.2, 39.2, 36.3, 35.6, 35.1, 30.3, 29.7, 29.1, 28.2, 26.5, 26.4, 26.4, 25.9, 23.7, 21.0, 21.0, 20.8, 18.1, 17.7, 15.9,  $-4.0$ ,  $-4.8$ .

**HRMS** (ESI):  $[\text{M}+\text{H}]^+$  calcd for  $\text{C}_{40}\text{H}_{64}\text{O}_{10}\text{Si}$ ; 733.4341 found 733.4339.

$[\alpha]_{\text{D}}^{25} -8.905$  ( $c = 0.35$ ,  $\text{CH}_2\text{Cl}_2$ ).

**IR** (film,  $\text{cm}^{-1}$ ) 3494, 2928, 2856, 1777, 1620, 1245, 1079.



**Rhodexin B (3-3): 3-76** (7.0 mg, 9.55  $\mu\text{mol}$ ) was dissolved in methanol (0.5 mL) and 1N HCl in MeOH (100  $\mu\text{L}$ ) was added to the reaction vial dropwise. The reaction mixture was stirred at room temperature for 2 h. Then, solid  $\text{NaHCO}_3$  was added until  $\text{pH}=7$ , filtered through celite, adsorb on silica and purified by column chromatography ( $\text{CH}_2\text{Cl}_2$ : MeOH = 1:0 to 10:1 to 5:1) to afford rhodexin B (**3-3**) in 87% yield (4.8 mg, 8.3  $\mu\text{mol}$ ) as a white film,  $R_f = 0.45$  (10% MeOH in  $\text{CH}_2\text{Cl}_2$ ).

**m.p.** 238-240  $^\circ\text{C}$  (decomposition), **Reported m.p.:** 242-244  $^\circ\text{C}$ .

**$^1\text{H NMR}$**  (500 MHz,  $\text{CD}_3\text{OD}$ )  $\delta$  6.00 (s, 1H), 5.50 (td,  $J = 9.2, 2.4$  Hz, 1H), 5.04 (dd,  $J = 18.5, 1.9$  Hz, 1H), 4.97 (dd,  $J = 18.5, 1.8$  Hz, 1H), 4.79 (d,  $J = 1.8$  Hz, 1H), 3.98 (t,  $J = 2.8$  Hz, 1H), 3.78 (dd,  $J = 3.4, 1.7$  Hz, 1H), 3.70 (td,  $J = 9.8, 3.3$  Hz, 2H), 3.66 (d,  $J = 2.9$  Hz, 1H), 3.39 (t,  $J = 9.5$  Hz, 1H), 3.29 (d,  $J = 8.7$  Hz, 1H), 2.81 (dd,  $J = 15.6, 9.6$  Hz, 1H), 1.96 (s, 3H), 1.93 (d,  $J = 4.9$  Hz, 1H), 1.89 (d,  $J = 2.5$  Hz, 1H), 1.85 (m, 1H), 1.81 (m, 1H), 1.73 (dd,  $J = 12.0, 3.0$  Hz, 1H), 1.68 (dd,  $J = 13.6, 3.5$  Hz, 2H), 1.63 (dd,  $J = 11.6, 3.3$  Hz, 1H), 1.60–1.54 (m, 2H), 1.51-1.48 (br, s, 1H), 1.47 (br, s, 1H), 1.44 (br, s, 1H), 1.29 (m, 4H), 1.27 (s, 2H), 1.25 (s, 2H), 1.23–1.19 (m, 1H), 1.21 (m, 1H), 0.98 (s, 3H), 0.96 (s, 3H).

**$^{13}\text{C NMR}$**  (126 MHz,  $\text{CD}_3\text{OD}$ )  $\delta$  176.7, 172.1, 171.6, 121.7, 99.9, 85.0, 77.6, 76.0, 74.1, 73.6, 73.0, 72.5, 70.0, 57.4, 51.4, 42.7, 41.4, 40.0, 38.1, 36.7, 36.3, 31.6, 30.8, 27.8, 27.5, 24.3, 22.2, 22.0, 20.9, 18.0, 16.4.





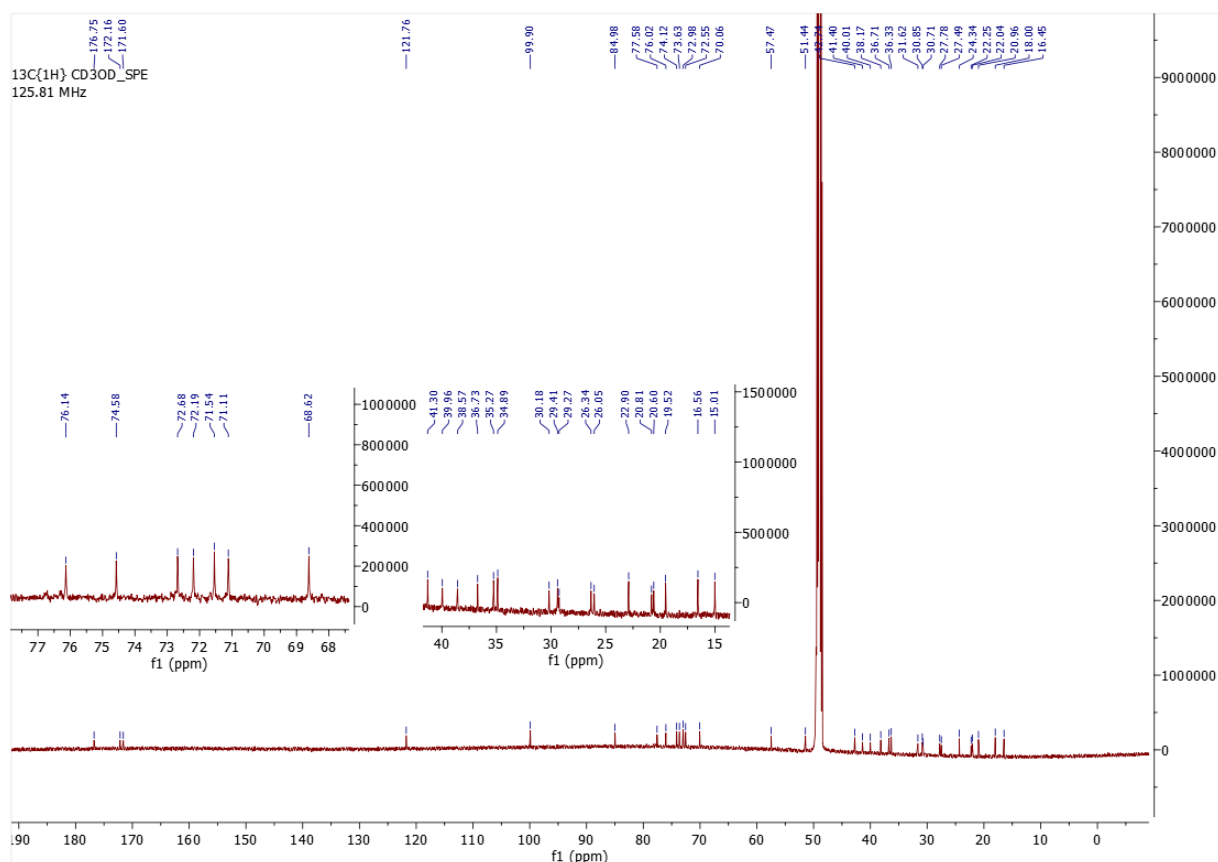


**Figure 3.33.**  $^{13}\text{C}$  NMR spectrum corresponding to rhodexin B (**3-3**).

Pan et. al. <sup>9</sup>	Synthetic ( <b>3-3</b> )
5.98 (s)	6.00 (s, 1H)
5.46 (m)	5.50 (td, $J = 9.2, 2.4$ Hz, 1H)
5.02 (dd, $J = 13.5$ Hz, $J = 1.5$ Hz)	5.04 (dd, $J = 18.5, 1.9$ Hz, 1H)
4.96 (dd, $J = 13.5$ Hz, $J = 1.5$ Hz)	4.97 (dd, $J = 18.5, 1.8$ Hz, 1H)
4.77 (d, $J = 1.0$ Hz)	4.79 (d, $J = 1.8$ Hz, 1H)
3.95 (br, s)	3.98 (t, $J = 2.8$ Hz, 1H)
3.75 (br, s)	3.78 (dd, $J = 3.4, 1.7$ Hz, 1H)
3.68 (m)	3.70 (td, $J = 9.8$ Hz, $3.3$ Hz, 2H)

3.65 (m)	3.66 (d, $J = 2.9$ Hz, 1H)
3.36 (t, $J = 11.5$ Hz, $J = 9.5$ Hz)	3.39 (t, $J = 9.5$ Hz, 1H)
3.27 (d, $J = 8.5$ Hz)	3.29 (d, $J = 8.7$ Hz, 1H)
2.78 (m)	2.81 (dd, $J = 15.6, 9.6$ Hz, 1H)
1.93 (s)	1.96 (s, 3H)
1.90 (m)	1.93 (d, $J = 4.9$ Hz, 1H)
1.84 (m)	1.89 (d, $J = 2.5$ Hz, 1H)
1.80 (m)	1.85 (m, 1H)
1.79 (m)	1.81 (m, 1H)
1.71 (m)	1.73 (dd, $J = 12.0, 3.0$ Hz, 1H)
1.66 (m)	1.68 (dd, $J = 13.6, 3.5$ Hz, 2H)
1.62 (m)	1.63 (dd, $J = 11.6, 3.3$ Hz, 1H)
1.61 (m)	1.60–1.54 (m, 2H)
1.54 (m)	--
1.52 (m)	1.51-1.48 (br, s, 1H)
1.46 (m)	1.47 (br, s, 1H)
1.44 (m)	1.44 (br, s, 1H)
1.42 (m)	--
--	1.29 (m, 4H)
1.26 (m)	1.27 (s, 2H)
1.24 (m)	1.25 (s, 2H)
1.23 (t, $J = 6.5$ Hz)	1.23–1.19 (m, 1H)
1.19 (m)	1.21 (m, 1H)

0.94 (s)	0.98 (s, 3H)
0.92 (s)	0.96 (s, 3H)

---

**Table 3.5.**  $^1\text{H}$  NMR ( $\text{CD}_3\text{OD}$ ) comparison of isolated (left) vs. synthetic (right) rhodexin B (i.e. tupichinolide) with reported data from the literature.

Pan et. al. <sup>9</sup>	Synthetic ( <b>3-3</b> )
176.7	<b>176.7</b>
172.1	<b>172.1</b>
171.6	<b>171.6</b>
121.7	<b>121.7</b>
99.8	<b>99.9</b>
84.6	<b>85.0</b>
77.5	<b>77.6</b>
75.9	<b>76.0</b>
74	<b>74.1</b>
73.5	<b>73.6</b>
72.9	<b>73.0</b>
72.5	<b>72.5</b>
70	<b>70.0</b>
57.4	<b>57.4</b>
51.4	<b>51.4</b>
42.7	<b>42.7</b>

41.3	<b>41.4</b>
39.9	<b>40.0</b>
38.1	<b>38.1</b>
36.6	<b>36.7</b>
36.2	<b>36.3</b>
31.5	<b>31.6</b>
30.8	<b>30.8</b>
27.7	<b>27.8</b>
27.4	<b>27.5</b>
24.3	<b>24.3</b>
22.2	<b>22.2</b>
22	<b>22.0</b>
20.9	<b>20.9</b>
17.9	<b>18.0</b>
16.4	<b>16.4</b>

---

**Table 3.6.**  $^{13}\text{C}$  NMR ( $\text{CD}_3\text{OD}$ ) comparison of isolated (left) vs. synthetic (right) rhodexin B (i.e. tupichinolide) with reported data from the literature.

### 3.7 References

- (1) (a) Neshar M.; Shpolansky U.; Rosen H.; Lichstein D., *Life Sci.* **2007** *80* 2093; (b) Bagrov A. Y.; Shapiro J. I.; Fedorova O. V.; *Pharm. Rev.* **2009** *61* 9 .
- (2) (a) Babula P. Masarik M. Adam V. Provaznik I. Kizek R. F; *Agents Med. Chem.* **2013** *13* 1069 1087; (b) Cerella , C.; ; Simoes , C. M. O.; ;Diederich , M. *Molecules* **2017** , *22* , 1932 .
- (3) (a) Cai H. Wang H.-Y. L. Venkatadri R. Fu D.-X. Forman M. Bajaj S. O. Li H. O’Doherty, O Doherty G. A. Aravboger R. *ACS Med. Chem. Lett.* **2014** *5* 395-399; Stoilov , F; P. ; Lingwood, C. ; Brown , M. ; Cochrane , A.;. *J. Virol.* **2017** , *91*.
- (4) Jacob P. L.; Leite J. A.; Alves A. K.; Rodrigues Y. K.; Amorim F. M.; Neris P. L.; Oliveira M. R.; Rodrigues-Mascarenhas S.; *Prasitol. Res.* **2013** *112* 1313.
- (5) (a) Orellana , A. M. ; Kinoshita , P. F. ; Leite , J. A. ; Kawamoto , M. ; Scavone , C.. *Front. Endocrinol.* **2016** , *7* , 1 10 (b) Cavalcante-Silva , L. H. A. ; de Almeida Lima , E. A. ; Carvalho , D. C. M. ; de Sales- Neto, J. M.; de Sales-Neto, de Abreu Alves , A. K. ; GalvaoGalvão , J. G. F. M. ; de FrancaFrança da SilvaSilv , J. S. ; Rodrigues-Mascarenhas , S. *Front. Physiol.* **2017** , *8* , 859-895.
- (6) (a) Plante K. S.; Dwivedi V.; Plante J. A.; Fernandez D.; Mirchandani D.; Bopp N.; Aguilar P.; V. Park J.-G.; Tamayo P. P.; Delgado J. Shivanna V. Torrelles J. B. Martinez-Sobrido L. Matos R. Weaver S. C. Sastry K. J. Newman R. *Biomed. Pharmacother.* **2021** *138* 111457. (b) Newman R. A. Sastry K. J. Avrav-Boger R. Cai H. Matos R. Harrod R. *J. Exp. Pharmacol.* **2020** *12* 503. (c) Kumar A. De T. Mishra A. Mishra A. K. *Pharmacogn. Rev.* **2016** *10* 147.; (d) Kanwal N.; Rasul A.; Hussain G.; Anwar H.; Shah M. A.; Sarfraz I.; Riaz A. ;Batoool R.; Shanbaz M.; Hussain A.; Selamoglu Z. *Food Chem. Toxicol.* **2020** *143* 111570; (e) Yang P.; Menter D. G.; Cartwright C.; Chan D.; Dixon S.; Suraokar M.; Mendoza G.; Llansa N.; Newman R. A. *Mol. Cancer Ther.* **2009** *8* 2319.
- (7) (a) Pathak S.; Multani A. S.; Narayan S.; Kumar V.; Newman R. A., *Anticancer Drugs* **2000** *11* 455; (b) Mekhail T.; Kaur H.; Ganapathi R.; Budd T. G.; Elson P.; Bukowski R. M.; *Invest New Drugs* **2006** *24* 423.
- (8) (a) Dunn D. E.; He D. N.; Yang P.; Johansen M.; Newman R. A.; Lo D. C., *J. Neurochem.* **2011** *119*; (b) Plante , K. S.; Dwivedi , V.; Plante , J. A.; Fernandez , D.; Mirchandani , D.; Bopp , N.; Aguilar , P. V. ; Park , J.-G. ; Tamayo , P. P. ; Delgado , J. ; Shivanna , V. ; Torrelles , J. B. ; Martinez-Sobrido , L. ; Matos , R. ; Weaver , S. C. ; Sastry , K. J. ; Newman , R. A. *Biomed. Pharmacother.* **2021** , *138* , 111457.
- (9) Pan, Z.-H.; Li, Y.; Liu, J.-L.; Ning, D.-S.; Li, D.-P.; Wu, X.-D.; Wen, Y.-X. *Fitoterapia* **2012**, *83*, 1489.
- (10) (a) Doskotch, R. W.; Mailk, Y. M.; Hufford, C. D.; Malik, S. N.; Trent, J. E.; Kubelka, W. R. *J. Pharm. Sci.* **1972**, *61*, 570. (b) Jung, J.-W.; Baek, N.-I.; Hwang-Bo, J.; Lee, S.-S.; Park, J.

- Seo, K.-H.; Kwon, J.-H.; Oh, E.-J.; Lee, D.-Y.; Chung, I.-S.; Bang, M.- H. *Molecules* **2015**, *20*, 20823
- (11) (a) Heasley, B. *Chem. - Eur. J.* **2012**, *18*, 3092. (b) Michalak, M.; Michalak, K.; Wicha, J. *Nat. Prod. Rep.* **2017**, *34*, 361. (c) Khatri, H. R.; Carney, N.; Rutkoski, R.; Bhattarai, B.; Nagorny, P. *Eur. J. Org. Chem.* **2020**, *21*, 755
- (12) (a) Zhang, H.; Reddy, M. S.; Phoenix, S.; Deslongchamps, P. *Angew. Chem., Int. Ed.* **2008**, *47*, 1272. (b) Reddy, M. S.; Zhang, H.; Phoenix, S.; Deslongchamps, P. *Chem.- Asian J.* **2009**, *4*, 725. (c) Renata, H.; Zhou, Q.; Baran, P. S. *Science* **2013**, *339*, 59. (d) Renata, H.; Zhou, Q.; Dunstl, G.; Felding, J.; Merchant, R. R.; Yeh, C.-H.; Baran, P. S. *J. Am. Chem. Soc.* **2015**, *137*, 1330. (e) Mukai, K.; Urabe, D.; Kasuya, S.; Aoki, N.; Inoue, M. *Angew. Chem., Int. Ed.* **2013**, *52*, 5300– 5304. (f) Mukai, K.; Kasuya, S.; Nakagawa, Y.; Urabe, D.; Inoue, M. *Chem. Sci.* **2015**, *6*, 3383.
- (13) Michalak, K.; Morawiak, M.; Wicha, J. *Org. Lett.* **2016**, *18*, 6148. (b) Michalak, K.; Rarova, L.; Kubala, M.; Cechova, P.; Strnad, M.; Wicha, J. *Eur. J. Med. Chem.* **2019**, *180*, 417. (c) Michalak, K.; Rarova, L.; Kubala, M.; Stenclova, T.; Strnad, M.; Wicha, J. *Eur. J. Med. Chem.* **2020**, *202*, 112520.
- (14) a) Kaplan, W.; Khatri, H. R.; Nagorny. *J. Am. Chem. Soc.* **2016**, *138*, 7194. Khatri, H. R.; Bhattarai, B.; Kaplan, W.; Li, Z.; Curtis Long, M. J.; Aye, Y.; Nagorny, P. *J. Am. Chem. Soc.* **2019**, *141*, 4849.
- (15) Fernández-Mateos, A.; Pascual, C. G.; Rubio, G. R.. *Tetrahedron*, **2005**, *61*, 8699.
- (16) Shimizu, S.; Hagiwara, K.; Itoh, H.; Inoue, M., *Org. Lett.* **2020**, *22*, 8652.
- (17) Ishii, K.; Hashimoto, T.; Dan, G.; Sakamoto, M.; Taira, Z.; Asakawa, Y. *Chem. Lett.* **1990**, 501.
- (18) Mukaiyama, T.; Yamada, T.. *Bull. Chem. Soc. Jpn.* **1995**, *68*, 17.
- (19) Bhattarai, B.; Nagorny, *Org. Lett.* 2018, *20*, 154.
- (20) (a) Reese, C. B.; Stewart, J. C. M.. *Tetrahedron Lett.* **1968**, *9*, 4273. (b) Hanamoto, T.; Sugimoto, Y.; Yokoyama, Y.; Inanaga, J. *J. Org. Chem.* **1996**, *61*, 4491.
- (21) Yang, J.; Cooper-Vanosdell, C.; Mensah, E. A.; Nguyen, H. M. *J. Org. Chem.* **2008**, *73*, 794

## Chapter 4

### Site-Selective Glycoside Cleavage

#### 4.1 Introduction

Non-enzymatic hydrolysis of alkyl glycopyranosides is a very well-studied reaction with a well-established mechanism.<sup>1</sup> The process is specific-acid-catalyzed where the rate determining step is the formation of a cyclic oxocarbenium ion intermediate. The rate constants of this reaction are an expression of the energy difference between the neutral reactant state and the transition state leading to this oxocarbenium ion. The mechanism now accepted was first suggested by Edward.<sup>2</sup> For example, with methyl O-D-glucopyranoside (**4-1**), it involves a rapid, equilibrium-controlled protonation of the glycosidic oxygen to give the corresponding conjugate acid (**4-2**). In the slow, rate-determining step, the acid decomposes in a unimolecular heterolysis with formation of an alcohol and a carbonium-oxonium ion (**4-3**), which is most likely present in a half-chair conformation. Finally, water is rapidly added, giving glycoside (**4-4**) and a hydronium ion.

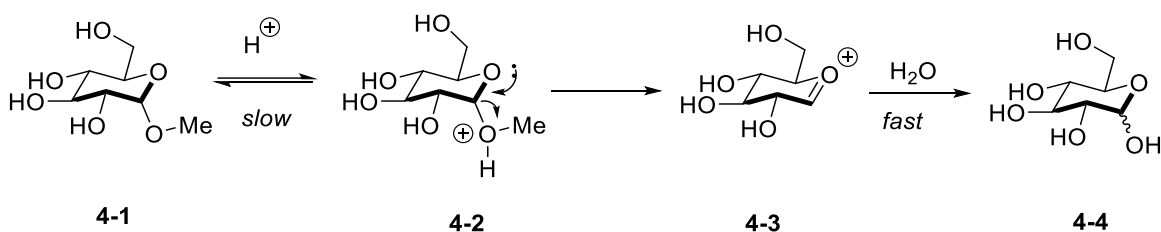


**Figure 4.1.** Classic mechanism for glycoside hydrolysis

This classic article by Edward<sup>2</sup> is mainly known for the observation of pyranosides with axial anomeric substituents supposedly being more stable than their equatorial counterparts was given

the name, anomeric effect, also known as the Edward-Lemieux effect<sup>2,3,4</sup> It can also be generalized to any cyclohexyl or linear system with the general formula C-Y-C-X, where Y is a heteroatom with one or more lone pairs, and X is an electronegative atom or group.

Edward's rationale for the varying reactivity of different glycosides had to do with steric strain with axial substituents allowing for easier rotation which better facilitates a more flattened half-chair conformation<sup>2</sup>. Many groups since then have deduced that in fact, steric effects only play a small role<sup>5,6</sup>. Electronic field effects induce a more significant effect on the rate of hydrolysis where hydroxyl group replacement with a fluorine for example, reduces reactivity and deoxygenation enhances reactivity through destabilization of the oxocarbenium ion transition state.<sup>5</sup> Bols<sup>7</sup> describes a major difference with whether the electron-deficient functionalities were placed either axially or equatorially. Bols<sup>8</sup> further disproved Edward's hypothesis with a more rigorous experimental study to conclude that deoxygenation of the 4-position of a sugar had a stronger effect than if the substituent was either axial or equatorial.

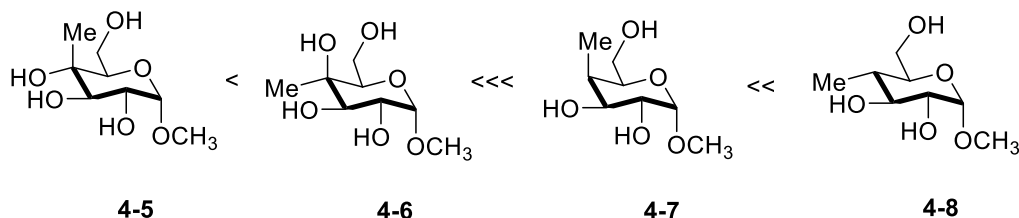


**Figure 4.2.** Bols<sup>8</sup> findings for understanding substituent effects for glycoside hydrolysis reactivity.

Typically, glycosidic cleavage is carried out in aqueous conditions, which can constrain how hydrolysis methods can be adjusted for improving selectivity of glycosidic cleavage for anomeric-specific targets. In aqueous solution, the environment is limited to the strength of the acid and how many hydronium ions exist in solution at any one time, which limits the selection of mineral acids to be either hydrochloric acid (HCl) or sulfuric acid (H<sub>2</sub>SO<sub>4</sub>). These acids are the most beneficial



to achieve a pH environment of around 2-3. Most glycosylation procedures also require elevated temperatures (60-75+ °C) along with extensive reaction times.<sup>9</sup> All of these limitations make it difficult to limit side reactions or cause the formation of elimination side products which can limit the event of rare sugar harvesting.<sup>10,11</sup>

Organic acids, like BINOL-derived acids, can be modulated to have different pK<sub>a</sub> levels, just with simple substitutions. They are similar to mineral acids in regard to the hydronium ion produced for hydrolysis in aqueous solution. However, if the glycoside acid cleavage was conducted in organic solvent, the pK<sub>a</sub> could be modified significantly and could be adjusted based on the solvent of choice. Of course, in order to stabilize the oxocarbenium intermediate necessary to carry out the hydrolysis reaction, the solvent needs to be able to support the reactive intermediate.<sup>12, 13</sup> For example, in acetonitrile (MeCN), HCl has a pK<sub>a</sub> of 10.6, and sulfuric acid, has a pK<sub>a</sub> of 8.7, respectively. Whereas triflic acid (TfOH) is -14 in water, but 0.7 in MeCN.

Our group has had a long-standing interest in the development of more economical, robust, simple, and efficient protocols for selective chemical glycosylations of natural products. In line with this, sometimes natural product sources can contain “rare-sugar” moieties that can either be difficult to synthesize or are polysaccharides that could be streamlined from chemical feedstocks through site-selective cleavage. From this, we sought to commence investigations into developing a simple, mild method for using organic solvents to conduct mild glycoside hydrolysis.

#### **4.2 Research Aim: Site-selective deglycosylation**

Many natural products (i.e. erythromycins, cardiotonic steroids) can contain more than one sugar moiety, which makes selective cleavage of a glycosidic linkage in the presence of others, leads to an interesting potential that may provide valuable intermediates for the subsequent SAR or medicinal chemistry studies. While this is sometimes achieved by acidic hydrolysis of weaker

linkages,<sup>14,15</sup> such transformations still cannot out compete enzymes in terms of selectivity and generality. To the best of our knowledge, no chiral catalyst-controlled site-selective deglycosylation reactions have been reported to date. However, we believe that these transformations could be accomplished with strong chiral Brønsted acids as the catalysts.

Our preliminary studies conducted by previous members of the Nagorny lab, Jeongyho Lee and Jeremy O'Brien, indicate that arylated disulfonimides are sufficiently strong Brønsted acids (similar to HBr in strength)<sup>15,16,17</sup> and can promote the cleavage of glycosidic linkages. In aprotic solvents may promote deglycosylation or transglycosylation reactions (Figure 4.3). The selective cleavage of epimeric alcohol glycosides was observed ( $S = 2.7$ ).

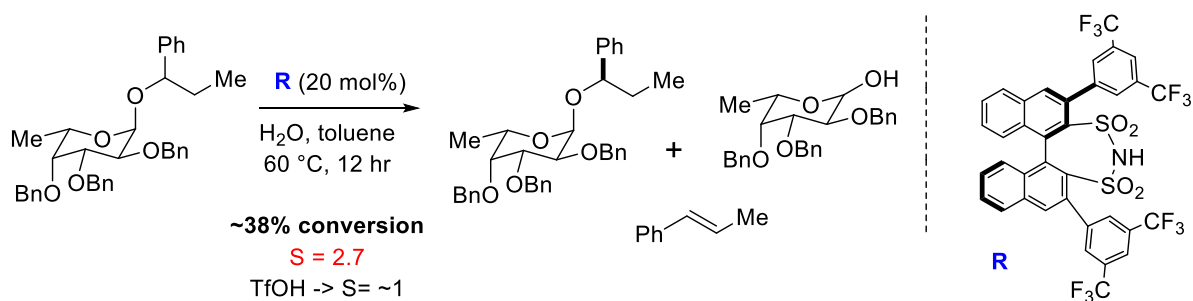


**Figure 4.3.** Previous preliminary results for mimicking glycosylases. (by Jeongyho Lee and Jeremy O'Brien).

With these promising findings for anomeric site-selective reactions, the next objective was to find more mild conditions that would lead to glycoside cleavage and to investigate the relative stabilities of glycosides towards the cleavage with different nucleophiles other than water with relative rates of the hydrolysis. Instead, the systems investigated anhydrous organic solvents (acetonitrile, etc.) to allow us to potentially accelerate the reactions by using superacids stronger than TfOH (Figure 4.4)

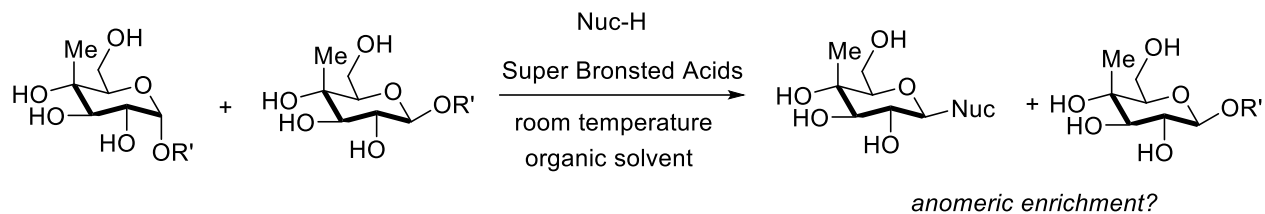


**Figure 4.4.** Proposal for potential anomeric enrichment of glycosides in organic solvents

### 4.3 Superacid reactions in literature

The term "superacid" was first used in 1927 when James Bryant Conant found that perchloric acid could protonate ketones and aldehydes to form salts in nonaqueous solution.<sup>18</sup> The magic acid system was developed in the 1960s by George Olah and was to be used to study stable carbocations. Lebedel<sup>19</sup> used NMR analysis to understand the ion effects of superacids to create a platform for exploring glycosyl cations. They used their strategy to explore the effects of deoxygenation and halogen substitution at the C2 position in a series of 2-halogenoglycosyl, galactosyl, and mannosyl donors. They were able to characterize these cationic intermediates by using low temperature *in situ* NMR experiments supported by DFT calculations. Lebedel et. al.<sup>19</sup> took inspiration from the work from Olah and Prakash, who unlocked large areas of carbocation chemistry exploiting nonnucleophilic superacid conditions<sup>18</sup> In their studies, Lebedel<sup>19</sup> used a superacidic medium of HF/SbF<sub>5</sub> as both a reagent and solvent and found that the oxocarbenium ions are quenched by the weakly coordinating SbF<sub>6</sub> anions. recently generated and characterized glycosyl cations in a condensed phase<sup>20</sup> This proof-of-concept study has been limited to glycosyl cations bearing only equatorial substituents. They recently published a general strategy for the direct characterization of glycosyl cations, the impact of halogens at C2 on the superacid-mediated transient and key glycosyl, galactosyl, and mannosyl cation formation, structure, and stability.

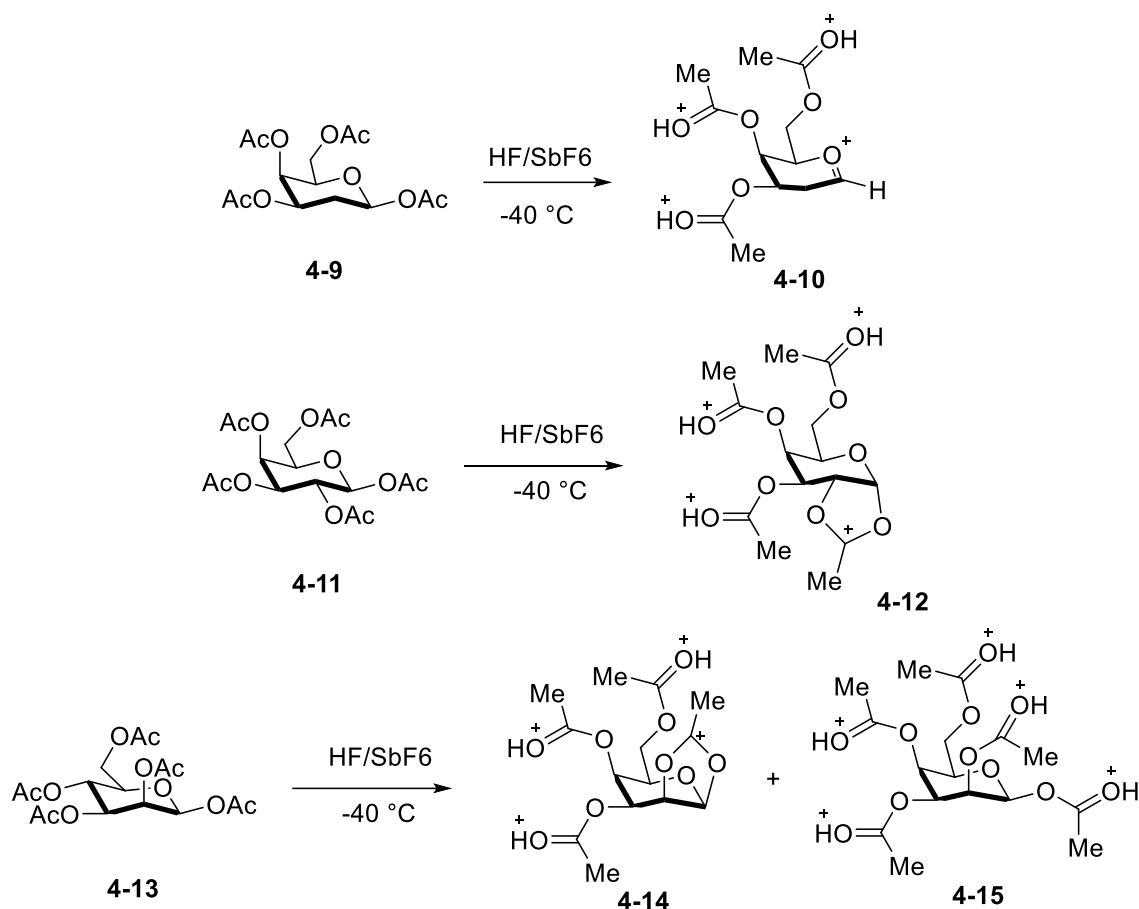


**Figure 4.5.** Observed NMR intermediates for glycosyl donors in superacid medium.

Some select examples were taken from their publication for showcasing C2 glycosylated derivatives. For comparison, the 2-deoxygalactopyranosyl donor **4-9** was first studied to evaluate the effect of an axial electron-withdrawing substituent at C4, which has shown through-space stabilization of the transient glycosyl cation.<sup>21</sup> The 2-deoxygalactopyranosyl donor **4-9** was submitted to HF/SbF<sub>5</sub> conditions and cleanly furnished a polycationic species. Detailed NMR analysis of this species was in excellent agreement with the 2-deoxy-galactopyranosyl cation **4-10**, and the quality of the recorded NMR spectra allowed complete analysis of the homonuclear NMR coupling constants. The three substituents adopted a pseudoequatorial orientation to minimize charge repulsion. The acetate at C4 remains axial, the 2-OAc group was participating to

give the dioxalenium ion **4-12** when studying peracetylated D-galactosyl donor **4-11**, potential participation of the 4-OAc of **4-9** was not observed. This led them to postulate that instantaneous protonation of this ester in the superacid was precluding its anchimeric assistance, unlike with the 2-OAc in the galactosyl donor **4-11**. The peracetylated- $\beta$ -D-mannopyranose **4-13** was treated with HF/SbF<sub>5</sub>, and it was found that the mannoopyranose **4-13** furnished a mixture of the expected dioxalenium ion **4-14**, observed as a distorted 4C1 conformer, along with some unreacted mannosyl donor in its polyprotonated form **4-15**, emphasizing the singular reactivity of this isomeric sugar.

#### **4.4 Initial studies with pseudo-disaccharides**

To begin our studies for developing milder deglycosylation conditions, model saccharide substrates were synthesized from commonly used sugars, glucose, mannose and galactose.

The glucose model began from commercially available peracetylated- $\beta$ -D-glucose **4-16** was transformed into thioglycoside **4-17** in 87% yield. From there, **4-17** was transformed into **4-18** and subsequently transformed in **4-19** and after column chromatography, an enriched mixture of glucose anomers was recovered in 54% yield and a 9:1  $\beta$ : $\alpha$  ratio.

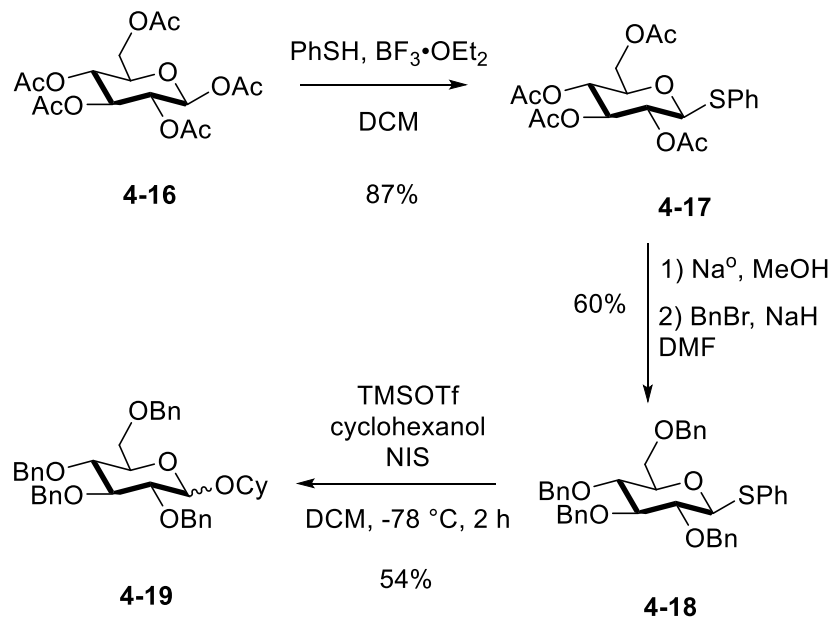


**Figure 4.6.** Synthesis of glucose pseudo-disaccharide model **4-19**.

**4-24** was synthesized from mannose by first acetylating then making thioglycoside **4-22**. Then, deprotection and benzylation to make **4-23**. Similar conditions used for the glucose variant to produce the cyclohexyl pseudo disaccharide variants of galactose and mannose (**4-29** and **4-24**, respectively). and for mannose derivative **4-24** was 2:1 ( $\beta$ : $\alpha$ ).

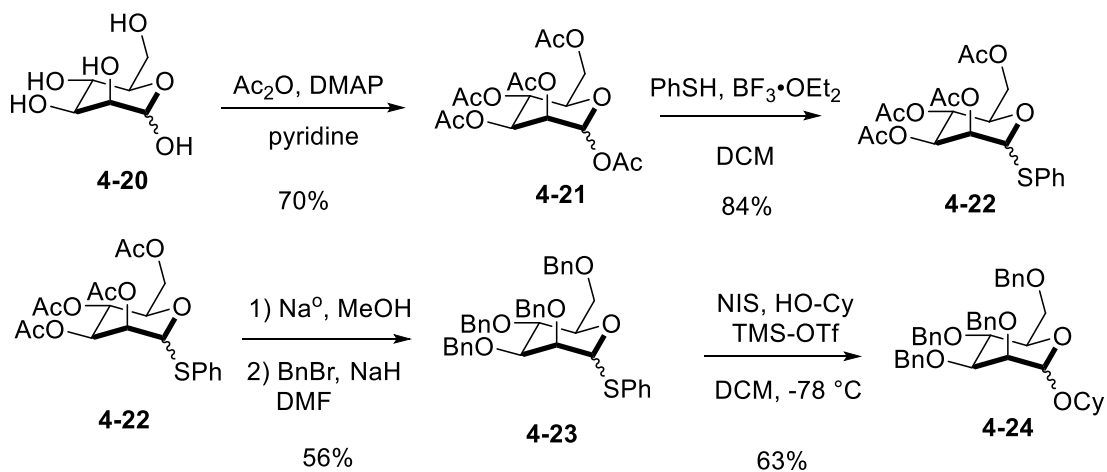


**Figure 4.7.** Synthesis of mannose pseudo-disaccharide model.

The final ratio of anomers for the galactose derivative **4-29** was 1:2 ( $\beta$ : $\alpha$ )

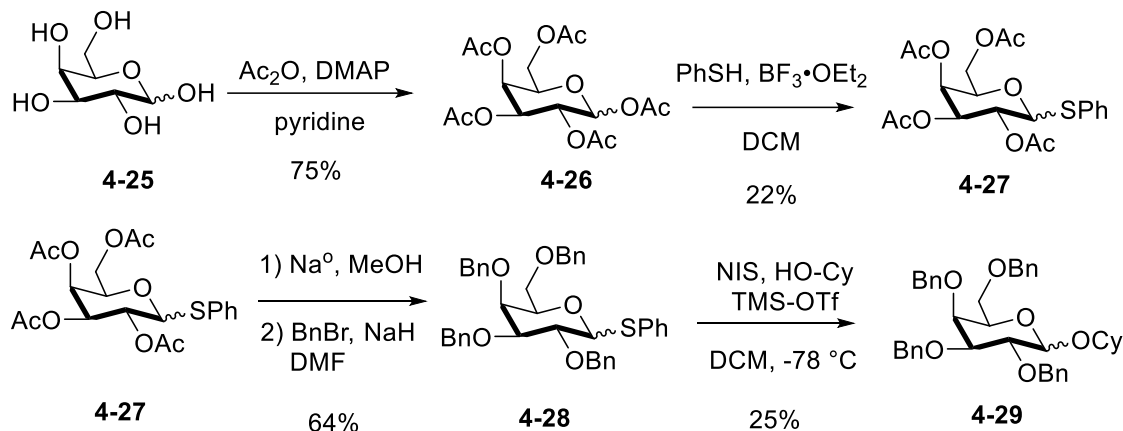


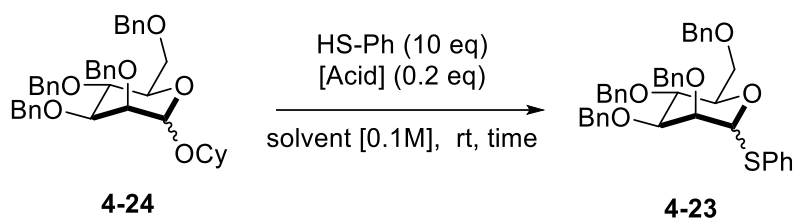
**Figure 4.8.** Synthesis of galactose pseudo-disaccharide model.

With the pseudo-disaccharide models in hand, the next phase was to screen various acids and observe if superacids in organic solvent have any bias for selectivity of the anomeric mixtures. Leito<sup>12</sup> published an informative publication detailing the large differences in acidity for many common mineral and organic acids. They obtained acidity values to characterize the acidities of molecules themselves rather than acidities of the media. Their scale is complementary to the Hammett acidity function ( $H_0$ ) scale, since they are both used for very concentrated solutions of strong acids, including superacids in the information they provide. For Leito's<sup>12</sup> studies, the solvent used is 1,2-dichloroethane (DCE), which has very weak basic properties, but sufficient polarity, and is an appropriate solvent for measuring acidities of very strong acids. DCE acidities of well-known superacids ( $\text{TfOH}$ ,  $(\text{Tf})_2\text{NH}$ , cyanocarbon acids, etc.) as well as common mineral acids ( $\text{H}_2\text{SO}_4$ ,  $\text{HI}$ ,  $\text{HBr}$ , etc.) are reported. The scale spans 15 orders of magnitude (from picric acid to 1,1,2,3,3-pentacyanopropene) and is a useful tool.

To begin our studies, we wanted to use common, commercially available superacids and the easiest to obtain was  $(\text{Tf})_2\text{NH}$  and it has the added benefit of being slightly more acidic than  $\text{TfOH}$  for comparison.

The studies were first conducted on the more reactive mannose substrate **4-24**. TfOH was first used, and it produced very little product. HNTf<sub>2</sub> that was kept in the freezer in open air, gave very little conversion (Table 4.1, Entry 2). But, when another acid sample was kept in a glovebox for storage, the conversion was significantly increased (Table 4.1, Entry 10). Interestingly, when solvents were switched to toluene, more of **4-24** was consumed through the reaction. While the conversion is good, the aim was to achieve anomeric enrichment. When compared to other common acids, (Table 4.1, Entries 3-5) no productive reaction was observed. We also wanted to see if an even more acidic superacid than HNTf<sub>2</sub> could achieve conversion and it was found that there is a limit to acids that can be used. HCTf<sub>3</sub> (Table 4.1, Entries 6-7) seemed to be forming **4-23** over time however, it seemed to be limited to how much superacid was in the reaction.



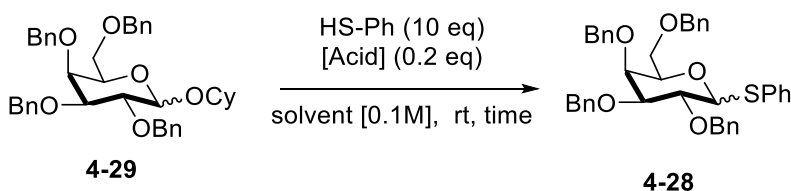
**Table 4.1.** Comparison study of various acids for the deglycosylation of **4-24**.

Entry <sup>a</sup>	Acid	Solvent	Time (h)	Conversion <sup>b</sup>	4-24 ( $\alpha$ : $\beta$ ) <sup>c</sup>	4-23 Yield
1	TfOH	DCM	5	trace	90%	2%
2	NHTf <sub>2</sub> (wet)	DCM	5	trace	95%	n.d.
3	BF <sub>3</sub> -Et <sub>2</sub> O	DCM	5	none	n.d.	n.d.
4	H <sub>2</sub> SO <sub>4</sub>	DCM	5	N/A	n.d.	n.d.
5	HBr	DCM	5	none	n.d.	n.d.
6	CHTf <sub>3</sub>	Et <sub>2</sub> O	5	trace	90%	3%
7	CHTf <sub>3</sub>	DCM	21	minor	80%	20%
8	HNTf <sub>2</sub>	PhMe	5	major	20% (4.4:1)	21%
9	HNTf <sub>2</sub>	THF	5	minor	50% (1.1:1)	2%
10	HNTf <sub>2</sub>	DCM	5	major	50% (6.2:1)	25%
11	HNTf <sub>2</sub>	MeCN	5	major	30% (48:1)	15%
12	HNTf <sub>2</sub>	DCE	5	major	25% (9.5:1)	20%

<sup>a</sup>Starting anomeric ratio = 1:2 ( $\alpha$ : $\beta$ ). <sup>b</sup>Conversion was based on TLC and crude <sup>1</sup>HNMR analysis; trace meant only observable by RP-HPLC. <sup>c</sup>Determined by RP-HPLC analysis.

With the optimized conditions established from Table 4.1, the galactose model **4-29** was investigated next. Surprisingly, the galactose variant gave higher amounts of thioglycoside product compared to the mannose derivative.

**Table 4.2.** Comparison study of various acids for the deglycosylation of **4-29**.



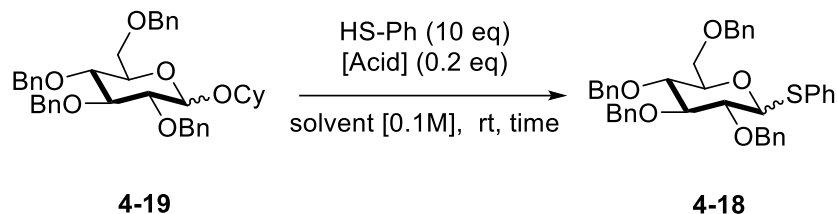
Entry <sup>a</sup>	Acid	Solvent	Time (h)	Conversion <sup>b</sup>	4-29	4-28
					( $\alpha$ : $\beta$ ) <sup>c</sup>	Yield
1	CHTf <sub>3</sub>	Et <sub>2</sub> O	5	none	90%	5%
2	CHTf <sub>3</sub>	DCM	21	minor	70%	20%
3	HNTf <sub>2</sub>	DCM	4	major	20% (4.4:1).	40%
4	HNTf <sub>2</sub>	toluene	5	minor	40% (1:1.5).	30%

<sup>a</sup>Starting anomeric ratio = 2:1 ( $\alpha$ : $\beta$ ). <sup>b</sup>Conversion was based on TLC and crude <sup>1</sup>HNMR analysis; trace meant only observable by RP-HPLC. <sup>c</sup>Determined by RP-HPLC analysis.

The study was continued with the glucose disaccharide model **4-19**. The most interesting finding from these experiments was that solvent choices played a major role in determining the overall reaction and how the ratio of products was enriched. Toluene, DCM, acetonitrile, and DCE all had high conversions but did not give much enrichment of the starting material **4-19**. But the most interesting case was with THF (Table 4.3, Entry 2) where the product enrichment was the most significant with giving mainly the  $\beta$ -**4-19** product. However, the thioglycoside product was not recovered to great degree, leading us to think that the product itself is not very stable to the

reaction conditions. Further optimization is needed to find a fitting nucleophile that will not be subsequently hydrolyzed during the reaction.

**Table 4.3.** Comparison study of various acids for the deglycosylation of **4-19**.



Entry <sup>a</sup>	Acid	Solvent	Time (h)	Conversion <sup>b</sup>	4-19	4-18
					( $\alpha$ : $\beta$ ) <sup>c</sup>	Yield
1	HNTf <sub>2</sub>	PhMe	5	major	15% (3.3:1).	35%
2	HNTf <sub>2</sub>	THF	5	minor	30% (1:28).	1%
3	HNTf <sub>2</sub>	DCM	5	major	10% (4.4:1).	30%
4	HNTf <sub>2</sub>	MeCN	5	major	10% (1:1.5).	30%
5	HNTf <sub>2</sub>	DCE	5	major	10% (2.8:1)	25%

<sup>a</sup>Starting anomeric ratio = 1:9 ( $\alpha$ : $\beta$ ). <sup>b</sup>Conversion was based on TLC and crude <sup>1</sup>HNMR analysis; trace meant only observable by RP-HPLC. <sup>c</sup>Determined by RP-HPLC analysis.

## 4.5 Conclusions

From the superacid studies conducted, a trend has been discovered for potential glycoside site-selective cleavage with anomeric mixtures of disaccharides. It is noteworthy that thiophenol behaves as a suitable nucleophile for intercepting the oxocarbenium ion resulting from the Bronsted acid-catalyzed glycosidic bond cleavage. It should also be noted that in organic solvent, acid strengths can differ greatly<sup>13</sup>. Based on our findings in this preliminary investigation, the next stage will be to develop chiral Bronsted acids that possess a similar, or lower pK<sub>a</sub> value than

HNTf<sub>2</sub>. This opens a door to the possibility of creating a safe and simple method for enriching sugar substrates without needing to worry about sensitive functional groups that may be present.

### Future Directions

In the future, with the findings described in this chapter, we plan to develop a library of chiral Bronsted acids that have low pK<sub>a</sub>'s but can also be soluble in various organic solvents. The benefit of organic solvents is that the acidic species is not dependent on water, permitting facile access for the organic super acid to promote deglycosylation uninhibited. The other benefit of the organic solvents and super acids is that other acid stable functionalities can be utilized as conjugate bases, without needing to be deprotonated first. Thiols have shown to be fantastic early candidate for these types of studies.

One avenue we envision is to dictate site-selective glycoside cleavage by using the natural chirality of a sugar linkage (*cf.* Figure 4-9). Long sugar linkages have alternating chirality built into their structure. If the correct chiral Bronsted acid is chosen, it has the potential to cleave at a specific anomeric site of a polysaccharide, effectively acting as an enzyme. This could be instrumental in developing a simple efficient method to cleave polymeric glycosides into their fragmented form, selectively.

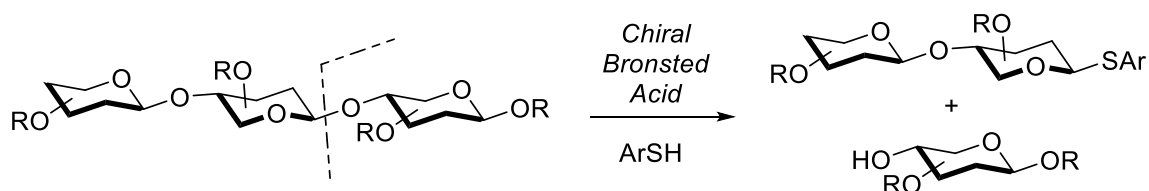


**Figure 4.9.** Proposal for poly-saccharide site recognition with chiral Bronsted acid catalysts.

## 4.6 Experimental information

### Methods and Reagents :

Unless otherwise stated, all reagents and solvents were purchased from commercial sources and were used as received without further purification unless otherwise specified. DCM, DMF, Et<sub>2</sub>O, THF, PhMe, were purified by Innovative Technology's Pure-Solve System using basic alumina. All reactions were carried out under a positive pressure of nitrogen in flame- or oven-dried glassware with magnetic stirring. Reactions were cooled using a cryocooler or external cooling baths (ice water (0 °C), sodium chloride/ice water (-20 °C), dry ice/acetonitrile (-40 °C), or dry ice/acetone (-78 °C)). Heating was achieved by use of a silicone oil bath with heating controlled by an electronic contact thermometer. Deionized water was used in the preparation of all aqueous solutions and for all aqueous extractions. Solvents used for extraction and chromatography were ACS or HPLC grade. Purification of reaction mixtures was performed by flash chromatography using SiliCycle SiliaFlash P60 (230-400 mesh). Yields indicate the isolated yield of the title compound with ≥95% purity as determined by <sup>1</sup>H NMR analysis. Diastereomeric ratios were determined by <sup>1</sup>H NMR analysis. <sup>1</sup>H NMR spectra were recorded on a Varian vnmrs 700 (700 MHz), 600 (600 MHz), 500 (500 MHz), 400 (400 MHz), Varian Inova 500 (500 MHz), or a Bruker Avance Neo 500 (500 MHz) spectrometer and chemical shifts (δ) are reported in parts per million (ppm) with solvent resonance as the internal standard (CDCl<sub>3</sub> at δ 7.26, D<sub>3</sub>COD at δ 3.31, C<sub>6</sub>D<sub>6</sub> at δ 7.16). Tabulated <sup>1</sup>H NMR Data are reported as s = singlet, d = doublet, t = triplet, q = quartet, qn = quintet, sext = sextet, m = multiplet, ovrlp = overlap, and coupling constants in Hz. Proton-decoupled <sup>13</sup>C NMR spectra were recorded on Varian vnmrs 700 (700 MHz) spectrometer and chemical shifts (δ) are reported in ppm with solvent resonance as the internal standard (CDCl<sub>3</sub> at δ 77.16, D<sub>3</sub>COD at δ 49.0, C<sub>6</sub>D<sub>6</sub> at δ 128.06). High resolution mass spectra

(HRMS) were performed and recorded on Micromass AutoSpec Ultima or VG (Micromass) 70-250-S Magnetic sector mass spectrometers in the University of Michigan mass spectrometry laboratory. Infrared (IR) spectra were recorded as thin films a Perkin Elmer Spectrum BX FT-IR spectrometer. Absorption peaks are reported in wavenumbers ( $\text{cm}^{-1}$ ). Optical rotations were measured at room temperature in  $\text{CHCl}_3$  or  $\text{H}_3\text{COH}$  on a Jasco P-2000 polarimeter. The diastereomeric ratio of product mixtures were analyzed using a Shimadzu RP-HPLC with Waters Nova-Pak C18 column ( $60\text{\AA}$ ,  $4\mu\text{m}$ ,  $3.9 \times 150\text{mm}$ ).

**Instrumentation:**

All spectra were recorded on Varian vnmrs 700 (700 MHz), Varian vnmrs 500 (500 MHz), Varian MR400 (400 MHz), Varian Inova 500 (500 MHz) spectrometers and chemical shifts ( $\delta$ ) are reported in parts per million (ppm) and referenced to the  $^1\text{H}$  signal of the internal tetramethylsilane according to IUPAC recommendations. Data are reported as (br = broad, s = singlet, d = doublet, t = triplet, q = quartet, qn = quintet, sext = sextet, m = multiplet; coupling constant( $S$ ) in Hz; integration). High resolution mass spectra (HRMS) were recorded on MicromassAutoSpecUltima or VG (Micromass) 70-250-S Magnetic sector mass spectrometers in the University of Michigan mass spectrometry laboratory. Infrared (IR) spectra were recorded as thin films on NaCl plates on a Perkin Elmer Spectrum BX FT-IR spectrometer. Absorption peaks were reported in wavenumbers ( $\text{cm}^{-1}$ ). The diastereomeric ratio of product mixtures were analyzed using a Shimadzu RP-HPLC with Waters Nova-Pak C18 column ( $60\text{\AA}$ ,  $4\mu\text{m}$ ,  $3.9 \times 150\text{mm}$ ).

#### General Procedure for Acetylation:

Glycoside was dissolved in pyridine (11 eq) under a N<sub>2</sub> atmosphere in an ice bath. Then, Ac<sub>2</sub>O (8 eq.) and was added along with DMAP (0.1 eq). The reaction was left to stir while warming to room temperature and monitored by TLC for complete conversion to the product. The reaction mixture was diluted with DCM and quenched with 1 N HCl. The mixed phases were introduced to separatory funnel. The organic phase was then subsequently washed with aq. sat. NaHCO<sub>3</sub>, then dI H<sub>2</sub>O, then brine. The organic layers were combined and dried over Na<sub>2</sub>SO<sub>4</sub>, filtered and all volatiles were removed *in vacuo*. Crude residue was purified by column chromatography (SiO<sub>2</sub>, EtOAc/hexanes).

#### General Procedure for Forming Thioglycoside:

Peracetylated glycoside was dissolved in anhydrous DCM (0.1 M) under an atmosphere of nitrogen. The solution was cooled to 0 °C and BF<sub>3</sub>·Et<sub>2</sub>O (3.0 eq.) was added dropwise. Afterwards, thiophenol (1.50 eq.) was added dropwise. Then, TBAI (0.1 eq) was added and the reaction mixture was stirred for 18 h and warmed up to room temperature. Reaction monitored by TLC (40% EtOAc/hexanes) showed complete conversion of the starting material. The reaction was stopped, and aq. sat. NaHCO<sub>3</sub> solution was added slowly. The reaction mixture was transferred to a separatory funnel and was extracted with DCM (3x). The organic layers were combined and dried over Na<sub>2</sub>SO<sub>4</sub>, filtered and all volatiles were removed *in vacuo*. The crude product was purified by column chromatography (Hex/EtOAc 2:1).

#### General Procedure for Benzylated Thioglycoside:

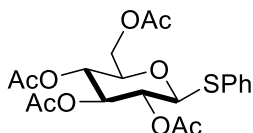
The acetylated thioglycoside was dissolved in methanol (0.2 M). Sodium methoxide (1.05 eq) was added. The reaction mixture was stirred at rt for 2 h. Reaction monitored by TLC showed complete conversion of the starting material. The reaction mixture was neutralised with 3 M AcOH. The reaction mixture was filtered over celite and a silica plug with MeOH/DCM (1:10) and all volatiles are removed *in vacuo*. The product was obtained as a colourless oil and used without further purification. Then, sodium hydride (8.00 eq., 60% dispersion on mineral oil) was suspended in anhydrous DMF (0.4 M) under an atmosphere of N<sub>2</sub> and placed in an ice bath. The unprotected thioglycoside was dissolved in anhydrous DMF under an atmosphere of N<sub>2</sub> and was taken up by syringe. This solution was added to the 0 °C cooled sodium hydride suspension in a dropwise fashion. The reaction mixture was stirred for 1 h at 0 °C. Benzyl bromide (8 eq.) was added and the reaction mixture was stirred for 16 h days and was slowly warmed up to room temperature in the meanwhile. Reaction monitored by TLC showed complete conversion of the starting material. Dilute with EtOAc, wash organic phase with dI H<sub>2</sub>O, then brine. The aqueous layer was extracted with EtOAc (3x). The organic layers were combined and extracted with H<sub>2</sub>O, sat. NaHCO<sub>3</sub>-solution and brine. The organic layer was dried over Na<sub>2</sub>SO<sub>4</sub>, filtered and concentrated *in vacuo*. The crude residue was purified by column chromatography. (SiO<sub>2</sub>, EtOAc/hexanes).

#### General Procedure for Anomeric Substitution with Cyclohexanol:

Benzylated thioglycoside is dissolved in anhydrous DCM (0.1 M) and chilled to -78 °C under atmosphere of N<sub>2</sub>. Then a solution of NIS (0.2 eq) in DCM (0.1 M) is added to the reaction solution. Followed by dropwise addition of TMSOTf (0.2 eq), and then cyclohexanol (1.2 eq) at -78 °C.



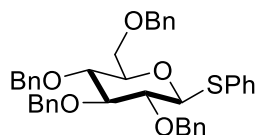
The reaction is left to stir at that temperature while monitoring by TLC until all starting material is consumed. Then, the reaction is quenched with sat. aq. NaHCO<sub>3</sub>, diluted with EtOAc and transferred to a separatory funnel. The organic phase is then washed with sat. aq. NaHCO<sub>3</sub>, and then brine. The organic phase is then dried over Na<sub>2</sub>SO<sub>4</sub>, filtered and concentrated *in vacuo*. The crude product was purified by column chromatography. (SiO<sub>2</sub>, EtOAc/hexanes).



**4-17**

Peracetylated glucose **4-16** (500 mg, 1.3 mmol) was dissolved in anhydrous DCM (10 mL) under an atmosphere of nitrogen. The solution was cooled to 0 °C and BF<sub>3</sub>·Et<sub>2</sub>O (0.86 mL, 3.84 mmol, 3.0 eq.) was added dropwise. Afterwards, thiophenol (200 μL, 1.92 mmol, 1.50 eq.) was added dropwise. Then, TBAI (48 mg, 0.13 mmol, 0.1 eq) was added and the reaction mixture was stirred for 18 h and warmed up to room temperature. Reaction control by TLC (40% EtOAc/hexanes) showed complete conversion of the starting material. The reaction was stopped, and aq. sat. NaHCO<sub>3</sub>-solution was added slowly. The reaction mixture was transferred to a separatory funnel and was extracted with DCM (3x 20 mL). The organic layers were combined and dried over Na<sub>2</sub>SO<sub>4</sub>, filtered and all volatiles were removed *in vacuo*. The crude product was purified by column chromatography (Hex/EtOAc 2:1). The product was obtained as a colorless oil. (490 mg, 11.2 mmol, 87%). R<sub>f</sub>: 0.4)

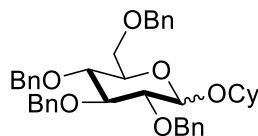
Characterizations of product match with previously reported data.<sup>21</sup>



**4-18**

This compound was prepared according to the general procedure for benzylation using glucose **4-17** (682 mg, 1.54 mmol, 1.00 Eq.), methanol (8 mL), sodium metal (40 mg, 1.68 mmol, 1.1 eq), sodium hydride (490 mg, 12.24 mmol, 8.00 eq.), DMF (10 mL), benzyl bromide (1.45 mL, 12.24 mmol, 8 eq.) The crude product was purified by column chromatography (Hex/EtOAc 3:1). Yield: 580 mg (0.92 mmol, 60%), colorless oil.  $R_f = 0.5$  (Hex/EtOAc 3:1).

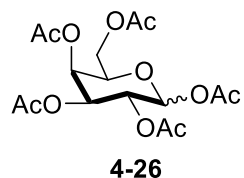
Characterizations of product match with previously reported data.<sup>22</sup>



**4-19**

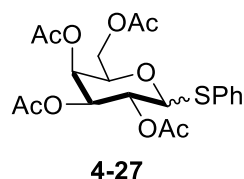
This compound was prepared according to the general procedure for cyclohexanol substitution using glucose **4-18** (1.3 g, 2.05 mmol, 1.00 Eq.), anhydrous DCM (10 mL), NIS (692 mg, 3.08 mmol, 1.5 eq), TMSOTf (75  $\mu$ L, 0.41 mmol, 0.2 eq), DMF (10 mL), cyclohexanol (320  $\mu$ L, 3.08 mmol, 1.5 eq) The crude product was purified by column chromatography (Hex/EtOAc 3:1). Yield: 580 mg (0.92 mmol, 60%), colorless oil.  $R_f = 0.5$  (Hex/EtOAc 3:1). Anomeric ratio was found to be 1:9 ( $\alpha$ : $\beta$ ).

Characterizations of product match with previously reported data for both anomers.<sup>22</sup>



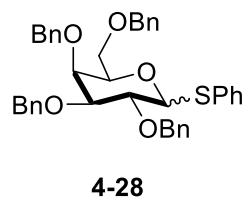
This compound was prepared according to the general procedure for acetylation using galactose **4-25** (500 mg, 2.77 mmol, 1.00 Eq.), pyridine (2.45 mL, 30.5 mmol, 11.0 Eq.), Ac<sub>2</sub>O (2.09 mL, 22.16 mmol, 8.0 eq) and DMAP (34 mg, 0.277 mmol, 0.1 eq). The crude product was purified by column chromatography (Hex/EtOAc 3:1). Yield: 812 mg (2.08 mmol, 75%), colorless oil. R<sub>f</sub> = 0.3 (Hex/EtOAc 3:1).

Spectral data matches previously reported literature <sup>23</sup>



This compound was prepared according to the general procedure for thioglycoside formation using galactose **4-26** (2 g, 5.12 mmol, 1.00 Eq.), BF<sub>3</sub>·Et<sub>2</sub>O (4 mL, 15.4 mmol, 3.0 eq.), thiophenol (0.79 mL, 7.9 mmol, 1.50 eq.) and TBAI (190 mg, 0.51 mmol, 0.1 eq) The crude product was purified by column chromatography (Hex/EtOAc 4:1). Yield: 1.8 g (4.1 mmol, 80%), colorless oil. R<sub>f</sub> = 0.4 (Hex/EtOAc 4:1).

Spectral data matches previously reported literature <sup>23</sup>

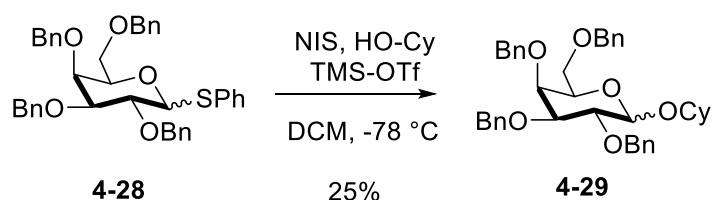


This compound was prepared according to the general procedure for benzylation using galactose **4-27** (200 mg, 0.45 mmol, 1.00 Eq.), methanol (2.25 mL), sodium metal (12 mg, 0.5 mmol, 1.1

eq), sodium hydride (144 mg, 3.6 mmol, 8.00 eq.), DMF (1.5 mL), benzyl bromide (0.43 mL, 3.6 mmol, 8 eq.) The crude product was purified by column chromatography (Hex/EtOAc 3:1).

Yield: 184 mg (0.29 mmol, 64%), colorless oil. Rf = 0.5 (Hex/EtOAc 3:1).

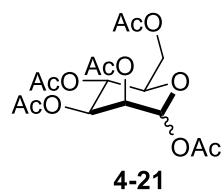
Spectral data matches previously reported literature <sup>24</sup>



This compound was prepared according to the general procedure for cyclohexanol substitution using galactose **4-28** (1.3 g, 2.05 mmol, 1.00 Eq.), anhydrous DCM (10 mL), NIS (692 mg, 3.08 mmol, 1.5 eq), TMSOTf (75  $\mu$ L, 0.41 mmol, 0.2 eq), DMF (10 mL), cyclohexanol (320  $\mu$ L, 3.08 mmol, 1.5 eq) The crude product was purified by column chromatography (Hex/EtOAc 3:1).

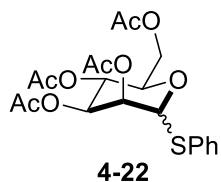
Yield: 580 mg (0.92 mmol, 60%), colorless oil. Rf = 0.4 (Hex/EtOAc 3:1). Anomeric ratio was found to be 2:1 ( $\alpha$ : $\beta$ ).

Characterizations of product match with previously reported data for both anomers. <sup>23</sup>



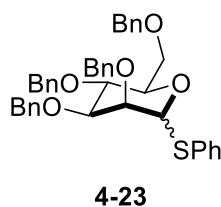
This compound was prepared according to the general procedure for acetylation using mannose **4-20** (500 mg, 2.77 mmol, 1.00 Eq.), pyridine (2.45 mL, 30.5 mmol, 11.0 Eq.), Ac<sub>2</sub>O (2.09 mL, 22.16 mmol, 8.0 eq) and DMAP (34 mg, 0.277 mmol, 0.1 eq). The crude product was purified by column chromatography (Hex/EtOAc 3:1). Yield: 760 mg (1.94 mmol, 70%), colorless oil. Rf = 0.3 (Hex/EtOAc 3:1).

Spectral data matches previously reported literature <sup>25</sup>



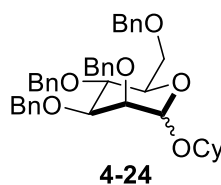
This compound was prepared according to the general procedure for thioglycoside formation using mannose **4-21** (760 mg, 1.95 mmol, 1.00 Eq.),  $\text{BF}_3 \cdot \text{Et}_2\text{O}$  (1.5 mL, 5.85 mmol, 3.0 eq.), thiophenol (0.30 mL, 2.93 mmol, 1.50 eq.) and TBAI (72 mg, 0.19 mmol, 0.1 eq) The crude product was purified by column chromatography (Hex/EtOAc 4:1). Yield: 721 mg (1.64 mmol, 84%), colorless oil.  $R_f = 0.4$  (Hex/EtOAc 4:1).

Spectral data matches previously reported literature <sup>21</sup>



This compound was prepared according to the general procedure for benzylation using mannose **4-22** (721 mg, 1.64 mmol, 1.00 Eq.), methanol (8.2 mL), sodium metal (43 mg, 1.8 mmol, 1.1 eq), sodium hydride (525 mg, 13.2 mmol, 8.00 eq.), DMF (4.1 mL), benzyl bromide (2.2 mL, 13.2 mmol, 8 eq.) The crude product was purified by column chromatography (Hex/EtOAc 3:1). Yield: 581 mg (0.92 mmol, 56%), colorless oil.  $R_f = 0.5$  (Hex/EtOAc 3:1).

Spectral data matches previously reported literature <sup>26</sup>

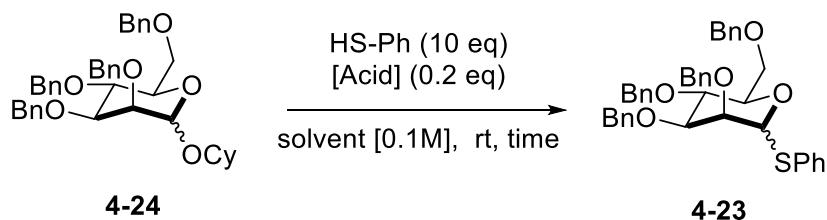


This compound was prepared according to the general procedure for cyclohexanol substitution using mannose **4-23** (580 g, 0.92 mmol, 1.00 Eq.), anhydrous DCM (10 mL), NIS (41 mg, 0.18

mmol, 0.2 eq), TMSOTf (33  $\mu$ L, 0.18 mmol, 0.2 eq), cyclohexanol (114  $\mu$ L, 1.09 mmol, 1.2 eq)  
The crude product was purified by column chromatography (Hex/EtOAc 3:1). Yield: 361 mg (0.58 mmol, 63%), colorless oil.  $R_f$  = 0.5 (Hex/EtOAc 3:1). Anomeric ratio was found to be 1:2 ( $\alpha$ : $\beta$ ).  
Characterizations of product match with previously reported data for both anomers<sup>25</sup>

General Procedure for HNTf<sub>2</sub> deglycosylation:

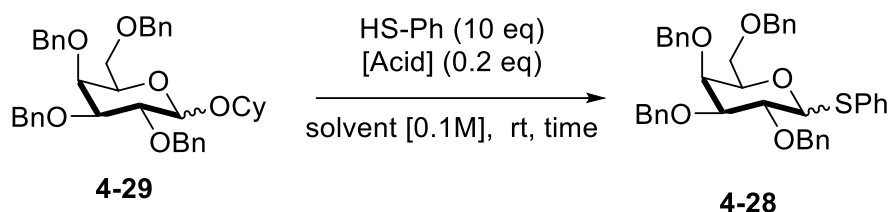
Cyclohexyl glycoside is dissolved in anhydrous solvent (0.1 M) under nitrogen atmosphere. In a separate flame-dried vial, HNTf<sub>2</sub> dissolved in DCM (0.1 eq, 0.1 M). Both the reaction vial and the acid vial were cooled to 0 °C in an ice-bath. The solution containing the sugar was added dropwise to the acid-containing vial and stirred at 0 °C for 15 mins. Then, thiophenol (10 eq) was added dropwise to the reaction flask and the reaction was left to stir for 5 h while warming to room temperature. After starting material was consumed by TLC monitoring, sat. aq. NaHCO<sub>3</sub> was added to quench the reaction. The aqueous layer was extracted with DCM (3x) and washed with brine. The organic phase was dried over Na<sub>2</sub>SO<sub>4</sub>, filtered and concentrated *in vacuo*. Column chromatography was used to purify the reaction (SiO<sub>2</sub>, Hexanes to 100% EtOAc over 10% increments). RP-HPLC was used to determine ratios of remaining glycoside anomers by quenching the mixture, filtered through a silica plug, eluting with 1:3 EtOAc:Hexanes, then concentrated, redissolved in 1mL MeCN, and analyzed by RP-HPLC (Nova-Pak C18, 80% MeCN, 20% H<sub>2</sub>O)



This compound was prepared according to the general procedure for superacid deglycosylation using cyclohexyl mannoside **4-24** (20 mg, 0.032 mmol), anhydrous DCM (320  $\mu$ L), HNTf<sub>2</sub> (2 mg,

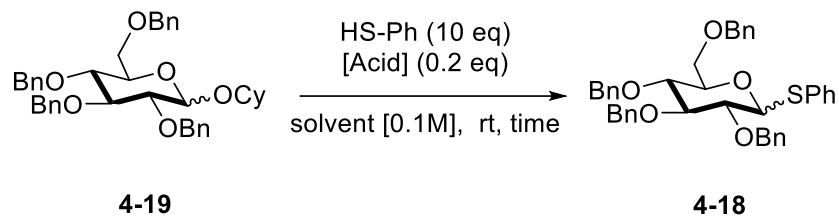
0.006 mmol, 0.1 eq), thiophenol (32.6  $\mu$ L, 0.32 mmol, 10 eq) Column chromatography was used to purify the reaction (SiO<sub>2</sub>, Hexanes to 100% EtOAc over 10% increments). RP-HPLC was used to determine ratios of remaining glycoside anomers. Isolated **4-24** (10 mg, 0.016 mmol, 50%, (6.2:1  $\alpha$ : $\beta$ ) RP-HPLC-Nova-Pak C18, 80% MeCN,  $t_R$ =13.47 min for  $\beta$  and,  $t_R$ =14.99 min for  $\alpha$ . Thioglycoside mixture  $t_R$  = 9.26 min.

Characterizations of product match with previously reported data for both anomers of remaining cyclohexyl glycoside and benzylated thioglycoside.<sup>25, 26</sup>



This compound was prepared according to the general procedure for superacid deglycosylation using cyclohexyl galactoside **4-29** (20 mg, 0.032 mmol) anhydrous DCM (320  $\mu$ L), HNTf<sub>2</sub> (2 mg, 0.006 mmol, 0.1 eq), thiophenol (32.6  $\mu$ L, 0.32 mmol, 10 eq) Column chromatography was used to purify the reaction (SiO<sub>2</sub>, Hexanes to 100% EtOAc over 10% increments). RP-HPLC was used to determine ratios of remaining glycoside anomers. Isolated **4-29** (4 mg, 0.006 mmol, 20%, (4.4:1  $\alpha$ : $\beta$ ) RP-HPLC (Nova-Pak C18, 80% MeCN, 20% H<sub>2</sub>O  $t_R$  = 12.9 min for  $\beta$  and,  $t_R$  = 13.4 min for  $\alpha$ . Thioglycoside mixture  $t_R$  = 9.2 min).

Characterizations of product match with previously reported data for both anomers of remaining cyclohexyl glycoside and benzylated thioglycoside.<sup>23, 26, 27</sup>



This compound was prepared according to the general procedure for superacid deglycosylation using cyclohexyl glucoside **4-19** (20 mg, 0.032 mmol) anhydrous DCM (320  $\mu\text{L}$ ), HNTf<sub>2</sub> (2 mg, 0.006 mmol, 0.1 eq), thiophenol (32.6  $\mu\text{L}$ , 0.32 mmol, 10 eq) Column chromatography was used to purify the reaction (SiO<sub>2</sub>, Hexanes to 100% EtOAc over 10% increments). RP-HPLC was used to determine ratios of remaining glycoside anomers. Isolated **4-19** (2 mg, 0.003 mmol, 10%, (4.4:1  $\alpha$ : $\beta$ ) RP-HPLC (Nova-Pak C18, 80% MeCN, 20% H<sub>2</sub>O  $t_{\text{R}}$  = 15.2 min for  $\alpha$  and,  $t_{\text{R}}$  = 18.6 min for  $\beta$ . Thioglycoside mixture  $t_{\text{R}}$  = 12.7 min).

Characterizations of product match with previously reported data for both anomers of remaining cyclohexyl glycoside and benzylated thioglycoside.<sup>22</sup>



## 4.7 References

- (1) Overend, W. G.; Rees, C. W.; Sequeira, J. S. *J. Chem. Soc.* **1962**, 3429..
- (2) Thatcher, G. R. J., Ed.; *ACS Symposium Series; American Chemical Society: Washington, D.C.*, **1993**; 539.
- (3) Wolfe, S.; Shi, Z. *Israel Journal of Chemistry* **2000**, *40* (3–4), 343–355.
- (4) Wolfe, S.; Rauk, A.; Tel, L. M.; Csizmadia, I. G. *J. Chem. Soc. B* **1971**, *0* (0), 136–145.
- (5) Withers, S. G.; Percival, M. D.; Street, I. P., *Carbohydrate Research*, **1989**, *187*, 1, 43–66.
- (6) Namchuk, M. N.; McCarter, J. D.; Becalski, A.; Andrews, T.; Withers, S. G.. *J. Am. Chem. Soc.* **2000**, *122* (7), 1270–1277.
- (7) Jensen, H. H.; Lyngbye, L.; Bols, M.. *Angewandte Chemie International Edition* **2001**, *40* (18), 3447–3449.
- (8) (a) Jensen, H. H.; Bols, M. *Org. Lett.* **2003**, *5* (19), 3419–3421. (b) Bols, M.; Liang, X.; Jensen, H. H.. *J. Org. Chem.* **2002**, *67* (25), 8970–8974.
- (9) Timell, T. E. *Can. J. Chem.* **1964**, *42* (6), 1456–1472.
- (10) Wolfenden, R.; Lu, X.; Young, G. *J. Am. Chem. Soc.* **1998**, *120* (27), 6814–6815.
- (11) Namchuk, M. N.; McCarter, J. D.; Becalski, A.; Andrews, T.; Withers, S. G. *J. Am. Chem. Soc.* **2000**, *122* (7), 1270–1277.
- (12) Kütt, A.; Rodima, T.; Saame, J.; Raamat, E.; Mäemets, V.; Kaljurand, I.; Koppel, I. A.; Garlyauskayte, R. Yu.; Yagupolskii, Y. L.; Yagupolskii, L. M.; Bernhardt, E.; Willner, H.; Leito, I.. *J. Org. Chem.* **2011**, *76* (2), 391–395.
- (13) Kütt, A.; Leito, I.; Kaljurand, I.; Sooväli, L.; Vlasov, V. M.; Yagupolskii, L. M.; Koppel, I. A. *J. Org. Chem.* **2006**, *71* (7), 2829–2838.
- (14) Edge, A. S. B. *Biochemical Journal* **2003**, *376* (2), 339–350.
- (15) Shuai, L.; Pan, X. *Energy Environ. Sci.* **2012**, *5* (5), 6889.
- (16) Leito, I.; Kaljurand, I.; Koppel, I. A.; Yagupolskii, L. M.; Vlasov, V. M.. *J. Org. Chem.* **1998**, *63* (22), 7868–7874.
- (17) Kaupmees, K.; Tolstoluzhsky, N.; Raja, S.; Rueping, M.; Leito, I. *Angewandte Chemie International Edition* **2013**, *52* (44), 11569–11572.

- (18) Olah, G. A.. *J. Org. Chem.* **2005**, *70* (7), 2413–2429.
- (19) Lebedel, L.; Ardá, A.; Martin, A.; Désiré, J.; Mingot, A.; Aufiero, M.; Aiguabella Font, N.; Gilmour, R.; Jiménez-Barbero, J.; Blériot, Y.; Thibaudeau, S. *Angewandte Chemie International Edition* **2019**, *58* (39), 13758–13762.
- (20) Martin, A.; Arda, A.; Désiré, J.; Martin-Mingot, A.; Probst, N.; Sinaÿ, P.; Jiménez-Barbero, J.; Thibaudeau, S.; Blériot, Y. *Nature Chem* **2016**, *8* (2), 186–191.
- (21) Krumb, M.; Lucas, T.; Opatz, T., *Eur. J. Org. Chem.*, **2019**, 4517-4521.
- (22) Bernardes, G. J. L.; Grayson, E. J., Thompson, S.; Chalker, J. M.; Errey, J. C.; Oualid, F. E., Claridge, T. D. W.; Davis, B. G., *Angew, Int. Ed.*, **2008**, *47*, 2, 2244-2248.
- (23) Guo, H.; Si, W.; Li, J.; Yang, G.; Tang, T.; Wang, Z.; Tang, Jie.; Zhang, J., *Synthesis* **2019**, *51*, 2984–3000
- (24) Dinkelaar, J.; Jong, A. R.; Meer, R.; Somers, M.; Lodder, G.; Overkleef, H. S.; Codee, J. D. C. Marel, G. A., *JOC*, **2009**, *74*, 14, 4982-4991.
- (25) Toshima, K.; Nagai, H.; Kasumi, K.; Kawahara, K.; Matsumura, S., *Tetrahedron* **2004**, *60* 5331–5339.
- (26) Lee, Y. J.; Back, J. Y.; Lee, B-Y.; Kang, S. S.; Park, H-S.; Jeon H. B.; Kim, K S., *Carbohydrate Research*, **2006**, *341*,10, 1708-1716.
- (27) Grube, M.; Lee, B-Y.; Garg, M.; Michel, D.; Vilotijevic, I.; Malik, A.; Seeberger, P. H.; Silva, D. V., *Chem. Eur. J.* **2018**, *24*, 3271-3282.

## Chapter 5

### Closing Remarks

Described herein is the development of novel strategies for derivatizing D-ring functionalities of steroid cores. Research conducted included building bufadienolide core-scaffolds by investigating selective hydrogenation techniques and developing optimizations towards a more efficient route of photooxidation of furan carbonyl moieties toward bufadienolides. Since direct, regioselective hydrogenation was more challenging than expected, this led us to investigate masking groups to add potential steric intervention. This proved unfruitful; however, we still aim to explore other effects that can potentially dictate the electronic environment of the pyrone olefins.

In summary, the work described in this Chapter 2 shows the importance of bufadienolides while also showcasing their inherent sensitivity. This can be attributed to the pyrone's duality being both a conjugated carbonyl that can coexist between two *cis*-alkene systems, with one being within the pyrone ring itself, and the other between the pyrone ring and the  $\Delta^{16}$ -steroid alkene. Pyrones also share characteristics with aromatic compounds, meaning that conditions that can reduce them, can be sometimes more engaging to the pyrone moiety. All in all, discoveries towards the development of synthetic methods for making bufadienolides is a worthy development. There is still a considerable vacancy for methods describing how to make bufadienolides, with or without any complex functional groups present. Since most bufadienolides are isolated from extracts of natural sources, their scarcity leads to a limited number of isolatable compounds. This limits scientific knowledge and understanding of therapeutic potential and interactions for medicinal chemistry studies. Together with their side effects and adverse drug interactions, this class of

therapeutics would require more investigations before they are included among standard medicines.

With the difficulties surrounding the selective hydrogenation of the pyrone-  $\Delta^{16}$ -steroid, we took inspiration from Wiesner's method of novel synthetic method for transforming furans-carbonyls into pyrones via an endo-peroxide, singlet-oxygen Diels-Alder rearrangement. This method allowed for one of the first total syntheses of bufalin and related derivatives from a common starting intermediate in testosterone or digitoxigenin. The limitation in their method includes the total step count of their route and how different stereocenters are incorporated and manipulated. We aimed to create a more efficient process of making pyrones from furan amides which could eliminate the additional oxidation operation in Wiesner's route. On a model phenyl substrate, our furan amide substrates were worked well with acid cyclization with *p*-TsOH. The issue came when applying the method on a steroid model system. Even with changing temperatures, solvents, or acids, only complex or decomposition pathways were observed. With these challenges, we look to the future by focusing on mild conditions for promoting the cyclization of the bis-allylic alcohol toward making pyrones.

Chapter 3 discussed the strategies and methods used for completing the first synthetic route for the synthesis of rhodexin B via glycosylation of oleandrigenin. To the best of our knowledge, glycosylations in the presence of C16-OAc functionalities have been reported to date. The additional novelty of this synthetic method is for the most efficient route towards the synthesis of oleandrigenin by showcasing a House-Meinwald rearrangement strategy of a furan-epoxy steroid. We aim to develop other functionalities of oleandrigenin for investigating the potential medicinal chemistry potential that other structural modifications may induce. This can range from other glycosides being introduced at the C3 position, or other functionalities, like amine stereocenters.

With the optimized House-Meinwald rearrangement, we will also investigate developing other novel C-17 isosteres that possess the additional C-16 oxidated appendage.

Chapter 4 describes ongoing studies for developing a library of chiral Bronsted acids that have low  $pK_a$  values but can also be soluble in various organic solvents. The benefit of organic solvents is that the acidic species is not dependent on water. The other benefit of the organic solvents and super acids is that other acid stable functionalities can be utilized as conjugate bases, without needing to be deprotonated first. This serves a useful platform to develop a simple method that could be universally used in complex polysaccharide cleavages.

This thesis has showcased methods that have added to the scientific literature, pertaining to D-ring modifications, specifically D-ring oxidized steroids, while also addressing current issues involved in making sensitive  $\alpha$ -pyrones in the presence of late-stage C-14 and C-16-OH functionalities in an effort to improve the synthesis of steroids in general for the scientific literature. The efforts invested in the synthesis of rhodexin B led to the discovery of a novel C-16-OH installation, and will lead to potential medicinal chemistry investigations involving C-16 modifications, and utilizing the House-Meinwald rearrangement in the presence of other sensitive heterocyclic moieties, including C-17  $\alpha$ -pyrones, and related isosteres.